الجمهورية الجزائرية الديمقراطية الشعبية

PEOPLE'S DEMOCRATIC REPUBLIC OF ALGERIA

MINISTERY OF HIGHER EDUCATION AND SCIENTIFC RESEARCH

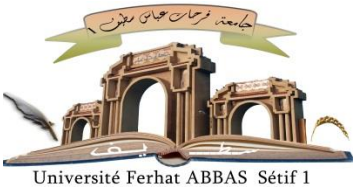

SETIF 1 UNIVERSITY FERHAT ABBES (ALGERIA)

FACULTY OF TECHNOLOGY

A thesis presented to the Faculty of Technology

Department of Electrical Engineering

in fulfilment of the requirement for the degree of

DOCTOR of SCIENCES

in Electrical Engineering

Presented by

SAHLI Zahir

Thesis Title:

Optimal planning of reactive power in electrical networks using metaheuristics

Presented on:

Mr. RADJEAI Hammoud	Professor	Univ. Ferhat Abbas Sétif 1	Chair of committee
Mr. HAMOUDA Abdellatif	Professor	Univ. Ferhat Abbas Sétif 1	Supervisor
Mr. SAYAH Samir	Professor	Univ. Ferhat Abbas Sétif 1	Co-Supervisor
Mr. MESSALTI Sabir	Professor	Univ. Mohamed Boudiaf, M'Sila	Examiner
Mr. MEDDAD Mounir	Professor	Univ. M^{ed} El Bachir El Ibrahimi, BBA	Examiner
Mr. BELHOUCHET Khaled	MCA	Univ. Mohamed Boudiaf, M'Sila	Examiner
Mr. TRENTESAUX Damien	Professor	Univ. Polytechnique Hauts-de-France	Invited
Mr. BEKRAR Abdelghani	Professor	Univ. Polytechnique Hauts-de-France	Invited

DEDICATION

.... dedicate

To my PhD Supervisor Pr., HAMOUDA Abdellatif, for his patience, motivation, immense knowledge and loving of scientific research.

To my beloved Wife and my children: Lina, Malak, Younes, Soundes and Rihab

To my wonderful friend SAYAH Samir

To My Family members for their continuous support and encouragement

List of Publications

Journal Publications

1. Zahir Sahli, Abdellatif Hamouda, Abdelghani Bekrar, Damien Trentesaux, "Reactive Power Dispatch Optimization with Voltage Profile Improvement Using an Efficient Hybrid Algorithm", Energies 2018, 11(8), 2134; doi.org/10.3390/en11082134.

2. Z. Sahli, A. Hamouda, S. Sayah, D. Trentesaux, and A. Bekrar, "Efficient Hybrid Algorithm Solution for Optimal Reactive Power Flow Using the Sensitive Bus Approach", Eng. Technol. Appl. Sci. Res., vol. 12, no. 1, pp. 8210–8216, Feb. 2022.

Conference Proceedings

1. Sayah Samir; Sahli Zahir; Zehar Khaled. Differential Evolution Algorithm for Economic Load dispatch considering Valve-Point Effect International conference on Electrical and Electronics Engineering ICEEE'08, Laghouat, Algeria

2. Mustapha Sarra, Zahir Sahli, Abdelmadjid Chaoui, Kamel Djazia. Real time control of a Power System Stabilizer using an Artificial Neural Network, International Conference on Applied Informatics ICAI09, BBA, Algeria.

3. Sahli Z., Bekrar A., Trentesaux D. Application of Evolutionary Algorithms for Optimal Dispatch of Reactive Power in electrical networks, 2nd regional day for PhD students in automation JRDA 2013, University of Valenciennes, France.

4. Sahli Z., Bekrar A., Trentesaux D. (2014). Hybrid PSO algorithm for the solving of the Optimal Reactive Power Problem. P. Siarry, L. Idoumghar, J. Lepagnot, International Conference on Swarm Intelligence Based Optimization (ICSIBO'2014), Mulhouse, France, pp. 45-46, may

5. Sahli Z., Bekrar A., Trentesaux D., Hamouda A. (2014). Hybrid PSO-tabu search for the Optimal Reactive Power Dispatch Problem. IEEE IECON'2014, Dallas, TX, USA, pp. 3536-3542, October.

ACKNOWLEDGEMENT

First, of all, thanks to Almighty Allah who gave me the strength and confidence to complete this Thesis; through ALLAH's generosity and mercy, I was able to complete this work. I would like also to express my deepest gratitude to Professor Abdellatif HAMOUDA, my thesis supervisor, for their invaluable guidance, unwavering support, and insightful feedback throughout the entire process of researching and writing this thesis. Their expertise and encouragement have been instrumental in shaping the direction of my work. I am also indebted to Professor SAYAH Samir, my thesis co-supervisor for their thoughtful critique and constructive suggestions, which greatly enhanced the quality of this thesis.

My deepest gratitude is also due to the members of the jury: Pr. RADJEAI Hammoud, Pr. MESSALTI Sabir, Pr. MEDDAD Mounir, Dr. BELHOUCHET Khaled, for serving as my committee members and taking the time to revise my thesis.

I would like to express my gratitude and thanks to Professor Damien TRENTESAUX from the University of Valenciennes. Special thanks to Professor Bekrar Abdelghani, Valenciennes University, for his invaluable discussions and brilliant comments.

I would also like to thank my friends and colleagues in the electrical engineering department of the University of Sétif 1.

Sincerely

Zahir SAHLI

2024

Table of Content

List of figures

List of Tables

List of Abbreviations

Acronyms

ABC	Artificial Bee Colony Algorithm
AC	Alternating Current
ACO	Ant Colony Optimization
AEO	Artificial Ecosystem-Based Optimization
AGA	Adaptive Genetic Algorithm
AHA	Artificial Hummingbird Algorithm
AIS	Artificial Immune Systems
ALO	Ant Lion Optimizer
ANOVA	Analysis Of Variance
APOPSO	Hybrid Artificial Physics Optimization–Particle Swarm
ARCBBO	Adaptive Real Coded Biogeography-Based Optimization
BA	Bat Algorithm
BBO	Biogeography-Based Optimization
BCFO	Bacterial Colony Foraging Optimization
BCO	Bee Colony Optimization
BHA	Black Hole Algorithm
BSA	Backtracking Search Optimization Algorithm
CA	Coordinated Aggregation
CBO	Colliding Bodies Optimization
CGA	Canonical Genetic Algorithm
CLPSO	Comprehensive Learning PSO
CMAES	Covariance Matrix Adopted Evolutionary Strategy
CSA	Cuckoo Search Algorithm
CSO	Chicken-Swarm-Optimization
CVs	Control Variables
DDE	Double Differential Evolution
DE	Differential Evolution Algorithm
DVR	Dynamic Voltage Restorers
EMS	Energy Management System
EP	Evolutionary Programming
ES	Evolution Strategies
FACTS	Flexible Alternating Current Transmission Systems
GA	Genetic Algorithm

GP	Genetic Programming
GPAC	General passive congregation
GSA	Gravitational Search Algorithm
GSO	Glowworm Swarm Optimization
GUI	Graphical User Interface
GWO	Grey Wolf Optimizer
HSA	Harmony Search Algorithm
HVDC	High Voltage Direct Current
ICA	Imperialist Competitive Algorithm
ICBO	Improved Colliding Bodies Optimization
IP	Interior Point
IP-OPF	Interior-Point Optimal Power Flow
IQR	Interquartile Range
IWO	Invasive Weed Optimization
KHA	Krill Herd Algorithm
LCA	League Championship Algorithm
L-DE	Local search-DE
LPAC	Local Passive Congregation
L-SACP-DE	DE with Local search Self-Adapting Control Parameters
L-SADE	Local search Self-Adaptive Differential Evolution
MAPSO	Multi-agent-Based PSO
MBA	Mine Blast Algorithm
MFO	Moth Flam Optimizer
MGBTLBO	Modified Gaussian Barebones Teaching–Learning-Based Optimization
MICA-IWO	Modified Imperialist Competitive Algorithm-Invasive Weed Optimization
MNSGA-II	Modified Non-dominated Sorting Genetic Algorithm
MOPSO	Multi-objective Particle Swarm Optimization
MSA	Moth Swarm Algorithm
MTLA	Modified Teaching Learning Algorithm
MTLA-DDE	Modified Teaching Learning Algorithm Double Differential Evolution
NBA	Novel Bat Algorithm
NLP	Nonlinear Programming Method
NSGA-II	Non-dominated Sorting Genetic Algorithm II
OGSA	Opposition Gravitational Search Algorithm
OPF	Optimal Power Flow
ORPD	Optimal Reactive Power Dispatch

Ploss	Power Losses
PMU	Phasor Measurement Unit
PSO	Particle Swarm Optimization
PSO-CF	PSO with Constriction Factor
PSO-TS	Particle Swarm Optimization – Tabu Search
PSO-TVAC	PSO-Time Varying Accelerating Constant
PSO-w	PSO with adaptive inertia weight
QOTLBO	Quasi-Oppositional Teaching Learning Based Optimization
RGA	Real-coded Genetic Algorithm
SA	Simulated Annealing
SARGA	Self-Adaptive Real-coded Genetic Algorithm
SCA	Sine Cosine Algorithm
SCADA	Supervisory Control and Data Acquisition
SD	Standard Deviation
SFLA	Shuffled Frog-Leaping Algorithm
SGA	Simple Genetic Algorithm
SKH	Stud Krill Herd Algorithm
SOA	Seeker Optimization Algorithm
SPSO-TVAC	Standard PSO with TVAC
SSSC	Static Synchronous Series Compensator
STATCOM	Static Synchronous Compensators
STATCON	Static Condensers
SVC	Static Var Compensators
TVD	Total of Voltage Deviation
TCPAR	Thyristor Controlled Phase Angle Regulators
TCR	Thyristor Controlled Reactor
TCSC	Thyristor Controlled Series Compensators
TLBO	Teaching–Learning-Based Optimization
TS	Tabu Search
TSC	Thyristor Switched Capacitor
TSP	Traveling Salesman Problem
TSR	Thyristor Switched Reactor
UPFC	Unified Power Flow Controllers
VAR	Volt-Amperes Reactive
VNS	Variable Neighborhood Search
VRP	Vehicle Routing Problem

VSI	Voltage Stability Index
WCA	Water Cycle Algorithm
WOA	Whale Optimization Algorithm

Symbols

P	Active power
Q	Reactive power
S	Apparent power
V	Bus voltage magnitude
δ	Bus phase angle
R_l	Line resistance
X_l	Line reactance
Y	Admittance matrix
P_{loss}	Real Power loss / Active power losses
δ_{ij}	The voltage angle difference between bus i and bus j
N_{PV}, N_{PQ}	The number of *PV* and *PQ* buses respectively
G_{ij}	Conductance of k^{th} branch connected between bus *i* and *j*
V_i, V_j	Voltage magnitude at bus *i* and *j*
$\left\|Y_{ij}\right\|$ / S_i	The elements of bus admittance matrix/apparent power flow in branch *i*
$P_{L,N_{PQ}}, Q_{L,N_{PQ}}$	The active and reactive power at each load bus
$V_i^{\max}, V_i^{\min}$	The maximum and minimum bus voltage magnitude at bus *i*
$Q_{Gi}^{\min}, Q_{Gi}^{\max}$	The minimum and maximum value of power generation at bus *i*
$T_k^{\max}$ / $T_k^{\min}$	The maximum/minimum tap ratio of k^{th} tap changing transformer
$Q_{Ci}^{\min}, Q_{Ci}^{\max}$	The minimum and maximum VAR injection limits of shunt capacitor banks
S^{max}	The maximum apparent power flow limit
c_1, c_2	Acceleration coefficients
g	Set of equality constraints
h	Set of inequality constraints
J	Objective function
K_P, K_V, K_Q, K_S	Penalty factors
L_k	Voltage stability index
N_B	Total number of buses
N_C	Number of shunt capacitors
N_G	Number of generator buses

N_L	Number of transmission lines
N_{PQ}	Number of PQ buses
N_T	Number of tap transformers
P_{Di}, Q_{Di}	Active and reactive power demand at bus i
$P_{G,\text{slack}}$	GReal power generation at slack bus
P_{Gi}, Q_{Gi}	Active and reactive power of the ith generator
P_{gi}	Active power generation at generator i
Q_C	Shunt VAr compensator
Q_{ci}	Reactive power compensation source at bus i
S_L	Line apparent power
T_i	Tap ratio of transformer i
u	Control variables vector
V_{Gi}	Voltage magnitude at generator bus i
V_i	Voltage magnitude at bus i
V_j	Voltage magnitude at bus j
V_{Li}	Voltage magnitude at load bus i
V_{ref}	Voltage reference
v_i^k	Current velocity of particle i at iteration k
w_{max}, w_{min}	Upper and lower limits of the inertia weighting factor
w_i	Inertia weight
x	State or dependent variables vector

Chapter 1

INTRODUCTION

1.1. Overview of the Thesis

Modern power systems are becoming more vulnerable to operating limit violation and voltage instability problems due to large transmission networks, deregulation of the electricity industry and utilization of various renewable energy sources as well as different load patterns. The power system, at this stage, can become insecure and prone to voltage collapse due to lack of reactive power support. Generators have the capability of providing reactive power but are limited to a certain extent. Moreover, the reactive power produced by the generators cannot be effectively utilized if the demand for the reactive power is far from its location [1]. Optimal reactive power dispatch (ORPD) in electrical transmission networks is an essential area of electrical engineering aimed at maintaining the stability and quality of the power system. Reactive energy is required to maintain a stable voltage in the power system. Optimizing reactive power flow involves effectively managing the production and consumption of reactive energy in order to minimize energy losses, optimize the use of equipment and maintain stable voltages in the network. The various key points linked to optimizing reactive power flow in transmission networks are as follows:

- ✓ Reactive energy is needed to maintain the voltage at an appropriate level in the electrical network.
- ✓ Energy generators, such as power stations, can produce reactive energy, while loads, such as electric motors, consume it. The aim is to coordinate the production and consumption of reactive energy to meet the needs of the network.
- ✓ Reactive power compensators, such as capacitors and inductors, can be used to adjust the reactive energy in the network. Automatic control systems adjust these devices to maintain voltages within acceptable ranges.
- ✓ To optimize the flow of reactive energy, electrical engineers use network modelling and analysis software to simulate the behavior of the network under different load and generation conditions.
- ✓ Optimizing reactive energy reduces energy losses in the network, improves energy efficiency and extends the life of electrical equipment.
- ✓ Proper management of reactive energy is crucial to maintaining the stability of the

electricity network. Excessive voltage variations can lead to network disturbances and outages [2].

Optimal Reactive Power Dispatch (ORPD) is a subproblem of OPF, which has the objective of improving the system voltage profile and minimizing system transmission losses. This is achieved through redistribution of reactive power in the network through optimal setting of generator terminal voltage or reactive power outputs, transformer tapings and output of other compensating devices such as shunt capacitors, reactors, synchronous condensers etc. The fast progress in the field of power electronics, has resulted into introduction of new devices for more flexible operation of the power systems known as Flexible AC Transmission System (FACTS) devices. These devices include Static Var Compensators (SVC), Thyristor Controlled Series Compensators (TCSC), Thyristor Controlled Phase Angle Regulators (TCPAR), Static Condensers (STATCON), Unified Power Flow Controllers (UPFC), etc. These devices have been mainly studied and applied for minimizing active power losses and improving the voltage profile of the power system.

This thesis is mainly based on the application of metaheuristic optimization techniques to address the optimal reactive power dispatch (ORPD) problem. The metaheuristic algorithms are used to investigate the best combination of control variables including generators voltage, transformers tap setting as well as reactive compensators sizing to achieve minimum total power loss and minimum voltage deviation.

1.2. Problem statement

The electrical energy from the generating station is delivered to the consumer terminals via transmission and distribution networks. The generating stations supply both active and reactive power to the consumers. The Reactive power is critical to the operation of the power networks on both safety aspects and economic aspects. Rational reactive power dispatch scheme can improve the power quality as well as reduce the real power loss. On the contrary, if the reactive power is unreasonably allocated, then it will bring great economic losses and might even threaten the security of the power grid. Consumer terminals require a substantially constant voltage for satisfactory operation, but in practice electrical loads are time-varying, which means that consumer loads change over time, causing power and current fluctuations. Reactive power requirements vary continuously according to load and system configuration. These changes in reactive power generation cause fluctuations in system voltage levels. Any change in the design of the system or in the demand for energy can alter the voltage levels in the system. The injection of reactive power into the electrical network increases voltages, while the absorption of reactive power from the network decreases them. The main task of a power system is to

sustain the load bus voltages within the nominal range for consumer satisfaction and minimizing power losses especially in a deregulated or restructured power industry. For the purpose of minimizing the real power loss, utility companies can either change the structure of the power grid or replace the old wiring with lower impedance lines. However, both of these methods require investing large amounts of money. The simplest and most economical way remains reactive power dispatch method. In the early days, the starting point of reactive power dispatch is to improve the power factor at each end user by installing reactive power compensators. This situation can be improved by the operator by reallocating the production of reactive power in the system by modelling it as an ORPD optimization problem. In an electrical power system, there is a constant need for the efficient management and dispatch of reactive power to maintain grid stability, voltage regulation, and power quality. The primary objective of the ORPD problem is to optimize the allocation and control of reactive power resources to minimize system losses, ensure voltage levels remain within acceptable limits. Solving the ORPD problem effectively involves mathematical optimization techniques and sophisticated control algorithms to find the optimal settings for devices that can generate or absorb reactive power. The result of solving this problem is a set of control actions for reactive power resources that minimize system losses and ensure the reliable and efficient operation of the electrical power system. The compensation of the reactive power can be done ether by FACTS (Flexible Alternating Current Transmission Systems) devices or classical reactive resources which play essential roles in managing reactive power in electrical power systems, but they differ in their operation, capabilities, and characteristics. FACTS devices are advanced power electronics-based devices that can control various parameters of the electrical grid, including voltage, impedance, and phase angle. They use real-time control algorithms to adjust these parameters and enhance the overall system performance. FACTS devices are highly flexible and can rapidly respond to changing grid conditions. The classical reactive resources include conventional devices such as synchronous generators and capacitors. These devices provide or absorb reactive power but typically do not have the same level of dynamic control and flexibility as FACTS devices. Their operation is often based on setpoints and may not adapt as quickly to grid changes.

1.3. Major contributions of the Thesis.

The main contributions of this dissertation can be summarized in the following points:

- Different Bio-inspired optimization algorithms were proposed namely MFO, GWO, ALO and AHA and applied on little, medium and large-scale power systems (IEEE 14-bus, IEEE-30 bus, IEEE-57 bus, IEEE-118 bus).

- Statistical analysis has been achieved in this study using Box-and-whisker plot and One-way ANOVA test system, to give a certain level of confidence to our study and evaluate which algorithms are most suitable in solving the ORPD problem.
- A novel method based on Hybridization of PSO (Particle Swarm Optimization) and TS (Tabu Search) named PSO-TS have been proposed for ORPD problem in standard IEEE power systems with 30 and 57 bus and with the practical large-scale Algerian 114-bus power test system in order to evaluate the performance of the power system in terms of active power losses and voltage profile.
- The proposed PSO-TS optimization method has also been applied to solve mixed integer optimization problem with discrete variables, which reflect the real nature of the variables.
- The proposed PSO-TS algorithm has been implemented to solve ORPD problem considering FACTS devices
- Programming a Windows application to display all the simulations carried out during the various system tests.
- Creation of a model for controlling SVC devices via a man-machine interface running under Windows and Android
- Direct control of the SVC devices via GUI MATLAB using a microcontroller.

1.4. Organization of the Thesis.

This thesis has been organized into seven chapters which are below detailed:

Chapter 1 highlights the Overview of the thesis, the problem statement and the major contributions of the research work.

The second chapter deals with reactive energy then it presents the general background, objective functions, constraints, and problem formulation of (ORPD). The conventional algorithm techniques are presented and several metaheuristic methods based ORPD in the literature are summarized.

The third chapter provides an overview of a range of Bio-inspired algorithms drawn from a natural phenomenon including MFO (Moth Flame Optimization), GWO (Grey Wolf Optimizer), AHA (Artificial Hummingbird Algorithm) and ALO (Ant Lion optimization). These bio-inspired algorithms were described and presented. The proposed algorithms based ORPD problem were applied on different IEEE test systems (from smallest to largest electrical transmission networks), and their results were compared with each other and with those of other optimization methods presented in the literature.

In Chapter 4 an efficient hybrid PSO with TS techniques called PSO-TS is implemented to solve the ORPD problem. First, the proposed Hybrid algorithm is implemented considering

continuous control variables. In the second part, a new approach to identify the sensitive buses was presented and was implemented to solve the ORPD problem with two distinct objective functions, namely, active power losses and voltage deviation. Afterwards the PSO-TS method based ORPD considering discrete control variables is presented and tested on IEEE 14-bus, IEEE 30-bus, IEEE 57-bus and the practical Algerian electric 114-bus power system.

In Chapter 5 a general presentation and modeling of the FACTS technology are presented. Afterwards the proposed PSO-TS method has been applied to the ORPD problem considering SVC and TCSC devices. The first time, only one type of FACTS was considered. Subsequently, both types of facts, i.e. SVC and TCSC, were installed simultaneously.

In Chapter 6 a mock-up to test the control and command of the SVC devices via a human-machine interface running under Windows and Android is built. A Windows application designed to visualize all the simulations carried out during our thesis work.

The conclusion and future-work are discussed in Chapter 7.

Chapter 2

OPTIMAL REACTIVE POWER DISPATCH PROBLEM AND METAHEURISTIC METHODS

2.1. Conventional methods for the ORPD problem

One of the most important conditions for economic and secure operation of electric power system is the optimal reactive power dispatch (ORPD). The ORPD is achieved by appropriate coordination of the equipment which manage the reactive power flows to minimize the real power loss and/or improve the voltage profile of the power system. Mathematically, the ORPD problem can be formulated as a constrained nonlinear optimization problem. Initially the conventional methods were used to solve the optimal reactive power dispatch problem. The application of these methods had been an area of active research in the recent past. The conventional methods are based on mathematical programming approaches and used to solve different size of OPF problems. To meet the requirements of different objective functions, types of application and nature of constraints, the popular conventional methods are further sub divided into: Gradient Method, Newton Method, Linear Programming Method, Quadratic Programming Method and Interior Point Method. Even though, excellent advancements have been made in classical methods, they suffer from the following disadvantages: In most cases, mathematical formulations have to be simplified to get the solutions because of the extremely limited capability to solve real-world large scale power system problems. They are weak in handling qualitative constraints. They have poor convergence, may get stuck at local optimum, they can find only a single optimized solution in a single simulation run, they become too slow if number of variables are large and they are computationally expensive for solution of a large system. In contrast, metaheuristics approach problems differently. They employ strategies like randomness, iteration, and exploration to navigate solution spaces more effectively. Recently meta-heuristic optimization techniques were successfully used to solve the ORPD problem [37]. These metaheuristics don't guarantee an optimal solution but excel in finding good solutions.

2.2. Introduction

One of the most important conditions for economic and secure operation of electric power system is the optimal reactive power dispatch (ORPD). The optimal reactive power dispatch problem is a critical aspect of power system operation, focusing on the efficient control and management of reactive power in electrical grids. Reactive power is essential for voltage control and ensuring the reliability and stability of the power system. The goal of optimal reactive

power dispatch is to minimize system losses, improve voltage profiles, and enhance the overall system performance while meeting operational constraints. The ORPD is achieving by appropriate coordination of the equipment which manage the reactive power flows. The ORPD problem solution aims to minimize a chosen objective function, such as power losses (Ploss) or the total of voltage deviation (TVD), through optimal adjustment of the power system control variables, under specified active power outputs of all generators (except at the slack bus), while at the same time satisfying various operating constraints [3]. In the literature, many methods of solving the ORPD problem have been used up to date. At the beginning, several classical methods such as gradient based [4] [5], linear programming [6] [7], nonlinear programming [8] [9], quadratic programming [10], and interior point [11], were successfully used to solve this problem. However, these methods have some disadvantages in the process of solving the complex ORPD problem. The drawbacks of these algorithms are the premature convergence properties, the algorithmic complexity and the fact that solutions can be trapped in local minima [12]. In order to overcome these disadvantages, researchers have, in recent years, successfully applied evolutionary and meta-heuristic algorithms such as Genetic Algorithm (GA) [13], Differential Evolution (DE) [14], Evolutionary programming (EP) [15], Particle Swarm Optimization (PSO) [16] [17], Biogeography Based Optimization (BBO) [18], Gravitational Search Algorithm (GSA) [19] [20], Krill Herd Algorithm (KHA) [21] [22], Harmony Search Algorithm (HSA)[23], Teaching–Learning-Based Optimization [24], Differential Search Algorithm [25], Ant Colony Optimization Algorithm [26], Artificial Bee Colony Algorithm (ABC) [27] and Enhanced Marked Algorithm [28]. The main advantage of these methods compared to the classical (deterministic) optimization methods is that they are not limited with requirements for differentiability, nonconvexity, and continuity of the objective function or types of control variables. Moreover, these methods can be used for practical power systems taking into account various types of objective function and constraints. The essence of metaheuristic methods is iterative correction of solutions, i.e., generating new populations by applying stochastic search operators on individuals from the current population. The main performances of metaheuristics are fast search of large solution spaces, ability to find global solutions, and avoiding local optimum.

2.3. Reactive power

Reactive power is an electric power quantity that oscillates between the source and reactive components, like capacitors or inductors, in an alternating current (AC) circuit. Unlike active power (measured in watts), which performs useful work, reactive power (measured in volt-amperes reactive or VARs) doesn't perform any work but is crucial for maintaining voltage levels and enabling the operation of inductive and capacitive loads. In simple terms, reactive

power arises due to the phase difference between voltage and current in AC circuits. Inductive loads (like motors, transformers) cause the current to lag behind the voltage, creating reactive power in the form of magnetizing energy stored in the inductor. Capacitive loads (like capacitors) cause the current to lead the voltage, generating reactive power in the form of electric field energy stored in the capacitor. Utilities manage both active and reactive power in power grids to ensure efficient transmission and distribution of electricity, maintaining voltage stability and minimizing losses. Devices like capacitors and inductors are employed to regulate reactive power, improve power factor, and reduce wastage in electrical systems.

2.3.1. Importance of reactive power

Reactive power, while essential for the proper functioning of electrical systems, also comes with certain limitations and considerations:

- Increased Transmission Losses: Reactive power does not perform useful work but still needs to be generated, transmitted, and distributed. This process incurs losses in the power system, leading to inefficiencies in the transmission and distribution of electrical energy.
- Voltage Stability: Inadequate reactive power support can result in voltage fluctuations or drops in the electrical system. This instability can lead to equipment malfunction, reduced efficiency, and even system failures if not managed properly.
- Power Factor Issues: Low power factor, caused by excessive reactive power relative to active power, can increase the current needed to deliver a certain amount of power. This results in increased losses in transmission lines, reducing overall system efficiency.
- Equipment Overheating: Reactive power flows can cause additional current to flow through system components, leading to increased heating in transformers, motors, and other equipment. Over time, this can decrease equipment lifespan and efficiency.
- Additional Equipment Costs: Managing reactive power often requires additional equipment such as capacitors or synchronous condensers. Installing, maintaining, and operating these devices add to the overall cost of the electrical system.
- Grid Congestion: Inadequate reactive power management can lead to congestion in the grid, affecting the smooth transmission of electricity and potentially causing disruptions in power supply.

Efforts to address these limitations involve improving power factor, employing reactive power compensation devices, and implementing better grid management techniques to optimize reactive power flow and minimize its adverse effects on the electrical system.

2.3.2. Reactive power planning

Reactive power planning aims to enhance power system stability, efficiency, and reliability by effectively managing the flow of reactive power throughout power network, ensuring voltage levels are maintained within acceptable limits, and optimizing the utilization of reactive power resources. Reactive energy planning includes the following points

- Analyzing the system's needs by conducting studies and assessments to determine the required levels of reactive power support. This includes evaluating the system's power factor, voltage stability, and the demand for reactive power by various loads.
- Identifying and deploying sources of reactive power. These can include synchronous condensers, shunt capacitors, static VAR compensators (SVCs), static synchronous compensators (STATCOMs), and other devices capable of generating or absorbing reactive power.
- Determining the optimal locations and capacities for reactive power compensation devices within the electrical grid. Strategic placement ensures effective voltage support and power factor improvement across the system.
- Implementing control strategies and regulation mechanisms to manage the flow and distribution of reactive power. These strategies ensure that reactive power resources are utilized efficiently and dynamically to meet the system's changing demands.
- Using modeling and simulation tools to simulate different scenarios, assess the impact of reactive power support on the system, and optimize the deployment and operation of reactive power devices.
- Conducting cost-benefit evaluations to assess the economic implications of deploying reactive power resources. This includes considering the costs associated with installing and operating reactive power devices against the benefits derived from improved system performance and reduced losses.
- Ensuring compliance with regulatory standards and grid codes governing reactive power support, including requirements for voltage regulation, power factor correction, and system stability.
- Establishing maintenance schedules and monitoring protocols for reactive power devices to ensure their optimal performance and longevity.

By effectively planning and managing reactive power resources, utilities can enhance system stability, improve voltage regulation, optimize power factor, reduce losses, and ensure efficient operation of electrical systems.

2.3.3. Reactive power compensation

Reactive power compensation in electric transmission systems involves the deliberate adjustment of reactive power levels to enhance the efficiency, stability, and reliability of the power grid. This compensation is crucial for maintaining voltage levels, improving power factor, and minimizing losses in transmission lines. Here are the main methods of reactive power compensation:

- Capacitor Banks: Shunt capacitors are commonly used for reactive power compensation. These capacitors are connected in parallel with the transmission lines and supply reactive power to counteract the lagging effect caused by inductive loads. They improve the power factor by reducing the reactive power drawn from the system.
- Synchronous Condensers: These devices operate like rotating machines (similar to synchronous motors or generators) but operate without a mechanical load. Synchronous condensers provide or absorb reactive power as needed to regulate voltage and support the grid. They can rapidly supply or absorb reactive power, aiding in voltage control and stabilization.
- Static VAR Compensators (SVCs): SVCs are power electronics-based devices that provide fast and dynamic reactive power compensation. They can both generate and absorb reactive power rapidly, contributing to voltage control and stability. SVCs are capable of responding quickly to fluctuations in the grid and are often used in high-voltage transmission systems.
- Static Synchronous Compensators (STATCOMs): These are also power electronics-based devices used for reactive power compensation. STATCOMs offer rapid and precise control of reactive power, helping to stabilize voltage levels and support the grid during transient conditions.
- Line Reactors and Transformers: These components are designed to mitigate voltage fluctuations and harmonics caused by reactive power issues. They help regulate voltage and reduce losses in transmission lines.
- Dynamic Voltage Restorers (DVRs): DVRs are used to compensate for voltage sags or interruptions caused by reactive power imbalances. They inject reactive power into the system when needed to rapidly restore voltage to acceptable levels.

By employing these methods of reactive power compensation, utilities can optimize the power flow, improve voltage stability, enhance power quality, reduce losses, and ensure the efficient and reliable operation of electric transmission systems. The choice of compensation method depends on factors like grid requirements, load characteristics, and the specific needs of the transmission network.

2.4. Optimal Reactive Power Dispatch (ORPD)

Power systems are complex networks used for generating and transmitting electric power, which is expected to consume minimal resources while providing maximum security and reliability. One of the most important conditions for economic and secure operation of electric power system is the optimal reactive power dispatch (ORPD). The ORPD is achieving by appropriate coordination of the equipment which manage the reactive power flows. The ORPD is a specific optimal power flow (OPF) problem which is a major and powerful tool for operating and planning of power systems first formulated by Carpentier in 1960s. The ORPD has a significant influence on the secure and economic operation of power systems [3] . In the modern power system operation, each variation for demand-load, results a proper adjustment of reactive power generations for keeping the balance between supply and demand with minimum real power loss. Hence, the stability of electric grid is preserved. This is can be accomplished locally by proper reactive power management.

The objective of the ORPD in power system is generally to minimize active power losses and to improve the voltage profile by minimizing the load bus voltage deviation while satisfying a given set of operating and physical constraints. The objective can be achieved by providing optimal control variable settings such as generator bus voltages (continuous variable), tap changing transformers, and shunt capacitors/reactors (discrete variables). However, some authors include as objective function an additional improvement of voltage stability [24]. Other possible objective functions may be cost-based, which means to minimize the possible cost related with ORPD such as variable and fixed Var installation cost, real power loss cost, and fuel cost. It is also reasonable to use a multi-objective model as the goal of the ORPD formulation. Due to the presence of continuous and discrete control variables, ORPD becomes a complex combinatorial optimization problem involving non-linear functions having multiple local minima.

2.4.1. ORPD problem formulation

ORPD is a highly constrained non-linear optimization problem in which a specific objective function is to be minimized while satisfying a number of nonlinear equality and inequality constraints. The ORPD can be solved as a single objective as well as a multi objective optimization problem. The ORPD has commonly been formulated as a complicated constrained optimization problem. The general formulation of ORPD is:

$$\begin{cases} \min \boldsymbol{J}(\boldsymbol{x},\boldsymbol{u}) \ \boldsymbol{subject\ to} \\ \quad \mathbf{g}(\boldsymbol{x},\boldsymbol{u}) = \mathbf{0} \\ \quad \boldsymbol{h}(\boldsymbol{x},\boldsymbol{u}) \leq \mathbf{0} \end{cases} \tag{2. 1}$$

Where:

- *J(x,u)* is the objective function
- *g* and *h* are the set of equality and inequality constraints respectively.
- *x* is the state or dependent variables vector.
- *u* is the control or independent variables vector.

The elements of the state variables vector "*x*" are load buses voltage (V_L), generators reactive power output (Q_G) and lines apparent power flow (S_L). The control variables vector "*u*" includes the generation buses voltage (V_G), the transformer tap settings (*T*) and the shunt VAR compensators (Q_C)

2.4.1.1. *Objective functions*

In general, the possible objectives of ORPD problems are active the minimization of active power losses and the improvement of the voltage profile by minimizing the voltage deviation. In addition to that, it is also common to find as an objective function the improvement of the voltage stability index. However, some researchers also consider other objective functions such as the minimization of the investment cost of shunt compensation devices and the minimization of the fuel cost.

a. Minimization of total active power losses

The first objective to be minimized is the system transmission active power losses (P_{loss}). This objective function is expressed as follows [3].

$$\boldsymbol{J_1(x,u) = P_{loss} = \sum_{k=1}^{N_L} g_k(V_i^2 + V_j^2 - 2V_iV_jcos\theta_{ij})} \quad (2.2)$$

where:

- J_1 is the objective function
- P_{loss} is the total active loss of the system
- N_L is the number of transmission lines.
- V_i and V_j are the voltage magnitude at buses *i* and *j*, respectively.
- g_k is the conductance of branch *k* between buses *i* and *j*.
- θ_{ij} is the voltage angle difference between bus *i* and bus *j*.

The elements of the state variables vector "*x*" are load buses voltage (V_L), generators reactive power output (Q_G) and lines apparent power flow (S_L). The control variables vector "*u*" includes the generation buses voltage (V_G), the transformer tap settings (*T*) and the shunt VAR compensators (Q_C).

Accordingly, the *x* vector can be written as follows:

$$\boldsymbol{x^T = [V_{L_1} \dots V_{L_{N_{PQ}}}, Q_{G_1} \dots Q_{G_{N_G}}, S_{L_1} \dots S_{L_{N_L}}]} \quad (2.3)$$

where N_G is the number of generators; N_{PQ} is the number of PQ buses (load buses); The control variables vector u can be expressed as:

$$\boldsymbol{u^T = [V_{G_1} \dots V_{G_{N_G}}, T_1 \dots T_{N_T}, Q_{C_1} \dots Q_{C_{N_C}}]} \quad (2.4)$$

where:

- N_T is the number of tap regulating transformers.
- N_C is the number of shunt VAR compensations.

b. Voltage-Profile Improvement.

Another important objective of ORPD study is to regulate the voltage at each node/bus of power system. For stable operation of power system, the bus voltage in power system should be as smooth as possible. The degree of voltage regulation is computed through total of voltage deviation (TVD) which measures the bus voltage deviation from reference voltage (1.0 p.u) at each bus. The bus voltage is one of the most important security and service quality indices. Improving the voltage profile can be achieved by minimizing the total voltage deviation (TVD), which is modeled as follows [3] :

$$\boldsymbol{J_2(x,u) = SVD = \sum_{1}^{N_{PQ}} |V_{L_i} - V_{ref}|} \quad (2.5)$$

where:

- J_2 is the objective function.
- SVD is the total voltage deviation (TVD)
- V_{Li} is the voltage magnitude at load bus *i*.
- V_{ref} is the voltage reference value which is equal to 1 p.u.

c. Minimization of voltage stability index

The minimization of voltage stability index refers to the process of reducing or optimizing a metric associated with the stability of the electrical grid concerning voltage levels. Voltage stability is crucial in power systems to ensure a continuous and reliable electricity supply. Some authors include as an objective function the improvement of a voltage stability index. The operating interval of index L is set in [0, 1] [30]. The voltage stability index (VSI) is modeled as below [31].

$$\boldsymbol{F^{Lmax}} = \boldsymbol{min\ L_{max}} = \min [\mathbf{max}\, \boldsymbol{L_k}]\ \mathbf{k} \in \mathbf{N_L} \quad (2.6)$$

$$\boldsymbol{L_k} = \left| \mathbf{1} - \sum_{i=1}^{N_G} \boldsymbol{F_{ji}} \frac{\boldsymbol{V_i}}{\boldsymbol{V_j}} < \{\boldsymbol{\theta_{ij}} + (\boldsymbol{\delta_i} - \boldsymbol{\delta_j})\} \right| \quad (2.7)$$

$$\boldsymbol{F_{ji} = -[Y_{ij}]^{-1}[Y_{ij}]} \quad (2.8)$$

Where $\boldsymbol{F^{Lmax}}$ is the objective function, L_k is the voltage stability index (L-index) of buses; F_{ji} is the value of the element $ij^{th}$of the sub matrix obtained by the partial inversion of Y_{bus}; Y_{jj} is the admittance matrix of the j^{th} buses; Y_{ji} is the mutual admittance between the i^{th} and j^{th} buses; θ_{ij} is the phase angle of the term F_{ij}; δ_i, δ_j are the phase angle of the voltage in the i^{th} and j^{th} buses, respectively; N_G is the number of generation buses.

d. Minimization of VAR cost

Minimizing VAR (Volt-Ampere Reactive) cost involves optimizing the reactive power flow in an electrical grid while minimizing associated costs. Minimizing VAR cost is significant in power system management as it optimizes the reactive power flow, reduces operational expenses, and enhances the overall efficiency of the grid. It involves balancing the need for reactive power support with cost-effectiveness to maintain a stable and reliable power system. The cost of a reactive power source can be divided into two parts: fixed installation costs and operating costs. The fixed costs are mainly the sum of the capital and installation costs of the equipment. The variable costs consist of the cost of heating losses and maintenance costs, etc. However, operating costs can vary from year to year. A better formulation of the VAR costs minimization can be expressed as min ($F^{VARcost}$) [32].

$$\boldsymbol{F^{VARcost}} = \mathbf{C_0} + \mathbf{C_1}.\mathbf{Q_c} \qquad (2.\ 9)$$

Where C_0 is the fixed cost prorated per hour ($/hour), $C_1.Q_c$ is the variable cost ($/hour), C_1 is the operational cost of compensation device and Q_c is VAR source installments

e. Minimization of Fuel cost

The objective function in OPF incorporates the total fuel cost associated with generating electric power. It involves the cost of fuel consumed by each generator, considering their fuel types, efficiencies, and cost curves. The goal is to minimize the total cost of generating electricity. The fuel cost objective function is usually well-defined as the sum of the individual polynomial cost function of real power injections for each generator. It can be presented as [33]:

$$\boldsymbol{F^{fuelcost}} = \sum_{\boldsymbol{i=1}}^{\boldsymbol{N_g}} \left(\boldsymbol{a_i} + \boldsymbol{b_i P_{gi}} + \boldsymbol{c_i P_{gi}^2}\right) \qquad (2.\ 10)$$

Where $P_{gi}$is the active power generation at unit i, $a_i, b_i, and c_i$are the cost coefficients of the i^{th}generator, $N_g$is the number of thermal units

f. Multi-objective function

In the optimal power flow (OPF) problem, employing a multi-objective function allows for the consideration of multiple conflicting objectives simultaneously. It involves optimizing the power system while balancing various, sometimes conflicting, goals. In real world application, it usually contains simultaneous optimization of multiple-objectives, which generally conflict with each other. Multi-objective problems have a set of solutions, the reason for their optimality

is that no one can be considered to be better than any other towards all objective functions. In a multi-objective OPF, multiple objectives are considered, such as minimizing costs, minimizing emissions, minimizing active power losses, minimizing of total voltage deviation. etc. These objectives might conflict, for instance, minimizing costs might increase emissions. The multi-objective function aims to find trade-offs among these conflicting objectives. A general multi-objective optimization problem comprises a number of objectives that has to be optimized simultaneously and is connected with a number of equality and inequality constraints. It can be formulated as follows [34]:

$$\boldsymbol{Minimize\ F(X)\ =\ F1(X), F2(X), \ldots\ \ldots, Fn(X)} \qquad (2.\ 11)$$

subject to equality and inequality constraints.

where X is a determination vector that presents a solution, n is the number of objectives.

the number of equality and inequality constraint, respectively.

the aim objective of ORPD is to provide the system with efficient VAR compensation to allow the system to be operated under a correct balance between security and economic concerns. Generally, ORPD problem has been formulated as multi-objective optimization problem. Several methods have been presented to handle the multi-objective formulation of the ORPD problem. The most multi-objective methods for ORPD are:

- Weighted Sum Method: A common approach is to create a single aggregated objective by assigning weights to each objective and summing them. For instance, cost might be prioritized over emissions by assigning higher weight to cost in the combined objective function.
- Pareto-based Approaches: Using Pareto optimization, where solutions lie on the Pareto front, showing the best trade-offs between conflicting objectives without aggregating them into a single function.

2.4.1.2. *Problem Constraints*

These constraints are crucial in formulating the optimization problem for reactive power dispatch to ensure a solution that meets operational requirements while minimizing system losses and maintaining stability. Optimization algorithms and techniques are applied to find the optimal settings for controlling reactive power in the system while adhering to these constraints. In the optimal reactive power dispatch problem, several constraints need to be considered to ensure the efficient and reliable operation of the power system. Some of the key constraints include:

- Voltage Limits: Ensuring that the bus voltages are within acceptable limits to maintain system stability and prevent voltage collapse. Both upper and lower voltage limits at different buses in the network need to be considered.

- Reactive Power Limits: Limits on the reactive power generation at generator buses and other devices like shunt capacitors. These limits ensure that devices operate within their reactive power capability.
- Line Flow Limits: Constraints on power flow through transmission lines to prevent overloading and ensure that the power flow remains within the equipment's thermal and voltage limits.
- Transformer Tap Limits: Restrictions on the tap settings of transformers, which can influence the reactive power flow and voltage levels in the system.
- System Balance: Maintaining the overall balance between reactive power generation and consumption to ensure the system's stability and reliability.
- Operational Limits: Operational constraints, such as minimum and maximum control settings for devices like capacitors, reactors, and voltage regulators, need to be considered.

The ORPD constraints are divided into equality and inequality constraints [3].

a. Equality Constraints

These constraints reflect the physical laws governing the electrical system known as power flow equations. They are the expression of the balance between load demand (power loss included) and generated power. The power flow equations are given by:

$$P_{Gi} - P_{Di} - V_i \sum_{j=1}^{N_B} V_j (G_{ij} \cos\theta_{ij} + B_{ij} \sin\theta_{ij}) = 0 \quad (2.12)$$

$$Q_{Gi} - Q_{Di} - V_i \sum_{j=1}^{N_B} V_j (G_{ij} \sin\theta_{ij} - B_{ij} \cos\theta_{ij}) = 0 \quad (2.13)$$

where:

- P_{Gi}, Q_{Gi} are the respective active and reactive power of the i^{th} generator.
- P_{Di}, Q_{Di} are the respective active and reactive power demand at bus i.
- N_B is the total number of buses; B_{ij}, G_{ij} are real and imaginary parts of $(i,j)^{th}$ element of the bus admittance matrix.

b. Inequality Constraints.

The inequality constraints of the ORPD reflect the limits on physical devices in the power system as well as the limits created to ensure system security. This section delineates all the necessary inequality constraints needed for the ORPD implementation in this thesis. These inequality constraints are as follows.

- Inequality Constraints on Security Limits
    - Active power generated at slack bus

$$P_{G,slack}^{min} \leq P_{G,slack} \leq P_{G,slack}^{max} \quad (2.14)$$

- Load bus voltage

Voltage buses are restricted by lower and upper limits as follows.

$$V_{L_i}^{min} \leq V_{L_i} \leq V_{L_i}^{max} \quad i \in N_{PQ} \quad (2.15)$$

- Generated reactive power

Reactive power generated by each generator in an electrical system is restricted by lower and upper limits as shown in Eq. 2.16

$$Q_{Gi}^{min} \leq Q_{Gi} \leq Q_{Gi}^{max} \quad i \in N_G \quad (2.16)$$

- Thermal limits: the apparent power flowing in line "*L*" must not exceed the maximum allowable apparent power flow value (S_L^{max})

$$S_L \leq S_L^{max} \qquad L \in N_L \quad (2.17)$$

- Inequality Constraints on Control Variable Limits

The different control variables are bounded as follows:

- Generator voltage limits

$$V_{G_i}^{min} \leq V_{G_i} \leq V_{G_i}^{max} \quad i \in N_{PV} \quad (2.18)$$

- Transformer tap limits

Load tap changing transformers have a maximum and minimum tap ratio as shown in Eq. (2.19), which can be adjusted. The magnitude of the load tap changer is a discrete variable because the tap is changing with a certain increment. This increment depends on the size of the specified transformer.

$$T_i^{min,} \leq T_i \leq T_i^{max} \quad i \in N_T \quad (2.19)$$

- Shunt capacitor limits

All capacitors in a power system are used as reactive power suppliers. These capacitors are restricted by lower and upper reactive power limit as in Eq. (2.20). This limit will retain the amount of the exported reactive power into the power system as per the needs.

$$Q_{C_i}^{min} \leq Q_{C_i} \leq Q_{C_i}^{max} \quad i \in N_C \quad (2.20)$$

where:

$P_{G,\text{slack}}$ is the real power generation at slack bus.

V_{Gi} is the voltage magnitude at generator bus *i*.

T_i is the tap ratio of transformer *i*.

Q_{ci} is the reactive power compensation source at bus *i*.

N_{PQ} is the number of *PQ* bus.

$(.)^{max}$ and $(.)^{min}$ are the upper and lower the limits of the considered variables, respectively.

The objective functions, equality and inequality constraints are non-linear functions and they depend upon control variables. The equality constraints given by Equations (2.12) and (2.13) are met by solving the load-flow problem. The inequality constraints given by Equations (2.18)-(2.20) should be maintained during the solution evolution, while the inequality Equations (2.14)-(2.17) should be handled by additional techniques. The difficulty in adapting meta-heuristics mainly involves the question of how to preserve the feasibility of solutions during different iterations. A variety of approaches can be used to deal with feasibility in constrained non-linear optimization problems, which largely fall into two classes namely Penalty function approaches and Approaches preserving feasibility throughout evolutionary computation. Each method has its advantages and disadvantages. A penalty function approach is used in this paper due to its simplicity of implementation and its proven efficiency for many constrained non-linear optimization problems [35]. Conversely, feasibility preserving methods are highly time-consuming. To use a penalty function method, a penalty factor associated with each violated constraint is added to the objective function in order to penalize infeasible solutions [36]. Therefore, the optimum is found when all the constraints are respected and the objective function is minimized.

2.4.1.3. *Penalty function*

The most efficient and easiest way to handle constraints in optimization problems is by the use of penalty functions. The direction of the search process and thus, the quality of the optimal solution are hugely impacted by these functions. A suitable penalty function has to be chosen in order to solve a particular problem. The main goal of a penalty function is to maintain the systems security. These penalty functions are associated with numerous user defined coefficients which have to be rigorously tuned to suit the given problem. This research used a quadratic penalty function method in which a penalty term is added to the objective function for any violation of constraints. The inequality constraints which include the generator constraints, reactive compensation sources and transformer constraints are combined into the objective function as a penalty term, while the equality constraints and generator reactive power limits are satisfied by the Newton-Raphson load flow method. By adding the inequality constraints to the objective function $J(x,u)$ in Eq. (2.1). By using the concept of the penalty function method, the constrained optimization problem is transformed into an unconstrained optimization problem in which the augmented objective function becomes the new objective function to be minimized. The ORPD objective function is then modified as follows [18]:

$$F_T = J(x,u) + K_P\left(P_{G,slack} - P_{G,slack}^{lim}\right)^2 + K_V \sum_{i=1}^{N_{PQ}} \left(V_{L_i} - V_{L_i}^{lim}\right)^2 \qquad (2.\ 21)$$

$$+ K_Q \sum_{i=1}^{N_G} \left(Q_{Gi} - Q_{Gi}^{lim}\right)^2 + K_S \sum_{i=1}^{N_L} \left(S_{L_i} - S_{L_i}^{lim}\right)^2$$

Where:

- F_T is the new modified objective function;
- K_P, K_V, K_Q and K_S are the penalty factors of the slack bus generator, bus voltage limits, generator reactive power limits, and line flow limits, respectively.

$P_{G,slack}^{lim}$, $V_{L_i}^{lim}$, Q_{Gi}^{lim} and $S_{L_i}^{lim}$ are defined as follows:

$$P_{G,slack}^{lim} = \begin{cases} P_{G,slack}^{min} \; if \;\; P_{G,slack} < P_{G,slack}^{min} \\ P_{G,slack}^{max} \; if \;\; P_{G,slack} > P_{G,slack}^{max} \end{cases} \quad (2.\ 22)$$

$$V_{L_i}^{lim} = \begin{cases} V_{L_i}^{min} \; if \;\; V_{L_i} < V_{L_i}^{min} \\ V_{L_i}^{max} \; if \;\; V_{L_i} > V_{L_i}^{max} \end{cases} \quad (2.\ 23)$$

$$Q_{Gi}^{lim} = \begin{cases} Q_{Gi}^{min} \; if \;\; Q_{Gi} < Q_{Gi}^{lim} \\ Q_{Gi}^{max} \; if \;\; Q_{Gi} > Q_{Gi}^{max} \end{cases} \quad (2.\ 24)$$

$$S_{L_i}^{lim} = \begin{cases} S_{L_i}^{max} \; if \;\; S_{L_i} > S_{L_i}^{max} \\ 0 \quad\quad if \;\; S_{L_i} \leq S_{L_i}^{max} \end{cases} \quad (2.\ 25)$$

2.5. Metaheuristic optimizations

The word heuristics comes from the Greek word ‘‘heurisko’’ which means ‘‘to find,’’ ‘‘to know,’’ or ‘‘to guide an investigation.’’ It implies that heuristic algorithms are actually algorithms created by experimentation in order to obtain a satisfactory solution [38]. Heuristic algorithms are problem-solving techniques that prioritize finding a satisfactory solution quickly, even if it might not be the optimal or globally best solution. Heuristics is a set of rules based on experience which are used in solving a problem. These algorithms use a step-by-step approach, evaluating alternatives based on specific criteria without exhaustively exploring all possibilities. The disadvantage of heuristic methods is that there is no guarantee of optimality of the solution obtained. However, for complex optimization problems, the primary goal is to get a solution, regardless of its quality. When some solution exists, various techniques can be applied to improve its quality. In fact, this is the basic idea for building metaheuristic optimization methods [39]. Classical heuristic methods were mainly developed to solve some specific, individual problems using the familiar features of a given problem in solving it. In contrast, the metaheuristic optimization methods consist of general set of rules that can be applied to solve a variety of optimization problems. Many metaheuristic optimization methods have been developed by mimic of some well-known processes, primarily in biology, physics, society, and nature in general [39]. Metaheuristic algorithms are higher-level strategies used to efficiently explore and navigate solution spaces in search of near-optimal solutions for complex

optimization problems. They are more generalized and flexible compared to heuristics. Metaheuristics encompass a broad class of algorithms that guide the search through the solution space by combining and adapting various heuristic strategies. Metaheuristics are suitable for a wide range of problems and are not tied to specific domains. They aim to efficiently explore large solution spaces, often using stochastic or iterative methods to find approximate solutions. The principle of metaheuristics is to minimize or maximize an objective function. Their advantage is that they find a global minimum for a minimization problem and do not get stuck on a local minimum.

A metaheuristic algorithm must be characterized by two major features in order to guarantee the search for the global optimum. These two main characteristics are exploration and exploitation. Exploration is the ability to extend the search space, while exploitation is the ability to find optima around a good solution. The main difference between existing metaheuristics is the way in which they try to strike a balance between exploration and exploitation. Metaheuristic optimization methods can be classified according to different criteria. A fundamental classification of metaheuristic optimization methods is based on the number of solutions in an iteration. According to this criterion, metaheuristic methods can be classified as follows [40]:

1. Single-solution-based metaheuristics, also called trajectory methods, such as simulated annealing (SA), tabu search (TS), greedy randomized adaptive search procedure, variable neighborhood search, guided local search, and iterated local search.
2. Population-based metaheuristics, such as genetic algorithm (GA), particle swarm optimization (PSO), gravitational search algorithm (GSA), and many others.

We can find other criteria for classifying metaheuristics, as we will see below.

2.5.1. Classification of metaheuristic algorithms

Metaheuristic algorithms encompass a wide range of optimization strategies that efficiently explore solution spaces to find near-optimal solutions. These algorithms are classified into different categories based on their underlying principles and characteristics. Some common classifications include:

2.5.1.1. *Single-Solution Metaheuristics:*

Single-solution metaheuristics are optimization algorithms that operate on a single candidate solution at a time, exploring and iteratively improving this solution to find near-optimal solutions in complex problem spaces. Unlike population-based algorithms that maintain and evolve a population of solutions, single-solution metaheuristics focus on refining a single solution through iterations. Some prominent single-solution metaheuristics include:

- Simulated Annealing (SA): Inspired by the annealing process in metallurgy, this algorithm probabilistically accepts worse solutions to escape local optima, gradually reducing exploration.
- Tabu Search (TS): Focuses on exploring the neighborhood of solutions while maintaining a memory structure to avoid revisiting previously explored areas.
- Variable Neighborhood Search (VNS): Uses multiple neighborhood structures to explore the solution space, shifting between different neighborhoods to diversify the search.

2.5.1.2. *Population-Based Algorithms:*

Population-based algorithms are a category of optimization techniques that operate on a population of potential solutions to iteratively evolve and search for optimal or near-optimal solutions within a given problem space. These algorithms maintain a population of candidate solutions and use various mechanisms to update, evaluate, and evolve this population across iterations. Some prominent population-based algorithms include:

- Genetic Algorithms (GAs): Evolutionary algorithms that use concepts like crossover, mutation, and selection to evolve a population of candidate solutions toward optimal or near-optimal solutions.
- Particle Swarm Optimization (PSO): Individuals (particles) within a swarm move through the solution space, adjusting their positions based on their own experience and the best experiences of the entire swarm.
- Differential Evolution (DE): An evolutionary algorithm that manipulates a population of candidate solutions to create new solutions using differences between randomly chosen individuals.

2.5.1.3. *Nature-Inspired Metaheuristics:*

Nature-inspired metaheuristics draw inspiration from natural phenomena or processes to develop optimization algorithms that mimic the behaviors observed in nature. These algorithms explore solution spaces and find near-optimal solutions by leveraging concepts from biology, physics, and social behavior. Here are some prominent nature-inspired metaheuristics:

- Evolutionary Algorithms: Algorithms inspired by biological evolution, like Genetic Algorithms (GAs), Evolution Strategies (ES), and Genetic Programming (GP). They use concepts such as mutation, selection, and recombination to evolve solutions.
- Swarm Intelligence: Algorithms based on the collective behavior of swarms or groups, such as Particle Swarm Optimization (PSO), Ant Colony Optimization (ACO), and Bee Colony Optimization (BCO). These algorithms simulate social behaviors like cooperation and communication among individuals.

- Artificial Immune Systems (AIS): Inspired by the human immune system, these algorithms mimic immune system processes like recognition, memory, and learning to solve optimization problems.

2.5.1.4. *Hybrid and Memetic Algorithms:*

Hybrid and memetic algorithms are optimization approaches that combine multiple techniques, to leverage their respective strengths and overcome limitations. They merge different optimization paradigms to enhance the search capability and improve the quality of solutions for complex problems. Their adaptability and ability to combine diverse strategies make them powerful tools for solving real-world problems.

- Hybrid Metaheuristics: Combine different metaheuristic techniques or integrate metaheuristics with other optimization methods like mathematical programming, local search, or machine learning algorithms.
- Memetic Algorithms: Blend evolutionary algorithms with local search methods, allowing for the exploitation of promising regions discovered by evolutionary processes.

2.5.2. Population-based metaheuristics

Population-based metaheuristics are a class of optimization algorithms inspired by natural processes like evolution, swarm behavior, and social interactions. They're designed to find high-quality solutions to optimization problems where finding an exact solution is impractical due to the problem's complexity. In the population-based metaheuristic optimization algorithms, the population is defined by a set of individuals (agents) which represent potential solutions of the optimization problem. The number of agents (N) is named as the size of the population. In general, an agent can be represented as vector whose elements are the values of the control variables of the optimization problem. The number of control variables (n) is the search space dimension of the optimization problem. The efficiency and performance of metaheuristic optimization methods are dependent on the proper setting of the corresponding algorithmic parameters. Their effectiveness often lies in their ability to strike a balance between exploring the search space widely and exploiting promising regions to converge toward optimal or near-optimal solutions, especially in complex, high-dimensional, and non-linear problem spaces. Moreover, these methods can be used for practical optimization problems taking into account various types of objective function and constraints. In recent years, various population-based metaheuristic optimization methods listed in Figure 2.1 have been proposed for solving the different problems. The basic elements of metaheuristic optimization methods can be defined as follows*:*

$x(t)$: is a candidate solution represented by an n-dimensional vector, where n is the number of control variables.

X: Space of possible solutions. It is an n-dimensional solution space which is defined by lower and upper limits of control variables.

Fitness is a direct metric of the performance of the individual population member (agent). The fitness of each agent of the population is calculated from the value of the function being optimized.

General structure of the metaheuristic optimization methods can be represented as follows:

Initialization

1. Defining the objective function *F(*x*)* and the space of possible solutions *X*;

2. Generate initial population of *N* agents

Usually, the initial positions of each agent are randomly selected between minimum and maximum values of the control variables.

Iterative procedure

3. Calculate the fitness value *F(*x*)* for each agent x in the current population

4. Generate new population by applying the algorithmic operators on search agents from the current population.

5. Repeat the iterative procedure until the stop criteria is reached.

6. The optimal solution x* is determined.

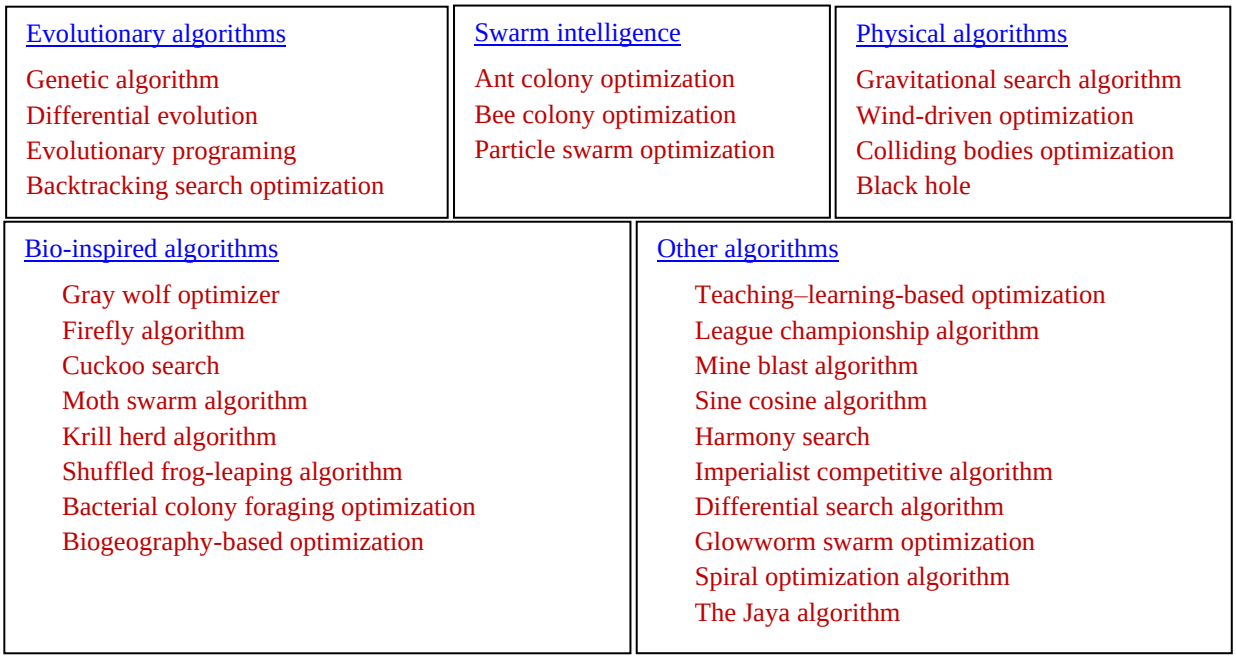

Figure 2.1. Population based-Metaheuristic classifications.

2.5.3. Summary of some popular metaheuristic optimization algorithms

2.5.3.1. *Genetic algorithm*

Genetic algorithms are search and optimization algorithms inspired by the process of natural selection and genetics. They are used to solve complex problems by mimicking the principles of evolution and natural selection. The basic idea behind genetic algorithms is to create a

population of candidate solutions, represented as a set of strings or "chromosomes." Each chromosome encodes a potential solution to the problem at hand. The chromosomes undergo a series of operations analogous to the processes of reproduction and evolution, such as selection, crossover, and mutation. [13]

2.5.3.2. *Differential evolution*

Differential Evolution (DE) is an evolutionary optimization algorithm that is particularly effective for solving continuous and global optimization problems. It was introduced by Rainer Storn and Kenneth Price in 1997. The main idea behind Differential Evolution is to maintain a population of candidate solutions (vectors) and use a combination of mutation, crossover, and selection operations to iteratively improve the population and search for the optimal solution. DE operates directly on the real-valued parameter space, making it suitable for problems with continuous variables. [14]

2.5.3.3. *Evolutionary programing*

Evolutionary Programming (EP) is an evolutionary computation technique that focuses on the evolution of computer programs or algorithms to solve complex problems. It was developed by Lawrence J. Fogel in the 1960s. In EP, a population of computer programs, often represented as strings of instructions or code, is evolved through a process of mutation, crossover, and selection. The goal is to optimize the behavior of the programs to solve a specific problem or perform a desired task. [41]

2.5.3.4. *Backtracking search optimization algorithm*

The Backtracking Search Optimization Algorithm (BSA) is a metaheuristic optimization algorithm that was introduced by Xin-She Yang in 2010. It is inspired by the process of backtracking, which is commonly used in problem-solving to find a solution by systematically exploring different paths. BSA is a population-based algorithm that aims to find the global optimum of a given problem by iteratively improving a set of candidate solutions. It combines local search with a backtracking mechanism to efficiently explore the search space and converge towards the optimal solution. The Backtracking Search Optimization Algorithm combines the exploitation capability of local search with the exploration capability of backtracking. This combination allows the algorithm to efficiently search the solution space, escape from local optima, and converge towards the global optimum. [42]

2.5.3.5. *Particle swarm optimization*

Particle Swarm Optimization (PSO) is a population-based optimization algorithm that was inspired by the collective behavior of bird flocking or fish schooling. It was first proposed by James Kennedy and Russell Eberhart in 1995. In PSO, a population of candidate solutions,

called particles, moves through the search space to find the optimal solution. Each particle represents a potential solution and keeps track of its position and velocity in the search space. The particles adjust their positions based on their own experience and the experience of the best-performing particle in the population. [12]

2.5.3.6. *Ant colony optimization*

Ant Colony Optimization (ACO) is a metaheuristic optimization algorithm that is inspired by the foraging behavior of ants. It was first introduced by Marco Dorigo in the early 1990s and has since been widely used to solve combinatorial optimization problems. ACO is particularly effective in solving problems that involve finding optimal paths or tours, such as the traveling salesman problem (TSP) or vehicle routing problem (VRP). The algorithm mimics the behavior of ants, which communicate with each other through pheromone trails to collectively find the shortest path between their nest and food sources. [26]

2.5.3.7. *Artificial bee colony*

The Artificial Bee Colony (ABC) algorithm is a population-based optimization algorithm inspired by the foraging behavior of honey bees. It was introduced by Dervis Karaboga in 2005. ABC aims to solve optimization problems by simulating the food foraging behavior of bees. In the ABC algorithm, the population is represented by a group of artificial bees. Each bee can be in one of three roles: employed bee, onlooker bee, or scout bee. These roles simulate different behaviors of bees in a real hive. [27]

2.5.3.8. *Gravitational search algorithm*

The Gravitational Search Algorithm (GSA) is a metaheuristic optimization algorithm inspired by the laws of gravity and motion. It was proposed by Esmat Rashedi, Hossein Nezamabadi-pour, and Saeid Saryazdi in 2009. GSA models the optimization problem as a system of masses interacting through gravitational forces. In the GSA algorithm, candidate solutions are represented as particles in a search space, and the optimization process mimics the gravitational interaction between these particles. The algorithm iteratively updates the positions and masses of the particles to find the optimal solution [43].

2.5.3.9. *Colliding bodies optimization*

The Colliding Bodies Optimization (CBO) algorithm is a metaheuristic optimization algorithm inspired by the physical phenomenon of colliding bodies. It was proposed by Zong Woo Geem in 2006 to solve optimization problems. In the CBO algorithm, candidate solutions are represented as particles in a search space, and the optimization process simulates the interaction and collision between these particles. The algorithm iteratively updates the positions and

velocities of the particles to converge towards the optimal solution.[44]

2.5.3.10. *Black hole algorithm*

The Black Hole Algorithm (BHA) is a metaheuristic optimization algorithm inspired by the behavior of black holes in the universe. It was proposed by Mirjalili, and Andrew Lewis in 2016. BHA aims to solve optimization problems by simulating the gravitational interactions of black holes and their influence on particles. In the BHA algorithm, candidate solutions are represented as particles, and their movements are influenced by the gravitational force of black holes. The algorithm iteratively updates the positions and velocities of the particles to search for the optimal solution. [45]

2.5.3.11. *Gray wolf optimizer*

The Gray Wolf Optimizer (GWO) is a metaheuristic optimization algorithm inspired by the social hierarchy and hunting behavior of gray wolves. It was proposed by Seyedali Mirjalili and Andrew Lewis in 2014. GWO aims to solve optimization problems by simulating the social interactions and hunting strategies of gray wolves. In the GWO algorithm, candidate solutions are represented as gray wolves, and their movements are influenced by the hierarchical structure and coordination within the wolf pack. The algorithm iteratively updates the positions of the wolves to search for the optimal solution. [46]

2.5.3.12. *Firefly algorithm*

The Firefly Algorithm (FA) is a metaheuristic optimization algorithm inspired by the flashing behavior of fireflies. It was proposed by Xin-She Yang in 2008. The algorithm aims to solve optimization problems by simulating the attractiveness and movement of fireflies. In the FA algorithm, candidate solutions are represented as fireflies, and their movements are influenced by the attractiveness of other fireflies. The algorithm iteratively updates the positions of the fireflies to search for the optimal solution. [47]

2.5.3.13. *Cuckoo search algorithm*

The Cuckoo Search Algorithm (CSA) is a metaheuristic optimization algorithm inspired by the behavior of cuckoo birds and their reproductive strategy known as brood parasitism. It was proposed by Xin-She Yang and Suash Deb in 2009. CSA aims to solve optimization problems by simulating the searching and breeding behaviors of cuckoos. In the CSA algorithm, candidate solutions are represented as cuckoos' eggs, and their movements are influenced by the fitness and diversity of the eggs in the population. The algorithm iteratively updates the positions of the eggs to search for the optimal solution. [48]

2.5.3.14. *Moth swarm algorithm*

The Moth Swarm Algorithm (MSA) is a metaheuristic optimization algorithm inspired by the behavior of moths, specifically their movements towards artificial light sources. It was proposed by Xin-She Yang and Suash Deb in 2010. MSA aims to solve optimization problems by simulating the attraction and movement of moths towards light sources. In the MSA algorithm, candidate solutions are represented as moths, and their movements are influenced by the brightness and distance to light sources. The algorithm iteratively updates the positions of the moths to search for the optimal solution. [49]

2.5.3.15. *Krill herd algorithm*

The Krill Herd Algorithm (KHA) is a metaheuristic optimization algorithm inspired by the collective behavior of krill swarms. It was proposed by Xin-She Yang and Suash Deb in 2010. KHA aims to solve optimization problems by simulating the movement and foraging behavior of krill in search of food. In the KHA algorithm, candidate solutions are represented as krill, and their movements are influenced by the feeding behavior of krill in response to food concentration and social interactions. The algorithm iteratively updates the positions of the krill to search for the optimal solution. [50]

2.5.3.16. *Shuffled frog-leaping algorithm*

The Shuffled Frog-Leaping Algorithm (SFLA) is a metaheuristic optimization algorithm inspired by the behavior of frogs and their ability to leap and communicate with each other to find food. It was proposed by Xin-She Yang in 2010. SFLA aims to solve optimization problems by simulating the leaping and sharing of information among frogs. In the SFLA algorithm, candidate solutions are represented as frogs, and their movements and interactions are influenced by the quality of the solutions and the information exchange among frogs. The algorithm iteratively updates the positions of the frogs to search for the optimal solution [51].

2.5.3.17. *Bacterial colony foraging optimization*

Bacterial Colony Foraging Optimization (BCFO) is a swarm intelligence-based optimization algorithm inspired by the foraging behavior of bacterial colonies. It was proposed by Daeshik Kang and Jong-Hwan Kim in 2009. BCFO aims to solve optimization problems by simulating the foraging and communication behavior of bacterial colonies in search of nutrients. In the BCFO algorithm, candidate solutions are represented as bacterial colonies, and their movements and interactions are influenced by the concentration of nutrients and the communication among colonies. The algorithm iteratively updates the positions of the colonies to search for the optimal solution [52].

2.5.3.18. *Biogeography-based optimization*

Biogeography-based optimization (BBO) is a nature-inspired optimization algorithm that is based on the principles of biogeography, which is the study of the distribution of species in different geographic regions. It was proposed by Dan Simon in 2008. BBO aims to solve optimization problems by simulating the migration and evolution of species across habitats. In the BBO algorithm, candidate solutions are represented as species, and their movements and interactions are influenced by the migration rates and exchange of information among species. The algorithm iteratively updates the positions of the species to search for the optimal solution [18].

2.5.3.19. *Teaching–learning-based optimization*

Teaching-Learning-Based Optimization (TLBO) is a population-based optimization algorithm inspired by the teaching-learning process in classrooms. It was proposed by Rao et al. in 2011. TLBO aims to solve optimization problems by simulating the teaching and learning interactions among individuals in a population. In the TLBO algorithm, candidate solutions are represented as individuals, and their movements and interactions are influenced by the teaching and learning processes. The algorithm iteratively updates the positions of the individuals to search for the optimal solution [36].

2.5.3.20. *League championship algorithm*

I apologize for the confusion in my previous response. The League Championship Algorithm (LCA) is a metaheuristic algorithm that was proposed by Alba et al. in 2013. LCA is inspired by the concept of sports league championships, where teams compete against each other to achieve the best possible ranking. The League Championship Algorithm aims to solve optimization problems by emulating the competition and ranking dynamics observed in sports leagues. It uses a population-based approach where candidate solutions, representing individuals or teams, compete against each other to improve their rankings [53] .

2.5.3.21. *Mine blast algorithm*

The Mine Blast Algorithm (MBA) is a nature-inspired optimization algorithm that was introduced by Zong Woo Geem in 2011. It is inspired by the blast effect of a mine explosion, where the explosion force is used as an analogy for the optimization process. The Mine Blast Algorithm aims to solve optimization problems by simulating the process of mine explosion and subsequent energy propagation. It is particularly suitable for solving continuous optimization problems [54].

2.5.3.22. *Sine cosine algorithm*

The Sine Cosine Algorithm (SCA) is a population-based optimization algorithm inspired by the sine and cosine functions. It was proposed by Seyedali Mirjalili in 2016 as a simple and efficient

algorithm for solving optimization problems. The Sine Cosine Algorithm aims to find the optimal solution by simulating the sine and cosine functions to update the positions of individuals in the population. It is a metaheuristic algorithm that can be applied to both continuous and discrete optimization problems [55].

2.5.3.23. *Harmony search*

The Harmony Search Algorithm (HSA) is a population-based metaheuristic optimization algorithm inspired by the musical improvisation process. It was proposed by Zong Woo Geem, Joong Hoon Kim, and G.V. Loganathan in 2001. The HSA mimics the process by which musicians improvise harmonies to find an optimal solution to an optimization problem. The Harmony Search Algorithm aims to find the best solution by simulating the improvisation of musical harmonies. It is particularly suitable for solving continuous optimization problems, but it can also be adapted for discrete and combinatorial problems [23].

2.5.3.24. *Imperialist competitive algorithm*

The Imperialist Competitive Algorithm (ICA) is a population-based optimization algorithm inspired by the concept of imperialism and competition among empires. It was proposed by Atashpaz-Gargari and Lucas in 2007 as a metaheuristic algorithm to solve optimization problems. The Imperialist Competitive Algorithm aims to find the optimal solution by simulating the process of imperialism, colonization, and competition. It is particularly suitable for solving continuous optimization problems, but it can also be adapted for discrete and combinatorial problems [56].

2.5.3.25. *Differential search algorithm*

I apologize for the confusion, but there is no widely known optimization algorithm called the "Differential Search Algorithm." It is possible that you may be referring to the Differential Evolution (DE) algorithm, which is a popular population-based optimization algorithm. Differential Evolution (DE) is a stochastic and evolutionary optimization algorithm that was introduced by Rainer Storn and Kenneth Price in 1997. DE is widely used for solving continuous optimization problems and has been applied to various domains [57].

2.5.3.26. *Glowworm swarm optimization*

Glowworm Swarm Optimization (GSO) is a population-based optimization algorithm inspired by the behavior of glowworms. It was proposed by Krishnanand and Ghose in 2005 as a metaheuristic algorithm to solve optimization problems. The Glowworm Swarm Optimization algorithm aims to find the optimal solution by simulating the behavior of glowworms in attracting and repelling each other based on their brightness. GSO is particularly suitable for solving optimization problems with multiple optima or in dynamic environments [58].

2.5.3.27. *Spiral optimization algorithm*

The Spiral Optimization Algorithm (SOA) is a population-based optimization algorithm inspired by the natural spiral patterns observed in various phenomena. It was proposed by Tuba and Yel in 2012 as a metaheuristic algorithm to solve optimization problems. The Spiral Optimization Algorithm aims to find the optimal solution by simulating the spiral movement observed in nature. SOA is particularly suitable for solving continuous optimization problems and has been applied to various domains [59].

2.5.3.28. *The Jaya algorithm*

The Jaya algorithm is a population-based optimization algorithm introduced by R. V. Rao in 2016. Jaya stands for "Jaya Algorithm for Optimization Inspired by the Nature of Optimization." It is a simple and efficient algorithm designed to solve optimization problems. The Jaya algorithm is inspired by the concept of cooperation and improvement in human society. It aims to improve the fitness of the entire population by encouraging cooperation between individuals and promoting the sharing of information [60].

2.5.3.29. *Whale Optimization Algorithm*

The Whale Optimization Algorithm (WOA) is a nature-inspired metaheuristic optimization algorithm that is based on the social behavior of humpback whales. It was developed by Seyedali Mirjalili in 2016 and is used to solve optimization problems. The algorithm mimics the social behavior of humpback whales, specifically their hunting strategy where they cooperate to encircle prey. In the WOA, potential solutions to an optimization problem are represented as individual whales in a population [61].

2.5.3.30. *Simulated Annealing*

Simulated Annealing (SA) is a probabilistic metaheuristic algorithm used to find the approximate global optimum in a large search space. It is inspired by the annealing process in metallurgy, where metals are heated and then slowly cooled to reach a low-energy crystalline state. This concept is adapted to solve optimization problems [62] .

2.5.3.31. *Water Cycle Algorithm*

The Water Cycle Algorithm (WCA) is a relatively new nature-inspired optimization algorithm inspired by the water cycle process in nature. Developed by Seyedali Mirjalili and Arash Mirjalili in 2016, this algorithm aims to solve optimization problems by mimicking the movement and behaviors of water molecules in the water cycle. The water cycle involves processes like evaporation, condensation, precipitation, and runoff. The WCA simulates these processes to explore the solution space and find optimal solutions in a similar manner [63].

2.5.3.32. *Artificial Hummingbird Algorithm.*

The Artificial Hummingbird Algorithm (AHA) is a nature-inspired optimization algorithm developed based on the foraging behavior of hummingbirds. This algorithm mimics the movement patterns and search strategies observed in hummingbirds when they forage for nectar, aiming to solve optimization problems efficiently [64] .

2.5.4. Literature of metaheuristic optimization algorithms-based ORPD.

Since ORPD is a very important aspect of power system operation and is a non-linear, non-convex optimization problem with both continuous and discrete control variables, various metaheuristic optimization algorithms have been attempted to solve it. The two most predominant and efficient classes of metaheuristic optimization algorithms are evolutionary algorithms and population-based algorithms. Table 2.1 summarizes some of the metaheuristics that have attempted to solve the ORPD problem using specified objective functions.

Table 2.1. Some metaheuristic algorithms applied to the ORPD problem

Methods	Authors	Ref	Objective function
HSA	A.H. Khazali, M. Kalantar	[23]	Ploss, Lmax, VPI
PSO	M.A. Abido	[12]	Fuel cost, VPI
FAPSO	Wen Zhang, Yutian Liu	[65]	Ploss, TVD, VPI
GA	D. Devaraj, J. Preetha Roselyn	[31]	VPI
SPEA2	Houssem Ben Aribia et al	[66]	Ploss, fuelcost, TVD
DE- ABC	Yuancheng Li et al	[67]	Ploss
ABC	M. Rezaei Adaryani, A. Karami	[68]	Ploss, VPI, Lmax,
GA	Ulas Kılıç	[69]	Ploss
CPVEIHBMO	Ali Ghasemi et al	[70]	Ploss, TVD, Lmax
FSSPSO	Marcela Martinez-Rojas et al	[71]	Ploss
CLPSO	K. Mahadevan, P.S. Kannan	[9]	Ploss, Lmax, VPI
GA	S.Durairaj, P.S.Kannan, et al	[72]	Ploss, VPI
GSA	R. Suresh et al	[73]	Ploss, TVD
DE	A.A. Abou El Ela et al	[14]	Ploss, Lmax, VPI
DE	M. Aradarajan, K.S. Swarup	[74]	Ploss
PPSO	Ying Li et al	[75]	Ploss
EGA–DQLF	M. SailajaKumari et al	[76]	Ploss, fuelcost, Lmax
HSA	K. Lenin	[77]	Ploss, TVD
GA	D. Devaraj	[78]	Ploss, Lmax
OGSA	Binod Shaw	[79]	Ploss, TVD, Lmax
TS	M. A. Abido	[80]	fuelcost
DE	M. Abdelmoumene et al	[81]	Ploss, VPI
SARGA	P.Subbaraj, P.N. Rajnarayananb	[82]	Ploss
BBO	P.K. Roy et al	[29]	Ploss, TVD
SPEA	M.A. Abido, J.M. Bakhashwain	[83]	Ploss, TVD
PSO	Pathak Smita, B.N.Vaidya	[84]	Qloss
SOA	ChaohuaDai et al	[85]	Ploss, Lmax, TVD
BB-BC	R.Suresh et al	[86]	Ploss, TVD
MASRL	Y. Xu et al	[87]	Ploss
WCA	A. A. Heidari et al	[88]	Ploss
MICA-IWO	M. Ghasemi et al	[89]	Ploss
ACO	Abou El-Ela AA et al	[26]	Ploss

ACO	K. Rayudu et al	[90]	TVD
PSO-TVAC	Medani KBO, Sayah S	[91]	Ploss
DMSDE	X. Zhang et al	[92]	Ploss
QOTLBO	B. Mandal, P.K. Roy	[24]	Ploss, TVD, Lmax
BBO	Aniruddha Bhattacharya et al	[18]	Ploss
MAPSO	B. Zhao et al	[3]	Ploss
GSA	S. Duman et al	[19]	Ploss, TVD, Lmax
MOAIA	H. Xiong, H. Cheng, H. Li	[93]	Ploss, TVD, Lmax
BFO	M. Tripathy, S. Mishra	[94]	Ploss, TVD
GBTLBO	M. Ghasemi et al	[95]	Ploss
OSAMGSA	Niknam et al	[20]	Ploss, TVD, Lmax
SA	Raha et al	[96]	Ploss
CSA	Sulaiman et al	[97]	Ploss
CSA	Raha, S.B et al	[98]	Ploss
MODE	Basu. M	[99]	Ploss, TVD, Lmax
FA-APT-FPSO	M.N. Gilvaei et al	[100]	Ploss, TVD, Lmax
EPSDE	L. Titare et al	[101]	Lmax
DE	Kumar SKN, Renuga P	[102]	Ploss, VAR cost
DEPSO	M.Vishnu, Sunil Kumar T. K	[103]	Ploss, TVD
APO–PSO	Tawfiq M. Aljohani et al	[104]	Ploss, TVD, Lmax
PSO-TS	Z. Sahli et al	[105]	Ploss, TVD
GAFGP	BijayBaran Pal et al	[106]	Ploss, Lmax, VPI
ABC	Essam A. Al-Ammar et al	[107]	Ploss, TVD
ECOA	Amlak Abaza et al	[108]	Ploss, TVD
GWO-PSO	Mohamed A.M. Shaheen et al	[109]	Ploss, TVD
FAHCLPSO	Naderi, E et al	[110]	Ploss, TVD
ICAPSO	Mehdinejad. M et al	[111]	Ploss, VD
HGAPSO	Lenin. K et al	[112]	Ploss, Lmax
ESPSO	Yapıcı. H et al	[113]	Ploss
DSPSO	Subbaraj. P et al	[114]	Ploss

2.6. Conclusion.

This chapter first presented the importance of reactive energy, its planning and compensation. Afterwards, a survey related to Optimal Reactive Power Dispatch problem has been presented. However, the chapter has described the following:

- Definition of ORPD problem and its important role in power system field.
- ORPD problem formulation, including the common objective functions of power system, control variables and operating constraints.
- The conventional methods that have been employed to solve ORPD problem.
- The metaheuristic optimization techniques that have been applied for ORPD. In addition. metaheuristic algorithms are classified into different categories based on their underlying principles and characteristics.
- A summarize of some metaheuristics that have attempted to solve the ORPD problem using specified objective functions.

However, the metaheuristic techniques have a superiority than the conventional techniques due

to the following merits:

These methods can be applied in both small and large-scale systems.

High reliability to obtain the optimal solutions.

These methods rarely suffer from stagnations or trapped in local minima solutions.

These methods converged rapidly to the optimal solution compared with conventional methods.

Chapter 3

ORPD PROBLEM BASED BIO-INSPIRED OPTIMIZATION ALGORITHMS

3.1. Introduction.

Meta-heuristics are powerful computational methods used to solve complex problems, often in fields such as optimization, operations research and artificial intelligence. Rather than following a strict algorithmic scheme, these techniques adopt a heuristic approach, seeking solutions intelligently and iteratively, often inspired by natural phenomena or optimization processes observed in various fields. These approaches are particularly effective for exploring vast search spaces, enabling solutions close to the optimum, or even the optimum itself. What makes meta-heuristics so attractive is their ability to adapt to different types of problem, even in the absence of detailed information about the structure of the problem itself. Although they do not always guarantee the best possible solution, meta-heuristics often offer very competitive results and are widely used to solve real problems in a variety of contexts. This ability to efficiently explore complex search spaces makes them a major area of research and application in computer science and engineering. The problem of the Optimal Reactive Power Dispatch (ORPD) is one of the problems that researchers have used meta-heuristics to solve. These kinds of methods offer powerful approaches to solve this type of optimization problem. In order to find the algorithm best suited to a particular problem, such as ORPD in our case, it may be a good idea to experiment with several meta-heuristics and compare their performance. Recently, bioinspired algorithms have received a great deal of attention. These algorithms transfer the biological activities of living organism algorithms into mathematical models, such as PSO, ant colony optimization, artificial bee colony, cuckoo search and others, in an optimized manner. In this chapter, we have used a number of bioinspired algorithms. We will describe the proposed algorithms in detail presenting their applications on a different IEEE test system (from the smallest to the largest), as well as a comparison of their results with each other and with those of other optimization methods presented in the literature. The methods used are MFO (Moth Flame Optimization), GWO (Grey Wolf Optimizer), AHA (Artificial Hummingbird Algorithm) and ALO (Ant Lion optimization).

3.2. Description of the bio-inspired algorithms

Nature is the best teacher and its designs and capabilities are extremely huge and mysterious, so researchers try to imitate nature in technology. Nature and technology have a much stronger link, as it seems entirely reasonable that new or persistent problems in computing may have

much in common with problems that nature encountered and solved long ago. Bio-inspired algorithms are computational techniques that draw inspiration from biological systems, or behaviors observed in nature to solve complex optimization and computational problems. These algorithms simulate the mechanisms found in natural systems to efficiently search for solutions in various domains. Bio inspired computing has come up as a new era in computing encompassing a wide range of applications, covering all most all areas including computer networks, security, robotics, bio medical engineering, control systems, power systems and many more [115]. Here are descriptions of the bio-inspired algorithms used in this study.

3.3. The proposed bio-inspired algorithms

3.3.1. Moth Flame Optimization algorithm (MFO)

The MFO (Moth Flame Optimization) algorithm is a recently developed meta-heuristic based on the behavior of moths attracted by the light of a flame. This approach seeks to optimize solutions by imitating the movement of moths attracted by a light source. Proposed by Seyedali Mirjalili [49], MFO algorithm is based on the simulation of the behavior of moths for their special navigation methods in night. The special navigation technique used by moths to travel at night called transverse orientation. The idea of transverse orientation is by maintaining a fixed angle of natural light such as the moon, which is a very effective mechanism for travelling long distance in a straight path because the moon is far away from the moth (Figure 3.1-a). As the moon is too far away, it remains stationary and provides a fixed point of reference for the moths to navigate in a straight line. However, with the advent of lamps, moths become disorientated and mistake the lamp light for an artificial moon. They try to keep a constant distance from it and end up circling the artificial light because it is too close (Figure 3.1-b). In MFO algorithm the Moths fly around flames in a Logarithmic spiral way and finally converges towards the flame.

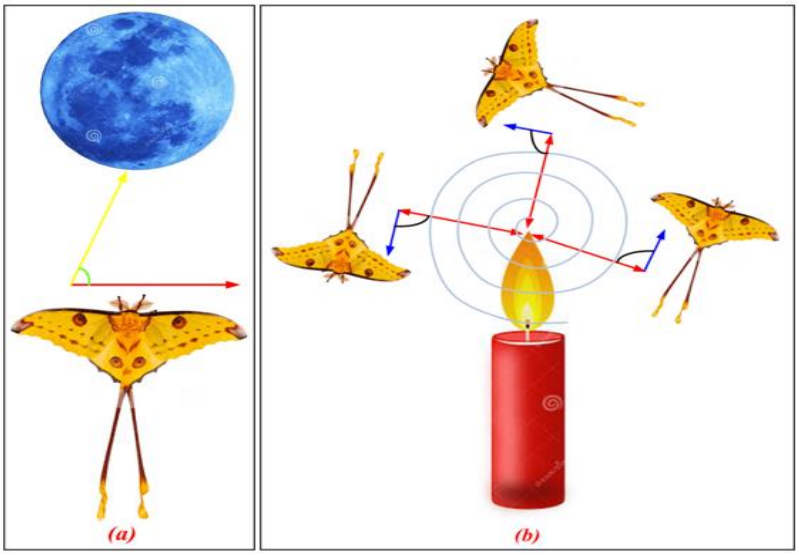

Figure 3.1. Moth movement mechanism [116]

In the MFO algorithm, each moth must move around a single corresponding flame, which allows better exploration of the search space and a lower probability of stagnation of local optima. Therefore, a set of flame locations can be represented in a matrix with the same dimensions as the moth positions. In addition, it should be noted that moths and flames are both solutions. The difference between them is the way they are processed and updated at each iteration. Moths are true search agents that move around the search space. Meanwhile, the flames are the best solutions obtained by the moths so far. In other words, the flames can be seen as flags or pins dropped by the moths as they explore a search space. Each moth searches around a flame and updates it if a better solution is found. With this mechanism, a moth never loses its best solution. In basic MFO, the individual moth represents a potential solution, and each position is expressed as a matrix of control variables given below [117].

$$\boldsymbol{M} = \begin{bmatrix} \boldsymbol{m_{1,1}} & \boldsymbol{m_{1,2}} & \cdots \boldsymbol{m_{1,d}} \\ \boldsymbol{m_{2,1}} & \boldsymbol{m_{2,2}} & \cdots \boldsymbol{m_{2,d}} \\ \vdots & \ddots & \vdots \\ \boldsymbol{m_{n,1}} & \boldsymbol{m_{n,2}} & \cdots \boldsymbol{m_{n,d}} \end{bmatrix} \tag{3. 1}$$

where n is the number of moths and d is the number of variables. The fitness values sorting can be given by the following array:

$$\boldsymbol{OM} = \begin{bmatrix} \boldsymbol{OM_1} \\ \boldsymbol{OM_2} \\ \vdots \\ \boldsymbol{OM_n} \end{bmatrix} \tag{3. 2}$$

The fitness value is the return value of each moth where all moths are passed through the fitness function. The output of the fitness function is identical to its fitness value in OM array. A basic matrix of MFO is represented by flames. Flames matrix can be described as follows:

$$\boldsymbol{F} = \begin{bmatrix} \boldsymbol{F_{1,1}} & \boldsymbol{F_{1,2}} & \cdots \boldsymbol{F_{1,d}} \\ \boldsymbol{F_{2,1}} & \boldsymbol{F_{2,2}} & \cdots \boldsymbol{F_{2,d}} \\ \vdots & \ddots & \vdots \\ \boldsymbol{F_{n,1}} & \boldsymbol{F_{n,2}} & \cdots \boldsymbol{F_{n,d}} \end{bmatrix} \tag{3. 3}$$

Dimension of moth's matrix is equal to the dimension of flames matrix. The fitness values of flames can be sorted in the following array:

$$\boldsymbol{OF} = \begin{bmatrix} \boldsymbol{OF_1} \\ \boldsymbol{OF_2} \\ \vdots \\ \boldsymbol{OF_n} \end{bmatrix} \tag{3. 4}$$

It is worth mentioning that both of moths and flames are solutions. It is possible to recognize the difference between them when analyzing the way to treat and update moths and flame positions during running process. Moths are the search agents seek for best position, while flames are the flags or the best position of moths. The mathematical equation represents the

movement of moths with respect to flame position, which can be formulated as follows [118]:

$$\boldsymbol{M_i = S\left(M_i, F_j\right)}. \tag{3. 5}$$

where M_i $i$ndicates the ith moth, F_j indicates the jth flame, and S is the spiral function.

In MFO algorithm, the movement of moths proceeds as logarithmic spiral function to update the position of each moth with respect to flame; any spiral movement should satisfy the following conditions: • Spiral movement starts from moth. • Spiral movement ending at flame position. • Domain of spiral movement is restricted by search space. MFO logarithmic spiral function can be given by the following equation:

$$\boldsymbol{S\left(M_i, F_j\right) = D_i \cdot e^{bt} \cdot cos(2\pi t) + F_j} \tag{3. 6}$$

$\boldsymbol{D_i}$ is the distance of the i-th moth for the jth flame, b is a constant that assigns the shape of spiral algorithm, t is a random number that lies in between [-1, 1]. The distance $\boldsymbol{D_i}$ can be calculated from the following equation:

$$\boldsymbol{D_i = \left|F_j - M_i\right|}. \tag{3. 7}$$

The lower the value of t, the closer the distance between the ith moth and the jth flame. Figure 3.2 depicts the spiral flight of a moth around its corresponding flame. If moths were required to move around N different flames all the time, this would deteriorate the exploitation of the best solution. To resolve this problem, the number of flames is adaptively decreased over the iterations as Eq. (3.8). After the reduction in the number of flames in each generation, the corresponding moth updates its position according to the worst flame position.

$$\boldsymbol{Flame\ number\ = round\left(N - l * \frac{N-1}{T}\right)} \tag{3. 8}$$

where l is the current iteration, N is the maximum number of flames, and T indicates the maximum number of iterations. The adaptive mechanism for the flame number provides an efficient balance between the exploration and exploitation in a solution space.

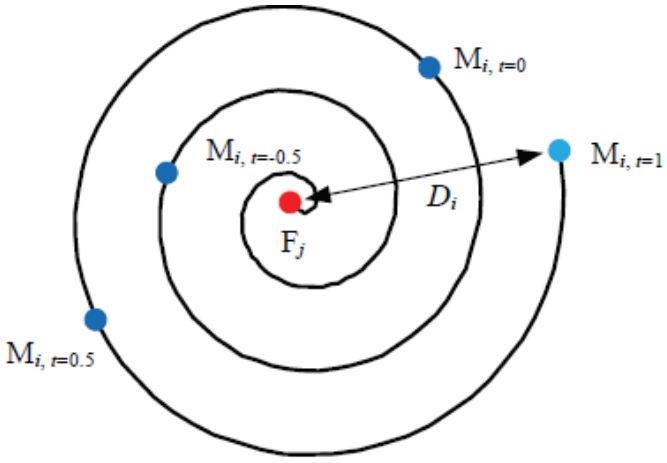

Figure 3.2. Spiral flight of a moth around its corresponding flame [118].

The main optimization steps of the MFO algorithm are illustrated on the flowchart below (Figure 3.3).

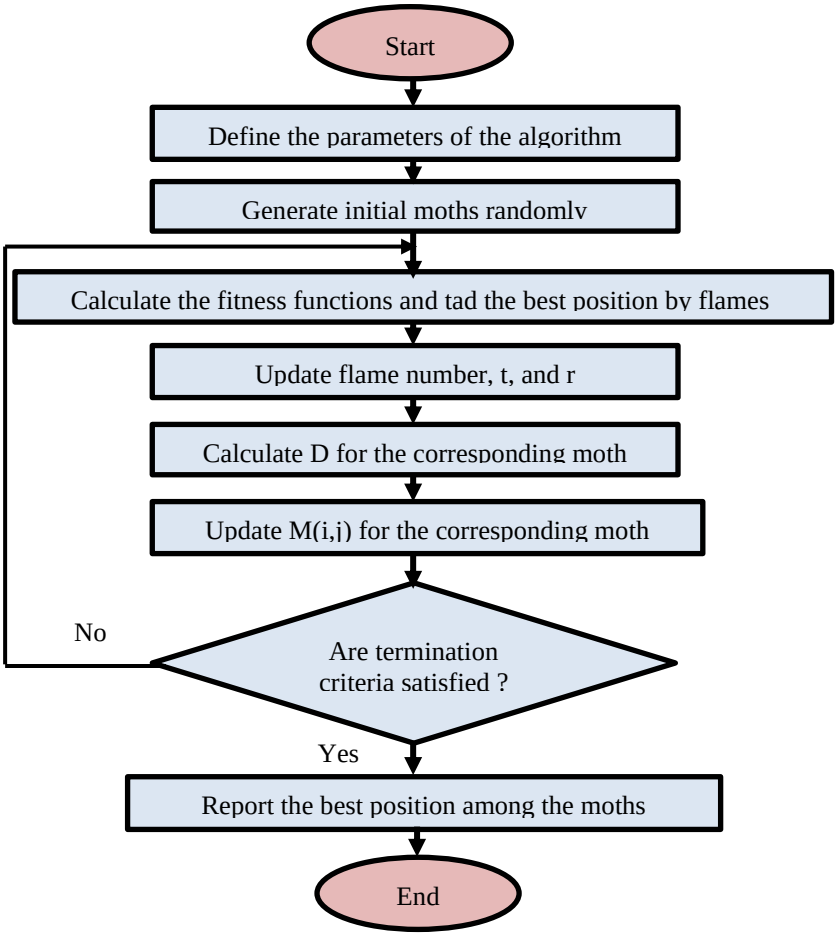

Figure 3.3. flowchart of MFO algorithm

3.3.2. Ant Lion Optimization Algorithm (ALO)

The ALO algorithm is modeled based on the hunting mechanism of Antlions in nature. The ALO algorithm simulates the interaction between antlions (predators) and ants (prey). In their larval period (2.5-3 years), antlions usually eat ants. Antlion digs a hole with a cone shape using its jaw. Then it hides in the bottom of the cone and waits. when an ant trap into the hole, it begins throwing sand towards the trap in order to bury the prey. After catching the prey and consumed it, Antlion throw the prey' leftover outside the trap as illustrated in Figure 3.5. Figure 3.4. illustrates different steps that describe the relationship between antlions and ants [119].

Figure 3.4. Different steps that describe the relationship between antlions and ants [119]

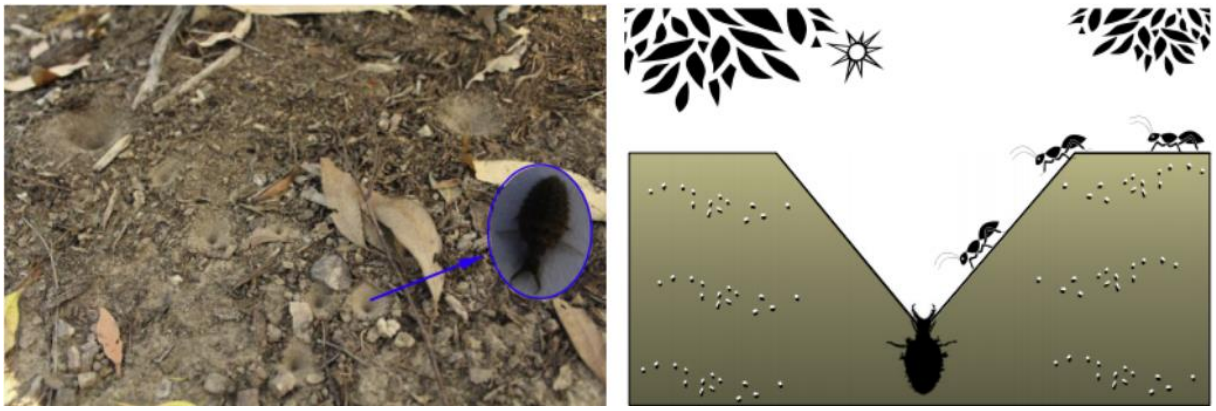

Figure 3.5. Cone-shaped traps and hunting behavior of antlions [119]

The ALO method mimics interaction between antlions and ants in the trap. To simulate these interactions, ants must to move over the search space, and antlions are allowed to hunt them and become fitter using traps. Since ants move stochastically in nature when searching for food like all other insects in nature (Figure 3.5), a random walk is chosen for modelling ants' movement as follows [119]:

$$\boldsymbol{X(t) = [0, cumsu(2r(t_1) - 1), cumsu(2r(t_2) - 1), \ldots\ldots, cumsu(2r(t_n) - 1)]} \quad (3.\ 9)$$

Where $X(t)$ is the random walks of ants, *cumsu* calculates the cumulative sum, n is the max_iterations, t_i is the step of random walk, and $\mathrm{r}(t_i)$ is a function defined as follows:

$$\mathbf{r}(\boldsymbol{t_i}) = \begin{cases} \mathbf{1} & \boldsymbol{if\ rand\ > 0,5} \\ \mathbf{0} & \boldsymbol{if\ rand\ < 0,5} \end{cases} \quad (3.\ 10)$$

where, rand is a randomly generated number uniformly distributed in the range of [0, 1].

The following steps describe the five main phases in hunting technique of ant lions.

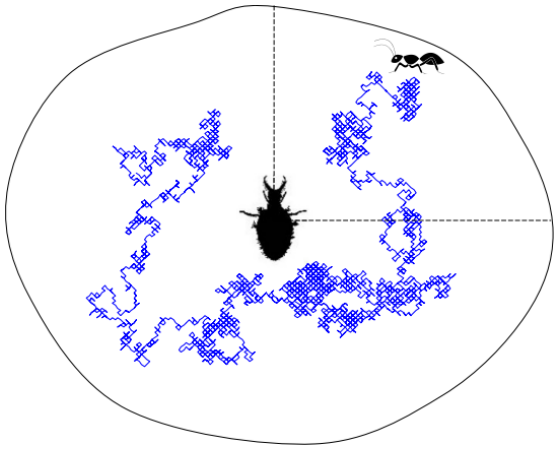

Figure 3.6. Random walk of an ant inside an antlion's trap **[119]**

In every step of optimization, ants update their positions to a random walk search (equation 3.9). To ensure that all the positions of ants are inside the boundary of the search space, they are normalized by using the following expression:

$$\boldsymbol{X_i^t = \frac{(X_i^t - a_i) \times (d_i^t - c_i^t)}{(b_i - a_i)} + c_i^t} \quad (3.\ 11)$$

Where a_i, b_i are respectively the minimum and maximum of random walk corresponding of i^{th} variable. c_i^t, d_i^t indicate respectively the minimum and maximum of i^{th} variable at the t^{th} iteration.

random walks of ants are affected by antlions' traps. In order to mathematically model this assumption, the following equations are proposed:

$$\boldsymbol{c_i^t = Antlion_j^t + c^t} \quad (3.\ 12)$$

$$\boldsymbol{d_i^t = Antlion_j^t + d^t} \quad (3.\ 13)$$

where c^t is the minimum of all variables at t^{th} iteration, d^t indicates the vector including the maximum of all variables at t^{th} iteration and $Antlion_j^t$ shows the position of the selected j^{th} antlion at t^{th} iteration.

Equations (3.12) and (3.13) show that ants randomly walk in a hyper sphere defined by the vectors c and d around a selected antlion. Figure 3.6 shows a two-dimensional search space. It may be observed that ants are required to move within a hypersphere around a selected antlion. During optimization, The ALO algorithm is required to use a roulette wheel operator for selecting Antlions based on their fitness for giving a high chance for catching ants.

With the mechanisms proposed so far, Antlions are capable to build traps proportional to their fitness, and ants are required to move randomly near the center of the pit. However, once Antlions realize that an ant is in the trap, they shoot sands outwards the center of the pit. This proposed mechanism is mathematically modeled as it follows:

$$\boldsymbol{c^t = \frac{c^t}{I}} \quad (3.\ 14)$$

$$\boldsymbol{d^t = \frac{d^t}{I}} \quad (3.\ 15)$$

I is a ratio, given by $I = 10^{\omega \frac{t}{T}}$, t is the current iteration T is the maximum number of iterations and ω is a constant defined as it follows:

$$\boldsymbol{\omega = \begin{cases} 2 \text{ if } 0.1T < t \leq 0.5T \\ 3 \text{ if } 0.5T < t \leq 0.75T \\ 4 \text{ if } 0.75T < t \leq 0.9T \\ 5 \text{ if } 0.9T < t \leq 0.95T \\ 6 \text{ if } t > 0.95T \end{cases}} \quad (3.\ 16)$$

The ants catching by predator and pit rebuilding in order to catch new prey are described by the following equation.

$$\boldsymbol{Antlion_j^t = Ant_i^t, if\ f(Ant_i^t) > f\left(Antlion_j^t\right)} \quad (3.\ 17)$$

where $Antlion_j^t$ is the j^{th} position of the selected antlion at iteration *t* and Ant_i^t is the position of the selected i^{th} ant at iteration *t*.

Elitism is one of the most important characteristics of evolutionary algorithms. In ALO algorithm, at any iteration the best antlion obtained (solution) is saved as elite. Since the elite is the fittest antlion which is able to guide the movements of the remaining ants along the iterations. The elitism mechanism mathematically described as follows.

$$\boldsymbol{Ant_i^t = \frac{R_A^t + R_E^t}{2}} \tag{3. 18}$$

where R_A^t is the random walk around the ant-lion selected by the roulette wheel at t^{th} iteration, R_E^t is the random walk around the elite at t^{th} iteration, and Ant_i^t denote the position of i^{th} ant at t^{th} iteration.

The main optimization steps of the ALO algorithm are shown in Fig 3.7.

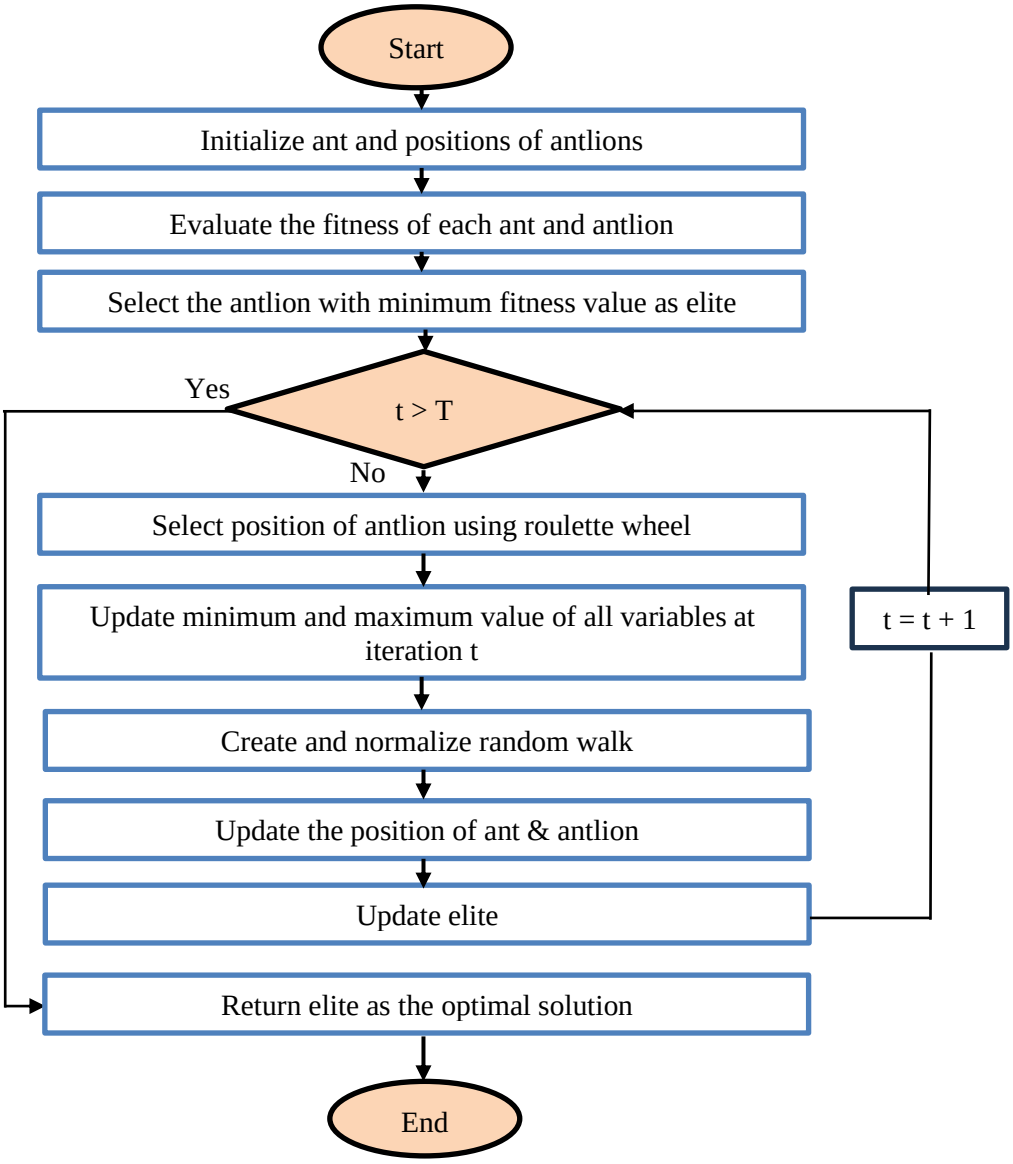

Figure 3.7. Flowchart of ALO algorithm

3.3.3. Grey Wolf Optimizer algorithm (GWO)

GWO is a nature-inspired optimization algorithm inspired from the real life of an organized group of Grey Wolf by analyzing their behavior and communication for hunting in nature. Naturally, grey wolves live in a group of between 5 to 12 individuals. Grey wolves sternly live in a social hierarchy. In the GWO to solve the optimization issues, the behavior of grey wolves for hunting is modelled. The social hierarchy of grey wolves consists of 4 categories alpha, beta, omega, and delta. The group is guided by a special leader, called alphas. The main task of the alphas is to make the most powerful decisions for hunting, choosing location for sleeping, to safe the group. A second category named betas works in coordination with the first group, agents from this sub group help the leader (alpha) in decision making to achieve the desired objectives of the pack. So, the knowledge of leader is improved by the feedback transferred from associated agents of this second category. Delta agent's category, have to achieve many tasks such as: scouts, sentinels, elders and hunters. They have to communicate their ideas to alpha and beta to guarantee the safety of the pack. Wolves within this category called also subordinate. The omega is the lowest ranking Grey Wolf in the pack, they are the last wolves that are allowed to eat. The omega plays role of scapegoat, the wolves of this category always have to submit to all the other individuals from dominant category [46]. The hierarchy structure of Grey Wolf is shown in Figure 3.8.

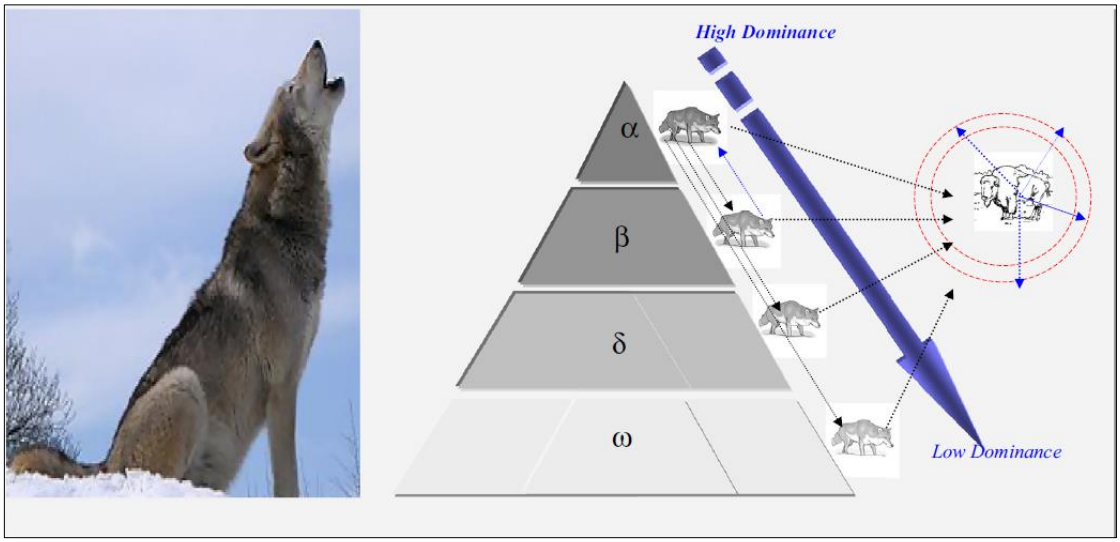

Figure 3.8. Hierarchy structure of Grey Wolf **[120]**

Besides the social hierarchy that exists in a group of grey wolves, collective hunting is another fascinating communal behavior of grey wolves. The grey wolves' hunting includes the steps represented in Figure 3.9.

For mathematical modeling of the algorithm, the best solution is considered as alpha (α). Then

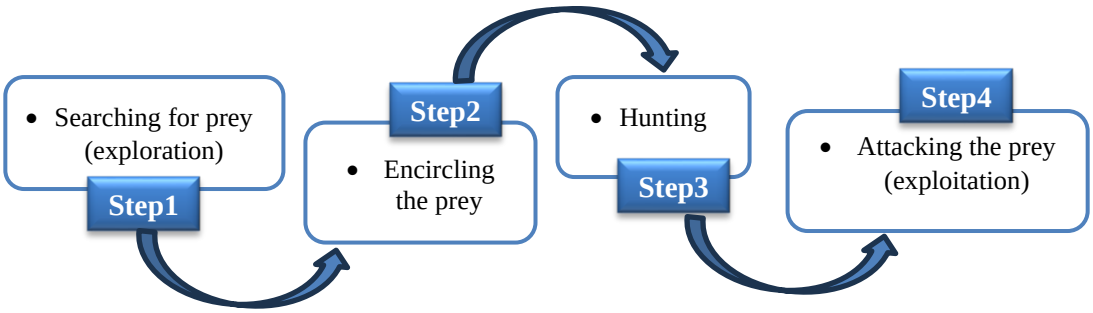

Figure 3.9. Grey Wolf Hunting process

beta (β), delta (δ) and omega (ω) are given priority respectively. During hunt the grey wolves encircle prey. The encircling behavior is modeled and described using the following equations [120]:

$$\vec{D} = \left|\vec{C} \cdot \vec{X}_p\,(t) - \vec{X}(t)\right| \quad (3.\ 19)$$

$$\vec{X}(t+1) = \left|\vec{X}_p\,(t) - \vec{A} \cdot \vec{D}\right| \quad (3.\ 20)$$

Where t indicates the current iteration, $\vec{A}$ and $\vec{C}$ are coefficient vectors, $\vec{X}_p$ is the position vector of the prey, and $\vec{X}$ indicates the position vector of a Grey Wolf. The two vectors $\vec{A}$ and $\vec{C}$ are calculated as follows:

$$\vec{A} = 2\vec{a} \cdot \vec{r}_1 - \vec{a} \quad (3.\ 21)$$

$$\vec{C} = 2 \cdot \vec{r}_2 \quad (3.\ 22)$$

where components of $\vec{a}$ are linearly decreased from 2 to 0 over the iterations, $\vec{r}_1$ and $\vec{r}_2$ are random vectors in [0, 1].

The location of prey is formulated by the combination of the best knowledge given by alpha and beta during the hunting process. The identification of the best location of the prey is based on the best solutions achieved during search process [46]. The basic equations describing and guiding the hunting process are formulated as follows:

$$\overrightarrow{D_\alpha} = \overrightarrow{C_1}.\overrightarrow{X_\alpha} - \vec{X} \quad (3.\ 23)$$

$$\overrightarrow{D_\beta} = \overrightarrow{C_2}.\overrightarrow{X_\beta} - \vec{X} \quad (3.\ 24)$$

$$\overrightarrow{D_\delta} = \overrightarrow{C_3}.\overrightarrow{X_\delta} - \vec{X} \quad (3.\ 25)$$

$$\vec{X}_1 = \vec{X}_\alpha - \vec{A}_1 \cdot \vec{D}_\alpha \quad (3.\ 26)$$

$$\vec{X}_2 = \vec{X}_\beta - \vec{A}_2 \cdot \vec{D}_\beta \quad (3.\ 27)$$

$$\vec{X}_3 = \vec{X}_\delta - \vec{A}_3 \cdot \vec{D}_\delta \quad (3.\ 28)$$

$$\vec{X}(t+1) = \frac{\vec{X}_1 + \vec{X}_2 + \vec{X}_3}{3} \quad (3.\ 29)$$

where $\vec{X}(t+1)$ is the position vector of prey at iteration ($t+1$), this position is updated based on the best information given by alpha, beta and delta agents during process search. Figure 3.11 shows how the search agent updates its position to match alpha, beta, and delta positions. Afterward, alpha, beta, and delta assess the hunt position, and the other wolves randomly update their positions around the hunt. This cycle repeats until the desired outcome is reached [46]. The main optimization steps of the GWO algorithm are shown in Fig 3.10.

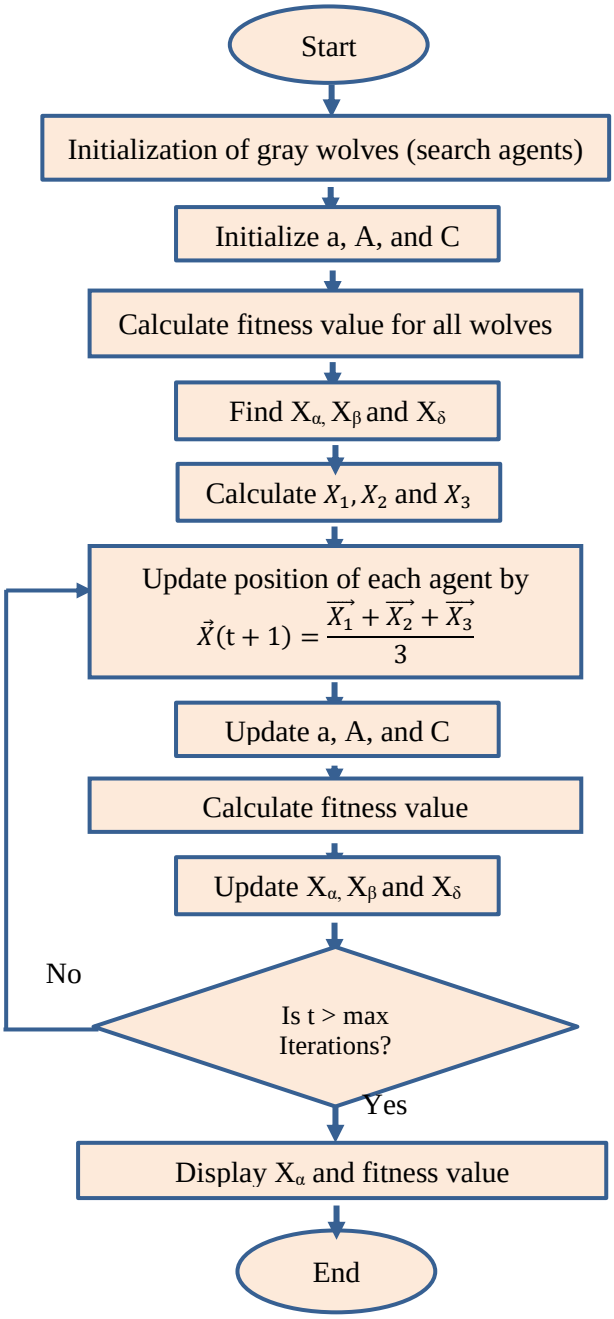

Figure 3.10. Flowchart of GWO algorithm

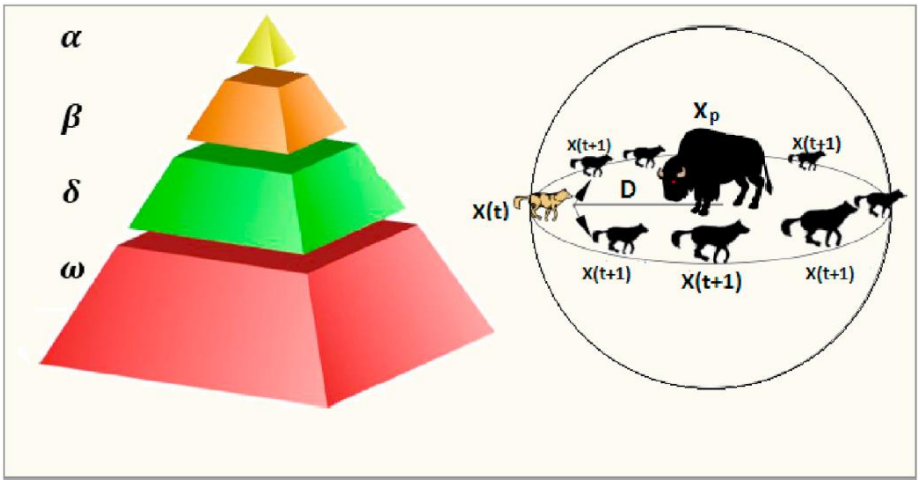

Figure 3.11. The update steps for Grey Wolves Position [121]

3.3.4. Artificial Hummingbird Algorithm (AHA)

The Hummingbird Optimizer algorithm is a nature-inspired optimization algorithm that is based on the behavior of hummingbirds. There are over 360 different hummingbird species in the globe, and the majority of them only have a 7.5 to 13 cm body length. Hummingbirds may beat their wings up to 80 times per second, which is the greatest rate of any bird. Hummingbirds consume a lot of flower nectar found inside flowers each day to provide them the energy they need to soar (Figure 3.12). Hummingbirds are unique in that they have a remarkable memory of finding food. The bird can also remember the spatial-temporal information about the food sources and use this information to avoid flowers (food sources), which were visited previously [122]. Hummingbirds have three special flight skills and three intelligently adjusted foraging strategies.

Figure 3.12. A foraging hummingbird **[64]**

The main inspirations behind AHA algorithm to solve optimization problems are the flight skills, memory capacity, and foraging strategies of hummingbirds. In the process of foraging, hummingbirds have three special flight skills: axial, diagonal, and omnidirectional flight.

Figure 3.13 describes the three flight behaviors in three-dimensional space. Figure 3.13(a) shows axial flight, in which the hummingbird can choose to fly in an arbitrary direction. Figure 3.13(b) reflects diagonal flight, in which the hummingbird can fly from any angle of the coordinate axis to its diagonal position. Figure 3.13(c) demonstrates omnidirectional flight, in which the hummingbird can fly in any direction [123].

Hummingbirds have also other sorts of search tactics, such as guided, migrating, and territorial foraging. These three foraging behaviors are depicted in Figure 3.14. Hummingbird tends to visit the food source with the highest nectar-refilling rate among the food sources with the same highest visit level. Each hummingbird is able to find its target food source via the visit table [64].

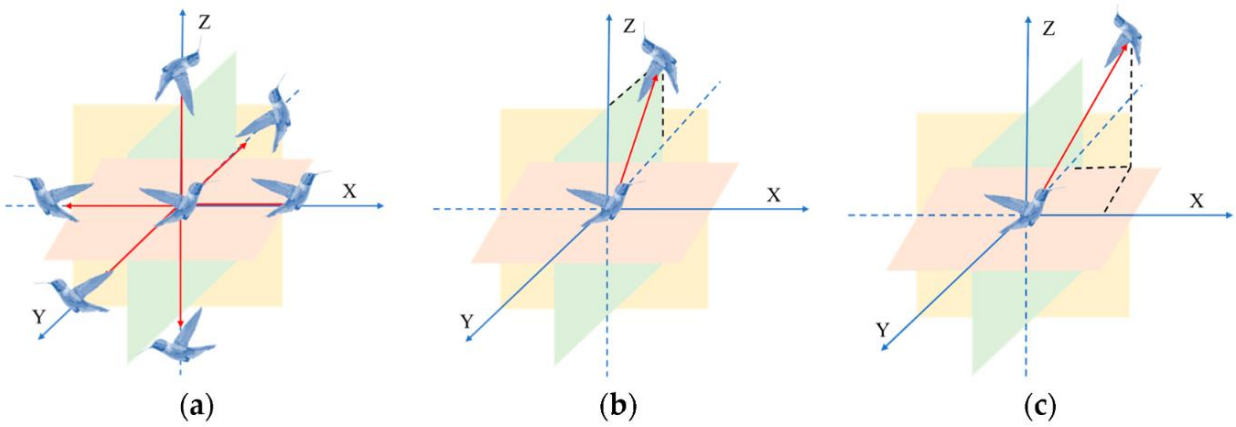

Figure 3.13. The special flight abilities of hummingbirds **[123]**

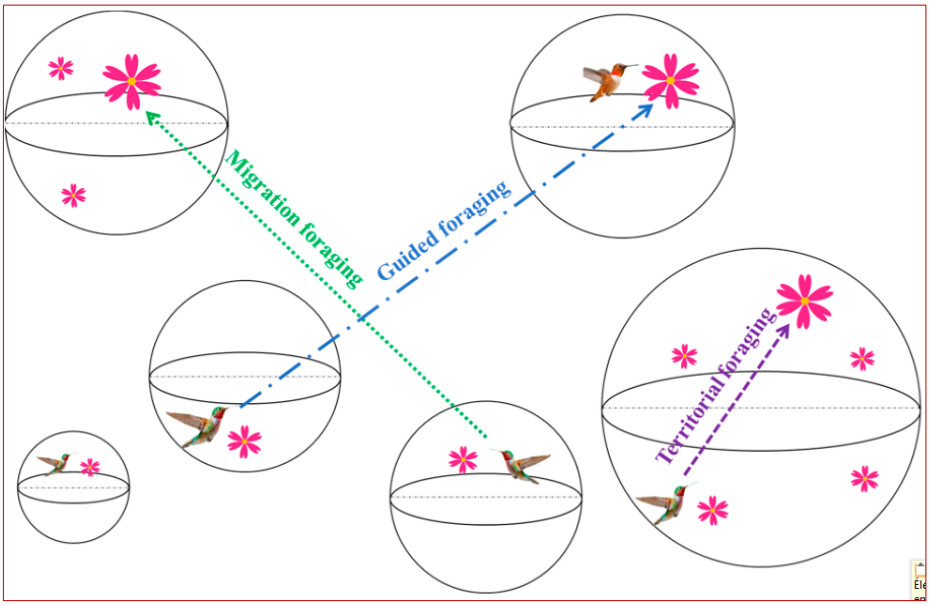

Figure 3.14. The different foraging behaviors of hummingbirds **[123]**

AHA algorithm uses the random initialization method to generate hummingbird population X, and randomly places n hummingbirds on n food sources, as described by Equation (3.30):

$$\boldsymbol{x_i = Lb + r \cdot (Ub - Lb), i = 1, \ldots, n,} \quad (3.30)$$

x_i is the location of the ith food source, Ub and Lb represent the boundaries of the search domain for a d-dimensional problem, r is a random value in [0, 1], n represents the population size. Moreover, the visit table of the food sources (best solutions) is formed as flows:

$$\boldsymbol{VT_{i,j} = \begin{cases} null & if\ i = j \\ 0 & if\ i \neq j \end{cases}\ i = 1, \ldots, n;\ j = 1, \ldots, n,} \quad (3.31)$$

Where $VT_{i,j}$ is the visit level, indicating the time period when the ith hummingbird did not reach the jth food source. In the case of $i = j$, $VT_{i,j} = null$ refers to the amount of food consumed by a hummingbird at a certain food source. $VT_{i,j} = 0$ refers to the jth hummingbird visiting the food source i.

A hummingbird is assumed to search for food at the maximum visit rate and then select the one with the maximum nectar-refilling rate from X as its optimal solution for the guided foraging behavior. This foraging makes use of the three flight abilities of omnidirectional, diagonal, and axial flight. In d-dimensional space, the expressions for simulating the axial, diagonal, and omnidirectional flight of hummingbirds are expressed by Equations (3.32) -(3.34), respectively.

$$\boldsymbol{D^{(i)} = \begin{cases} 1, if\ i = randi([1, d]) \\ 0, else \end{cases}\ i = 1, \ldots, d,} \quad (3.32)$$

$$\boldsymbol{D^{(i)} = \begin{cases} 1, if\ i = P(j), j = [1, q], P = randperm(q) \\ 0, else \end{cases}} \quad (3.33)$$

$$\boldsymbol{D^{(i)} = 1\ i = 1, \ldots, d,} \quad (3.34)$$

where $randi([1,d])$ is a randomly generated integer in $[1,d]$, q in [1, $[rand.(d\text{-}2)]$ +1], and $randperm(q)$ represents generating a random arrangement of integers from 1 to q. Hummingbirds use three flight skills in alternation to reach their food source, and they apply Equation (3.35) to simulate guided foraging and determine the position of a possible food source v_i.

$$\boldsymbol{v_i(t+1) = x_{i,aim}(t) + A \cdot D \cdot \left(x_i(t) - x_{i,aim}(t)\right)} \quad (3.35)$$

Where $v_i(t+1)$ is the position of the candidate solution in iteration $t+1$ and $x_i(t)$ is the i-th food source in iteration t. In addition, $x_{i,aim}(t)$ is the location of the target food source where the ith hummingbird will be located. A in $N(0,1)$ is the guiding parameter that obeys the normal distribution. The position of the i-th food source of the hummingbird is updated by Equation (3.36).

$$\boldsymbol{x_i(t+1) = \begin{cases} x_i(t), if\ f(x_i(t)) \leq f(v_i(t+1)) \\ v_i(t+1), if\ f(x_i(t)) > f(v_i(t+1)) \end{cases}} \quad (3.36)$$

where $f(x_i(t))$ and $f(v_i(t+1))$ represent the nectar replenishment rates of hummingbird food

sources and candidate food sources, respectively, that is, the fitness value of the function.

Once the flower nectar has been consumed, a hummingbird is more likely to search for a new source of food than to visit other flowers. As a result, the bird may readily migrate to a nearby spot inside its own territory, where a new food source could be located as a potential replacement for the existing one. The mathematical formula designed to simulate hummingbirds local foraging behavior and a potential food source is as follows:

$$\boldsymbol{v_i(t+1) = x_i(t) + B \cdot D \cdot x_i(t)} \quad (3.37)$$

Where $v_i(t+1)$ is the position of the candidate food source obtained by hummingbird i through territorial foraging in $t+1$ iterations, and B in $N(0,1)$ represents the territorial parameter obeying the normal distribution. Hummingbirds update the visit table after performing territorial foraging.

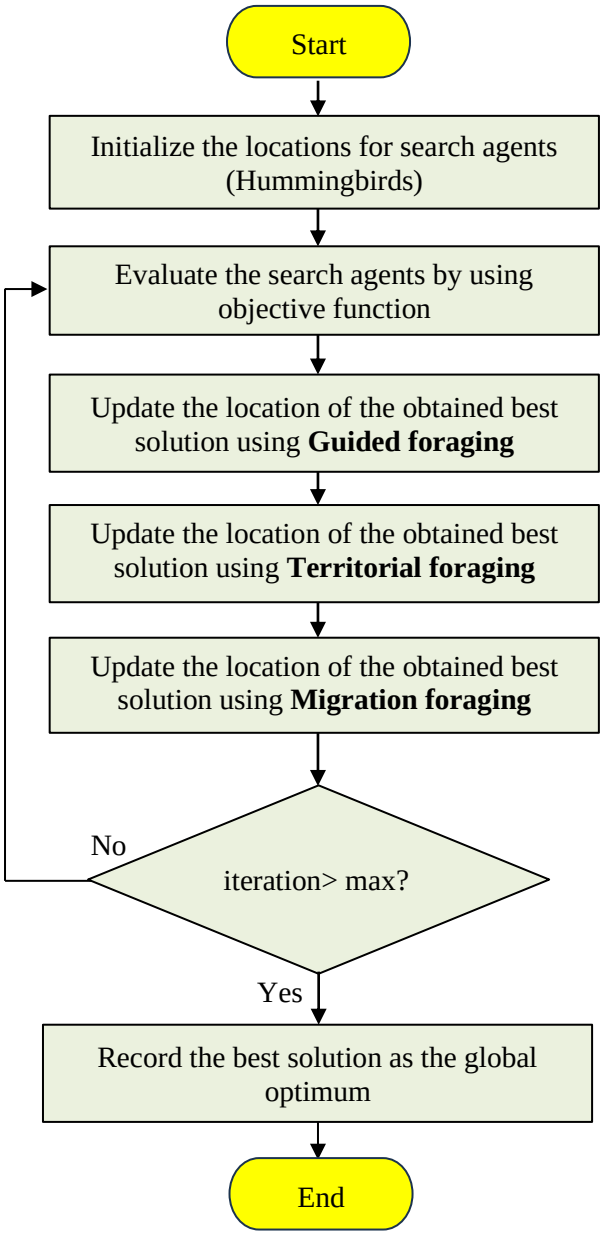

Figure 3.15. Flowchart of AHA algorithm

The mathematical formulation designed to simulate a hummingbird's migration foraging from the source with the lowest nectar-refilling rate to a new one produced at random is:

$$\boldsymbol{x_{wor}(t+1) = Low + r \cdot (Up - Low)} \quad (3.\ 38)$$

where x_{wor} is the food source with the worst nectar supplementation in the hummingbird population, and r is the random vector in [0,1]. Hummingbirds will update the visit table after migration and foraging. The flow shart of the AHA algorithm is given in Figure 3.15.

3.4. Optimal reactive power dispatch

In general, the goal of the ORPD study is to optimize the active power loss in the transmission network through optimal adjustment of the power system control parameters such as generator voltages, tap position of tap-changing transformers, and shunt capacitors while satisfying equality and inequality constraints at the same time. The ORPD may also have the objective of improving voltage profile by employing the reactive compensation devices such as automatic voltage regulators, transformer tap settings and shunt capacitors. ORPD is formulated as a general constrained optimization problem with continuous control variables. They may be classified as a group of equality constrains i.e. a power balance of load flow, as well as inequality constraints such as the physical limits of the system of control variables, or the physical limits of the system dependent variables. In this chapter we will study the ORPD problem by applying the proposed bio-inspired metaheuristics methods detailed in the previous section, namely MFO, GWO, AHA and ALO. To verify the effectiveness and efficiency of these proposed algorithms, different networks involving small, medium and large networks are used. First, the IEEE 14 bus test system is chosen. In 14 bus system, 10 control variables are considered including two shunt capacitors linked on buses 9 and 14. The IEEE 30 bus is used as second test system and 19 control variables are considered. In this system 9 buses were selected to receive shunt capacitors. The IEEE 57 bus is considered as third test system included 25 control variables. In this network, buses 18,25 and 53 were selected to receive shunt capacitors. The IEEE 118 bus is considered as fourth test system. There are 77 control variables in which 14 are shunt capacitors in this large test system. The Description of these studied test systems is depicted in Table 3.1. In all these test systems, the control variables are considered as continuous variables and the locations of the shunt capacitors are those used by most authors in the literature. Two different objective functions in the ORPD study are taken into consideration, namely: active power loss minimization and voltage deviation minimization (Equations 2.2 and 2.5). The shunt capacitor variable is modelled as a shunt admittance. This variable will modify the diagonal element Y_{ii} of the admittance matrix to which it has been connected. The diagonal elements of the nodal admittance matrix *Y* before connecting the shunt capacitor are given by the expression:

$$Y_{ii=}\sum_{\substack{j=1\\ j\neq i}}^{n}(y_{oij}+y_{ij}) \quad (3.\ 39)$$

Where y_{ij} is the serial admittance of the *i*-*j* branch and y_{oij} is the shunt admittance connected to node i.

When the capacitor (y_{Qshunt}) is connected at bus *i*, the new value of Y_{ii} becomes:

$$Y'_{ii} = Y_{ii+}y_{Qshunt} \quad (3.\ 40)$$

Table 3.1. Description of different power test systems

	IEEE 14-bus	IEEE 30-bus	IEEE 57-bus	IEEE 118-bus
Buses	14	30	57	118
Lines	20	41	80	186
Generators	5	6	7	54
Tap transformers	3	4	17	9
Shunt capacitors	2	9	3	14
Load buses	9	24	50	64
Control variables	10	19	25	77
P_{Load} (MW)	259.00	283.40	1250.80	4242
Q_{Load} (MVAR)	73.50	126.20	336.40	1438
$P_{Generators}$ (MW)	272.39	289.211	1279.26	4375.36
$Q_{Generators}$ (MVAR)	82.44	108.922	345.45	881.92
Initial P_{Loss} (MW)	13.393	5.811	28.462	132.863
Initial TVD (pu)	0.4962	0.4236	1.5528	1.4393

3.4.1. Population size of the proposed algorithms

Population size refers to the number of candidate solutions or individuals that coexist and evolve simultaneously within the algorithm's search space. Unlike traditional optimization techniques or local search metaheuristics that operate with a single solution, most metaheuristic algorithms utilize a population-based approach to explore the solution space more comprehensively. The choice of population size for the metaheuristic methods is often problem-specific and requires experimentation to find an optimal or satisfactory value. It is one of the important parameters influencing the quality of the result. Larger populations generally allow more extensive exploration of the search space, but can increase computational costs. Smaller populations can converge more quickly but risk getting stuck in local optima. Researchers often carry out experiments to determine the impact of population size on algorithm performance.

In this section, an empirical study was carried out to select the population size, i.e., we have investigated the effect of the population size (number of search-agents) on the performance of

the proposed methods (MFO, GWO, AHA and ALO), in which 30 trials runs were conducted for different population sizes (20, 30 and 40 search agents) for IEEE 14-bus, IEEE 30-bus, and IEEE 57-bus power systems. The results for the different population sizes for all the networks studied, have not all been presented, because there are a lot of graphs to be introduced. For this reason, we have only presented the results for the IEEE 57-bus (figure 3.16 to figure 3.19).

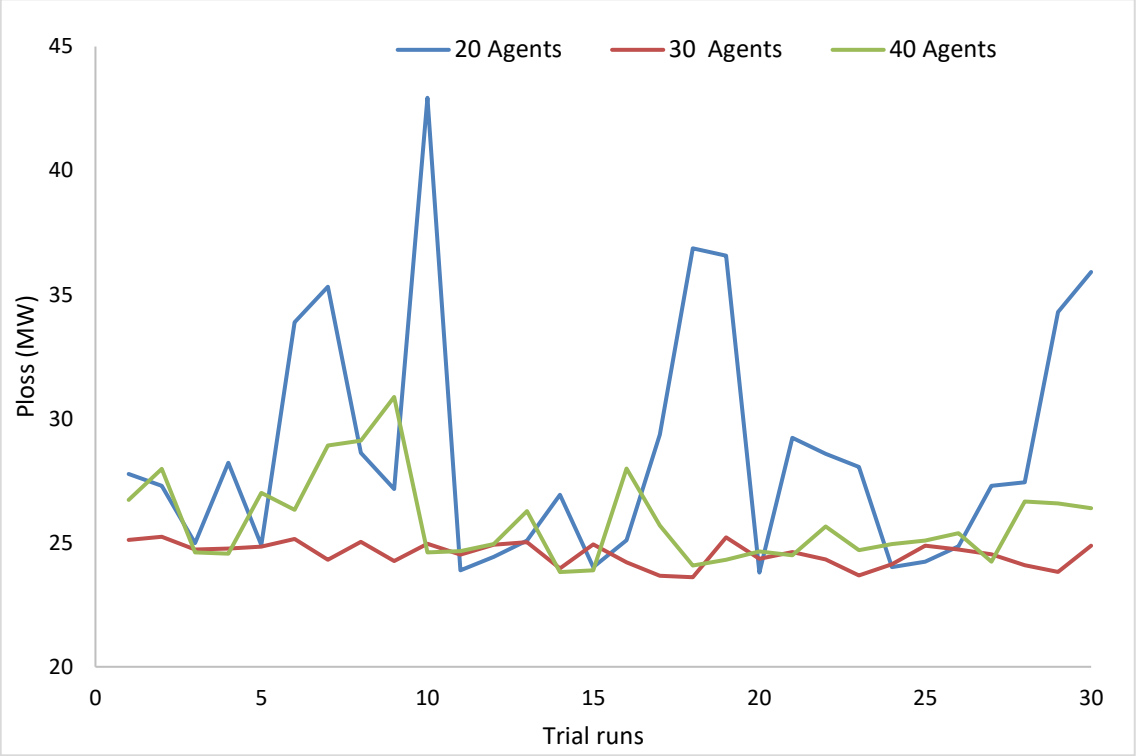

Figure 3.16. Active power losses for different population size, IEEE 57-bus (MFO method)

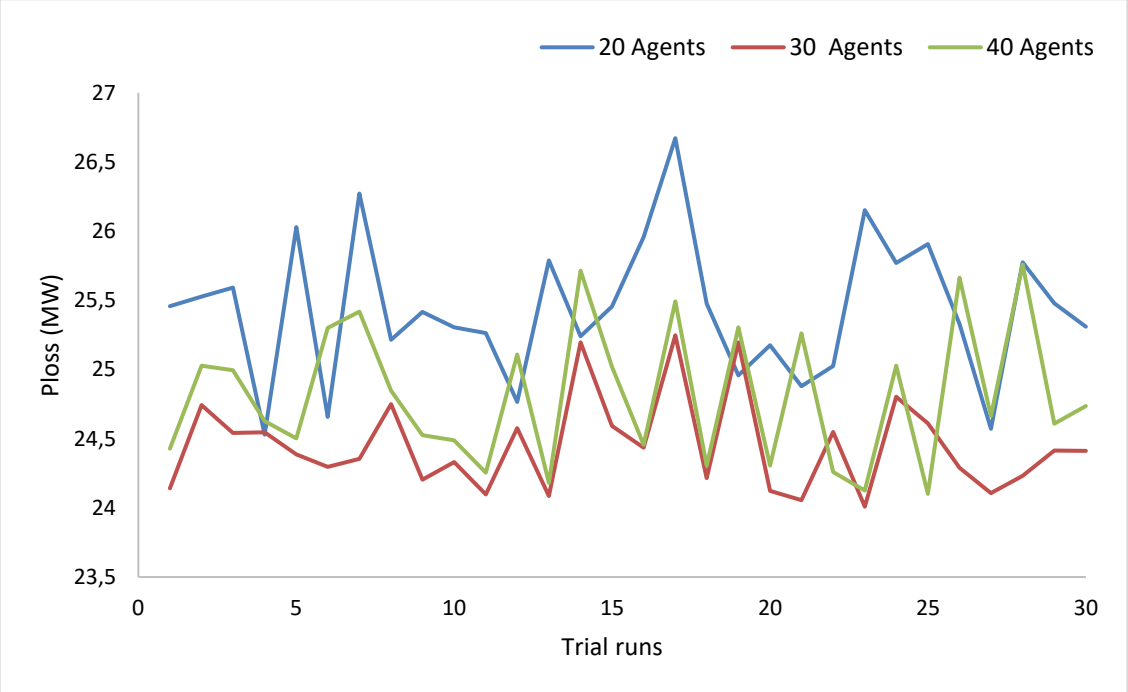

Figure 3.17. Active power losses for different population size (GWO method)

Figure 3.18. Active power losses for different population size (AHA method)

Figure 3.19. Active power losses for different population size, IEEE 57-bus (ALO method)

From the Figures above given (figure 3.16 to figure 3.27), it can be seen that 30 search agents are sufficient to obtain the best value closest to the optimum for the MFO and GWO methods but for the two methods ALO and AHA, it is observed that the best result is obtained for 40 search agents. In other words, 30 search agents for MFO and GWO methods and 40 search agents for ALO and AHA methods are good enough to get the near global optimum value of active power losses. For that reason, in all simulation cases, population size is specified as 30 for the MFO and GWO methods and 40 for ALO and AHA methods. The maximum number of iterations is fixed at 500. Since MFO, GWO, ALO and AHA are a random population-based techniques, multiple execution of theses algorithms is essential to assess its performance. For this work, the proposed methods are executed 40 times for all the test cases to solve the ORPD problem and the best results have been presented.

3.4.2. ORPD simulation (case of IEEE 14-bus test system)

Firstly, the proposed algorithms are applied on the IEEE 14-bus system shown in Figure 3.20. In this test system, there are 14 buses, out of which 5 are generator buses. Bus 1 is the slack bus, the buses number 2, 3, 6 and 8 are taken as generator buses and the rest are load buses. The network has 20 branches, 17 of which are transmission lines and 3 are tap-changing transformers. The shunt reactive power sources are considered at buses 9 and 14. Totally, there are 10 control variables, which consists of 5 generator voltages, 3 tap changing transformers and 2 shunt compensation reactive sources. The load demand is 259.00 MW and 73.5 MVAR on 100 MVA base. The initial active power losses are 13.4919 MW. The control variable limits are cited in Table 3.2. The system data and the initial operating conditions of the system are given from [17].

Table 3.2. The limits of the control variables for IEEE 14-bus test system

Variable limits	Lower limit (pu)	Upper limit (pu)
Generator buses voltage	0.9	1.1
Load buses voltages	0.9	1.1
Transformers tap setting	0.9	1.1
Shunt compensators (MVAR)	0	18

3.4.2.1. *Active power losses minimization*

In this case, the proposed algorithms namely MFO, GWO, AHA and ALO are applied to minimize the active power losses (Ploss). Table 3.3 summarizes the results of the optimal settings obtained by the proposed algorithms and shows the best results of active power losses. From this table it can be seen that MFO, GWO, ALO and AHA methods reduced active power losses by 7.745%, 7.922% 9.365% and 9.334% respectively. We can see also from Table 3.4,

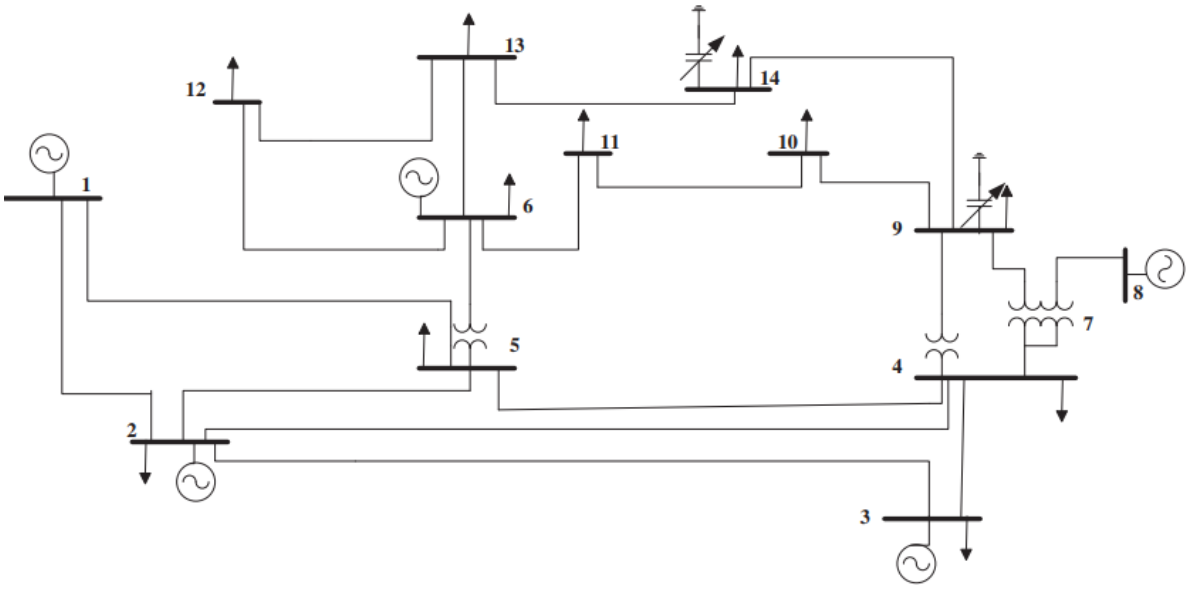

Figure 3.20. Single line diagram of IEEE 14 bus system

that the two methods ALO and AHA were able to find better results than MFO, GWO and the other algorithms from the literature. Figure 3.23 shows the convergence curves of the proposed optimizers and as it can be seen, the ALO algorithm converges to high quality solutions in less than 270 iterations. Figure 3.21 and figure 3.22 illustrate the performance of all proposed algorithms for 40 independent runs.

Table 3.3. Simulation results of proposed algorithms for IEEE 14-bus test system

Control variables	Initial	AHA	ALO	GWO	MFO
V_1	1.0600	1.1000	1.1000	1.1000	1.1000
V_2	1.0450	1.0857	1.0861	1.0776	1.0766
V_3	1.0100	1.0564	1.0571	1.0436	1.0409
V_6	1.0700	1.1000	1.1000	1.0622	1.0600
V_8	1.0900	1.0995	1.1000	1.1000	1.0666
T_{4-7}	0.9780	1.0309	0.9793	1.0735	1.0153
T_{4-9}	0.9690	0.9061	0.9696	0.9051	0.9648
T_{5-6}	0.9320	0.9864	1.0085	0.9495	0.9641
Q_{C9}	0.1800	17.9754	17.7316	3.9360	14.8082
Q_{C14}	0.1800	6.2070	5.9659	6.9710	6.4962
Ploss (MW)	13.4919	12.2325	12.2284	12.423	12.447
TVD (pu)	0.4962	0.7445	0.7560	0.4248	0.4084
Red (%) (Ploss)	-	9.334	9.365	7.922	7.745

Table 3.4. Comparative results of IEEE 14-bus test system

Methods	Ploss (MW)	Ploss Reduction (%)	Methods	Ploss Reduction (%)
PSO-TVAC [124]	12.279	8.989	CBA [125]	8.75
MGBTLBO [95]	12.310	8.756	MGBTLBO [125]	8.74
WOA [124]	12.255	9.167	BA [125]	8.70
PSO [124]	12.381	8.233	JAYA [125]	8.68
AHA	**12.232**	**9.334**	DE-ABC [125]	8.30
ALO	**12.228**	**9.365**	IGSACSS [125]	8.10
GWO	**12.423**	**7.922**	DE [125]	7.72
MFO	**12.447**	**7.745**	DEEP [125]	7.71

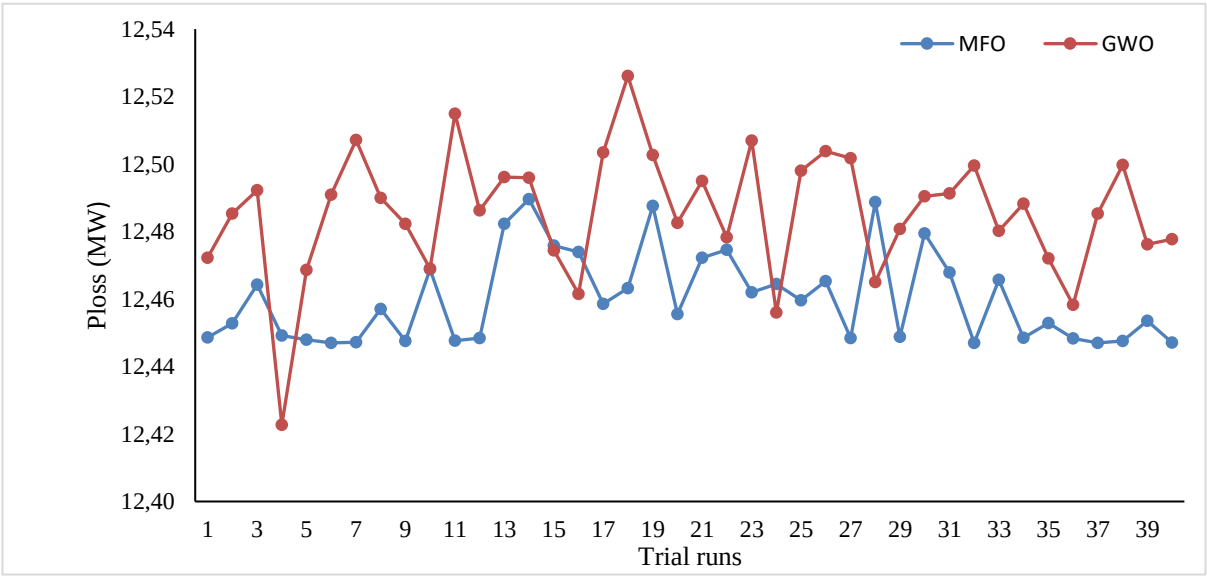

Figure 3.21. Performance of 30 search agents for 40 trial runs

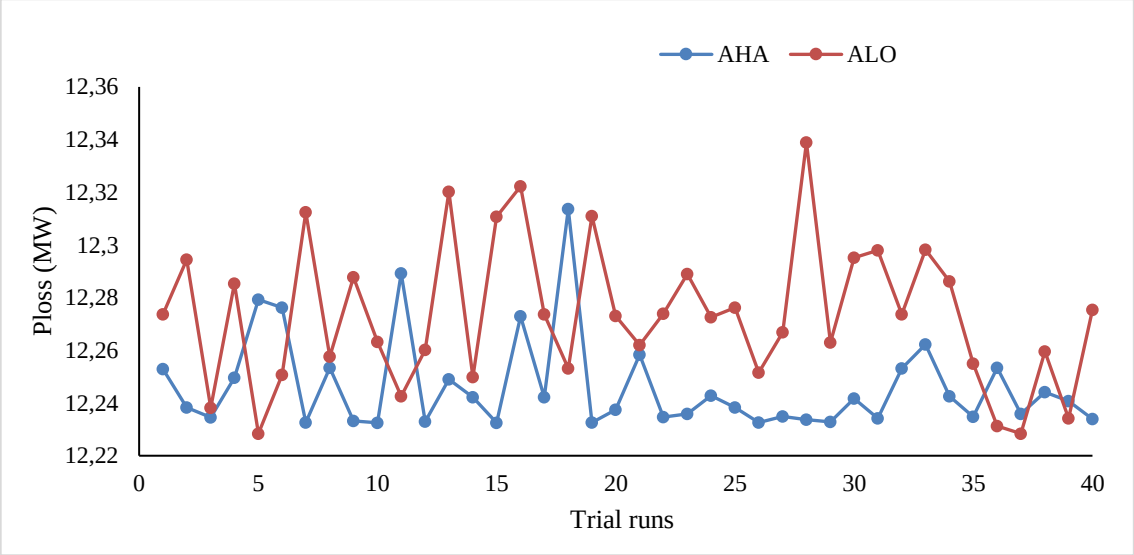

Figure 3.22. Performance of 40 search agents for 40 trial runs

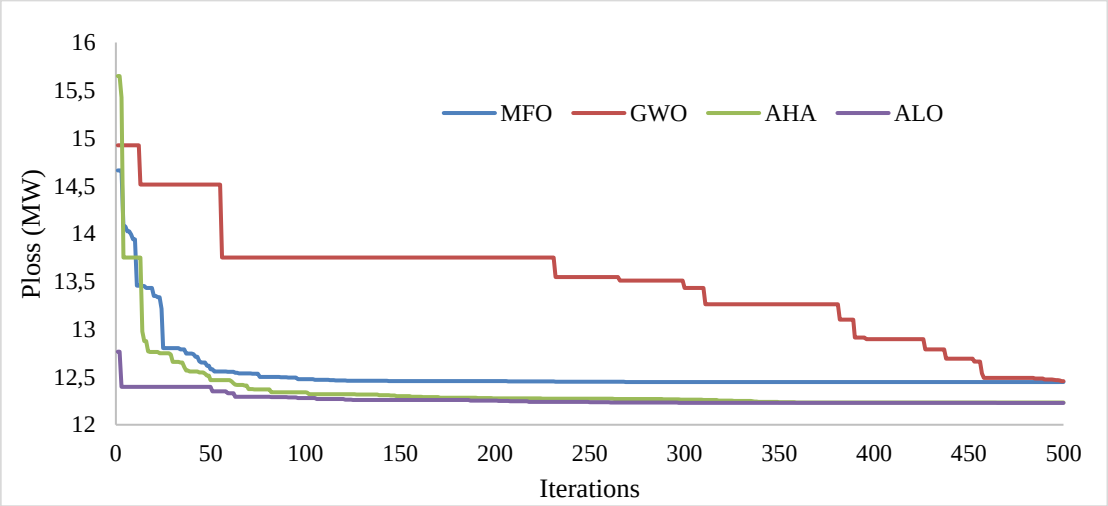

Figure 3.23. Convergence characteristic of IEEE 14-bus system for *PLoss* minimization

3.4.2.2. *Voltage Deviation minimization.*

In this section the proposed algorithms are applied to minimize the total voltage deviation (TVD). In this case, the best results of the voltage deviation minimization achieved by MFO, GWO, AHA and ALO are tabulated in Table 3.5. We note that practically all the methods produced good results except the GWO method. It can be pointed that MFO, GWO, AHA and ALO are able to reduce the voltage deviation by 98.347%, 98.347%, 97.501% and 98.387% respectively with respect to initial value. Figures 3.24 and 3.25 illustrate the performance of the four proposed algorithms for 40 independent runs. Figure 3.26 shows the TVD reduction process for MFO, GWO, AHA and ALO simultaneously. From this figure it can be seen that satisfactory results can be achieved by ALO and AHA methods after about 200 iterations, which reflects their good search capability over the other two techniques. Figure 3.27 shows the bus voltage profiles of the best solutions obtained using the proposed methods. It is clear from this figure that the voltage profile has been significantly improved.

Table 3.5. Simulation results of proposed algorithms for IEEE 14-bus test system

Control variables	Initial	AHA	ALO	GWO	MFO
V_1	1.0600	1.0563	0.9669	0.9315	0.9000
V_2	1.0450	1.0268	1.0527	1.0726	1.0521
V_3	1.0100	1.0012	1.0323	1.0817	1.0274
V_6	1.0700	1.0130	1.0128	1.0130	1.0129
V_8	1.0900	1.0274	0.9689	0.9215	0.9746
T_{4-7}	0.9780	1.0311	0.9622	0.9131	0.9681
T_{4-9}	0.9690	0.9879	0.9921	0.9426	0.9947
T_{5-6}	0.9320	0.9394	0.9996	1.0167	1.1000
Q_{C9}		0.1800	16.1616	16.6651	0.0603
Q_{C14}	0.1800	13.0441	12.9962	0.1484	13.0931
TVD (pu)	0.4962	0.0082	0.0082	0.0124	0.008005
*P*loss (MW)	13.4919	13.8139	23.3005	36.0771	37.4749
TVD Red (%)	-	98.347	98.347	97.501	98.387

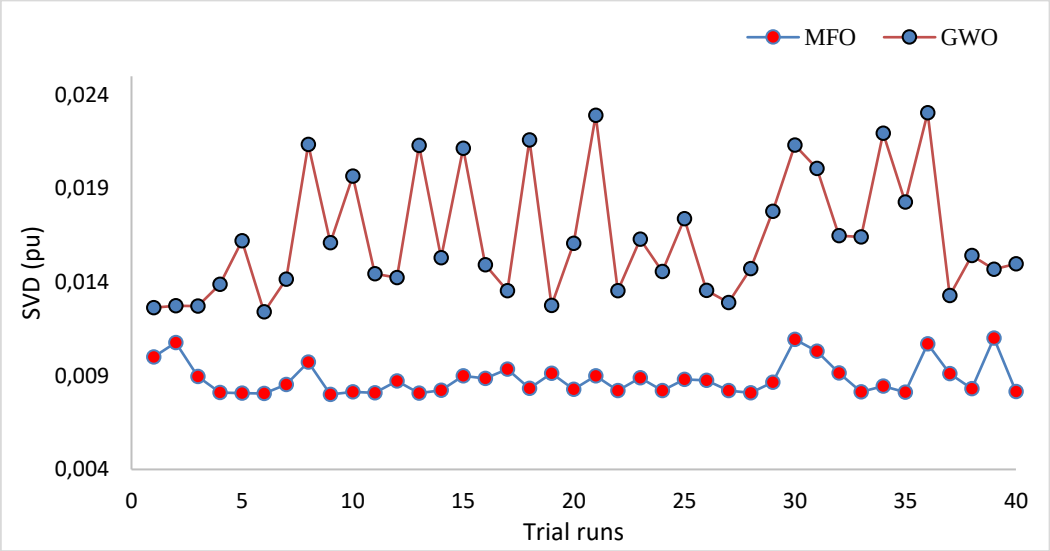

Figure 3.24. Performance of 30 search agents for 40 trial runs

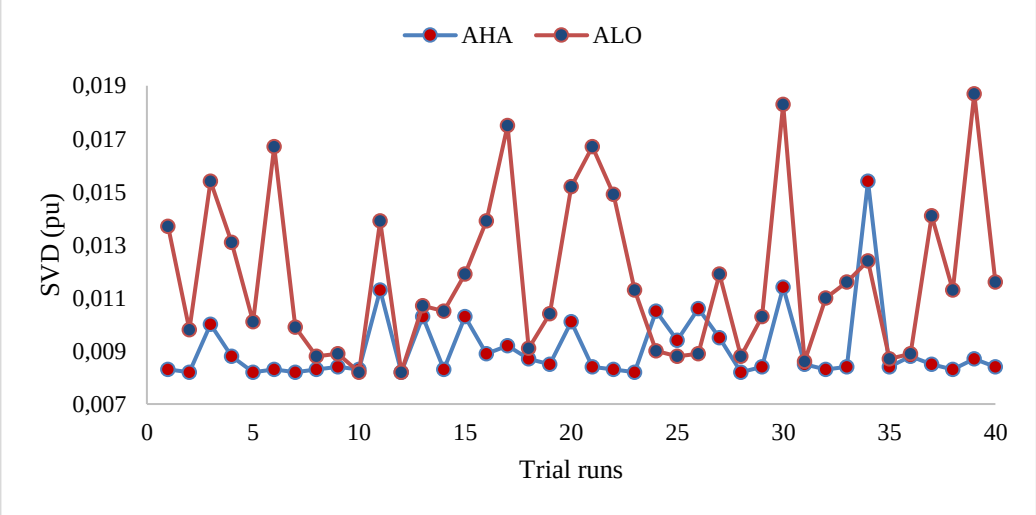

Figure 3.25. Performance of 40 search agents for 40 trial runs

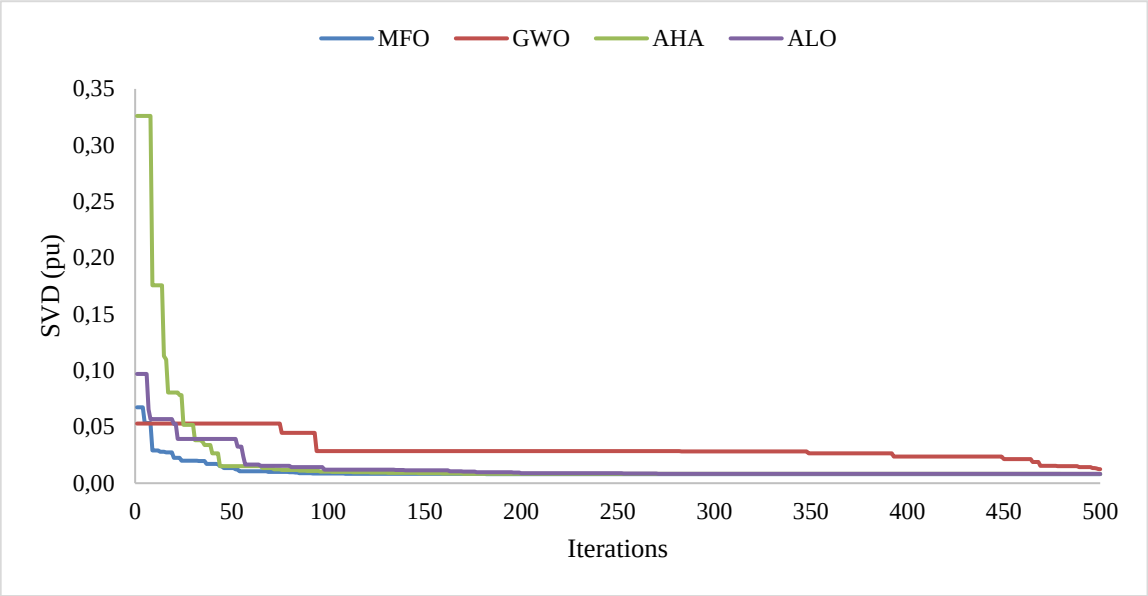

Figure 3.26. Convergence characteristic of IEEE 14-bus system for TVD minimization

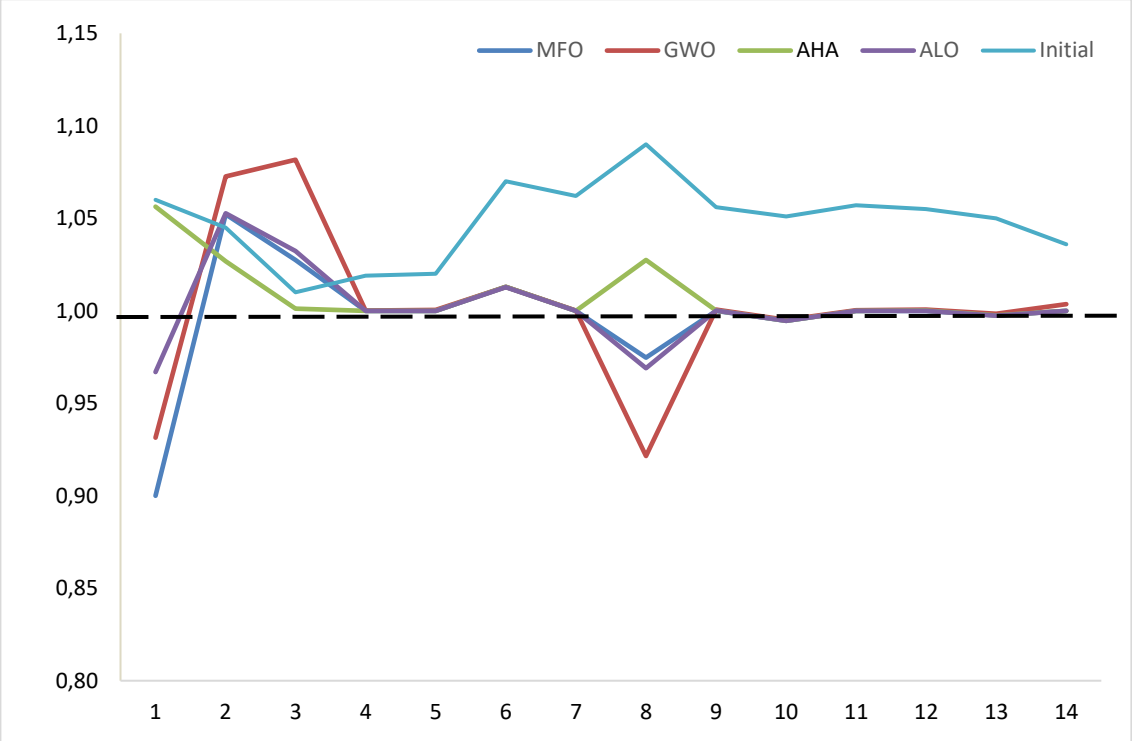

Figure 3.27. Voltage profiles of IEEE 14-bus system for TVD minimization

3.4.3. ORPD simulation (case of IEEE 30-bus test system)

In this case, the IEEE 30 bus system (figure 3.28) includes six generation buses connected on the bus number 1, 2, 5, 8, 11 and 13, 24 load buses and 41 branches. Four branches are transformers with tap changers in lines (6, 9), (6, 10), (4, 12) and (27, 28). In addition, buses 10, 12, 15, 17, 20, 21, 23, 24 and 29 were selected to receive shunt capacitors. This IEEE 30 bus test system included 19 control variables. The total system real power demand is 2.834 p.u. at 100 MVA base. The voltages of the load buses as well as generator buses have been constrained within limits between 0.9 p.u. and 1.1 p.u. The operating range of all tap

transformers is set between 0.9 and 1.1. The range of capacitor bank considered is between 0 and 5 MVAR (Table 3.6). The total active and reactive loads are P_{load} = 2.834 p.u and Q_{load} = 1.262 p.u.

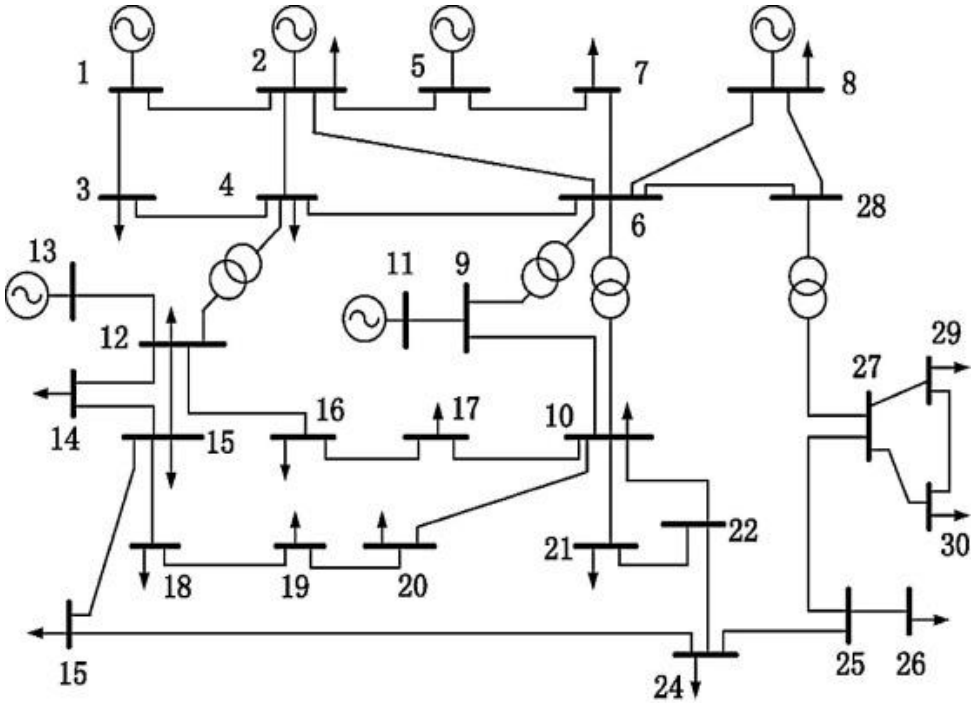

Figure 3.3.28. Single-line diagram of IEEE 30 bus test system.

Table 3.6. The limits of the control variables for IEEE 30-bus test system

Variable limits	Lower limit (pu)	Upper limit (pu)
Generator buses voltage	0.9	1.1
Load buses voltages	0.9	1.1
Transformers tap setting	0.9	1.1
Shunt compensators (MVAR)	0	5

3.4.3.1. *Active power loss minimization.*

Table 3.7 shows the optimum values of the control variables and the active power losses obtained by the proposed algorithms. Figures 3.29 and 3.30 illustrate the Performance of all the proposed algorithms for 40 trial runs. It can be seen that the active power losses obtained by AHA and ALO methods are 4.5127 MW and 4.5315 MW which means a reduction in losses of 17.88% and 17.54% respectively. The two others methods (MFO and GWO) have reduced active power losses by only 11.32% and 7.60% respectively. Table 3.8 compares the results obtained from MFO, GWO, AHA and ALO methods with the other methods in the literature. These results indicate that the two proposed ALO and AHA methods exceed all other methods in performance, except for the GSA method, which surpassed the ALO method by 0.0172 MW, resulting in a decrease of less than 0.31%. The best result in terms of loss reduction obtained by GSA is 17.859%, while the AHA and ALO methods are 17.888% and 17.546% respectively. Figure 3.31 shows the convergence characteristics of real power losses of the four proposed methods.

Table 3.7. Simulation results of proposed algorithms for IEEE 30-bus test system

Control variables	Initial	AHA	ALO	GWO	MFO
V_1	1.0600	1.1000	1.1000	1.0716	1.0705
V_2	1.0430	1.0941	1.0945	1.0625	1.0612
V_5	1.0100	1.0745	1.0753	1.0402	1.0382
V_8	1.0100	1.0759	1.0772	1.0386	1.0383
V_{11}	1.0820	1.0998	1.1000	1.0977	1.0397
V_{13}	1.0710	1.1000	1.1000	1.0511	1.0205
T_{6-9}	0.9320	1.0369	0.9864	1.0192	1.1000
T_{6-10}	0.9780	0.9003	0.9765	0.9869	0.9345
T_{4-12}	0.9690	0.9731	0.9878	0.9814	1.0275
T_{27-28}	0.9680	0.9634	0.9789	0.9795	1.0052
Q_{C10}	0.0000	4.9439	4.9981	2.2670	0.0000
Q_{C12}	0.0000	4.9917	4.9968	4.0813	3.0784
Q_{C15}	0.0000	4.8621	4.9318	1.6247	5.0000
Q_{C17}	0.0000	4.9837	4.6289	4.6196	5.0000
Q_{C20}	0.0000	4.1728	3.3762	2.8740	5.0000
Q_{C21}	0.0000	4.9996	4.9219	2.2094	5.0000
Q_{C23}	0.0000	2.6848	3.7978	2.8866	3.3328
Q_{C24}	0.0000	4.9622	4.8002	4.7419	5.0000
Q_{C29}	0.0000	2.2485	4.1211	2.6607	2.6378
Ploss(MW)	5.4958	4.5127	4.5315	4.8733	5.0776
TVD (pu)	0.4236	2.0899	2.0033	0.8205	0.3217
Ploss Red (%)	-	17.888	17.546	11.327	7.609

Table 3.8. Comparative results of IEEE 30-bus test system

Methods	Active power losses (MW)	Reduction (%)
PSO [124]	4.7779	13.062
PSO-TVAC [124]	4.6469	15.446
WOA [124]	4.5943	16.403
BBO [18]	4.5511	17.189
DE [14]	4.5550	17.118
CLPSO [9]	4.5615	17.000
PSO [9]	4.6282	15.786
SARGA [82]	4.5740	16.772
GSA [19]	4.5143	17.859
AHA	**4.5127**	**17.888**
ALO	**4.5315**	**17.546**
GWO	**4.8733**	**11.326**
MFO	**5.0776**	**7.609**

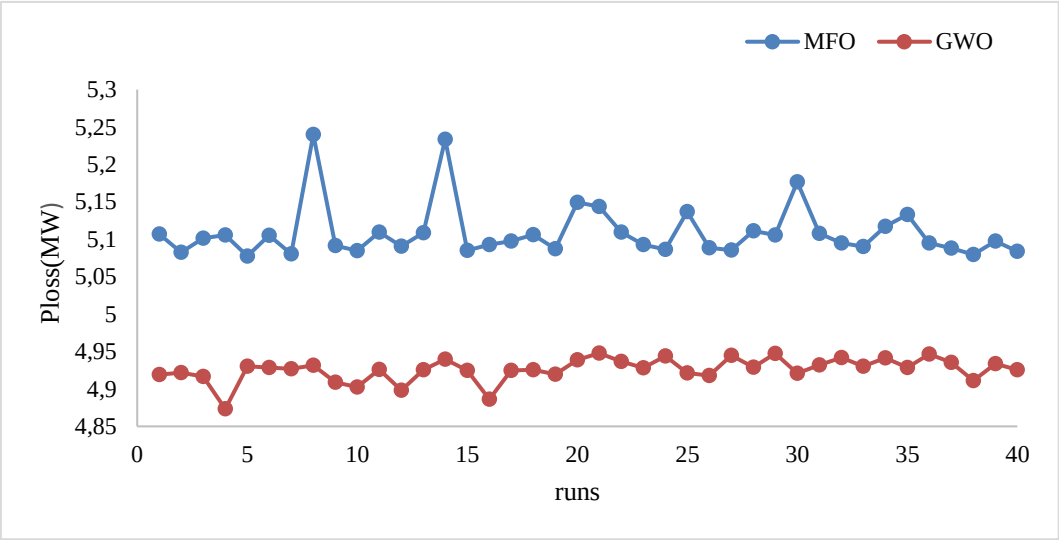

Figure 3.29. Performance of 30 search agents for 40 trial runs

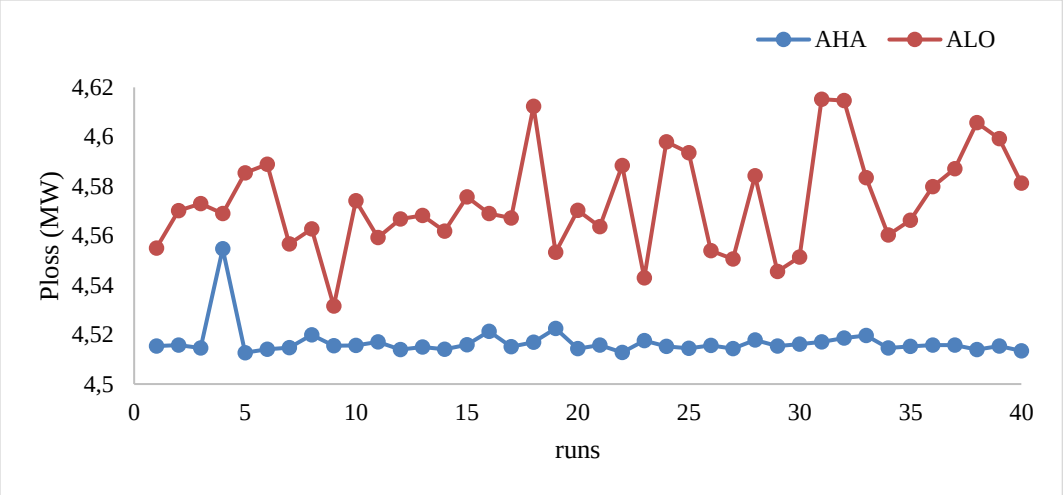

Figure 3.30. Performance of 40 search agents for 40 trial runs

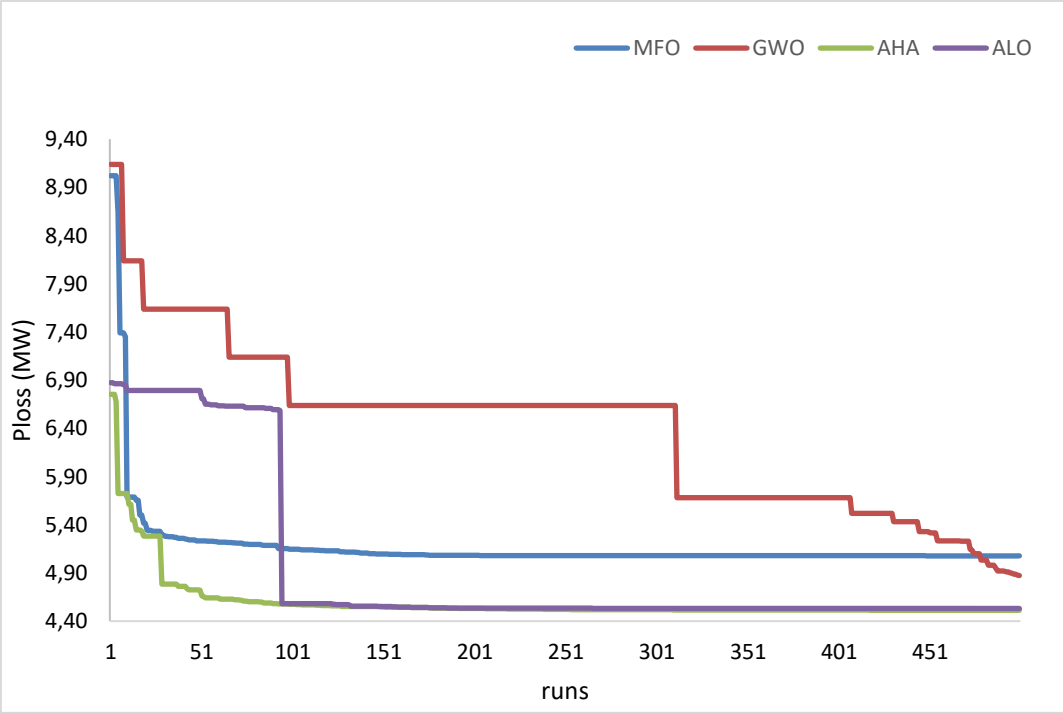

Figure 3.31. Convergence characteristic of IEEE 30-bus system for Ploss minimization

3.4.3.2. *Voltage Deviation minimization.*

In this case the total voltage deviation minimization (TVD) is considered and optimized using different proposed methods. The optimal values that obtained by these methods are listed in Table 3.9. Referring to this Table it is realized that the TVD is upgraded by 78.116% from AHA, 79.344% from MFO, 76.440% from ALO, and 73.654% from the GWO algorithm. These results show that AHA and MFO leads to obtain the highest reduction of TVD compared to ALO and GWO. The IEEE 30-bus Convergence characteristic for TVD minimization of AHA, MFO, ALO and GWO algorithms is displayed in Figure 3.34. The Performance of all methods for 40 trial runs are exhibited in Figure 3.32 and 3.33. The voltage profile at all buses for IEEE 30-bus is illustrated in Figure. 3.35. From this figure, we can see that the voltage profiles of this test system have been improved compared with the initial state in both AHA and MFO methods.

Table 3.9. Simulation results of proposed algorithms for IEEE 30-bus test system

Control variables	Initial	AHA	ALO	GWO	MFO
V_1	1.0600	1.0125	0.9956	0.9756	0.9958
V_2	1.0430	1.0084	1.0975	1.0006	0.9974
V_5	1.0100	1.0195	1.0175	1.0140	1.0195
V_8	1.0100	1.0028	1.0123	1.0028	1.0005
V_{11}	1.0820	1.0336	0.9077	1.0866	1.0593
V_{13}	1.0710	1.0203	0.9645	1.0661	1.0436
T_{6-9}	0.9320	1.0410	0.9127	1.0945	1.0786
T_{6-10}	0.9780	0.9107	0.9000	0.9083	0.9000
T_{4-12}	0.9690	0.9941	0.9010	1.0867	1.0402
T_{27-28}	0.9680	0.9581	0.9651	0.9489	0.9637
Q_{C10}	0.0000	4.9650	2.2691	0.0454	5.0000
Q_{C12}	0.0000	0.1328	0.4662	0.0206	0.1829
Q_{C15}	0.0000	4.8455	4.3654	0.0319	5.0000
Q_{C17}	0.0000	0.0018	1.7544	0.0243	0.0000
Q_{C20}	0.0000	4.9985	4.8976	0.0446	5.0000
Q_{C21}	0.0000	4.8327	3.7088	0.0164	5.0000
Q_{C23}	0.0000	4.9763	4.4438	0.0467	5.0000
Q_{C24}	0.0000	4.9472	3.1092	0.0417	5.0000
Q_{C29}	0.0000	1.6340	2.6276	0.5973	2.3118
TVD (pu)	0.4236	0.0927	0.0998	0.1116	0.0875
Ploss (MW)	5.4958	5.7020	15.8529	6.9918	8.1475
TVD Red (%)	-	78.116	76.440	73.654	79.344

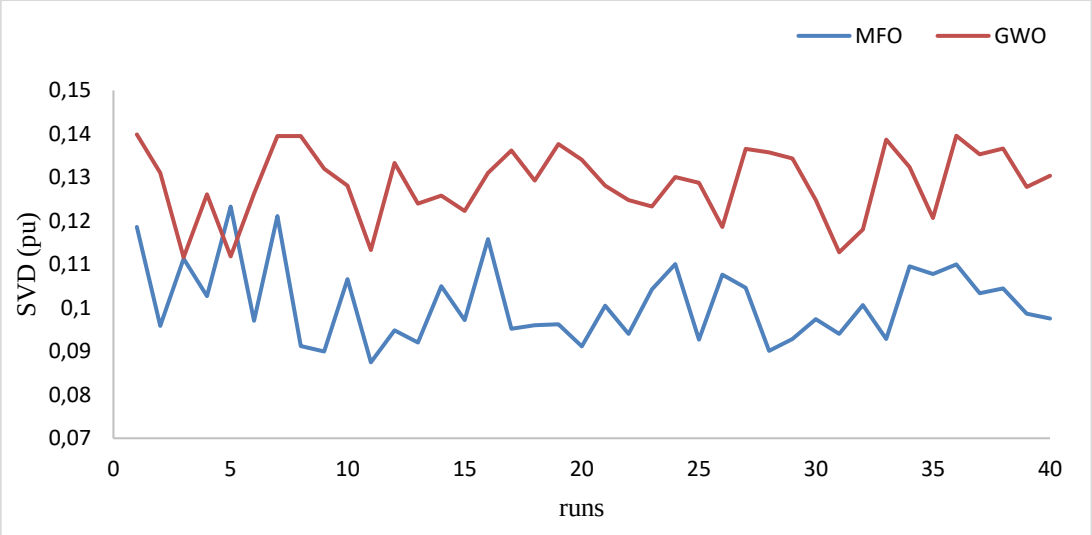

Figure 3.32. Performance of 30 search agents for 40 trial runs

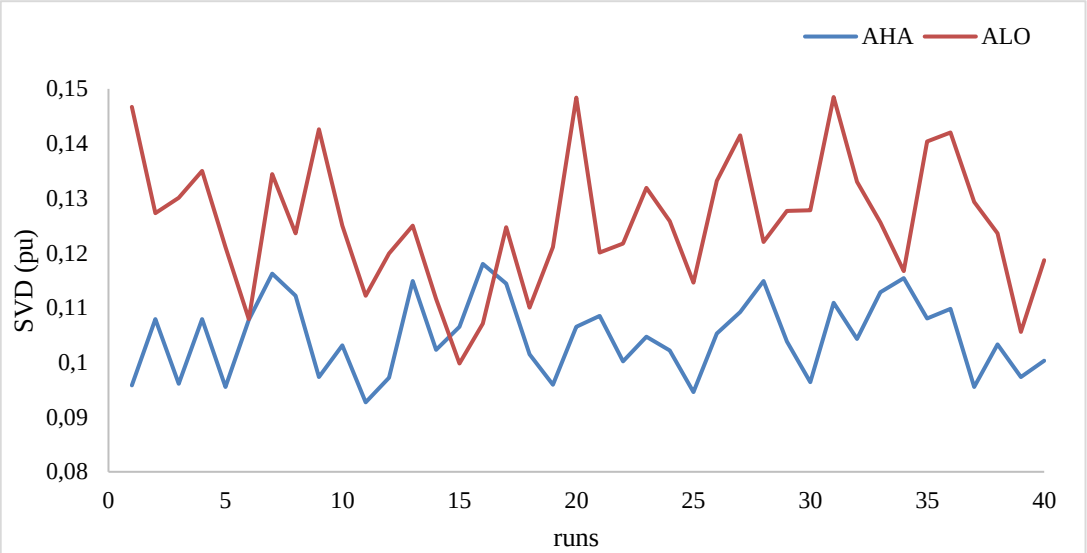

Figure 3.33. Performance of 40 search agents for 40 trial runs

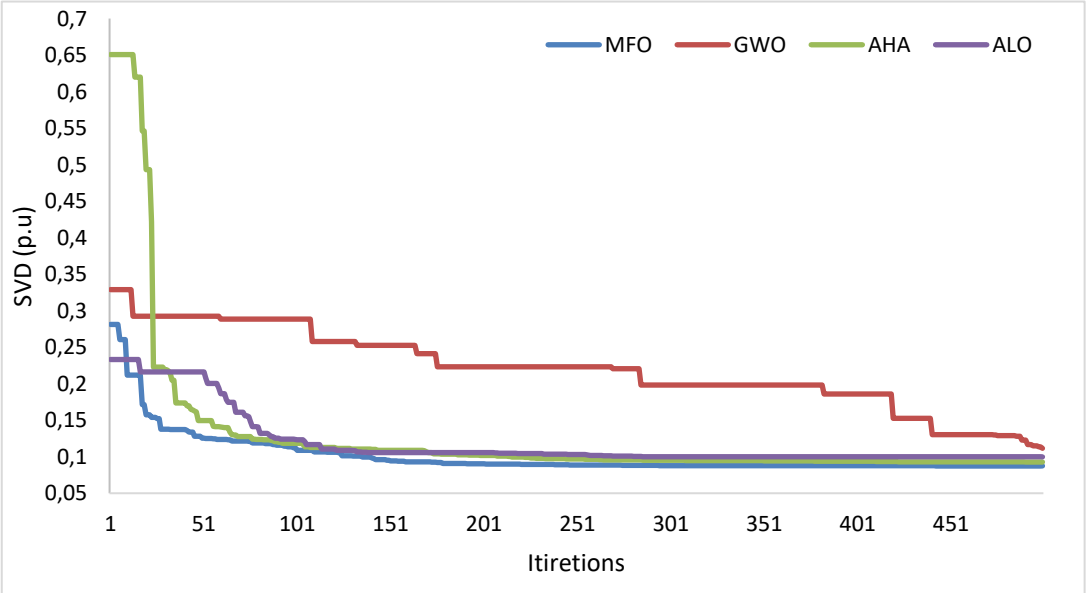

Figure 3.34. Convergence characteristic of IEEE 30-bus system for TVD minimization

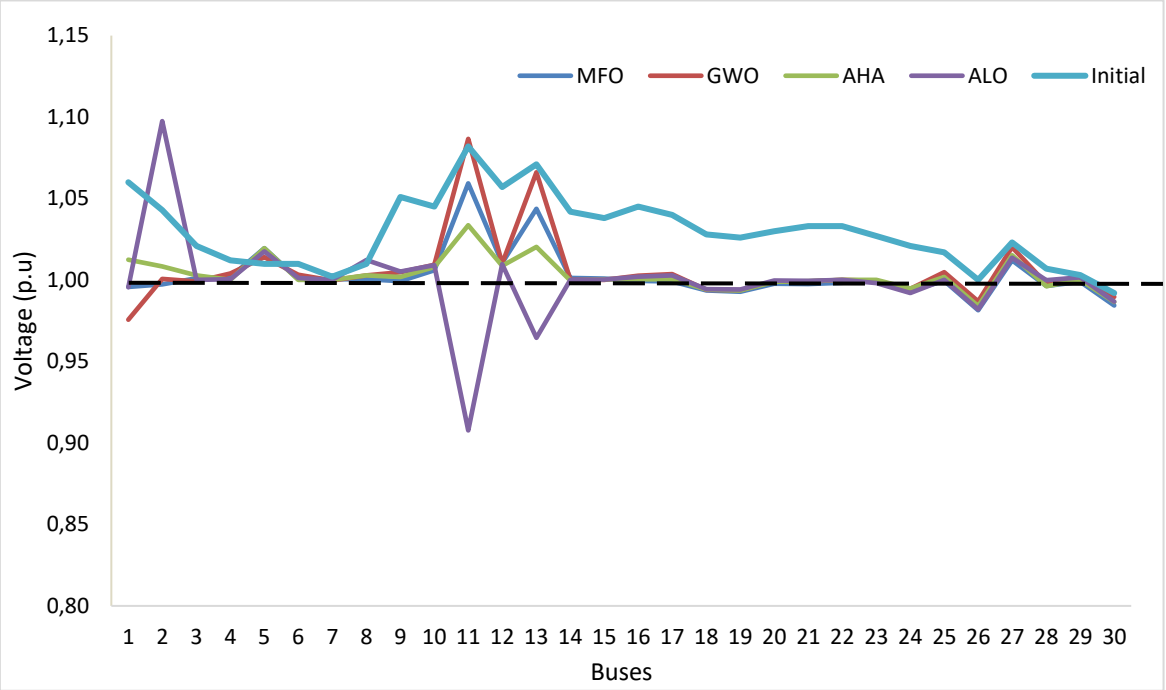

Figure 3.35. Voltage profiles of IEEE 30-bus system for TVD minimization

3.4.4. ORPD simulation (case of IEEE 57-bus test system)

To further evaluate the proposed methods, the IEEE 57-bus system is used (Figure 3.36). This benchmark is a medium-sized network, with 57 buses, 80 transmission lines, 7 generators at buses 1, 2, 3, 6, 8, 9 and 12. 15 branches are under load change tap transformers. Three shunt reactive power sources are installed at buses 18, 25 and 53. The system line data, bus data, variable limits and the initial values of the control variables were given in [126], [127]. The search space of this case system has 25 dimensions, including 7 generator voltages, 15 transformer taps and 3 reactive power sources. The upper and lower limits of Bus generator Voltages, Bus load Voltages, Tap setting transformers and Shunt compensators of the test system are given in Table 3.10. The system loads are given as follows: Pload = 12.508 p.u., Qload = 3.364 p.u. The initial total generations and power losses are as follows: PG = 12.7926 p.u., QG = 3.4545 p.u., Ploss = 0.28462 p.u.

Table 3.10. The limits of the control variables for IEEE 57-bus test system

Variables	Lower limit (pu)	Upper limit (pu)
Generator buses voltage	0.9	1.1
Load buses voltage	0.9	1.1
Transformers tap setting	0.9	1.1
Shunt compensators (MVAR)	0	30

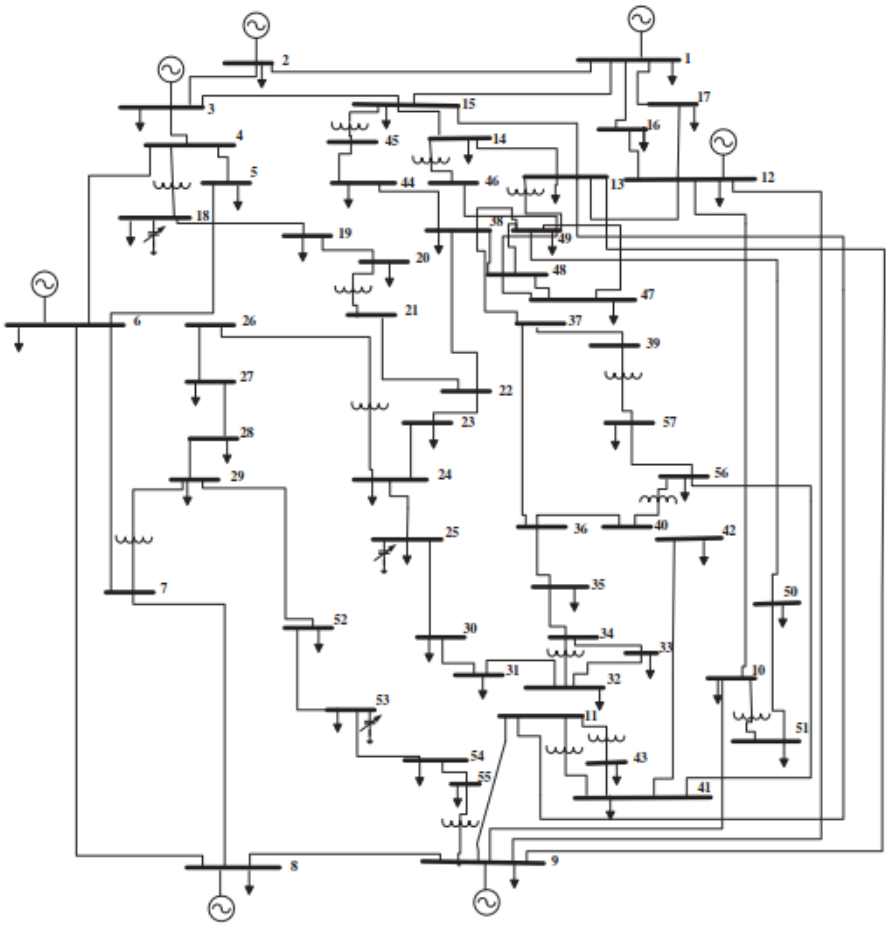

Figure 3.36. Single line diagram of IEEE 57 bus system

3.4.4.1. *Active power loss minimization.*

In this part, the objective function adopted is the minimization of the active power losses by means of the AHA, ALO, GWO and MFO algorithms. Table 3.11 shows the minimum value of power loss in MW and their percentage of loss reduction obtained by different proposed techniques. The total active power losses are reduced from the base case which is 28.462 MW to 21.4918 MW, 21.8631 MW, 24.0086 MW and 23.6101 MW by using AHA, ALO, GWO and MFO algorithms respectively. From this achievement, AHA algorithm is able to excel ALO, GWO and MFO algorithms. These methods produce respectively about 23.186 % 15.648 % and 17.050 % of loss reduction from the base case compared to AHA method which reduces losses by 24.490%. From Table 3.12, it is seen that the AHA algorithm outperforms many algorithms in literature. the best result was found by the CBA-IV method (22.83%), which is below the AHA result of 1.65%. Additionally, it can be noticed that the obtained control variables as shown in Table 3.12 are all within the range of the limit. Figure 3.37 and Figure 3.38 show the performance of the proposed algorithms for 40 independent runs. Figure 3.39. shows the convergence curves of the considered optimizers and it is noticeable that the AHA algorithm converges to a high-quality solution in the first quarter of iterations.

Table 3.11. Simulation results of proposed algorithms for IEEE 57-bus test system

Control variables	Initial	AHA	ALO	GWO	MFO
V_1	1.0400	1.1000	1.1000	1.0787	1.0751
V_2	1.0100	1.0967	1.0985	1.0685	1.0720
V_3	0.9850	1.0843	1.0871	1.0439	1.0548
V_6	0.9800	1.0769	1.0810	1.0366	1.0451
V_8	1.0050	1.0987	1.1000	1.0469	1.0654
V_9	0.9800	1.0833	1.0843	1.0335	1.0471
V_{12}	1.0150	1.0813	1.0791	1.0287	1.0406
T_{4-18}	0.9700	0.9316	0.9740	1.0158	0.9000
T_{4-18}	0.9780	0.9113	0.9282	0.9591	1.0933
T_{21-20}	1.0430	0.9987	0.9984	0.9618	1.0072
T_{24-26}	1.0430	0.9870	1.0377	0.9919	1.0039
T_{7-29}	0.9670	0.9074	0.9657	0.9834	0.9962
T_{34-32}	0.9750	0.9491	0.9754	0.9411	0.9520
T_{11-41}	0.9550	0.9062	1.0221	0.9225	0.9112
T_{15-45}	0.9550	0.9055	0.9095	0.9774	0.9913
T_{14-46}	0.9000	0.9053	0.9078	0.9729	0.9720
T_{10-51}	0.9300	0.9199	0.9228	0.9988	0.9854
T_{13-49}	0.8950	0.9007	0.9000	0.9420	0.9420
T_{11-43}	0.9580	0.9046	0.9941	0.9756	0.9789
T_{40-56}	0.9580	0.9997	1.0840	0.9881	0.9973
T_{39-57}	0.9800	0.9857	1.0583	0.9549	0.9681
T_{9-55}	0.9400	0.9125	0.9721	0.9838	0.9974
Q_{C18}	0.0000	10.6871	18.4544	0.0277	0.0968
Q_{C25}	0.0000	12.0956	16.6199	0.1165	0.1330
Q_{C53}	0.0000	10.3264	15.3966	0.1129	0.1278
Ploss (MW)	28.4623	21.4918	21.8631	24.0086	23.6101
TVD (p.u)	1.5528	6.7249	5.6735	1.1006	1.2372
Ploss Red (%)	-	24.490	23.186	15.648	17.05

Table 3.12. Comparative results of IEEE 57-bus test system

Methods	Ploss (MW)	Reduction (%)	Methods	Ploss (MW)	Reduction (%)
CFA [125]	24.2900	14,6590	SOA [125]	24.2654	14,7455
ABC [125]	23.9600	15,8536	BBO [125]	24.5440	13,7666
CKHA [50]	23.3800	17,8563	OGSA [125]	23.4300	17,6806
BA [125]	22.2716	21,7505	GSA [125]	23.4600	17,5752
ABC [125]	23.9666	15,7953	**GWO**	**24.0086**	**15,6477**
NGBWCA [125]	23.2700	18,2427	**MFO**	**23.6101**	**17,0478**
MICA-IWO [125]	24.2568	14,7757	**ALO**	**21.8631**	**23,1858**
CBA-IV [125]	21.9627	22,8358	**AHA**	**21.4918**	**24,4903**

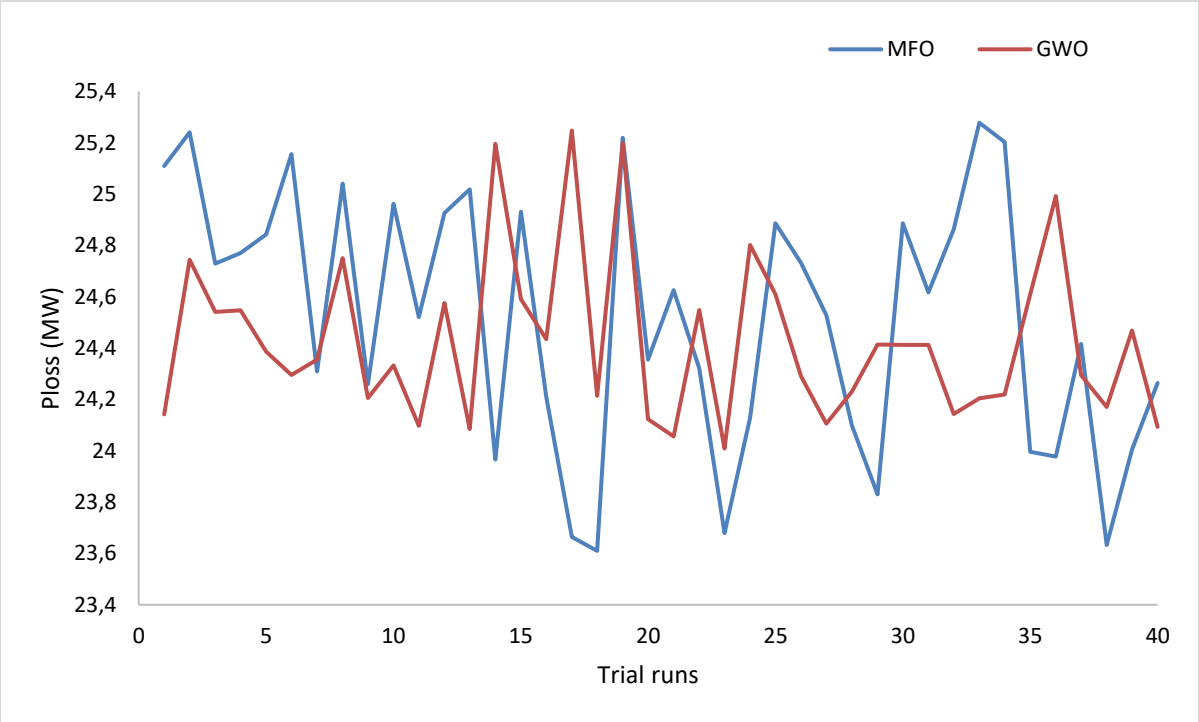

Figure 3.37. Performance of 30 search agents for 40 trial runs

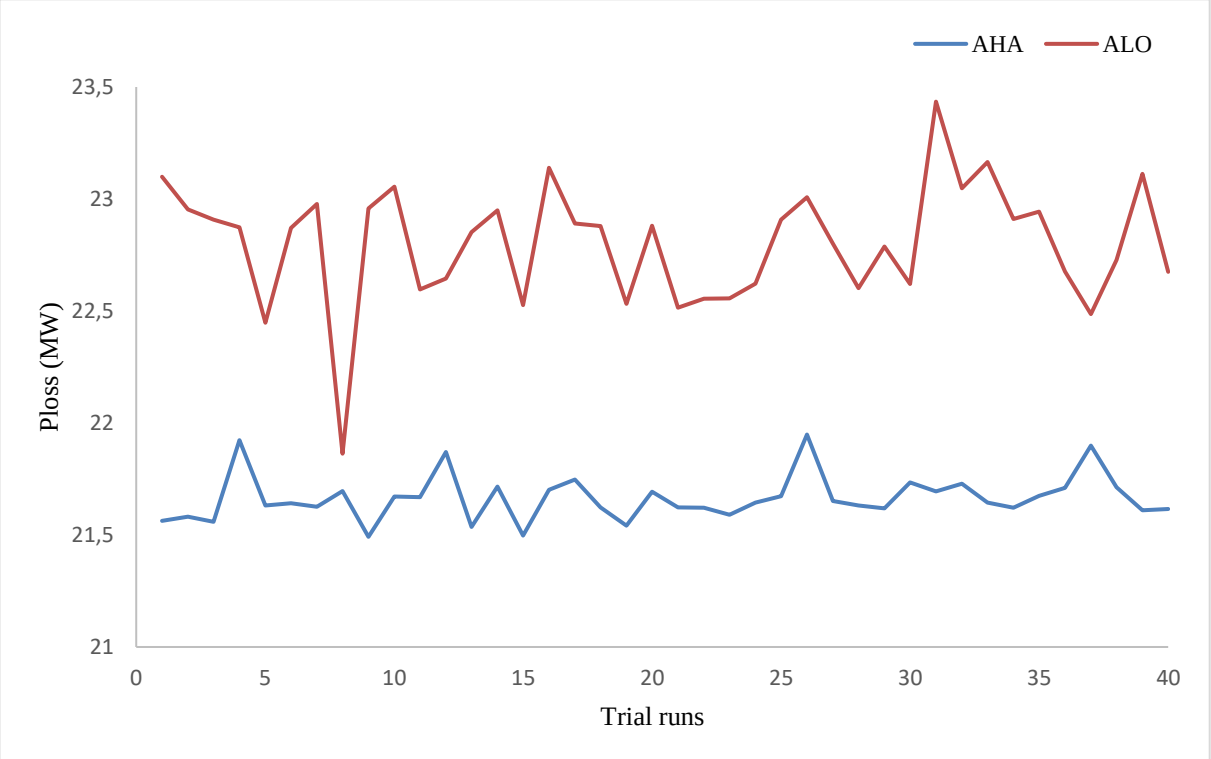

Figure 3.38. Performance of 40 search agents for 40 trial runs

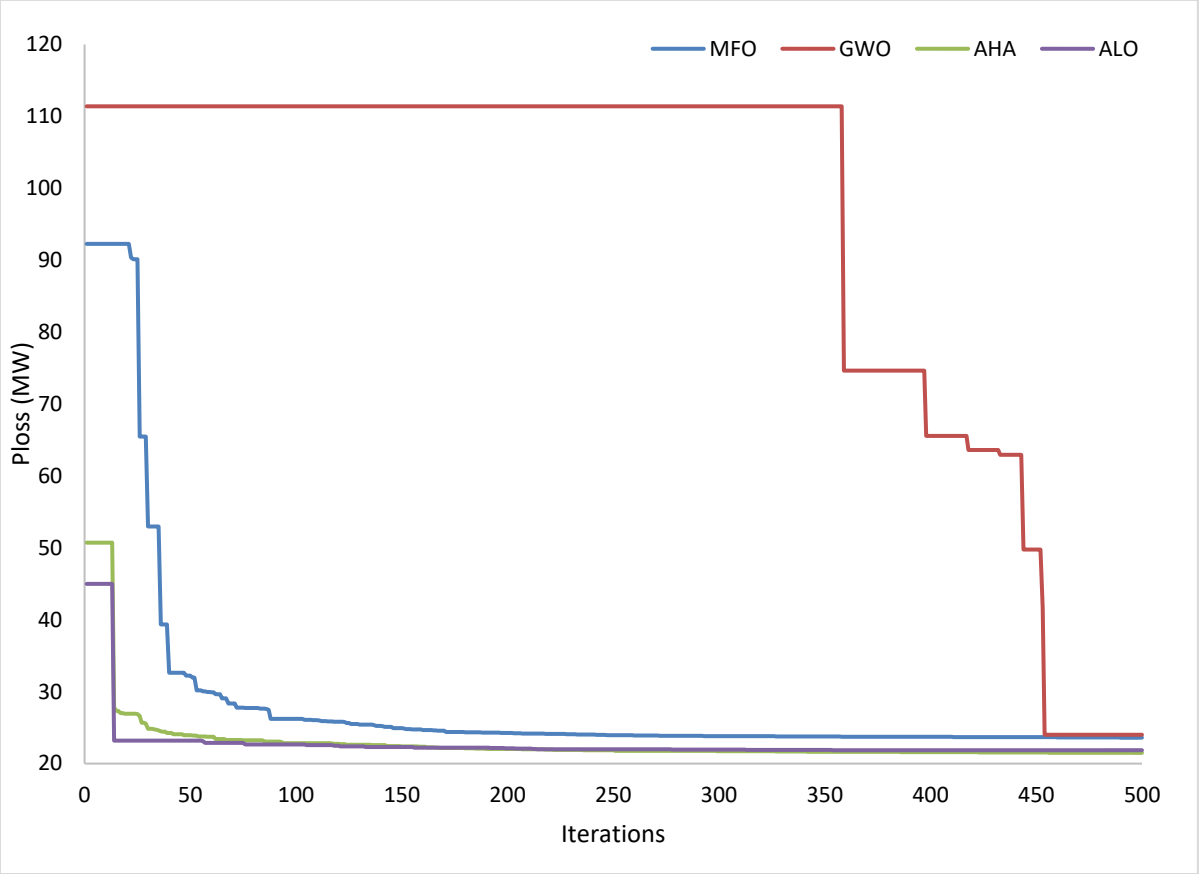

Figure 3.39. Convergence characteristic of IEEE 57-bus system for Ploss minimization

3.4.4.2. *Voltage Deviation minimization.*

The best results of control variables and power losses yielded by the proposed algorithms are tabulated in Table 3.13. According to this Table, it can be observed that the AHA yielded a TVD value of 0.5637 compared with the results 0.5747, 0.68197 and 0.6820 achieved by ALO, GWO and MFO respectively. It is also recognized from the same Table that an improvement of 63.698% in TVD has been achieved by using AHA in comparison to 62.989% with ALO, 56.081% with GWO and 56.079% with MFO. Figures 3.40 and 3.41 illustrate the Performance of all the proposed algorithms for 40 trial runs. These Figures clearly show that the proposed method AHA converges to lower value in comparison with ALO, GWO and MFO methods. The 57-bus convergence characteristics of MFO, GWO, AHA and ALO is displayed in figure 3.42. From this figure, it is clear that the convergence characteristics of TVD for the AHA and ALO outperform the two other algorithms. The voltage profile at all buses for IEEE 57-bus is depicted in Figure. 3.43. From this figure, we can see that the voltage profiles of this test system have been improved compared with the initial state in both AHA and ALO methods.

Table 3.13. Simulation results of proposed algorithms for IEEE 57-bus test system

Control variable	Initial	AHA	ALO	GWO	MFO
V_1	1.0400	1.0463	1.0173	1.0236	0.9941
V_2	1.0100	0.9288	0.9225	0.9808	0.9253
V_3	0.9850	1.0105	1.0104	1.0222	1.0429
V_6	0.9800	1.0019	1.0021	0.9768	0.9281
V_8	1.0050	1.0053	1.0070	1.0573	1.1000
V_9	0.9800	1.0461	1.0249	1.0264	0.9895
V_{12}	1.0150	0.9934	1.0078	1.0047	1.0490
T_{4-18}	0.9700	1.0268	1.0308	0.9799	0.9000
T_{4-18}	0.9780	0.9994	0.9572	1.0296	1.1000
T_{21-20}	1.0430	0.9776	0.9951	0.9832	0.9840
T_{24-26}	1.0430	1.0051	1.0042	0.9991	0.9940
T_{7-29}	0.9670	0.9818	0.9826	0.9942	1.0195
T_{34-32}	0.9750	0.9254	0.9324	0.9406	0.9320
T_{11-41}	0.9550	0.9002	0.9000	0.9013	0.9000
T_{15-45}	0.9550	0.9011	0.9250	0.9538	0.9506
T_{14-46}	0.9000	1.0031	0.9736	0.9562	0.9655
T_{10-51}	0.9300	1.0010	1.0033	0.9959	1.0096
T_{13-49}	0.8950	0.9000	0.9000	0.9002	0.9000
T_{11-43}	0.9580	0.9872	0.9874	0.9905	0.9932
T_{40-56}	0.9580	1.0052	0.9700	0.9814	0.9000
T_{39-57}	0.9800	0.9160	0.9130	0.9651	0.9511
T_{9-55}	0.9400	1.0465	1.0099	0.9892	0.9909
Q_{C18}	0.0000	13.4437	13.8252	0.1223	0.1588
Q_{C25}	0.0000	12.4409	15.1368	0.1609	0.1728
Q_{C53}	0.0000	25.9873	21.7412	0.0574	0.2855
TVD (pu)	1.5528	0.5637	0.5747	0.68197	0.6820
Ploss (MW)	28.4623	46.9736	41.0056	30.8434	91.0664
TVD Red (%)	-	63.698	62.989	56.081	56.079

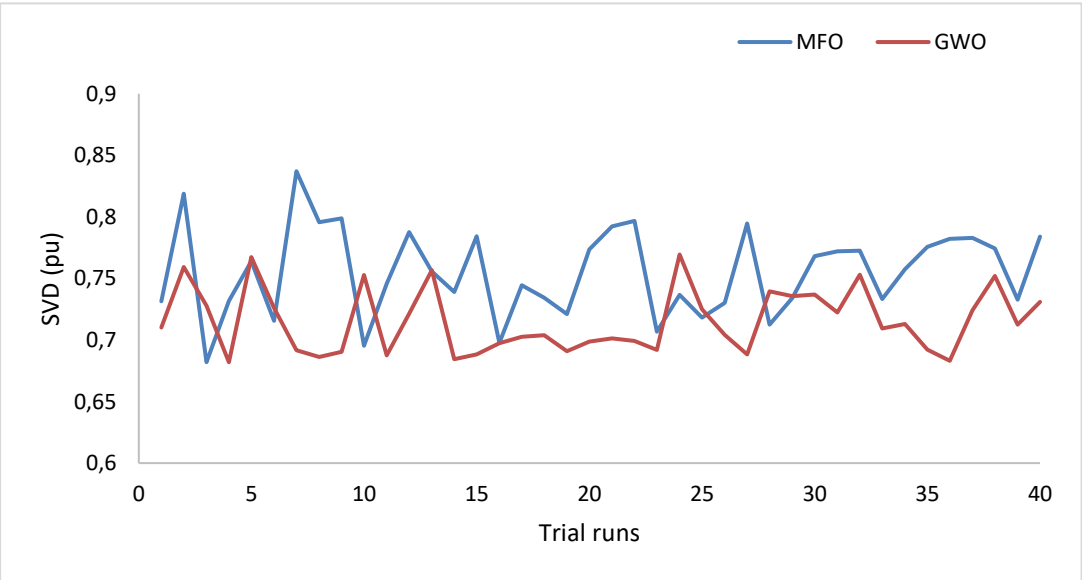

Figure 3.40. Performance of 30 search agents for 40 trial runs

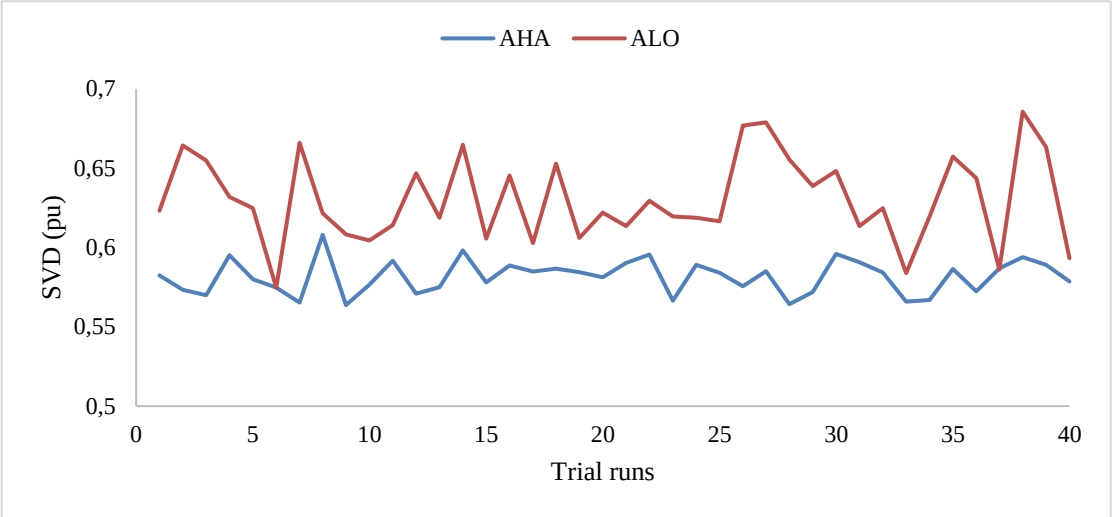

Figure 3.41. Performance of 40 search agents for 40 trial runs

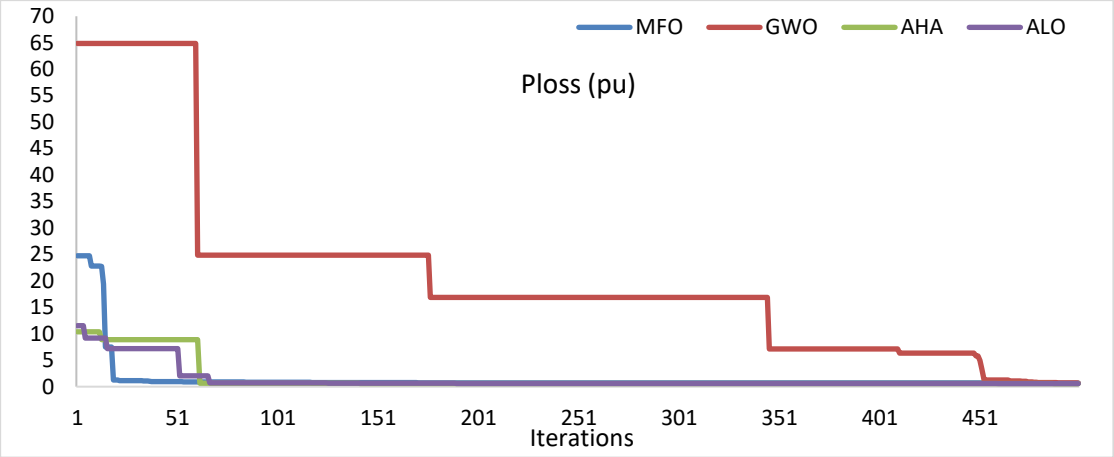

Figure 3.42. Convergence characteristic of IEEE 57-bus system for TVD minimization

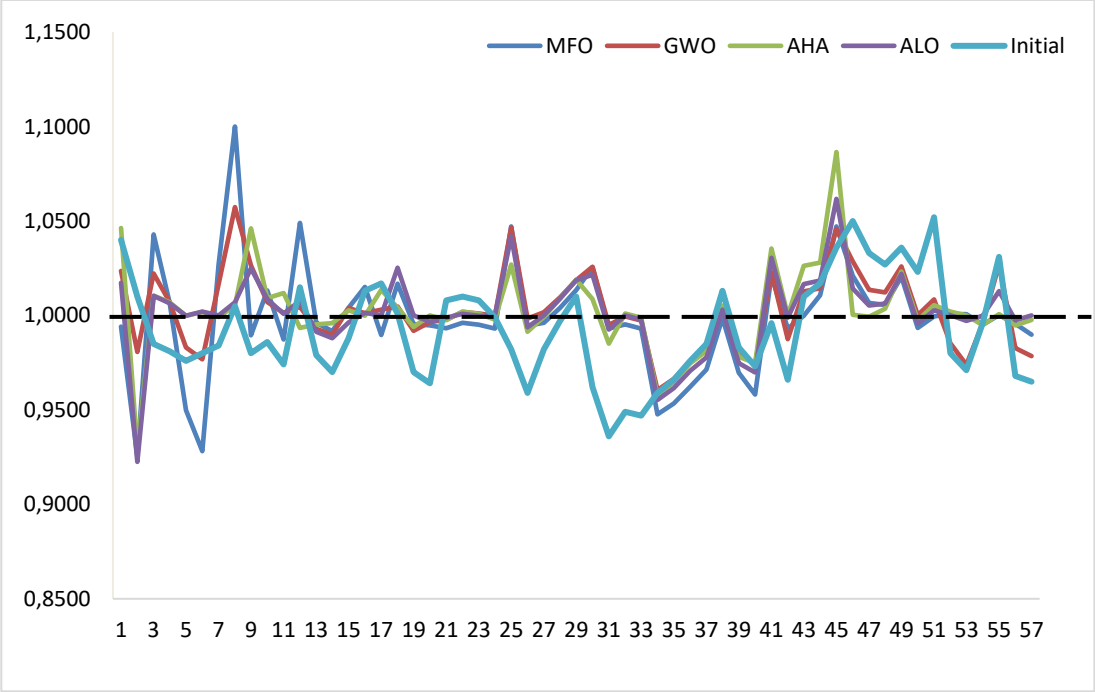

Figure 3.43. Voltage profiles of IEEE 57-bus system for TVD minimization

3.4.5. ORPD simulation (case of IEEE 118-bus test system)

To test the potential of proposed algorithms in solving large scale systems the standard IEEE 118 bus test system is considered. The single-line diagram of the IEEE 118-bus test system is shown in Figure 3.44. This test system has 54 generator buses, 64 load buses, 186 transmission lines, 9 transformer taps and 14 reactive power sources. In this case, the search space of this system has 77 dimensions, that is, 54 generator buses, 9 transformer taps and 14 reactive power sources. The system line data, bus data, variable limits and the initial values of control variables are available in [9],[128]. The load demand is 4242 MW and 1438 MVar on 100MVA base. The initial total generations and power losses are: P_G = 43.7536 p.u., Q_G = 8.8192 p.u., P_{loss} = 1.33357 p.u. the limits values of voltages for all generating units and tap setting transformer control variables are considered to be 0.9–1.1 in p.u, the maximum and minimum values for voltages at all load buses are 1.06 and 0.94 in p.u, respectively. In this large electrical test system two objective functions are considered, the active power losses and voltage deviation.

3.4.5.1. *Active power loss minimization.*

for this case, the proposed metaheuristic algorithms namely AHA, ALO, GWO and MFO are implemented to minimize active power losses. The best ORPD solutions and the corresponding control variables settings obtained by the proposed approaches in 40 trials are presented in

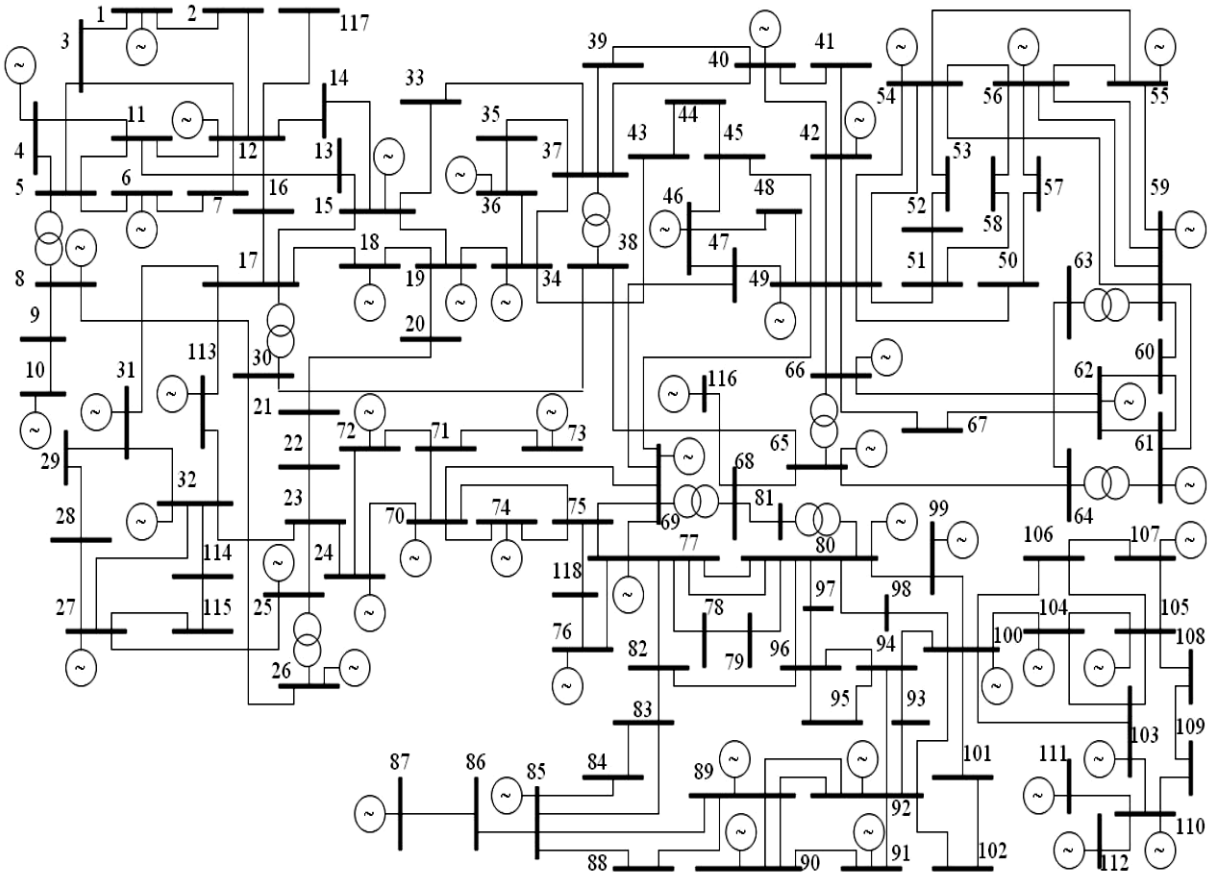

Figure 3.44. Single line diagram of IEEE 118 bus system

Figure 3.45 and Table 3.14. The results indicate that applying These methods lead to 107.6843 MW, 107.6475 MW, 122.878 MW and 111.4051 MW respectively. It can be seen also from Table 3.14 that a 18.979 % decrease (from the initial power loss of 132.8630 MW) in active power loss is achieved with the ALO algorithm, which performs better than AHA, GWO and MFO algorithms which reduced losses by only 18.951%, 7.515% and 16.150% respectively. Table 3.15 which compares the proposed algos with other algorithms in the literature, indicates that ALO approach achieved the biggest reduction of active power loss in comparison to that obtained by the other approaches in particular, SFS and QOTLBO which reduces active power losses by 14,934% and 15,493% respectively. The performance of AHA, ALO, GWO and MFO for 40 independent trial runs is shown in Figure 3.46 and 3.47. From these figures, it can be seen that the difference between worst and best solution doesn't exceed 1.8 MW for the ALO method and doesn't exceed 4 MW for the GWO and AHA methods. This clearly reflects the stability and robustness of the ALO algorithm in term of exploring the optimal solution at each trial, compared with the other algorithms. The convergence characteristics of all implemented algorithms for 118-bus system is shown in Figure 3.48. According to this Figure, it is clearly that ALO algorithm converges to optimal real power loss after less than 75 iterations. Based on the real power loss and convergence characteristics, it is come to an end that the ALO algorithm provides superior results than the other implemented algorithms.

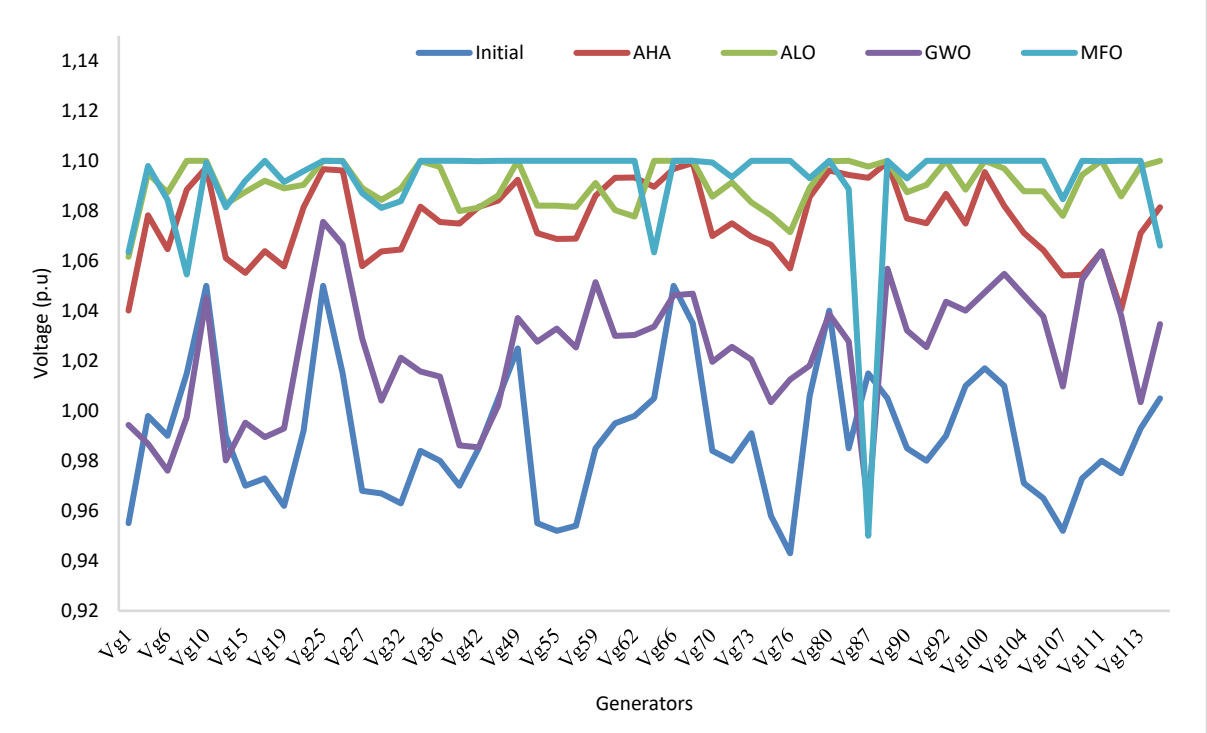

Figure 3.45. Generator voltages of IEEE 118 bus system

Table 3.14. Simulation results of proposed algorithms for IEEE 118-bus test system

Control Variables	Initial	AHA	ALO	GWO	MFO
T_8	0.9850	0.9963	1.0167	0.9624	0.9000
T_{32}	0.9600	1.0773	1.0096	1.0012	0.9000
T_{36}	0.9600	1.0005	1.0233	1.0011	0.9507
T_{51}	0.9350	0.9887	1.0227	0.9476	0.9000
T_{93}	0.9600	0.9875	1.0296	0.9179	0.9467
T_{95}	0.9850	0.9849	1.0706	0.9898	0.9000
T_{102}	0.9350	1.0197	1.1000	1.0619	1.0944
T_{107}	0.9350	0.9563	1.0792	0.9236	0.9000
T_{127}	0.9350	0.9644	1.0163	0.9326	0.9655
Q_{C5}	0.0000	-21.4094	-19.4555	-15.1507	-40.000
Q_{C34}	0.0000	2.4593	8.8726	4.1052	13.9977
Q_{C37}	0.0000	-2.8253	-10.5976	-12.6576	-15.0000
Q_{C44}	0.0000	5.6260	4.3510	9.6675	7.7034
Q_{C45}	0.0000	6.0608	9.6419	3.2449	7.9514
Q_{C46}	0.0000	4.8216	4.5536	6.8210	8.1223
Q_{C48}	0.0000	2.2088	8.5382	6.0974	10.0000
Q_{C74}	0.0000	4.5928	8.3175	2.4338	0.0000
Q_{C79}	0.0000	16.0019	1.4969	13.4165	19.9532
Q_{C82}	0.0000	17.8840	12.2959	6.2711	0.0000
Q_{C83}	0.0000	8.6921	3.4439	4.8435	0.0000
Q_{C105}	0.0000	8.5596	10.2205	12.6798	20.000
Q_{C107}	0.0000	3.0726	4.0117	2.8928	5.7356
Q_{C110}	0.0000	2.7430	2.1072	5.3290	4.4769
Ploss (MW)	132.8630	107.6843	107.6475	122.878	111.4051
TVD	/	4.5456	5.5389	1.1651	5.2609
Ploss Red (%)	/	18.951	18.979	7.515	16.150

Table 3.15. Comparative results of IEEE 118-bus test system

Methods	Ploss (MW)	Reduction (%)	Methods	Ploss (MW)	Reduction (%)
PSO-TVIW [129]	116,8976	12,016	SFS [129]	113,0213	14,934
PSO-TVAC [129]	124,3335	6,420	ABC [130]	117,9922	11,193
SPSO-TVAC [129]	116,2026	12,540	BRCFF [130]	116,5817	12,254
PSO-CF [129]	115,6469	12,958	TLA [130]	116,0682	12,641
PG-PSO [129]	116,6075	12,235	DE [130]	119,2770	10,226
SWT-PSO [129]	124,1476	6,5600	MTLA [130]	114,2213	14,031
PGSWTPSO [129]	119,4270	10,113	DDE [130]	116,4792	12,331
MPG-PSO [129]	115,0600	13,400	MTLA-DDE [130]	113,9814	14,211
SARCGA [129]	113,1200	14,860	**GWO**	**122,8780**	**7,5150**
HEP [129]	115,5800	13,008	**MFO**	**111,4051**	**16,150**
QOTLBO [24]	112,2789	15,493	**AHA**	**107,6843**	**18,951**
TLBO [24]	116,4003	12,391	**ALO**	**107,6475**	**18,979**

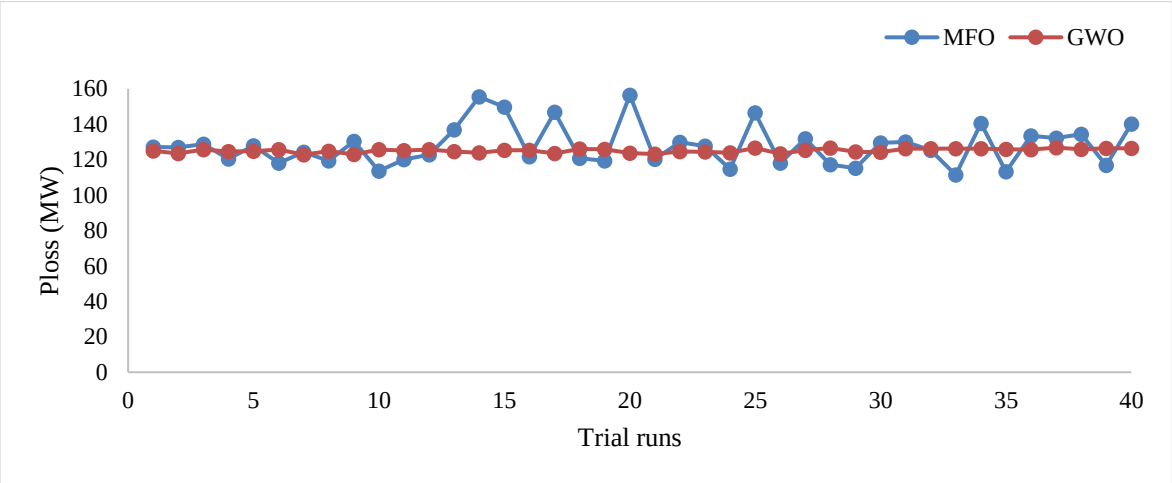

Figure 3.46. Performance of 30 search agents for 40 trial runs

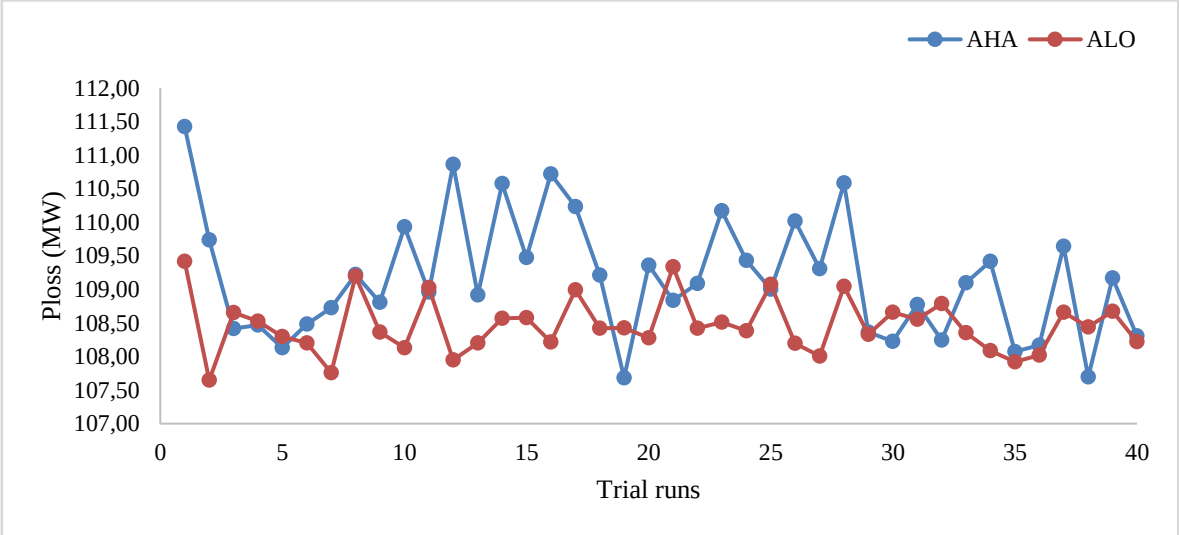

Figure 3.47. Performance of 40 search agents for 40 trial runs

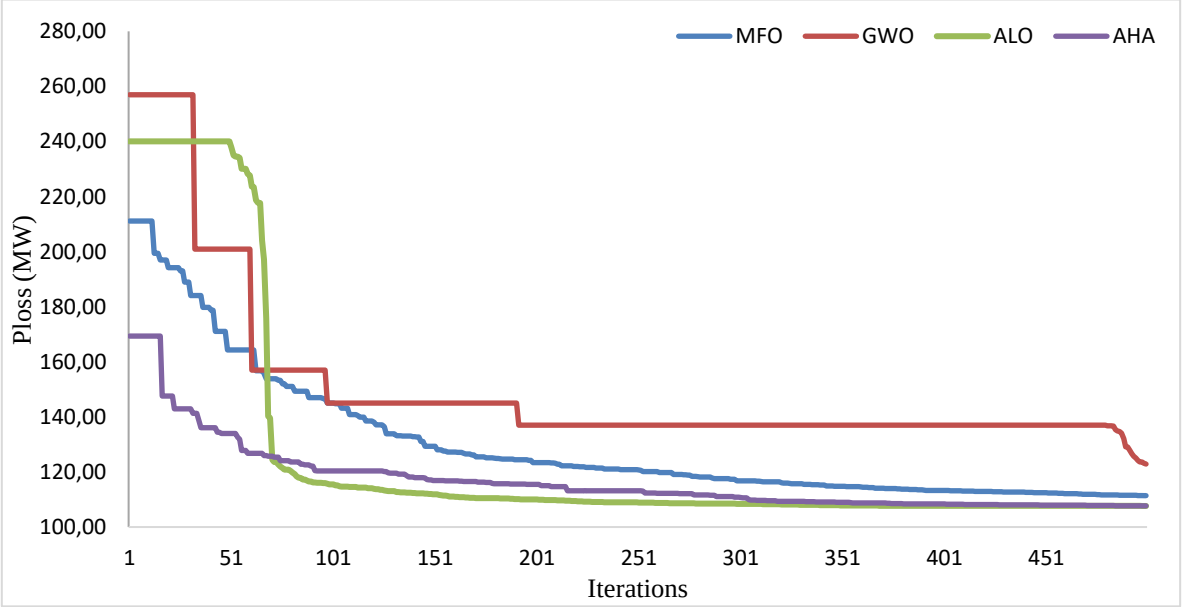

Figure 3.48. Convergence characteristic of IEEE 118-bus system for Ploss minimization

3.4.5.2. *Voltage Deviation minimization.*

The optimal solutions obtained by AHA, ALO, GWO and MFO for the objective of voltage profile improvement of IEEE 118 bus system are given in Figure 3.49 and Table 3.16. It may be noted that all the control variables are in their specified limits. It is observed from the simulation results of this table that, in the 40 independent runs performed, the proposed algorithms have substantially reduced voltage deviation. Initially, the total voltage deviation was 1.43933 p.u. It can be seen that the TVD obtained by AHA, ALO, GWO and MFO are 0.2203 p.u (84.694% reduction), 0.2638 p.u (81.669% reduction), 0.2859 p.u (80.132% reduction) and 0.3360 p.u (76.653% reduction) respectively. Moreover, it is observed that the voltage profile improvement is most significant for AHA among all the algorithms. Consequently, the proposed AHA algorithm not only benefits from high quality solutions, but also by guarantee the feasibility of solutions for large-scale test system. The voltage profiles of all load buses for this case of all proposed methods are depicted in Figure 3.53. It can be seen that all bus voltage magnitudes are within the admissible limits. The convergence curves of the total voltage deviation for IEEE 118-bus system for four implemented algorithms AHA, GWO and MFO is presented in Figure 3.52. According to this Figure, it is clearly that proposed algorithm converges to optimal TVD after less than 120 iterations. Figure 3.50 and Figure 3.51 disclose the performance of all proposed algorithms for 40 independent execution runs. It observed that the best and worst results of AHA are 0.2121 p.u and 0.3461 p.u, respectively in which difference between them is no longer than 0.134 p.u.

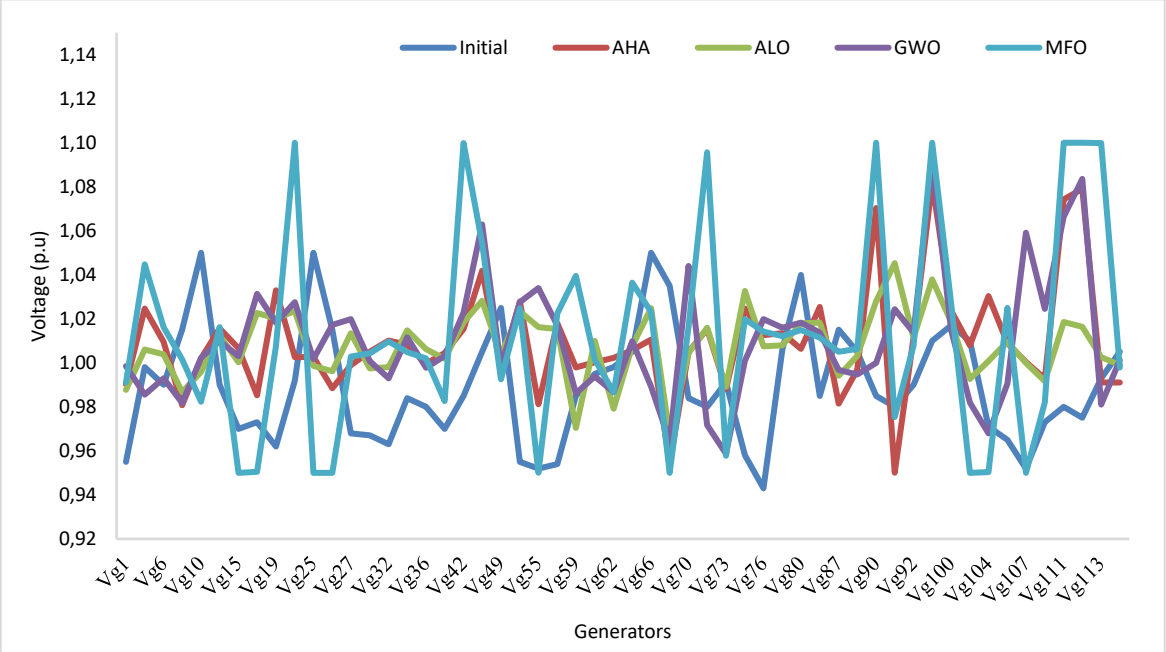

Figure 3.49. Generator voltages of IEEE 118 bus system

Table 3.16. Simulation results of proposed algorithms for IEEE 118-bus test system

Control Variables	Initial	AHA	ALO	GWO	MFO
T_8	0.9850	0.9798	0.9326	0.9387	1.0335
T_{32}	0.9600	1.0484	0.9440	0.9098	0.9000
T_{36}	0.9600	1.0065	0.9858	0.9954	0.9932
T_{51}	0.9350	0.9791	0.9731	0.9582	0.9717
T_{93}	0.9600	0.9888	1.0139	1.0263	0.9620
T_{95}	0.9850	0.9980	0.9975	0.9921	0.9696
T_{102}	0.9350	1.0076	0.9739	1.0178	0.9000
T_{107}	0.9350	1.0869	0.9872	0.9669	0.9149
T_{127}	0.9350	0.9793	0.9684	0.9616	0.9842
Q_{C5}	0.0000	-35.0337	-25.7814	-15.3768	-0.0725
Q_{C34}	0.0000	13.8517	5.2623	7.9276	0.0000
Q_{C37}	0.0000	-13.8341	-4.8685	-5.9316	-8.9112
Q_{C44}	0.0000	9.9654	1.1697	2.4040	8.8190
Q_{C45}	0.0000	9.4345	9.2826	8.7758	10.000
Q_{C46}	0.0000	7.3992	4.5030	2.6082	0.0000
Q_{C48}	0.0000	0.2283	4.7879	6.3307	0.0000
Q_{C74}	0.0000	6.4251	11.2930	8.6687	11.7248
Q_{C79}	0.0000	9.9770	8.8584	1.2169	0.0009
Q_{C82}	0.0000	19.7495	17.8508	16.7987	19.2552
Q_{C83}	0.0000	1.6203	5.8952	6.2343	10.0000
Q_{C105}	0.0000	10.2114	3.1191	3.1189	0.0000
Q_{C107}	0.0000	2.5711	5.4032	1.3913	0.0000
Q_{C110}	0.0000	0.6602	4.4634	2.3626	5.9861
TVD	1.43933	0.2203	0.26384	0.28597	0.33604
P_{Loss}(MW)	/	170.9650	144.8889	162.6252	237.8739
Red (%)	/	84.694	81.669	80.132	76.653

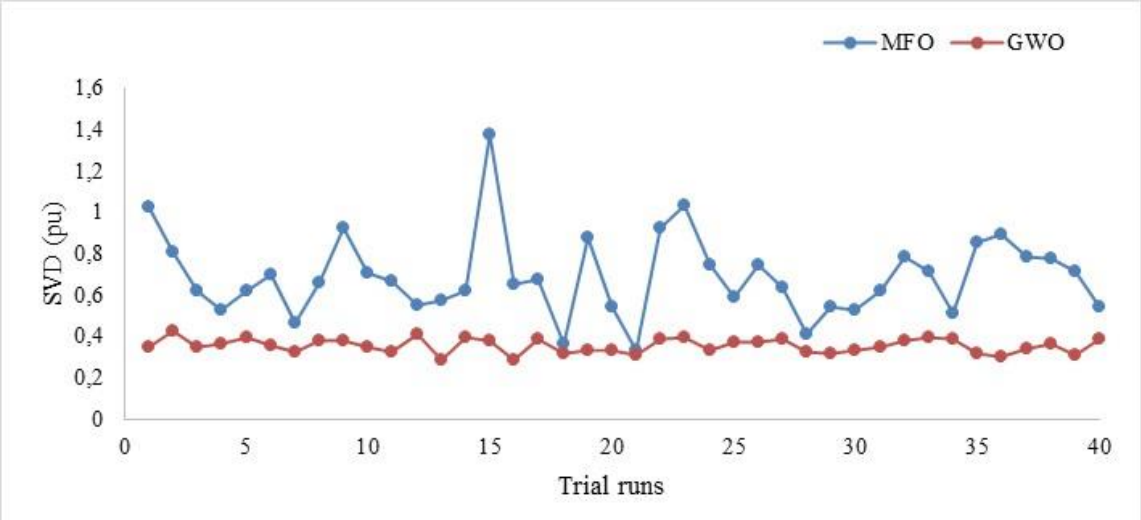

Figure 3.50. Performance of 30 search agents for 40 trial runs

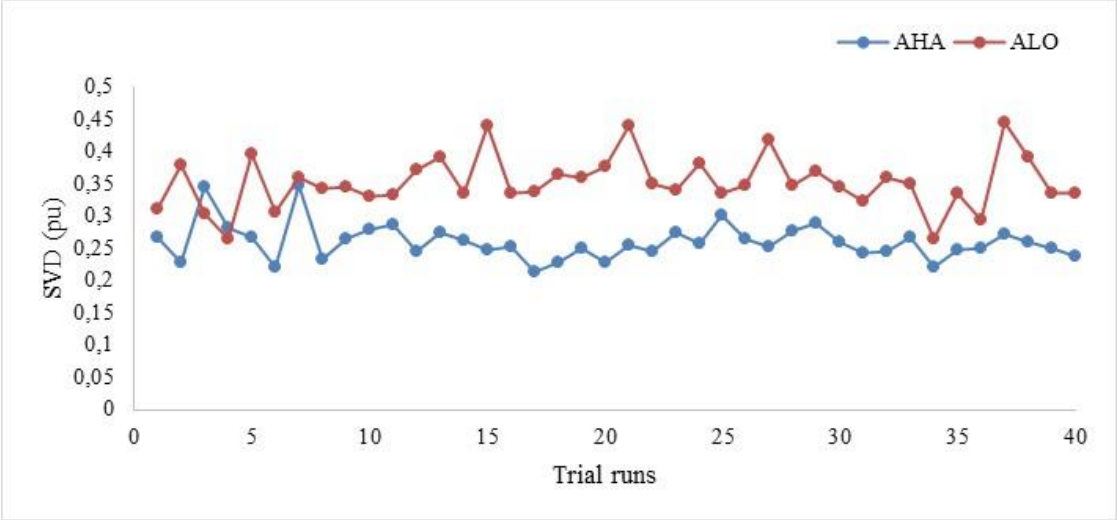

Figure 3.51. Performance of 40 search agents for 40 trial runs

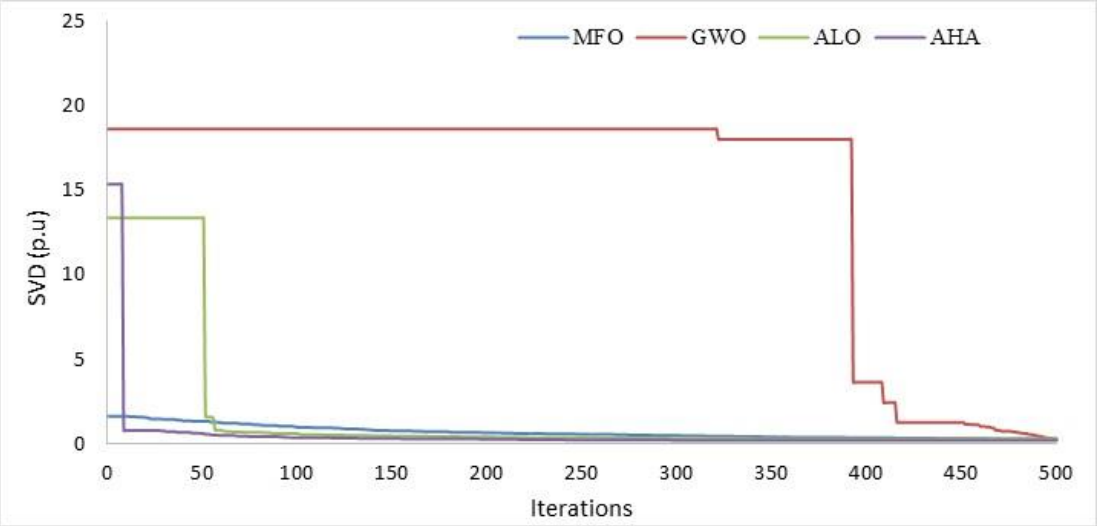

Figure 3.52. Convergence characteristic of IEEE 118-bus system for TVD minimization

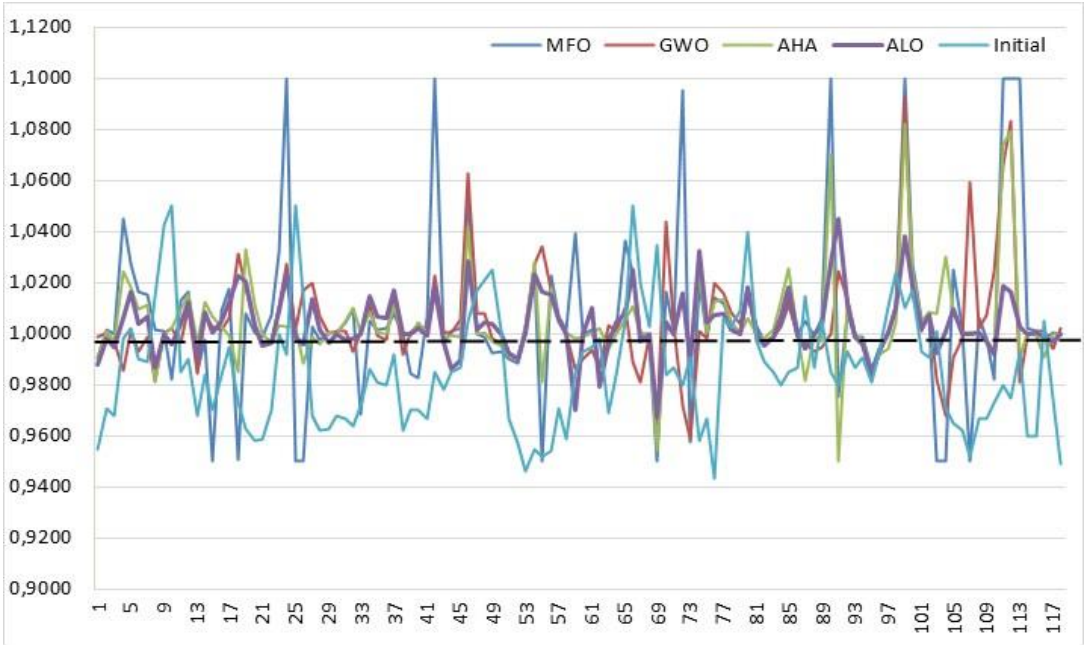

Figure 3.53. Voltage profiles of IEEE 118-bus system for TVD minimization

3.5. Statistical analysis

Several metaheuristic algorithms have been used to solve the optimal reactive power dispatch problem. The performance of these algorithms is strongly related to its parameterization and to the structure of the problem to optimize. The choice of the metaheuristic is a complex task that requires a good knowledge of the algorithm and the problem to be optimized. As these algorithms are iterative stochastic processes, evaluating their performance requires the use of the appropriate statistical tools [131]. Several tests were carried out throughout this work in order to conduct statistical studies to confirm the effectiveness of the proposed methods. For this reason, we are going to focus on two statistical study methods, namely: the Box-and-whisker plot also known as the Box plot and the analysis of a one-way Analysis of Variance (ANOVA). The statistical studies were carried out on the results obtained by AHA, ALO, GWO and MFO for the objective of voltage minimization of active power losses. These two statistical analysis methods (Box plot and One-way ANOVA) were applied to the results obtained by the different test systems namely IEEE 14-bus, IEEE 30-bus, IEEE 57-bus and IEEE 118-bus. The one-factor analysis of variance was carried out using Excel 2013, and the whisker box-plot using R software.

3.5.1. Box-and-whisker plot (Box-plot)

3.5.1.1. *Definition of Box-and-whisker plot*

The method to summarize a set of data that is measured using an interval scale is called a box and whisker plot and commonly also known as a boxplot. It is a statistical visualization that provides a graphical representation of the distribution of a dataset. In most cases, a histogram analysis provides a sufficient display, but a box and whisker plot can provide additional details. The box-plot is a useful way to compare different sets of data as you can draw more than one box-plot per graph. The shape of the box-plot shows how the data is distributed and it also shows any outliers. It is easy to see where the main bulk of the data is, and make that comparison between different groups. These can be displayed alongside a number line, horizontally or vertically. Box and whisker plot displays the five-number summary of a set of data:

- Minimum and Maximum: The smallest and largest values in the dataset, excluding outliers (if they exist).
- Quartiles (Q1, Q2(Median), Q3): Quartiles divide the dataset into four equal parts. Q1 represents the boundary below which 25% of the data falls, Q2 (the median) marks the midpoint where 50% of the data lies below and above it, and Q3 denotes the boundary below which 75% of the data falls.
- Interquartile Range (IQR): The range between Q1 and Q3, covering the middle 50% of the dataset.

- Whiskers: Lines extending from the box in both directions that indicate the range of the non-outlier data. They can represent different ranges, often calculated based on the IQR or extend to the minimum and maximum within a specified range.
- Outliers: Data points lying beyond the whiskers, considered as anomalies or extreme values in the dataset.

The Construction of a box plot is based around a dataset's quartiles, or the values that divide the dataset into equal fourths. The first quartile (Q1) is greater than 25% of the data and less than the other 75%. The second quartile (Q2) sits in the middle, dividing the data in half. Q2 is also known as the median. The third quartile (Q3) is larger than 75% of the data, and smaller than the remaining 25%. In a box and whiskers plot, the ends of the box and its center line mark the locations of these three quartiles (figure 3.54). Among the software that can create box plots is R, which offers solid capabilities for creating, visualizing and analyzing data using box-plots.

3.5.1.2. *The software "R"*

R is a programming language and software environment used primarily for statistical analysis, data visualization and graphics. It is an open-source software widely used in statistics, data science and academic research. It provides a wide variety of statistical and graphical techniques and is highly extensible with numerous packages available for various purposes. R is popular among statisticians, data miners, and analysts for its robustness in data analysis, visualization, and machine learning. It's an open-source platform, fostering a strong community that contributes to its evolution and the creation of new packages and functionalities. The R software environment includes an extensive collection of libraries, a command-line interface, and a graphical interface (like RStudio) that facilitate data analysis, statistical modeling, and the creation of visualizations and reports. Its flexibility and robustness have made it a popular choice among statisticians, data analysts, researchers, and anyone working with data-driven decision-making processes.

3.5.1.3. *Box-and-whisker plot applications on test systems*

3.5.1.4. *Box-plot applied on IEEE 14-bus test system*

Table 3.17 shows the mean, standard deviation (SD), interquartile range (IQR), median, first and third quartile, minimum and maximum of the trials for the three algorithms (AHA, ALO, GWO and MFO) for minimizing active power losses. Based on this data, we were able to produce a Box and whisker for this test system, considering 40 independent trials, as shown in Figure 3.55. It can be seen that the standard deviation of AHA, ALO, GWO and MFO are 0.01803617 (MW), 0.02724562 (MW), 0.01862761 (MW) and 0.01332164 (MW) respectively,

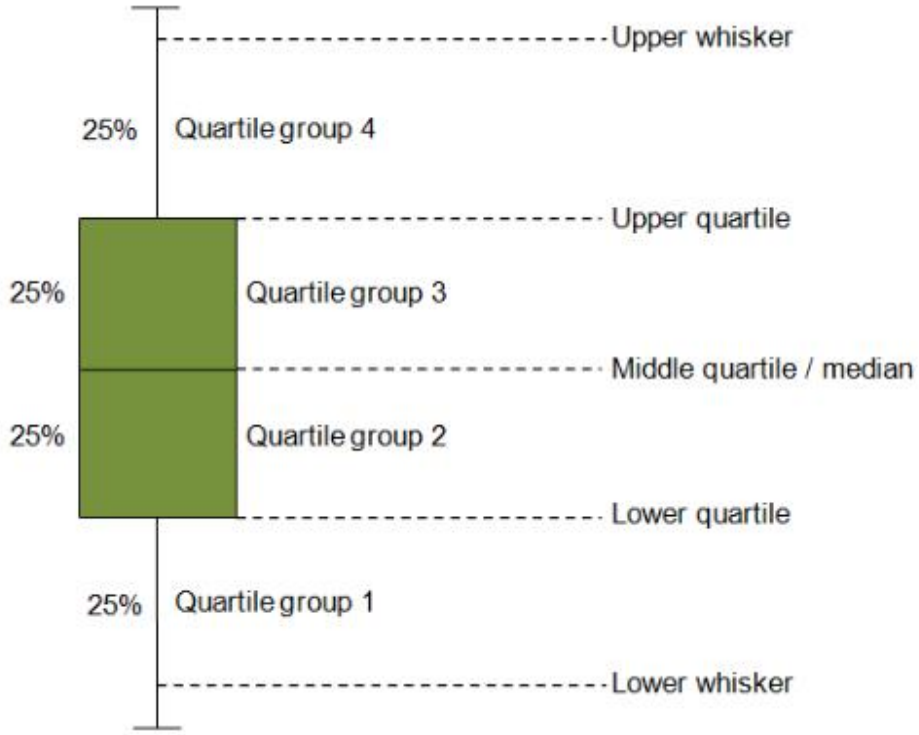

Figure 3.54. Different parts of Box-plot

Table 3.17. The statistical results of the experimental simulation (IEEE 14-bus test system)

Methods	Mean	SD	IQR	Min	1st quartile	Median	3rd quartile	Max
AHA	12.24619	0.01803617	0.018825	12.2325	12.23412	12.23950	12.25295	12.3136
ALO	12.27343	0.02724562	0.035900	12.2284	12.25445	12.27335	12.29035	12.3389
GWO	12.48572	0.01862761	0.022625	12.4227	12.47575	12.48730	12.49837	12.5261
MFO	12.46005	0.01332164	0.019750	12.4470	12.44837	12.45625	12.46813	12.4896

which means that the values obtained by these methods are all close to their means. The smallest value of the standard deviation is that of MFO (0.01332 MW). It is also notable that the interquartile range (0.018825) and the mean (12.24619) and the minimum solution (12.2325 MW) of AHA are lower than that of the other algorithms which means that AHA has the most homogeneous values. We can therefore conclude that the AHA method performs best in minimizing active losses in this network. More generally, we can say that the proposed method is the most efficient for solving the optimal power flow problems of the IEEE 14-bus system.

3.5.1.5. *IEEE 30-bus test system*

As with the previous test network, the same work was carried out on the IEEE 30-bus system. Table 3.18 shows the statistical results of the experimental simulation. We can see that the lowest (Best) value of active losses was found by the AHA method (4.5168 MW) and the

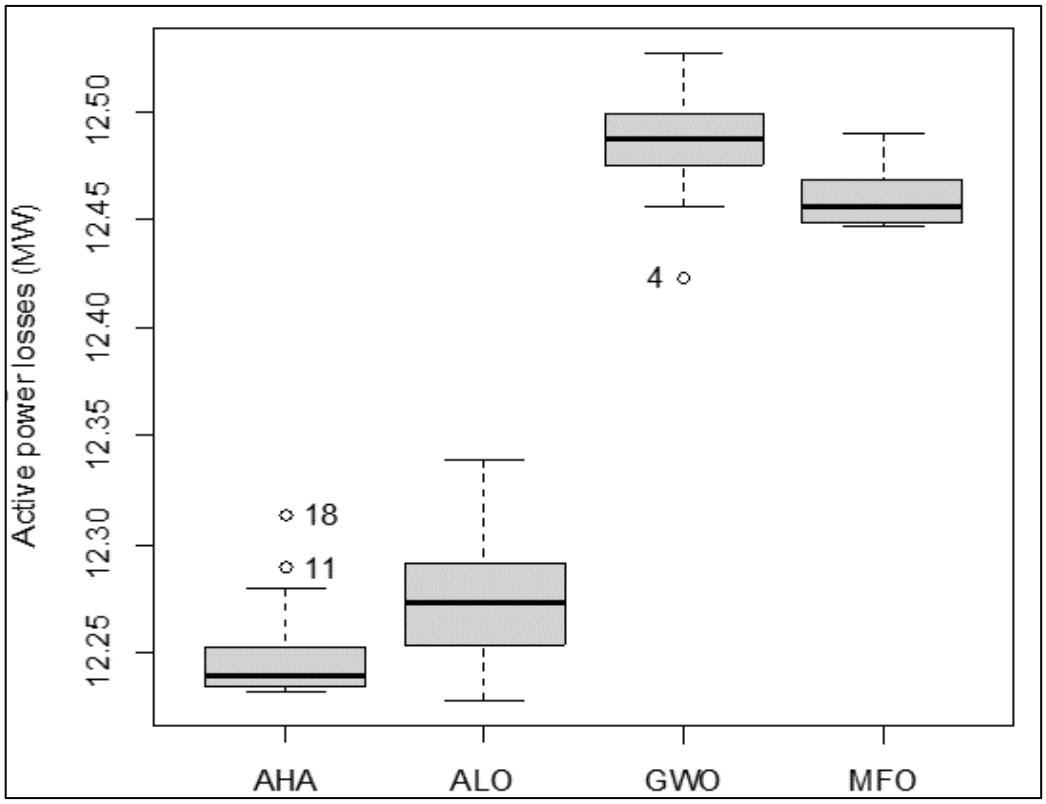

Figure 3.55. Box-and-whisker plot of IEEE 14-bus test system

highest by the MFO method (5.2400 MW). The best mean (4.516820 MW) is also found by the AHA method. Figure 3.56 shows three points beyond the maximum values of the AHA method, which represent the outliers (extreme values) of this method located in 4th and 10th position. The lowest standard deviation is that of the AHA method (0.006499515 MW), which means that its rate of dispersion around its mean is very low compared with the other methods. AHA also has the lowest standard deviation (0.006499515 MW), which means that its rate of dispersion around its mean is very low compared with other methods. AHA is also the most homogeneous of the other algorithms because its interquartile range (Q3-Q1) is the lowest (0.002375 MW). We can therefore conclude that, the AHA method performs very well when optimizing the IEEE 30-bus system and can determine the optimal solution.

Table 3.18. The statistical results of the experimental simulation (IEEE 30-bus test system)

Methods	Mean	SD	IQR	Min	1st quartile	Median	3rd quartile	Max
AHA	4.516820	0.006499515	0.002375	4.5127	4.514550	4.51540	4.516925	4.5547
ALO	4.573372	0.020012483	0.025800	4.5315	4.560025	4.56955	4.585825	4.6152
GWO	4.925835	0.015852179	0.015375	4.8733	4.920475	4.92745	4.935850	4.9478
MFO	5.108980	0.036282610	0.021475	5.0776	5.087925	5.09745	5.109400	5.2400

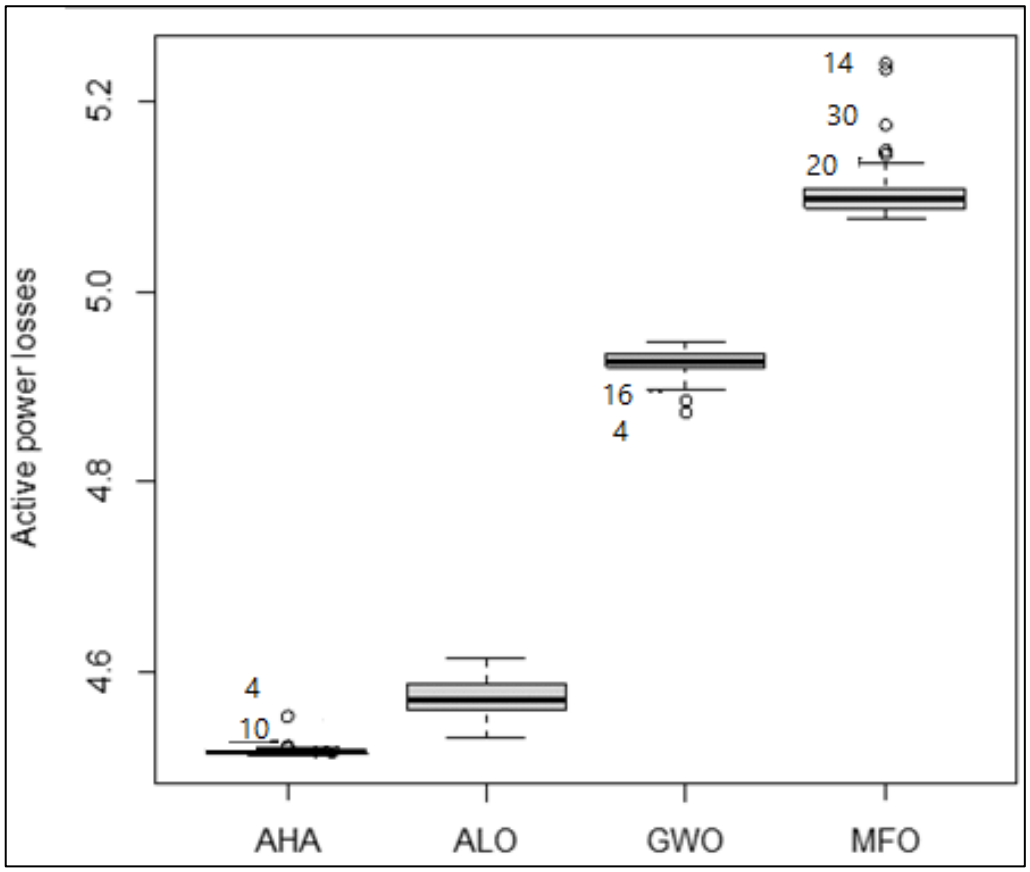

Figure 3.56. Box-and-whisker plot of IEEE 30-bus test system

3.5.1.6. *IEEE 57-bus test system*

Table 3.19 shows the statistical results of the experimental simulation. The best mean, the lowest standard deviation and the lowest IQR are found by the AHA method which are: 21.66581 MW, 0.1030830 and 0.085275 respectively. We can see also that the lowest value of active power losses is found by the AHA method (21.4918 MW) and the highest by the MFO method (25.2779 MW). From figure 3.57 we can see that, for the two methods ALO and GWO, the distribution is positively asymmetrical, as the top portion of the box and the top whiskers are longer than the bottom of the median. The distribution of the MFO method is approximately symmetrical, as the two halves of the box are of roughly equal length. The distribution of the AHA method is the most concentrated, as the interquartile range is 0.085275 compared with 0.339725 for ALO, 0.383850 for GWO and 0.805625 for MFO. which means that the rate of dispersion of AHA method around its mean is very low. The center of the distribution for the MFO method is the highest of the four methods (median at 24.52019). The distribution of the GWO method includes potentially extreme values. There are two extreme values, one at position 10 and the other at position 17. The statistical analysis of this research illustrated that AHA is able to produce competitive results by yielding lower power loss than the other algorithms.

Table 3.19. The statistical results of the experimental simulation (IEEE 57-bus test system)

Methods	Mean	SD	IQR	Minimum	1st quartile	Median	3rd quartile	Max
AHA	21.6658	0.1030830	0.085275	21.4918	21.61848	21.64490	21.70375	21.9483
ALO	22.8012	0.2705268	0.339725	21.8631	22.61530	22.87215	22.95502	23.4346
GWO	24.4286	0.3223250	0.383850	24.0086	24.19592	24.37025	24.57977	25.2475
MFO	24.5201	0.5028831	0.805625	23.6101	24.12148	24.57225	24.92710	25.2779

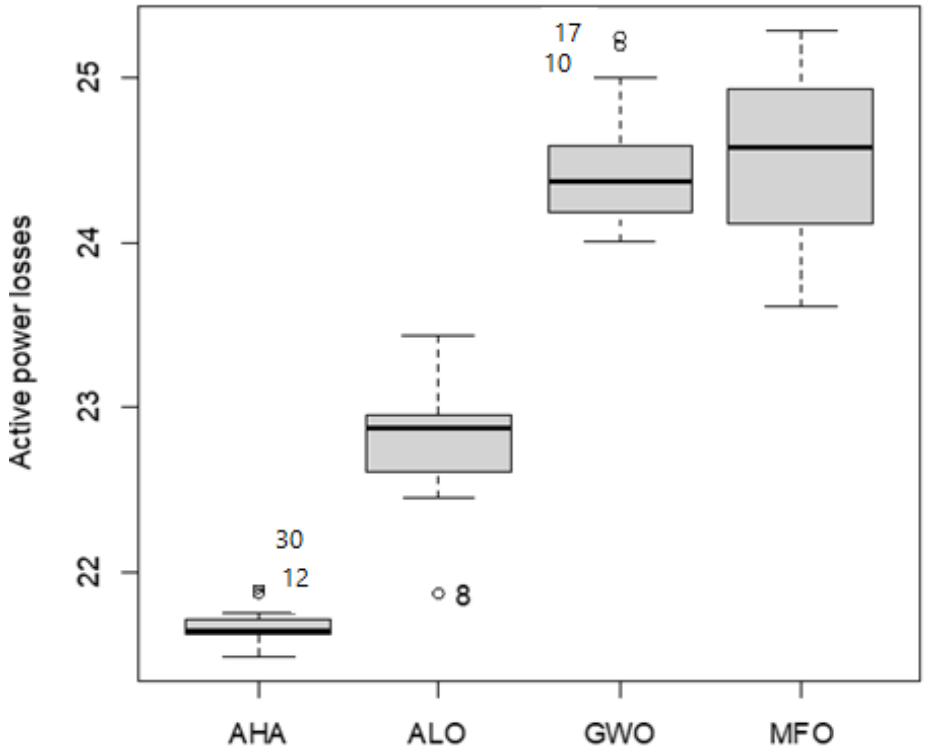

Figure 3.57. Box-and-whisker plot of IEEE 57-bus test system

3.5.1.7. *IEEE 118-bus test system*

The statistical performances like, mean, standard deviation, best solution and IQR of active power losses obtained in 40 trials are reported in Table 3.20. The results obtained show that the active power losses values obtained by AHA (107.6843 MW) and ALO (107.6475 MW) are nearer to their means (109.1746 MW, 108.4633 MW) respectively. The distribution of the AHA and ALO methods are the most concentrated with an IQR of 1.208100 and 0.455925 respectively. The Standard deviation of AHA method (0.9010233) and ALO method (0.4124813) are lesser than the other techniques. From figure 3.58. We can see that the range of AHA, ALO and GWO methods is very small, which means that the solutions found by these three methods are homogeneous. The distribution of MFO method is positively asymmetric. The centers of the distribution for the AHA and ALO method are the lowest (109.1746 and 108.4633) respectively. The statistical analysis of this research illustrated that AHA and ALO algorithms can be used for solving Optimal reactive power dispatch problems successfully.

Table 3.20. The statistical results of the experimental simulation (IEEE 118-bus test system)

Methods	Mean	SD	IQR	Min	1st quartile	Median	3rd quartile	Max
AHA	109.174	0.9010233	1.208100	107.684	108.4567	109.094	109.6648	111.423
ALO	108.463	0.4124813	0.455925	107.647	108.2037	108.421	108.6596	109.415
GWO	125.1201	1.1270939	1.618175	122.8780	124.3752	125.3768	125.9933	126.8411
MFO	127.9176	11.5391521	13.112600	111.4051	119.4520	127.0788	132.5646	156.5084

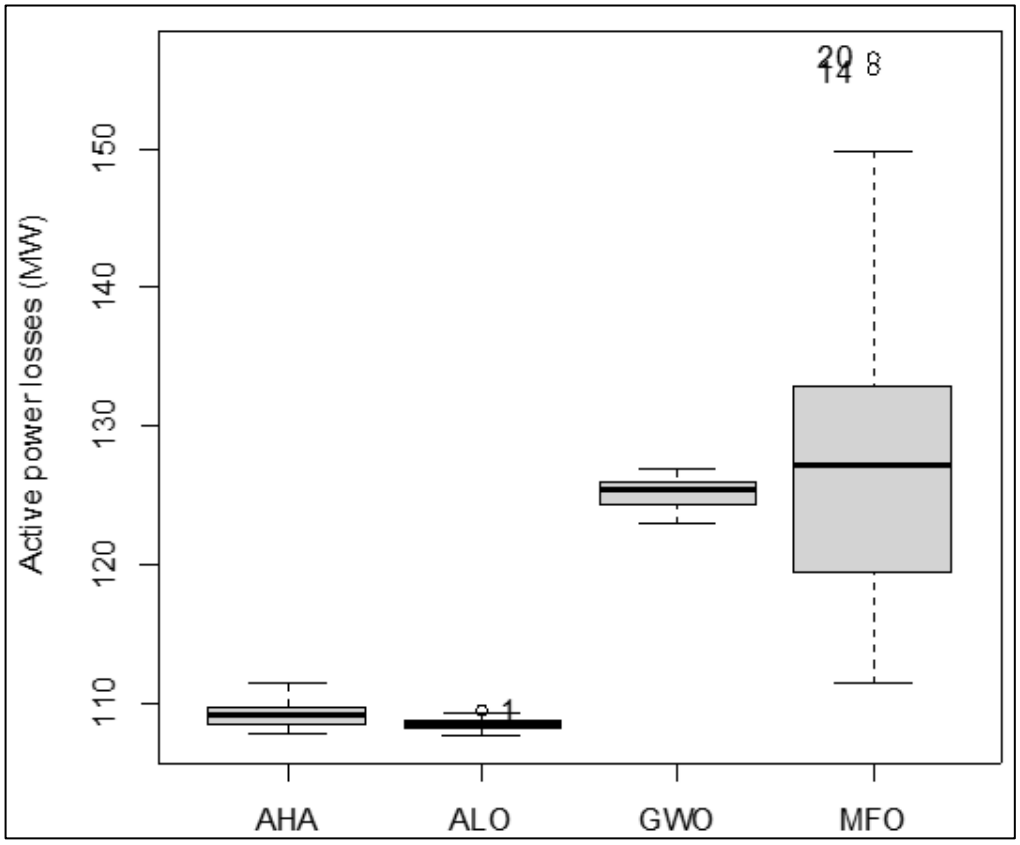

Figure 3.58. Box-and-whisker plot of IEEE 118-bus test system

3.5.2. Statistical test of one-way ANOVA

ANOVA is a statistical method used to compare the means of three or more groups in order to determine whether at least one of the group means is significantly different from the others. ANOVA examines the variance within the different groups and compares it to the variance between the groups. It is generally used when there is a single independent variable, or factor, and the objective is to check whether variations in this factor have a measurable effect on a dependent variable. We are interested in the main effects of these factors and the effect of their interaction on the quantitative (dependent) variable. The principle is to test the null hypothesis (H_0) that the means of three (or more) populations are equal, against the alternative hypothesis (H_a) that at least one mean is different. For k means, according to the official notation for statistical hypotheses, we write: H_0 if $\mu_1=\mu_2=\cdots=\mu_k$ or H_a if at least one of the means is different (where μ_k is the mean of the k^{th} level of the factor).

ANOVA generates an F-statistic and a p-value. The F-statistic indicates whether there are significant differences among the group means, and the p-value tells us the probability of

observing such differences due to random chance. If the p-value is below a certain significance level (often 0.05), it suggests that there's enough evidence to reject the null hypothesis, indicating that there are significant differences between at least two group means. In the case of our study, the stochastic nature of the proposed metaheuristic optimization algorithms requires to run each technique several times on the same objective function in order to obtain the best result values, which probably vary to each execution. In addition to the Box-and-whisker plot which gives us the mean, worst, best solution and standard deviation, one-way analysis of variance (ANOVA) has been performed to observe the statistical significance of the difference between the performance of different implemented algorithms. The one-way ANOVA results obtained from experimented algorithms on four test systems (IEEE 14-bus, IEEE 30-bus, IEEE 57-bus and IEEE 118-bus) are listed in Tables 3.21. In this study, the alternative hypothesis is considered. We can see that the value of the probability P is much lower than the 0.05 level of significance considered in all test systems. We can state also that the null hypothesis is rejected. We can conclude that there is a statistically significant difference between the means of the different groups. This is strong evidence that the mean values of the groups differ.

Table 3.21. Analysis of variance for the different study cases.

IEEE 14-bus test system						
Source of variance	SS	df	MS	F	P-value	F-crit
Between groups	1,84399107	3	0,61466369	1544,30226	9,972E-116	2,66256855
Within groups	0,06209117	156	0,00039802			
Total	1,90608224	159				
IEEE 30-bus test system						
Source of variance	SS	df	MS	F	P-value	F-crit
Between groups	9,6579222	3	3,2193074	6405,10798	4,615E-163	2,66256855
Within groups	0,07840804	156	0,00050262			
Total	9,73633024	159				
IEEE 57-bus test system						
Source of variance	SS	df	MS	F	P-value	F-crit
Between groups	226,813516	3	75,6045052	686,384449	1,2798E-89	2,66256855
Within groups	17,1832314	156	0,11014892			
Total	243,996747	159				
IEEE 118-bus test system						
Source of variance	SS	df	MS	F	P-value	F-crit
Between groups	12698,1234	3	4232,70778	125,039043	2,6612E-41	2,66256855
Within groups	5280,76989	156	33,851089			
Total	17978,8932	159				

SS: Sum of Squares; df: Degrees of Freedom; MS: Mean Squares

3.6. Conclusion

Bio inspired algorithms are going to be a new revolution in computer science since they are among the most powerful algorithms for optimization. In this chapter, a number of bioinspired algorithms were described and presented namely: MFO, GWO, AHA and ALO. These proposed bio-inspired algorithms based ORPD problem were applied on a different IEEE test systems (from the smallest to the largest), and their results were compared with each other and with those of other optimization methods presented in the literature. Considering the cases and comparative studies presented in this chapter, the proposed bio-inspired algorithms appear to be very effective in particular for their solutions quality as well as their significant active power losses and voltage deviation reductions. As these proposed algorithms are iterative stochastic processes, evaluating their performance requires the use of statistical tools. In this chapter, several tests were carried out in order to conduct statistical studies to confirm the effectiveness of the proposed methods. Two statistical study methods, namely: the Box-and-whisker plot and the analysis of a one-way Analysis of Variance (ANOVA) are presented. These two statistical analysis methods were applied to the results obtained by the different test systems namely IEEE 14-bus, IEEE 30-bus, IEEE 57-bus and IEEE 118-bus.

Chapter 4

HYBRID OPTIMIZATION BASED METAHEURISTIC METHODS FOR THE ORPD PROBLEM

4.1. Introduction

Optimization problems are of great importance in many fields. They can be tackled, for example, by approximate algorithms such as metaheuristics. Metaheuristic algorithms are problem-solving techniques used to find approximate solutions for optimization problems, especially in scenarios where exact solutions are either impractical or computationally infeasible due to the problem's complexity. These algorithms are general-purpose and don't guarantee an optimal solution but aim to efficiently explore the solution space to find good solutions. The first two decades of research on metaheuristics were characterized by the application of rather standard metaheuristics. However, in recent years it has become evident that the concentration on a sole metaheuristic is rather restrictive. A skilled combination of a metaheuristic with other optimization techniques, a so-called hybrid metaheuristic, can provide a more efficient behavior and a higher flexibility when dealing with real-world and large-scale problems. This can be achieved, by combining the complementary strengths of metaheuristics [132]. The use of hybrid algorithms is a new and successful trend in solving optimization problems. The main goal of this research is to obtain a more powerful algorithm that combines the advantages of individual algorithms. Hybrid algorithms benefit from this synergy. However, it is important to choose an appropriate combination of component algorithms to achieve a better overall performance in a particular situation or problem. This research tends to combine the PSO (Particle Swarm Optimization) and TS (Tabu Search) optimization techniques to form a hybrid tool that can outperform the algorithms when used individually in solving power system optimization problems. Generally, PSO has a more global searching ability at the beginning of the run and a local search near the end of the run. The PSO technique can generate high-quality solutions and has a more stable convergence characteristic than other stochastic methods. However, when solving complex multimodal problems, PSO can be trapped in local optima [3]. The PSO technique can generate high-quality solutions and has a more stable convergence characteristic than other stochastic methods. However, when solving complex multimodal problems, PSO can be trapped in local optima [79]. To overcome this drawback, PSO performance can be enhanced with few adjustments. Hybridization is one of these

modifications or techniques which, nowadays, is a popular idea being applied to evolutionary algorithms in order to increase their efficiency and robustness [133]. Recently, hybrid PSO has provided promising results for problems such as the power loss minimization problem [134]. In this section an efficient hybrid PSO with the tabu search (PSO-TS) method is implemented to solve the ORPD problem with two distinct objective functions, namely, active power losses and voltage deviation. The proposed optimization approach was tested on IEEE 14-bus, IEEE 30-bus, IEEE 57-bus and the practical Algerian electric 114-bus power system. To demonstrate the effectiveness of the proposed PSO-TS algorithm, the obtained results were compared with TS, PSO and with several methods published in the literature, namely: Biogeography Based Optimization (BBO) technique [29] , Differential Evolution (DE) algorithm [14], General passive congregation PSO (GPAC), local passive congregation PSO (LPAC), coordinated aggregation (CA) [134], CLPSO method [9], Interior point (IP) method [11].

4.2. The proposed Hybrid PSO-TS Algorithm

Hybridization is a way of combining two techniques in a judicious manner, so that the resulting algorithm contains positive features of both algorithms. The success of the meta-heuristics optimization algorithms depends to a large extent on the careful balance between two conflicting goals: exploration (diversification) and exploitation (intensification). In order to achieve these two goals, the algorithms use either local search techniques, global search approaches, or an integration of both, commonly known as hybrid methods [133]. For the ORPD problem, different hybridizations with PSO have been used to improve the algorithm's performance by avoiding premature convergence. For instance, PSO has been hybridized with the linear interior point method [135], fuzzy logic [136], Pareto optimal set [137], direct search method [114], differential evolution [33], a multi-agent systems [3], imperialist competitive algorithm [111], genetic algorithm [112] and eagle strategy [113]. Tabu search was used to solve OPF and optimal reactive power planning problems [80], [138] but the hybridization of TS with PSO has never been used even though it was effective in solving other optimization-constrained problems [139]. Both algorithms (PSO, TS) and their hybridization (PSO-TS) for solving the ORPD problem are discussed in the following sections.

4.2.1. Particle Swarm Optimization

The concept of PSO was first suggested by Kennedy and Eberhart in 1995 [140]. PSO is a population-based evolutionary computation technique. The main idea is to evolve the population (particles) of initial solutions in a search space in order to find the best solution. This evolution is an analogy of the behavior of some species as they look for food, like a flock of birds

or a school of fish [141]. These particles move through the search domain with a specified velocity in search of optimal solution. Each particle maintains a memory which helps it to keep track of its previous best position. The positions of the particles are distinguished as personal best and global best.

The swarm of particles evolves in the search space by modifying their velocities according to the following equations [133] :

$$\boldsymbol{v_i^{k+1} = w_i v_i^k + c_1 rand \times \left(pbest_i - x_i^k\right) + c_2 rand \times \left(gbest - x_i^k\right)} \quad (4.\ 1)$$

where:

- v_i^k is the current velocity of particle *i* at iteration *k*.
- w_i is the inertia weight.
- *rand* is a random number between 0 and 1.
- c_1 and c_2 are the acceleration coefficients.
- $pbest_i$ is the best position of the current particle achieved so far.
- $gbest$ is the global best position achieved by all informants.
- x_i^k is the current position of particle *i* at iteration *k*.

The new position of each particle is given by the following equation:

$$\boldsymbol{x_i^{k+1} = x_i^k + v_i^{k+1}} \quad (4.\ 2)$$

The inertia weighting factor for the velocity of particle *i* is defined by the inertial weight approach [134].

$$\boldsymbol{w_i = w_{max} - \frac{w_{max} - w_{min}}{iter_{max}} \times k} \quad (4.\ 3)$$

where:

- $iter_{max}$ is the maximum number of iterations.
- *k* is the current number of iteration.
- w_{max} and w_{min} are the upper and lower limits of the inertia weighting factor, respectively.

The efficiency of PSO has been proved for a wide range of optimization problems. However, constrained non-linear optimization problems have not been widely studied with this method. Hu and Eberhart were the first to try to adapt PSO to constrained non-linear problems [143]. The difficulty in adapting meta-heuristics mainly involves the question of how to preserve the feasibility of solutions during different iterations.

A variety of approaches can be used to deal with feasibility in constrained non-linear optimization problems, which largely fall into two classes:

- Penalty function approaches, and
- Approaches preserving feasibility throughout evolutionary computation,

Each method has its advantages and disadvantages. A penalty function approach is used in this thesis due to its simplicity of implementation and its proven efficiency for many constrained non-linear optimization problems [144]. Conversely, feasibility preserving methods are highly time-consuming. To use a penalty function method, a penalty factor associated with each violated constraint is added to the objective function in order to penalize infeasible solutions [36]. Therefore, the optimum is found when all the constraints are respected and the objective function is minimized. The ORPD objective function is then modified as follows [18]:

$$F_T = F + K_P\left(P_{G,slack} - P_{G,slack}^{lim}\right)^2 + K_V \sum_{i=1}^{N_{PQ}} \left(V_{L_i} - V_{L_i}^{lim}\right)^2 + K_Q \sum_{i=1}^{N_G} \left(Q_{Gi} - Q_{Gi}^{lim}\right)^2 + K_S \sum_{i=1}^{N_L} \left(S_{L_i} - S_{L_i}^{lim}\right)^2 \quad (4.4)$$

where F is equal to J_1 given by Equation (2.2) in the case of the power losses minimization or equal to J_2 given by Equation (2.5) in the case of the voltage deviation minimization; K_P, K_V, K_Q and K_S are the penalty factors of the slack bus generator, bus voltage limit violation, generator reactive power limit violation, and line flow violation, respectively.

$P_{G,slack}^{lim}$, $V_{L_i}^{lim}$, Q_{Gi}^{lim} and $S_{L_i}^{lim}$ are defined as follows:

$$P_{G,slack}^{lim} = \begin{cases} P_{G,slack}^{min} \; if \;\; P_{G,slack} < P_{G,slack}^{min} \\ P_{G,slack}^{max} \; if \;\; P_{G,slack} > P_{G,slack}^{max} \end{cases} \quad (4.5)$$

$$V_{L_i}^{lim} = \begin{cases} V_{L_i}^{min} \; if \;\; V_{L_i} < V_{L_i}^{min} \\ V_{L_i}^{max} \; if \;\; V_{L_i} > V_{L_i}^{max} \end{cases} \quad (4.6)$$

$$Q_{Gi}^{lim} = \begin{cases} Q_{Gi}^{min} \; if \;\; Q_{Gi} < Q_{Gi}^{lim} \\ Q_{Gi}^{max} \; if \;\; Q_{Gi} > Q_{Gi}^{max} \end{cases} \quad (4.7)$$

$$S_{L_i}^{lim} = \begin{cases} S_{L_i}^{max} \; if \;\; S_{L_i} > S_{L_i}^{max} \\ 0 \qquad if \;\; S_{L_i} \leq S_{L_i}^{max} \end{cases} \quad (4.8)$$

4.2.2. Tabu Search Method

In 1986, Fred Glover proposed a new approach, called “tabu search” (TS). TS is a meta-heuristic that guides a local heuristic search procedure to explore the solution space beyond

local optimality. This technique uses an operation called "move" to define the neighborhood of any given solution. One of the main components of TS is its use of adaptive memory, which creates a more flexible search behavior [145] [145]. The simplest of these processes consists of recording in a tabu list the features of the visited regions in the space search, which provides a means to avoid revisiting already inspected solutions and thus avoid becoming trapped in local optima. Generally, the advantages of the TS optimization technique can be summarized as follows [80]:

- TS is characterized by its ability to avoid entrapment in a local optimal solution and to prevent the same solution being found by using the flexible memory of the search history.
- TS uses probabilistic transition rules to make decisions, rather than deterministic ones. Hence, TS is a kind of stochastic optimization algorithm that can search a complicated and uncertain area to find the global optimum. This makes TS more flexible and robust than conventional methods.

- TS uses adaptive memory processes for guiding the seeking in the problem search space. Therefore, it can easily deal with non-smooth, non-continuous and non-differentiable objective functions.

4.3. Hybrid PSO-Tabu Search Approach Applied to ORPD

Several arguments support the hybridization of PSO with TS. Firstly, PSO is a global population-based algorithm while TS proposes fast local search mechanism. Secondly, the incorporation of TS into PSO enables the algorithm to maintain population diversity. Finally, TS is integrated to prevent PSO from falling into local optima. To this end, TS is proposed to serve as a local optimizer of the best local solutions (*pbest*). The *pbest* solutions of PSO are the inputs of the TS diversification procedure. For each solution "*s*", a list of neighborhoods is defined. Candidate solutions from these neighborhoods are examined and the best one becomes the new current solution that replaces "*s*". The move leading to the solution "*s*" is saved in the tabu list, called *best_list*. This process is repeated to produce successive new solutions until a defined stopping criterion is satisfied.

The neighborhoods of a solution "*s*" are defined by hyper-rectangles introduced in [146]. A hyper-rectangle of "*s*" with a radius "*r*" is the space containing solutions (*s'*) such that the distance between *s* and (*s'*) is less than "*r*". To generate m neighbors for the solution "*s*", *m* hyper-rectangles centered on "s" are created, and a point is randomly chosen from each

of them. The best of the m chosen points then replaces "*s*". The search procedure of PSO-TS algorithm will terminate whenever the predetermined maximum number of generations is reached, or whenever the global best solution does not improve over a predetermined number of iterations. The diversification procedure is outlined in Algorithm 4.1 while, the general and detailed flowcharts of the proposed PSO-tabu search are given in Figures 4.1 and 4.2, respectively.

Algorithm 4.1. Tabu search procedure (Diversification)

Inputs

pbest; // best historical solution of particles

pbestval; solutions values

m; //neighborhood size

r; //radius of hyper-rectangles

eps; //threshold for accepting new solution

best_list = (pbest, r); // Initializing the tabu list *best_list*

Repeat

For each solution $s(V_{Gi}, T_i, Q_{ci})$ in *pbest*

//generation of *m* neighbors

$i = 1$

While $i <= m$

Generate the hyper-rectangle of radius $r*i$ around *s*,

choose randomly a solution *NS* in the hyper- rectangle

If $NS \notin best\_list$ then

add the move to *best_list*;

if $eval(NS)$-$pbestval(s) \leq eps$ then update *pbestval* and *pbest*

$s = NS$,

End if

$i = i+1$;

End While

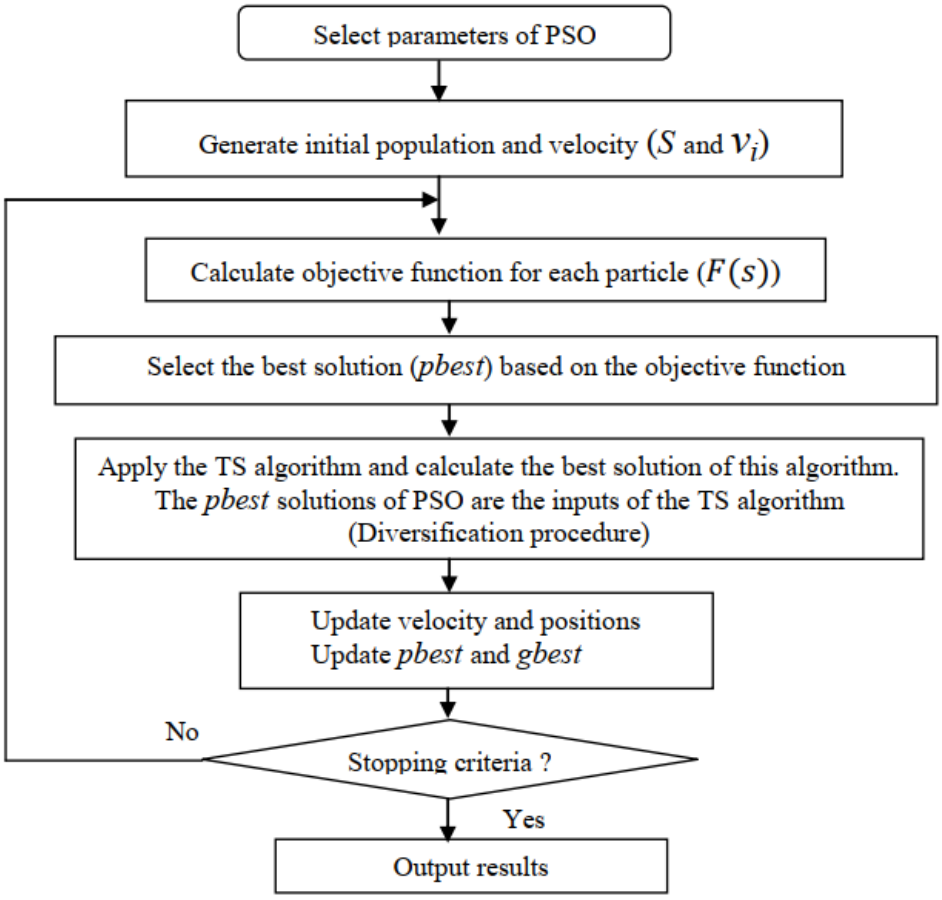

Figure 4.1. General flowchart of PSO-TS method.

4.4. Application and Results

4.4.1. PSO-TS algorithm based ORPD considering continuous control variables

In a first step we will consider that all control variables are continuous. In order to verify the performance and efficiency of the proposed PSO-TS algorithm, a test is carried out on IEEE 30-bus power system. For the purpose of comparison, two reactive power injection schemes have been considered:

- Case 1: IEEE 30 bus system with 12 control variables [147].
- Case 2: IEEE 30 bus system with 19 control variables [5].

For both cases, the two objective functions are considered: active power losses (P_{Loss}) (Equation (2.2)) and total of bus voltage deviation (TVD) (Equation (2.5)). In the study, all inequality constraints (Equations (2.14)– (2.20)) were taken into consideration. The PSO-TS parameter selection is a challenging task not only for this algorithm but also for other meta-heuristic algorithms. The parameter settings used in the proposed PSO-TS algorithm are determined through extensive experiments, including initial inertia weight, acceleration factors,

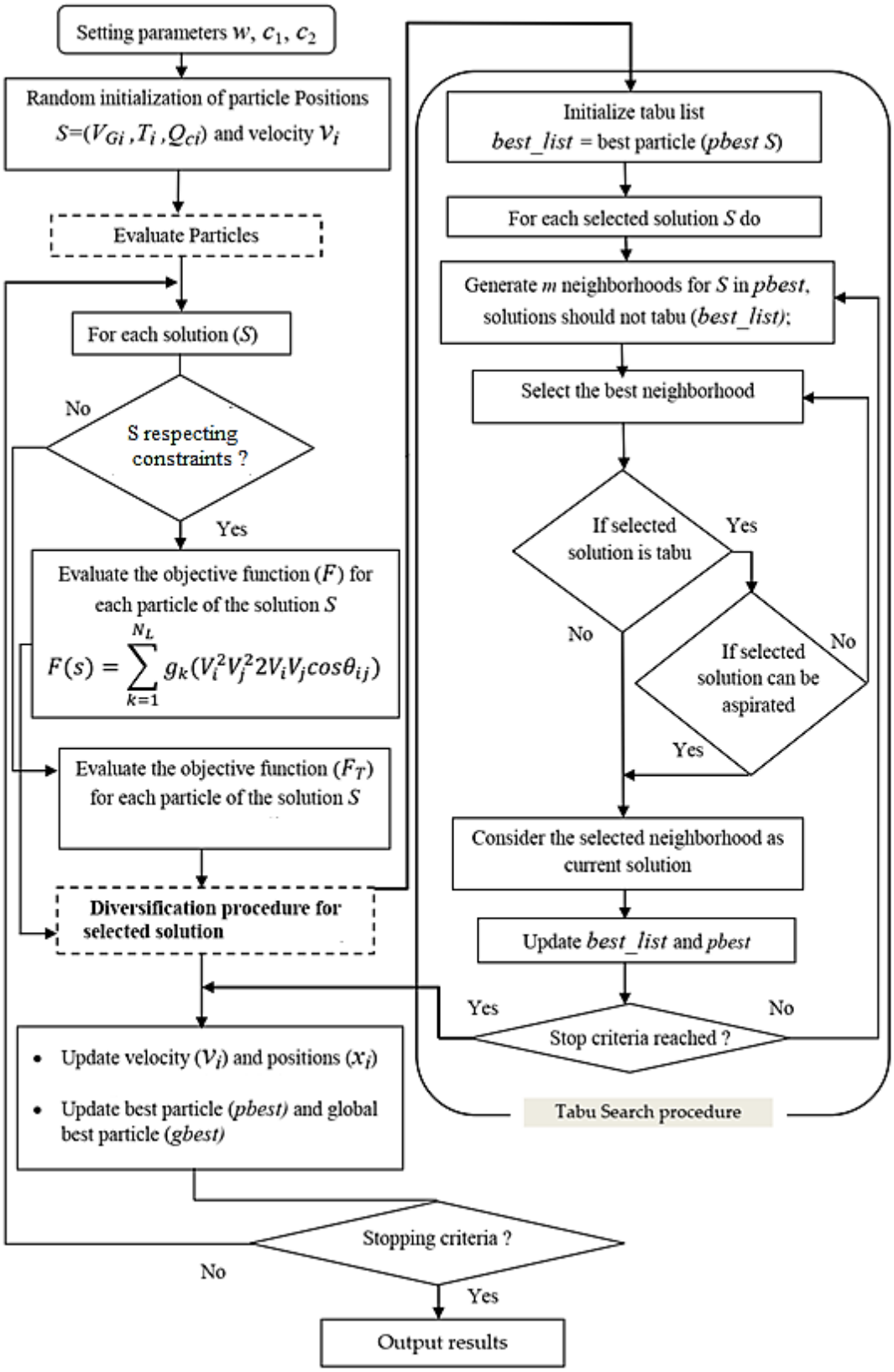

Figure 4.2. Detailed flowchart of the PSO-TS method

number of generations, swarm size, tabu list length, total number of neighborhood and radius of neighborhood. Based on these results, the control parameter settings shown in Table 4.1 have been used in the proposed PSO-TS algorithm and for all simulation studies in both objective functions.

Table 4.1. Control parameter settings.

Parameters	Value
Initial inertia weight w	decreased from 0.9 to 0.4
Acceleration factor c_1	2
Acceleration factor c_2	2
Maximum number of generations (PSO)	200
Swarm size	20
Tabu list length	7
Number of neighborhoods	3
Radius of neighborhood	0.1
Maximum number of generations (TS)	1000

4.4.1.1. *Case 1: IEEE 30 bus test system with 12 control variables*

In this case the IEEE 30 bus system contains six generator units connected to buses 1, 2, 5, 8, 11 and 13; four regulating transformers connected between the line numbers 6–9, 6–10, 4–12 and 27–28; and two shunt compensators connected to bus numbers 10 and 24. The transmission feeder numbers is of 41. The transmission line data and loads were taken from [147]. The generator voltages, transformer tap settings and VAR injection of the shunt capacitors were considered as continues control variables. The voltage magnitudes of all the buses were between 0.95 and 1.1 p.u, the transformer tap settings were within the range of 0.9–1.1 p.u and the shunt capacitor sizes were within the interval of 0 to 30 MVAR [134]. There are 12 control variables in this case, namely, 6 generator voltages, 4 transformer taps and 2 capacitor banks.

a. Simulation Results for Active Power Losses Minimization

The objective in this case is to minimize the total active power losses. Before minimization, the total power losses were 5.2783 MW. Minimum and maximum limit settings for tap setting transformers, reactive compensators and bus voltages are tabulated in Table.4.2. Table 4.3 summarize the results of the optimal settings and the system power losses obtained by PSO, TS and PSO-TS proposed approaches and methods reported in [134, 29], namely, CA, IP-OPF, LPAC, GPAC and BBO. These results show that the dispatch optimal solutions determined by the PSO-TS led to better results. Active power losses are lower than those given by TS, PSO and considered references. Using PSO-TS algorithm, power losses were reduced from 5.2783 MW to 4.6304 MW, indicating a reduction of 12.27%, while PSO and TS taken alone reduce

power losses by only 1.03% and 5.61%, respectively. For the other optimization algorithms, the best result is given by BBO algorithm [29] which reduces the losses by 5.93%. It can be concluded that the proposed PSO-TS method is able to determine the near-global optimal solution. At the same time, the proposed method succeeded in keeping the dependent variables within their limits. Figure 4.3 shows the supremacy of PSO-TS algorithm over the other methods. The convergence characteristics of power loss objective function for this case are plotted in Figure 4.4 which shows that while the PSO and TS algorithms converge faster than the PSO-TS, the minimum obtained by the latter is far better than those given by the former. As the hardware and the software environments significantly affect the computational time, it is not possible to compare the computational time requirements of the different methods unless all the methods are run on the same hardware and programmed using the same environment. As a rough guide, however, the average time taken by PSO-TS in this case is 19 s.

Table 4.2. IEEE 30-bus test system variable limits (case 1)

Variables	lower limits (p.u)	upper limits (p.u)
Generator buses voltage	0.95	1.1
Load buses voltage	0.95	1.1
Transformers tap setting	0.9	1.1
shunt compensators (MVar)	0	30

Table 4.3. Simulation results of TS, PSO and PSO-TS algorithms (Case 1)

Control variables	**CA[134]**	**IP-OPF[134]**	**LPAC[134]**	**GPAC[134]**	**BBO[29]**	**TS**	**PSO**	**PSO-TS**
V_1	1.02282	1.10000	1.02342	1.02942	1.1000	1.0684	1.1000	1.0992
V_2	1.09093	1.05414	0.99893	1.00645	1.0943	1.0933	1.0943	1.0948
V_5	1.03008	1.10000	0.99469	1.01692	1.0804	1.0893	1.1000	1.0766
V_8	0.95000	1.03348	1.01364	1.03952	1.0939	1.0853	1.1000	1.0977
V_{11}	1.04289	1.10000	1.01647	1.03952	1.1000	1.0017	0.9505	1.0837
V_{13}	1.03921	1.01497	1.01101	1.04870	1.1000	1.0780	1.1000	1.0754
T_{6-9}	1.07894	0.99334	1.04247	1.04225	1.1000	0.9979	1.0547	0.9257
T_{6-10}	0.94276	1.05938	0.99432	0.99417	0.9058	0.9008	1.1000	1.0291
T_{4-12}	1.00064	1.00879	1.00061	1.00218	0.9521	1.0337	0.9000	0.9265
T_{27-28}	1.00693	0.99712	1.00694	1.00751	0.9638	0.9441	0.9468	0.9422
Q_{Sh10}	0.15232	0.15253	0.17737	0.17267	0.2891	0.1395	0.3000	0.2864
Q_{Sh24}	0.06249	0.08926	0.06172	0.06539	0.1007	0.1838	0.0000	0.1363
P_{loss} (MW)	5.09209	5.10091	5.09212	5.09226	4.9650	5.2240	4.9819	4.6304

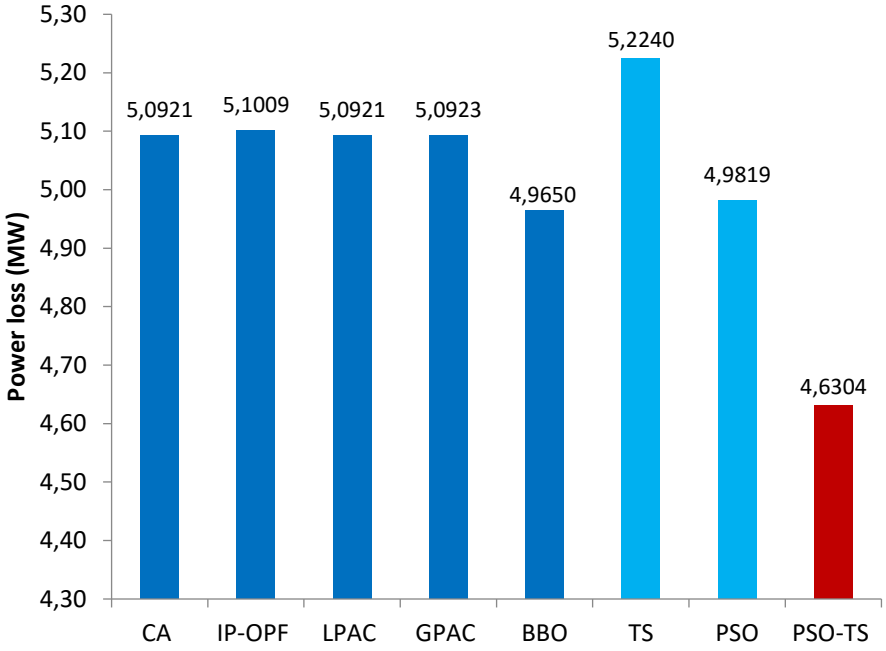

Figure 4.3. Comparative graph of the power losses (Case 1)

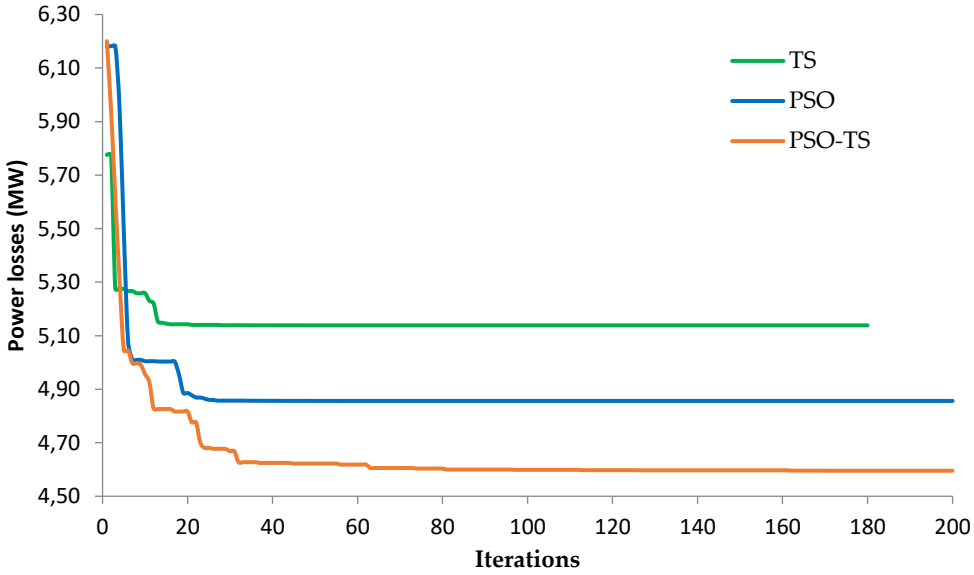

Figure 4.4 Convergence characteristic of the power losses (Case 1)

b. *Simulation results for total voltage deviation minimization*

The objective in this case is the minimization of the voltage deviation in order to improve the system voltage profile. The TVD and the optimal setting of control variables obtained by our PSO-TS algorithm and different considered methods (CA, IP-OPF LPAC, GPAC and BBO) [134, 29] are listed in Table 4.4 and figure 4.6. The convergence characteristics of the objective function obtained by TS, PSO and PSO-TS are illustrated in Figure 4.5. This figure shows that

PSO-TS converge faster than PSO and TS considered alone and gives also better results. Before minimization, the TVD was 0.619 p.u. As shown in Table 4.4, the obtained TVD using the proposed PSO-TS hybrid approach is 0.1113 p.u which means a reduction of 82.02% while the ones given by the mentioned methods are, respectively, 80.21%, 79.97%, 79.42%, 80.71%, 69.73% and 79.40%. These results clearly indicate that PSO-TS outperforms the other methods in term of solution quality (see Figure 4.6).

Table 4.4. Simulation results of TS, PSO and PSO-TS algorithms (Case 1)

Control Variables	CA [134]	IP-OPF [134]	LPAC [134]	GPAC [134]	BBO [29]	TS	PSO	PSO-TS
V_1	1.0890	1.10000	1.03879	1.00963	1.0033	1.0760	0.9875	1.0014
V_2	0.9500	0.99100	1.01776	1.00984	1.0071	1.0494	0.9513	1.0592
V_5	1.0860	0.96145	1.04863	1.01000	1.0189	1.0056	1.0641	1.0542
V_8	1.1000	0.95986	1.04993	1.03516	1.0148	1.0238	1.0596	1.0133
V_{11}	1.0021	1.10000	0.98373	1.03000	0.9908	1.0085	1.0972	0.9905
V_{13}	1.0279	0.95000	1.00524	1.00274	1.0697	0.9641	1.1000	1.0291
T_{6-9}	1.0287	0.99734	1.03054	1.02139	1.0039	0.9486	1.0344	0.9762
T_{6-10}	0.9000	1.08595	0.91429	0.93327	0.9000	0.9840	1.1000	1.0163
T_{4-12}	0.9929	1.00087	0.99469	0.99338	1.0490	0.9647	0.9000	0.9537
T_{27-28}	1.0248	1.00482	1.02078	1.02729	0.9546	1.0287	0.9516	0.9481
Q_{Sh10}	0.0000	0.11072	0.00000	0.04348	0.0924	0.0917	03000	0.2890
Q_{Sh24}	0.0000	0.15928	0.03586	0.00000	0.1244	0.2278	0.0440	0.0697

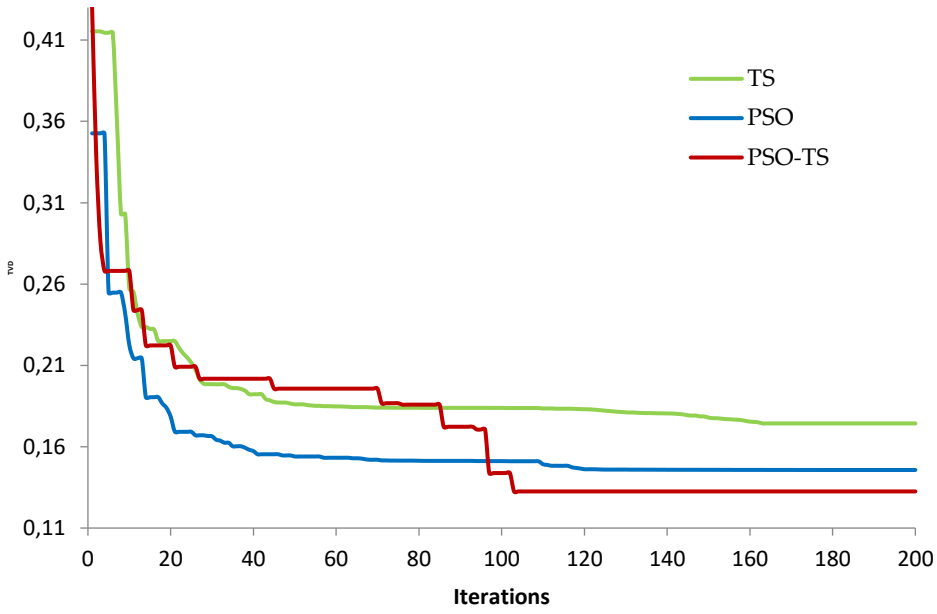

Figure 4.5. Convergence characteristic of the voltage deviation objective (TVD) (Case 1)

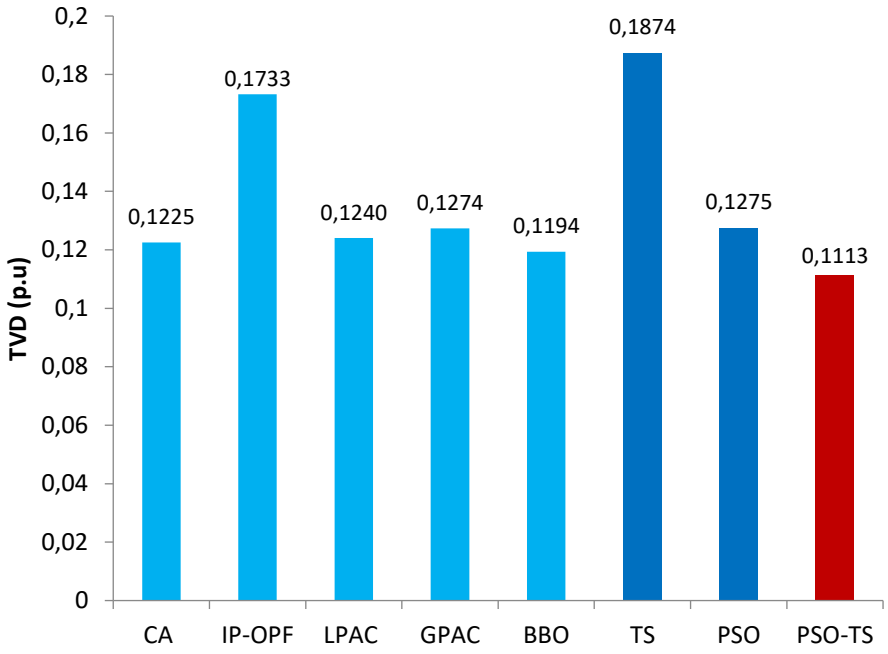

Figure 4.6. Comparative graph of the voltage deviation objective (TVD) (Case 1).

4.4.1.2. *Case 2: IEEE 30 bus system with 19 control variables*

In this case, the IEEE 30-bus system includes six generation buses, 24 load buses and 41 branches; 4 of them have tap-changing transformer as in the first case. In addition, buses 10, 12, 15, 17, 20, 21, 23, 24 and 29 were selected for receiving shunt capacitors. This IEEE 30-bus test system includes 19 control variables. The constraint limits of the generator voltage magnitude, the tap settings of the regulating transformers and the shunt capacitor sizes are tabulated in the table 4.5. The capacitor sizes are considered as continuous variables. The transmission line data and the loads were taken from [5]. The active and reactive total loads are P_{load} = 2.834 p.u and Q_{load} = 1.262 p.u. The power base value is 100 MVA

Table 4.5. IEEE 30-bus test system variable limits (case 2)

Variables	Lower limits (p.u)	Upper limits (p.u)
Generator buses voltage	0.95	1.1
Load buses voltage	0.95	1.1
Transformers tap setting	0.9	1.1
shunt compensators (MVAr)	0	5

a. Simulation Results for Active Power Losses Minimization

To demonstrate the superiority of the proposed algorithm in the minimization of transmission power losses, Table 4.6 shows the optimal setting of control variables obtained by our PSO-TS algorithm and different considered methods. Figure 4.7 illustrates the PSO-TS simulation results compared with those reported in the literature such as DE [14], BBO, comprehensive

learning PSO (CLPSO), Quasi-Oppositional Teaching Learning Based Optimization (QOTLBO) [24], teaching-learning-based optimization (TLBO) [24], Gravitational search algorithm (GSA) [47], Artificial ecosystem optimization (AEO) [148] and Novel bat algorithm (NBA) [148]. The initial conditions for all these methods are the same and are taken from [5]. The total active power losses which were initially 5.8322 MW, are reduced to 4.5213 MW by the proposed method, i.e., a reduction in power losses by 22.48%. Figure 4.7 shows also that the proposed PSO-TS outperforms the cited meta-heuristic methods. The convergence characteristics of TS, PSO and PSO-TS are given by Figure 4.8 which indicates a much better solution for the proposed hybrid algorithm.

Table 4.6. Simulation results of TS, PSO and PSO-TS algorithms (Case 2)

CVs	DE [14]	CLPSO [24]	BBO [24]	QOTLB [24]	TLBO [24]	GSA [47]	NBA [148]	AEO [148]	TS	PSO	PSO-TS
V_1	1.1000	1.1000	1.1000	1.1000	1.1000	1.0999	1.1000	1.1000	1.0835	1.1000	1.1000
V_2	1.0931	1.1000	1.0944	1.0942	1.0936	1.0743	1.0951	1.0944	1.0567	1.1000	1.0943
V_5	1.0736	1.0795	1.0749	1.0745	1.0738	1.0749	1.0775	1.0751	1.0671	1.0832	1.0749
V_8	1.0756	1.1000	1.0768	1.0765	1.0753	1.0768	1.0792	1.0770	1.0944	1.1000	1.0766
V_{11}	1.1000	1.1000	1.0999	1.1000	1.0999	1.0999	1.0960	1.1000	0.9873	0.9500	1.1000
V_{13}	1.1000	1.1000	1.0999	1.0999	1.1000	1.0999	1.0998	1.1000	1.0863	1.1000	1.1000
T_{6-9}	1.0465	0.9154	1.0435	1.0664	1.0251	1.0000	1.0313	1.0392	1.0745	1.1000	0.9744
T_{6-10}	0.9097	0.9000	0.9011	0.9000	0.9439	0.9300	0.9424	0.9000	0.9960	1.0953	1.0510
T_{4-12}	0.9867	0.9000	0.9824	0.9949	0.9992	0.9800	1.0009	0.9729	0.9678	0.9000	0.9000
T_{27-28}	0.9689	0.9397	0.9691	0.9714	0.9732	0.9700	0.9854	0.9632	1.0267	1.0137	0.9635
Q_{Sh10}	0.0500	0.0492	0.0499	5.0000	5.0000	3.7000	4.2055	4.9948	0.0146	0.0500	0.0500
Q_{Sh12}	0.0500	0.0500	0.0498	5.0000	5.0000	4.3000	5.0000	4.9963	0.0376	0.0500	0.0500
Q_{Sh15}	0.0500	0.0500	0.0499	5.0000	5.0000	3.700	3.3446	4.8409	0.0000	0.0000	0.0500
Q_{Sh17}	0.0500	0.0500	0.0499	5.0000	5.0000	2.200	5.0000	4.9985	0.0335	0.0500	0.0500
Q_{Sh20}	0.0440	0.0500	0.0499	4.4500	4.5700	3.100	4.3974	4.2895	0.0019	0.0500	0.0386
Q_{Sh21}	0.0500	0.0500	0.0499	5.0000	5.0000	3.9000	4.9844	5.0000	0.0242	0.0500	0.0500
Q_{Sh23}	0.0280	0.0500	0.0387	2.8300	2.8600	4.2000	4.8984	2.6464	0.0307	0.0500	0.0500
Q_{Sh24}	0.0500	0.0500	0.0498	5.0000	5.0000	4.4000	3.7526	4.9998	0.0294	0.0500	0.0500
Q_{Sh29}	0.0259	0.0500	0.0290	2.5600	2.5800	2.0000	2.8649	2.2293	0.0399	0.0260	0.0213

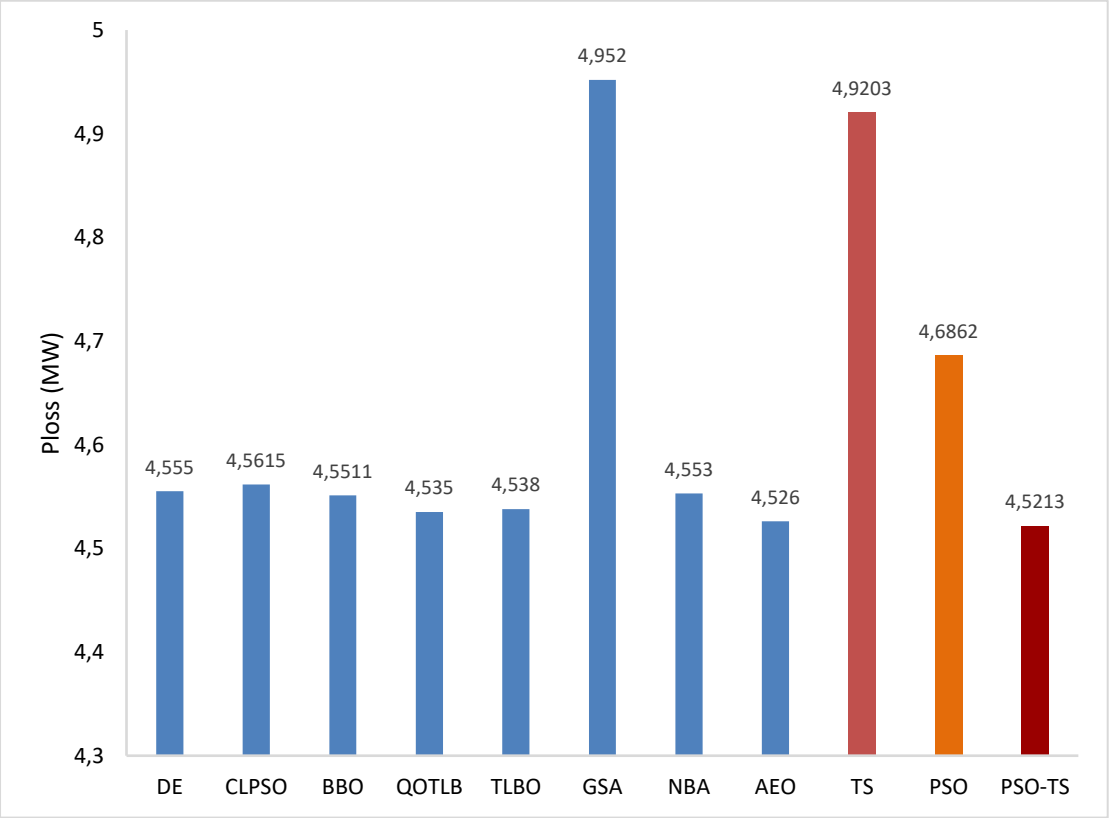

Figure 4.7. Comparative graph of the power losses (Case 2)

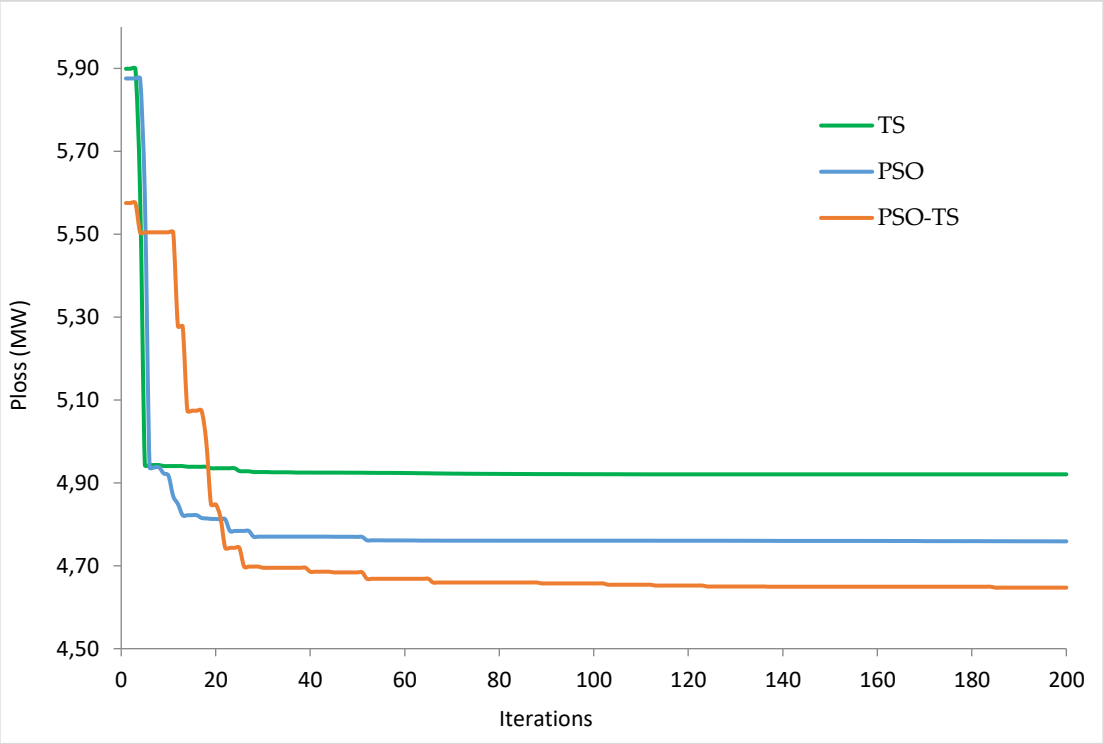

Figure 4.8. Convergence characteristic of the power losses (Case 2).

b. Simulation results for Total voltage deviation minimization

The TVD minimization has also been tested using the PSO-TS proposed method on the IEEE 30 bus with 19 control variables. The optimal control variables settings and the TVD obtained by the different methods are shown in Table 4.7 and Figure 4.9. These results show that the optimal solutions determined by PSO-TS lead to lower TVD than those found by TS, PSO, TLBO [24] and DE [14] (Figure 4.9). The PSO-TS algorithm has reduced the TVD from the initial state value of 1.1521 p.u to 0.0866 p.u representing a reduction of 92.48% while the TVD reductions given by TS, PSO, TLBO and DE are of 86.63%, 91.27%, 92.07% and 92.09% respectively. This shows that the PSO-TS is well capable of determining the global or near-global optimum solution. The proposed method succeeded also in keeping the dependent variables within their limits. Figure 4.10 gives the TVD evolution over iterations of TS, PSO and PSO-TS methods where it is shown that the PSO-TS algorithm converges to a much better minimum.

Table 4.7. Simulation results of TS, PSO and PSO-TS algorithms (Case 2)

Control Variables	DE **[14]**	TLBO **[24]**	TS	PSO	PSO-TS
V_1	1.0100	1.0121	0.9518	0.9898	0.9867
V_2	0.9918	0.9806	1.0888	0.9529	0.9910
V_5	1.0179	1.0207	1.0502	1.0493	1.0244
V_8	1.0183	1.0163	1.0052	0.9988	1.0042
V_{11}	1.0114	1.0293	1.0730	1.0749	1.0106
V_{13}	1.0282	1.0323	1.0637	1.0404	1.0734
T_{6-9}	1.0265	1.0435	1.0137	1.0548	1.0725
T_{6-10}	0.9038	0.9056	1.0342	1.1000	0.9797
T_{4-12}	1.0114	1.0195	0.9993	0.9115	0.9273
T_{27-28}	0.9635	0.9492	0.9652	0.9458	0.9607
Q_{Sh10}	0.0494	0.0484	0.0355	0.0500	0.0095
Q_{Sh12}	0.0108	0.0066	0.0419	0.0500	0.0215
Q_{Sh15}	0.0499	0.0500	0.0032	0.0486	0.0226
Q_{Sh17}	0.0023	0.0009	0.0008	0.0500	0.0005
Q_{Sh20}	0.0499	0.0500	0.0491	0.0500	0.0359
Q_{Sh21}	0.0490	0.0500	0.0134	0.0500	0.0401
Q_{Sh23}	0.0498	0.0495	0.0382	0.0500	0.0427
Q_{Sh24}	0.0496	0.0493	0.0426	0.0500	0.0374
Q_{Sh29}	0.0223	0.0024	0.0306	0.0000	0.0210

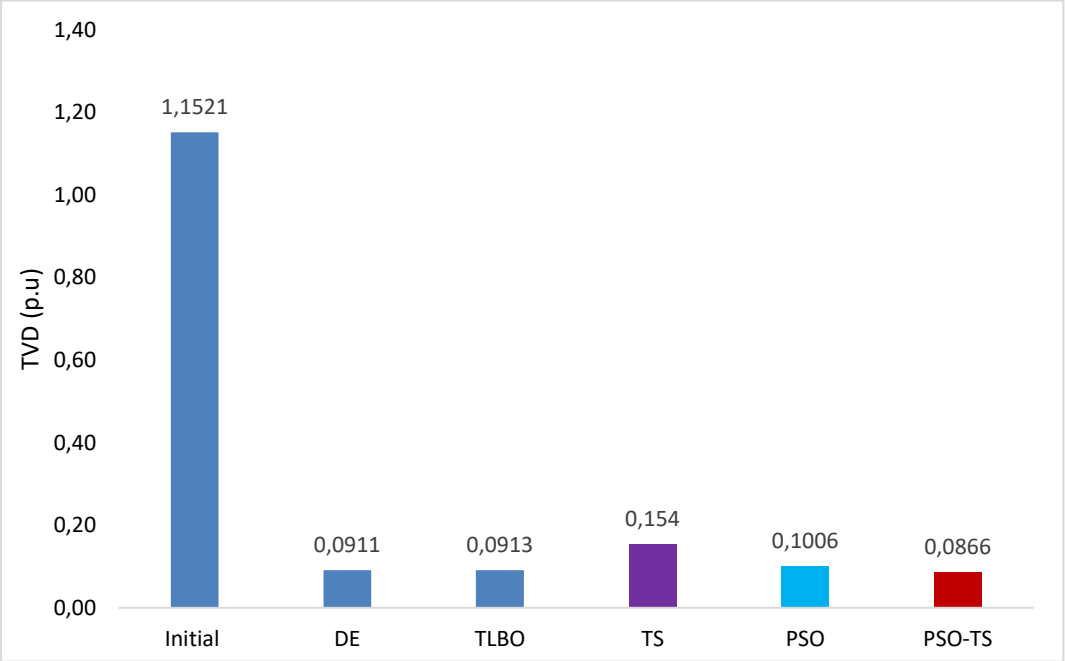

Figure 4.9. Comparative graph for the total voltage deviation (TVD) (Case 2).

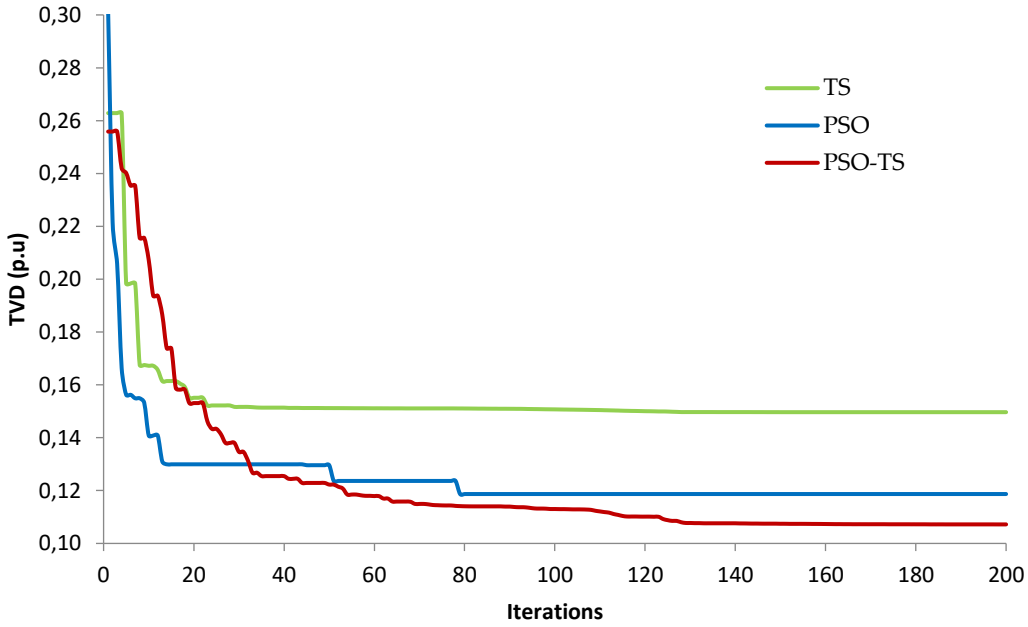

Figure 4.10. Convergence characteristic of the voltage deviation objective (TVD) (Case 2).

4.4.2. ORPD problem based PSO-TS using Sensitive Bus approach

The proposed PSO-TS approach using sensitive bus approach is used to find the settings of the control variables which minimize transmission active power losses and load buses voltage deviation. The bus locations of the shunt capacitors are identified according to sensitive buses. To show the effectiveness of the proposed method, it is applied to IEEE 14-bus, IEEE 30-bus, IEEE 57-bus and the Algerian 114-bus system and is compared with PSO and TS without hybridization, along with some other published approaches. Due to the stochastic nature of the

studied algorithms, it is imperative to run several trials on the same problem instance in order to obtain values that are close to the global optimum. Several tests have also been carried out for statistical study purposes. The values in relative unit (p. u) are taken in a base of 100 KV and 100 MVAR.

4.4.2.1. *Determination of sensitive buses*

In this study, the PSO-TS based reactive power optimization approach was applied to the IEEE 30-bus power system with 12 control variables. This system contains six generator units connected to buses 1, 2, 5, 8, 11 and 13, four regulating transformers connected between the line numbers 6–9, 6–10, 4–12 and 27–28 as in case 1. The difference in this case is that the buses where the shunt compensators will be installed are no longer buses 10 and 24 (locations that appear in the test network [134] taken into consideration by all the previous authors) but the shunt capacitors will be installed at the most sensitive buses. A sensitive bus is a load bus, which requires the installation of a shunt capacitor. To identify this type of buses and their number, we have studied three cases. The two first cases are based on the active power losses (P_{Loss}), and the third one is based on the total voltage deviation (TVD).

4.4.2.1.1. Determination of sensitive buses by removing the entire load (case 1)

To find the locations of the shunt compensators (sensitive buses) and their number, we remove the load from each load bus and calculate the active power losses (P_{Loss}) each time. The bus giving the least active power losses will be considered as the most sensitive. Table 4.8 shows the classification of the sensitive buses according to the new values of the active power losses when the loads of these buses are eliminated. This table shows the classification of the bus sensitivities, from the most sensitive (bus 7) to the least sensitive (bus 29).

Table 4.8. Classification of load buses based on the case 1

Load bus	New P_{loss} (MW)	Load bus	New P_{loss} (MW)
7	4.787	4	5.691
21	4.816	10	5.696
30	5.040	14	5.707
26	5.155	23	5.769
24	5.271	18	5.771
19	5.306	16	5.838
17	5.487	20	5.850
15	5.517	3	5.944
12	5.670	29	5.944

4.4.2.1.2. Determination of sensitive buses by removing the reactive load (case 2)

In order to find the locations of the shunt compensators in this case, we set each load bus

reactive power to zero and calculate the active power losses (P_{Loss}) each time. The bus giving the least active power losses will be considered as the most sensitive bus. Table 4.9 shows the classification of the sensitive buses according to the new values of the active power losses. We can see from this table that the most sensitive buses are 21, 24, 26, 17 and so on until bus 12.

Table 4.9. Classification of buses based on the case 2

Load bus	New P_{loss} value (MW)	Load bus	New P_{loss} value (MW)
21	5.3385	10	5.4766
24	5.3693	29	5.4792
26	5.4393	16	5.4817
17	5.4407	18	5.4826
19	5.4474	20	5.4850
7	5.4596	4	5.4879
30	5.4604	3	5.4912
23	5.4674	14	5.4914
15	5.4731	12	5.5096

4.4.2.1.3. Determination of sensitive buses based on the Voltage Deviation (case 3)

To find the sensitive buses based on the total voltage deviation we will follow the same method mentioned below. i.e., we remove the reactive load from each PQ load and calculate the total voltage deviation (TVD) instead of the active power losses. The bus giving the smallest value of the total voltage deviation will be considered the most sensitive bus. The table 4.10 gives us the classification of the buses based on the new values of the total of voltage deviation. The most sensitive buses from this table are 29, 3, 4, 30, 14 and 20

Table 4.10. Classification of buses based on the total of voltage deviation.

Load bus	New value of TVD (pu)	Load bus	New value of TVD (pu)
29	0.6976	16	0.7151
3	0.7003	23	0.7162
4	0.7014	10	0.7185
30	0.7027	15	0.7234
14	0.7032	19	0.7456
20	0.7073	12	0.7470
26	0.7082	17	0.7602
18	0.7098	24	0.7766
7	0.7151	21	0.8264

4.4.2.2. *Capacitors placement Process.*

Once the sensitivities of the nodes have been determined and classified, the number of capacitor banks to be placed on the network is determined by testing. The first capacitor bank is placed on the network, and its effect on active power losses is tested. If power losses have

been reduced, the second capacitor is placed and its effect on power losses is observed. If no significant decrease in active power losses is observed, the capacitor is removed and a single capacitor is placed on the network. Otherwise, two capacitors are required, and a third capacitor is placed on the grid and its effect on power losses examined. This process continues until there is no effect on power losses.

4.4.2.3. *Simulation results.*

Once the sensitive buses have been identified by the different methods described above (case 1, case 2 and case 3), we install the shunt capacitors on the sensitive busses found in each case by minimizing two objective functions, namely the active power losses (Ploss) and the total voltage deviation (TVD). The test system used is the IEEE 30-bus described above. The sensitive busses considered will be the busses that give the minimum active power losses. The number of shunt capacitors to be installed is two; beyond two, no improvement will be obtained. Once the sensitive busses approach has been validated on the IEEE 30-bus test system, we will continue to optimize the two objective functions mentioned above in larger test networks, i.e. IEEE 57-bus test system and the Algerian 114 bus network.

4.4.2.3.1. IEEE 30 bus test system

The test network to be studied is the IEEE-30 buses described in the section 4.4.1.1

a. Active Power Losses Minimization (Ploss)

After implementing the PSO-TS algorithm to minimize power losses for the different methods of determining sensitive nodes, three locations for the shunt capacitors were selected based on node sensitivities. The first and second cases are based on the calculation of the active power loss by removing the full load and the reactive load respectively and the third case is based on the calculation of the total voltage deviation. Table 4.11 summarize the results of the optimal settings and the system power losses obtained by the PSO-TS algorithm of the three cases. These results show that the optimal solutions determined by PSO-TS in the case 2 lead to lower P_{Loss} than those found by TS, PSO, PSO-TS and PSO-TS in case 1 and 3 (Figure 4.11). The PSO-TS algorithm in case 2 has reduced the power losses P_{Loss} from the initial state to 4.5872 MW representing a reduction of 13.09 % compared to TS, PSO, PSO-TS and PSO-TS (case 1) and PSO-TS (case 3), which reduced P_{Loss} by 1.02 %, 5.61 %, 12.27 %, 12.67 %, and 8.64 %, respectively. This shows that the installation of the shunt capacitors in sensitive buses found by the second method is well capable of determining better solution than the other cases and methods. The convergence characteristics of power losses objective function for the three cases

are shown in Figure 4.12 which shows a relatively slow convergence in the case of locations determined by the sensitivity of the nodes with respect to the reactive power of the loads, with however a much better.

Table 4.11. Simulation results for the Sensitive Buses Approach

Control variables	TS	PSO	PSO-TS	PSO-TS (case 1)	PSO-TS (case 2)	PSO-TS (Case 3)
V_1	1.0684	1.1000	1.0992	1.0990	1.1000	1.1000
V_2	1.0933	1.0943	1.0948	1.1000	1.0975	1.1000
V_5	1.0893	1.1000	1.0766	1.0687	1.0787	1.0753
V_8	1.0853	1.1000	1.0977	1.1000	1.1000	1.1000
V_{11}	1.0017	0.9505	1.0837	1.1000	1.1000	1.1000
V_{13}	1.0780	1.1000	1.0754	1.1000	1.0964	1.1000
T_{6-9}	0.9979	1.0547	0.9257	0.9072	0.9926	1.0307
T_{6-10}	0.9008	1.1000	1.0291	0.9399	1.0737	1.1000
T_{4-12}	1.0337	0.9000	0.9265	0.9000	0.9000	0.9000
T_{27-28}	0.9441	0.9468	0.9422	0.9149	0.9743	0.9976
Q_{Sh10}	0.1395	0.3000	0.2864	-	-	-
Q_{Sh24}	0.1838	0.0000	0.1363	-	0.0880	-
Q_{Sh07}	-	-	-	0.1285	-	-
Q_{Sh21}	-	-	-	0.2052	0.1393	-
Q_{Sh03}	-	-	-	-	-	0.0000
Q_{Sh29}	-	-	-	-	-	0.0193
P_{loss} (MW)	5.2240	4.9819	4.6304	4.6095	4.5872	4.8225

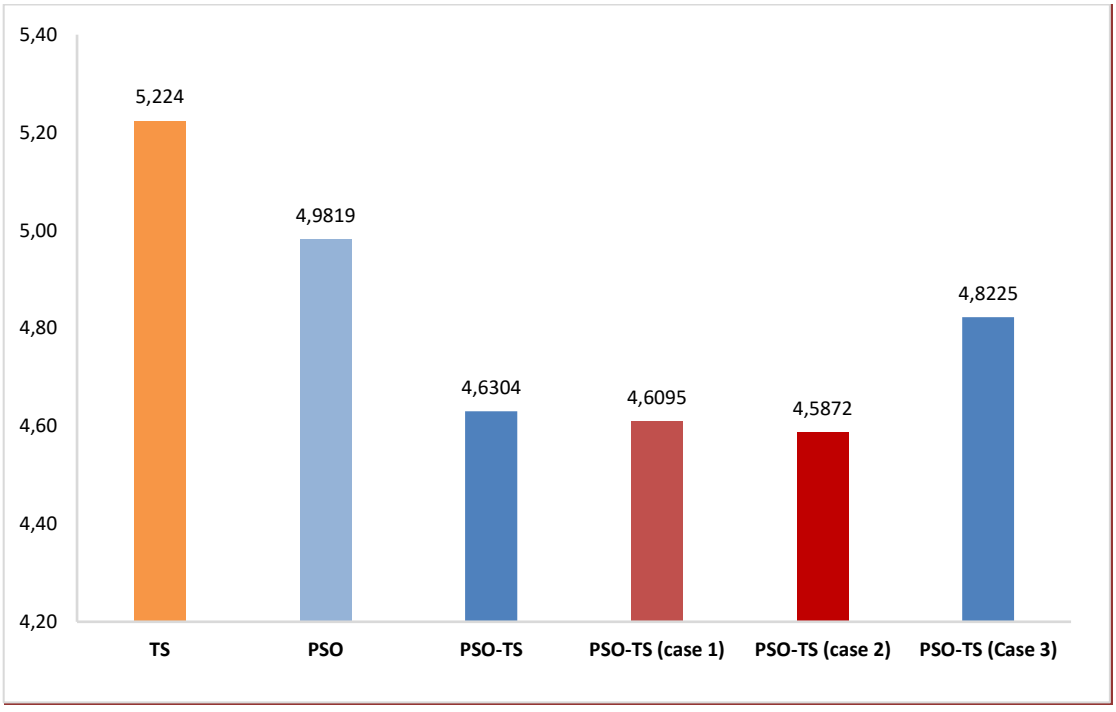

Figure 4.11. Comparative results of the power losses of the three cases

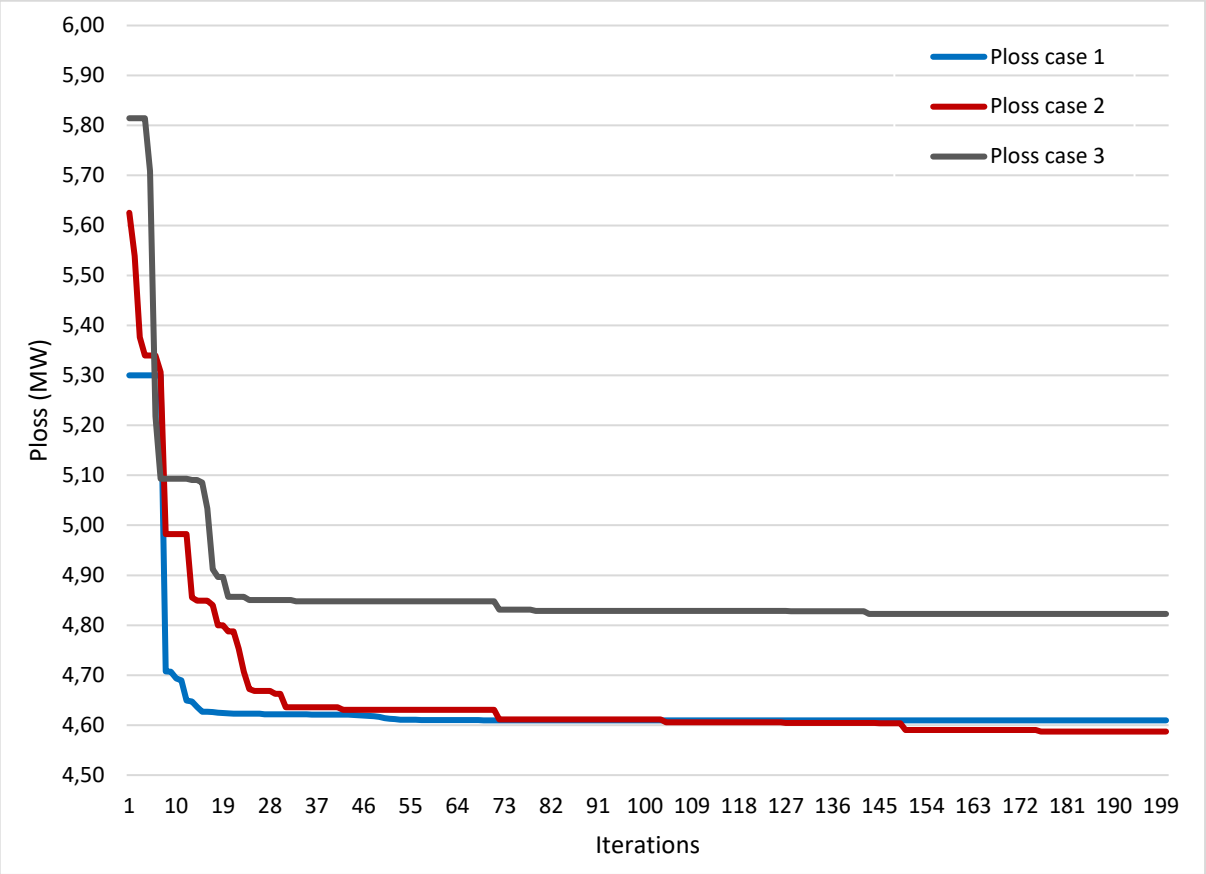

Figure 4.12. convergence characteristic of the power losses (case 1, 2 and 3)

b. Total voltage deviation minimization (TVD)

The hybrid PSO-TS algorithm in this case is to minimize the total of voltage deviation for the three cases (case 1, case 2 and case 3). The results tabulated in Table 4.12 shows that the optimal solutions determined by PSO-TS in the case 2 lead to lower TVD than those found by PSO-TS in case 1 and case 3 (Figure 4.13). The PSO-TS algorithm in case 2 has reduced the TVD from the initial state witch where 0.619 p.u to 0.1155 representing a reduction of 81.34 % compared with PSO-TS (case 1) and PSO-TS (case 3), which have reduced TVD by 79.85 % and 80.14 %, respectively. It can be seen that installing shunt capacitors on sensitive bus according to the second approach is more suitable for finding a better solution than other cases. The convergence characteristics of the TVD objective functions for the three cases are shown in Figure 4.14. From this figure the convergence curve of the proposed PSO-TS of the second case converges towards a high-quality solution compared with the other two cases. In this case, the algorithm converged in less than 180 iterations.

Table 4.12. Simulation results for the Sensitive Buses Approach

Control variables	TS	PSO	PSO-TS	PSO-TS (case 1)	PSO-TS (case 2)	PSO-TS (Case 3)
V1	1.0760	0.9875	1.0014	0.9960	0.9976	0.9796
V2	1.0494	0.9513	1.0592	1.0631	0.9714	1.0711
V5	1.0056	1.0641	1.0542	1.0702	1.0694	1.0675
V8	1.0238	1.0596	1.0133	0.9691	1.0594	1.0113
V11	1.0085	1.0972	0.9905	1.1000	0.9577	1.0994
V13	0.9641	1.1000	1.0291	1.0542	1.1000	1.0104
T6–9	0.9486	1.0344	0.9762	1.0129	1.0221	0.9556
T6–10	0.9840	1.1000	1.0163	1.0638	1.0056	1.0016
T4–12	0.9647	0.9000	0.9537	0.9000	0.9268	0.9000
T27–28	1.0287	0.9516	0.9481	0.9402	0.9493	0.9566
Q_{Sh10}	0.0917	03000	0.2890	-		-
Q_{Sh24}	0.2278	0.0440	0.0697	-	0.0785	-
Q_{Sh07}	-	-	-	0	-	-
Q_{Sh21}	-	-	-	0.1988	0.1748	-
Q_{Sh03}	-	-	-	-	-	0.1502
Q_{Sh29}	-	-	-	-	-	0.0206
TVD (p. u)	0.1874	0.1275	0.1113	0.1247	0.1155	0.1229
Reduction (%)	-	-	-	79.85	81.34	80.14

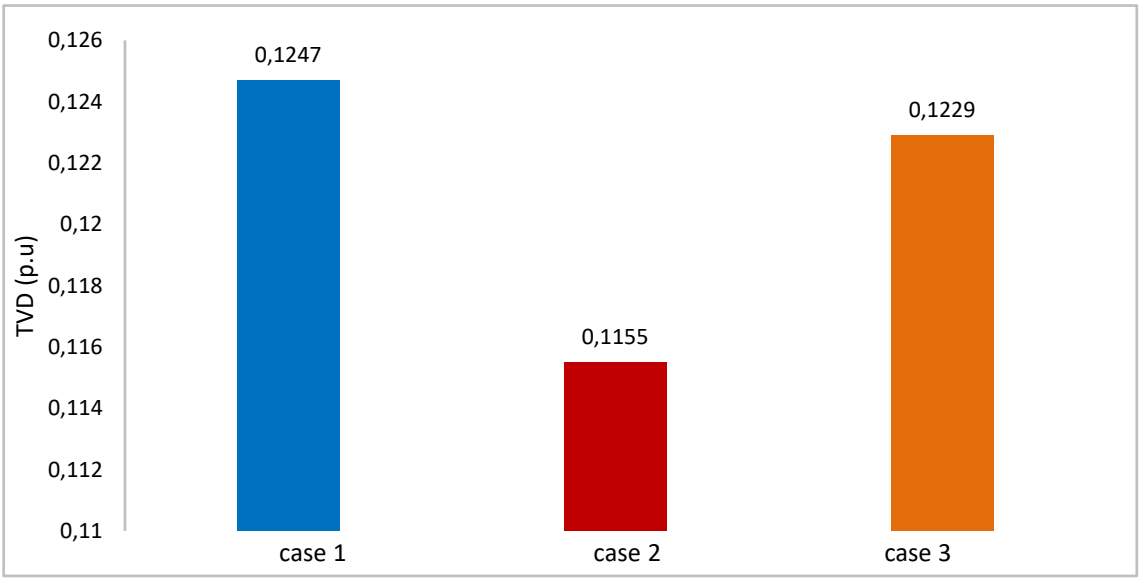

Figure 4.13. Comparative results of the TVD (3 cases)

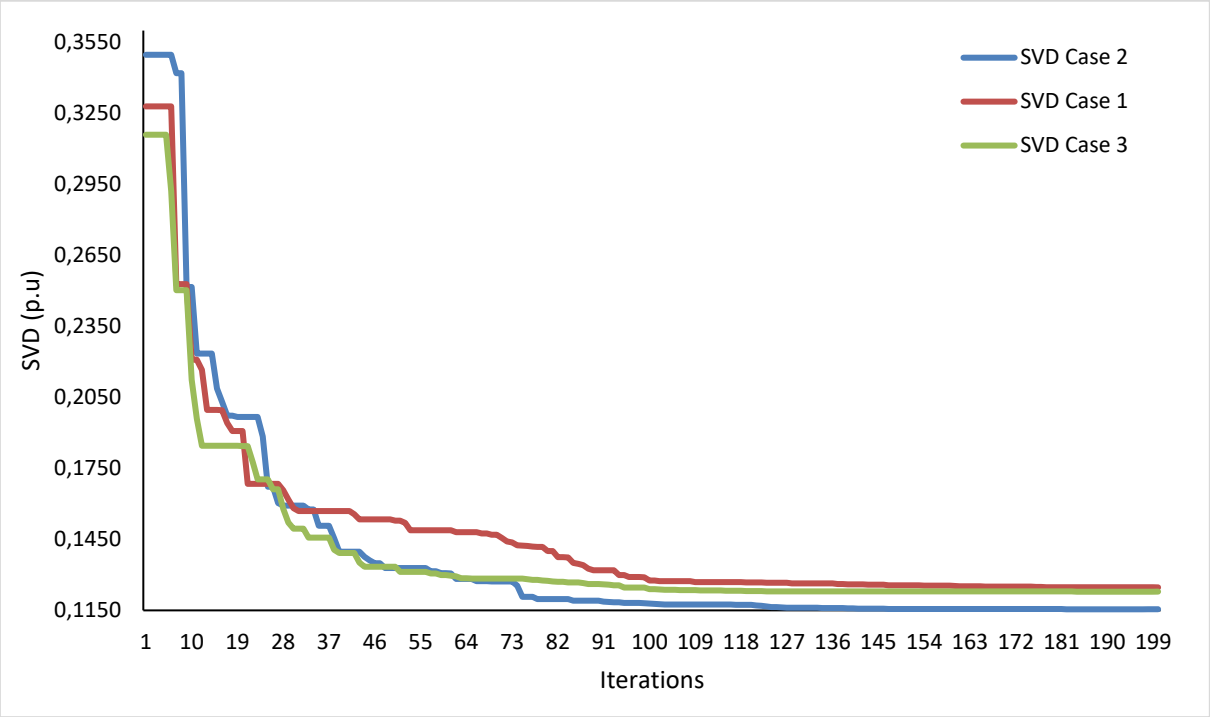

Figure 4.14. Convergence characteristic of the TVD (case 1, 2 and 3).

4.4.2.3.2. IEEE 57 bus test system

To confirm that the chosen method, based on the sensitivity to load reactive power, is the more appropriate and gives better results, the proposed hybrid algorithm have been implemented on the IEEE 57-bus test network. This system consists of 80 branches, seven generator-buses and 15 branches with load-tap setting transformers. The shunt reactive sources are at buses 18, 25 and 53 (standard buses). The bus one is the slack bus and the buses 2, 3, 6, 8, 9 and 12 are PV buses. The remaining nodes are PQ buses. Thus, the control variables vector is of length 25, i.e., seven generator voltages, 15 transformer taps, and three shunt reactive sources. The voltage magnitudes of all the buses are between 0.95 and 1.1 p.u, the transformer tap settings are within the range of 0.9–1.1 p.u and the shunt capacitor sizes are taken from 0 to 30 MVAR. The total system load is 1250.8 MW and 336.4 MVAr. The initial system active power loss is 28.462 MW. The classification of sensitive buses based on load reactive power is presented in table 4.13. For three capacitors and as given by Table 4.13, the most sensitive buses to be considered are 53, 31 and 38 (sensitive buses obtained using the second case approach). Beyond three capacitors, the active power losses do not improve. The proposed algorithm is tested and compared with other algorithms on optimal performance in terms of active power losses and total voltage deviation.

Table 4.13 Load reactive power-based classification (case 2)

Load bus	New P_{loss} value (MW)	Load bus	New P_{loss}value (MW)
53	28.1391	44	28.4060
31	28.2113	18	28.4112
38	28.2333	15	28.4139
35	28.2575	28	28.4164
25	28.2648	17	28.4265
47	28.2703	54	28.4298
42	28.2931	29	28.4318
50	28.3136	13	28.4361
33	28.3165	20	28.4366
30	28.3217	27	28.4470
49	28.3660	43	28.4481
56	28.3753	19	28.4495
57	28.3796	16	28.4526
52	28.3803	51	28.4552
23	28.3823	10	28.4559
14	28.3831	5	28.4581
41	28.3898	55	28.4715
32	28.3981	18	28.4112

a. Active power losses minimization

Table 4.14 lists the minimum power losses obtained by different methods, namely: PSO-TS in both cases (normal case and case 2), Canonical Genetic Algorithm (CGA), Adaptive Genetic Algorithm (AGA), Full Learning PSO (CLPSO) Gravitational Search Algorithm (GSA) [41]. From the results presented in this table, it is clear that the proposed algorithm with the sensitive bus approach performs much better than the other methods. The convergence characteristic for Ploss minimization of PSO-TS with sensitive bus approach is depicted in figure 4.15 which indicates a much better solution for the proposed hybrid algorithm and the performance of 30 independent runs of the proposed method is illustrated in figure 4.16. To have an idea of average performance of the proposed algorithm with sensitive bus approach, the best, worst, average minima and standard deviation are given respectively as follows: 21.3146, 22.2734, 21.5928 and 0.2977.

Table 4.14. Simulation results for the Sensitive Buses Approach

CVs	Initial	CGA [41]	AGA [41]	CLPSO [41]	GSA [41]	PSO-TS (normal case)	TS	PSO	PSO-TS (case 2)
V_1	1.0400	0.9686	1.0276	1.0541	1.0654	1.1000	1.0867	1.1000	1.1000
V_2	1.0100	1.0493	1.0117	1.0529	1.0682	1.0900	1.0721	1.1000	1.1000
V_3	0.9850	1.0567	1.0335	1.0337	1.0657	1.1000	1.0070	1.1000	1.0939
V_6	0.9800	0.9877	1.0010	1.0313	1.0432	1.1000	1.0790	1.1000	1.1000
V_8	1.0050	1.0223	1.0517	1.0496	1.0549	1.1000	1.0597	1.1000	1.1000
V_9	0.9800	0.9918	1.0518	1.0302	1.0598	1.1000	1.0724	1.1000	1.1000
V_{12}	1.0150	1.0044	1.0570	1.0342	1.0685	1.0747	1.0443	1.1000	1.0816
$T_{4\text{-}18}$	0.9700	0.9200	1.0300	0.9900	1.0300	0.9000	1.0734	1.1000	1.1000
$T_{4\text{-}18}$	0.9780	0.9200	1.0200	0.9800	1.0700	1.1000	1.0820	0.9000	0.9000
$T_{20\text{-}21}$	1.0430	09700	1.0600	0.9900	0.9500	1.1000	0.9911	1.1000	1.1000
$T_{24\text{-}26}$	1.0430	0.9000	0.9900	1.0100	1.0200	1.1000	0.9665	1.0007	1.0045
$T_{7\text{-}29}$	0.9670	0.91000	1.1000	0.9900	0.9800	1.0625	0.9018	0.9000	0.9000
$T_{34\text{-}32}$	0.9750	1.1000	0.9800	0.9300	1.0500	0.9000	1.0684	1.0053	0.9904
$T_{11\text{-}41}$	0.9550	0.9400	1.0100	0.9100	1.0800	0.9000	1.0536	0.9000	1.1000
$T_{15\text{-}45}$	0.9550	0.9500	1.0800	0.9700	0.9600	0.9840	1.0320	0.9000	0.9000
$T_{14\text{-}46}$	0.9000	1.0300	0.9400	0.9500	0.9400	1.0122	0.9965	0.9000	0.9000
$T_{10\text{-}51}$	0.9300	1.0900	0.9500	0.9800	1.0270	0.9832	1.0277	0.9040	0.9000
$T_{13\text{-}49}$	0.8950	0.900	1.0500	0.9500	1.0450	0.9658	0.9178	0.9000	0.9000
$T_{11\text{-}43}$	0.9580	0.900	0.9500	0.9500	1.0800	1.1000	0.9603	0.9000	0.9000
$T_{40\text{-}56}$	0.9580	1.0000	1.0100	1.0000	0.9900	1.1000	1.0155	0.9959	1.1000
$T_{39\text{-}57}$	0.9800	0.9600	0.9400	0.9600	1.0455	0.9879	1.0721	0.9814	1.1000
$T_{9\text{-}55}$	0.9400	1.0000	1.0000	0.9700	1.0247	1.0943	0.9256	0.9000	0.9000
Q_{sh18}	-	0.8400	0.0168	0.0988	0.07965	0.0000	-	-	-
Q_{sh25}	-	0.0081	0.01536	0.0542	0.00595	0.2994	-	-	-
Q_{sh53}	-	0.0536	0.03888	0.0628	0.04764	0.0000	0.1652	0.0990	0.0516
Q_{sh31}	-	-	-	-	-	-	0.1469	0.0536	0.3000
Q_{sh38}	-	-	-	-	-	-	0.1006	0.3000	0.0824
Ploss (Mw)	28.0080	25.2440	24.5648	24.5152	24.1264	24.3907	24.9508	24.4325	21.3146

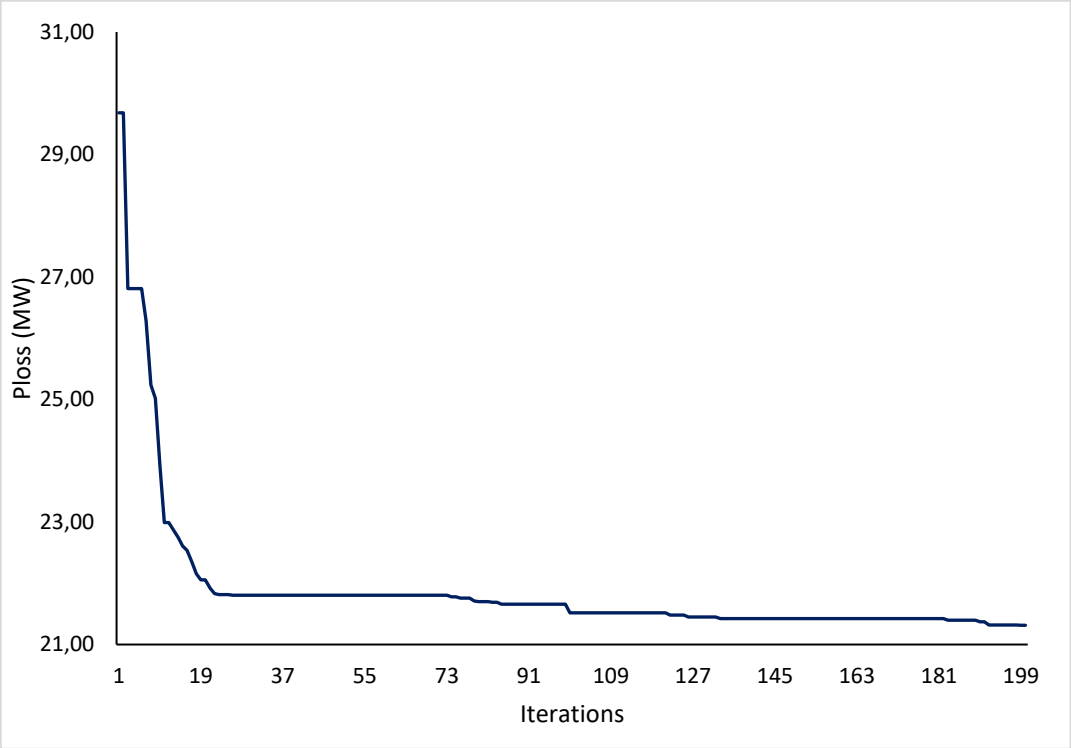

Figure 4.15. Convergence characteristic for active power losses minimization (case of sensitive bus approach)

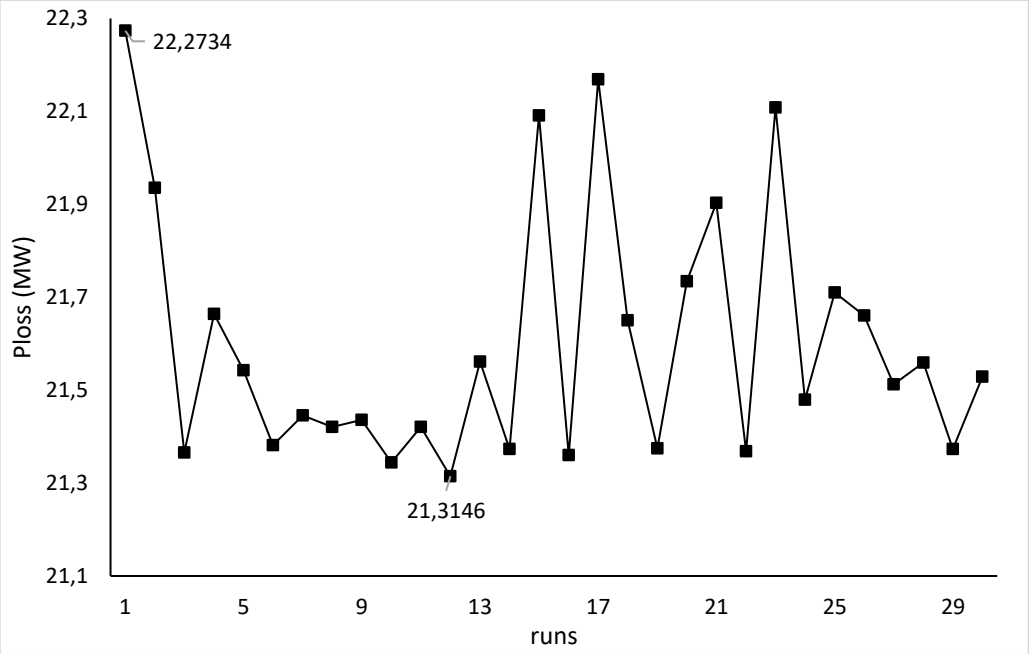

Figure 4.16. Performance of 30 independent runs (case 2)

b. Total voltage deviation minimization (TVD)

When the total voltage deviation is considered as objective function, the best results achieved by PSO-TS in both cases (normal case and case 2) are tabulated in Table 4.15. These results

show that the proposed algorithm with the sensitive bus approach (case 2) performs much better than the other methods namely: APOPSO (0.9430 pu), GSA (1.1100 pu), OGSA (0.6982 pu), PSO-TS (normal case) (0.9737 pu), TS (1.2184 pu), PSO (0.6998 pu). The convergence characteristic for TVD minimization of PSO-TS with sensitive bus approach is depicted in figure 4.17 and the performance of 30 independent runs of the proposed method is illustrated in figure 4.18. The best, worst, average minima and standard deviation are given respectively as follows: 0.67590, .8545, 0.7687 and 0.0560.

Table 4.15. Simulation results for the Sensitive Buses Approach

Control variables	APOPSO [149]	GSA [19]	OGSA [79]	PSO-TS (normal case)	TS	PSO	PSO-TS (case 2)
V_1	1.02	1.1	1.0138	1.0243	1.0319	1.0146	1.0015
V_2	1.009	1.1	0.9608	0.9529	1.0477	1.1000	0.9648
V_3	0.977	1.0737	1.0173	1.0400	0.9570	0.9500	0.9500
V_6	0.976	1.0422	0.9898	0.9500	1.0714	0.9735	1.1000
V_8	1.044	1.0523	1.0362	0.9500	1.0576	1.0456	0.9500
V_9	1.001	1.0455	1.0241	0.9500	1.0306	0.9500	0.9500
V_{12}	1.012	1.0468	1.0136	0.9500	1.0304	1.0681	1.1000
$T_{4\text{-}18}$	0.998	1.0100	0.9833	1.1000	0.9580	1.0436	0.9000
$T_{4\text{-}18}$	0.994	1.0100	0.9503	1.1000	0.9011	0.9196	1.0051
$T_{20\text{-}21}$	0.959	1.0300	0.9523	1.1000	1.0177	0.9700	1.0046
$T_{24\text{-}26}$	0.980	0.9800	1.0036	0.9000	1.0731	1.1000	1.0068
$T_{7\text{-}29}$	0.968	0.9800	0.9778	1.1000	0.9732	0.9764	0.9893
$T_{34\text{-}32}$	0.931	1.0200	0.9146	1.0625	0.9949	1.1000	1.0211
$T_{11\text{-}41}$	0.922	1.0000	0.9454	1.1000	0.9824	0.9000	0.9320
$T_{15\text{-}45}$	0.911	1.0000	0.9265	0.9831	0.9430	1.1000	0.9994
$T_{14\text{-}46}$	0.979	0.9800	0.9960	1.1000	0.9288	0.9400	0.9672
$T_{10\text{-}51}$	1.001	1.0200	1.0386	0.9821	0.9558	0.9909	0.9283
$T_{13\text{-}49}$	0.882	1.0000	0.9060	1.1000	1.0722	0.9000	0.9864
$T_{11\text{-}43}$	0.871	0.9900	0.9234	1.1000	1.0782	0.9318	0.9259
$T_{40\text{-}56}$	0.966	1.0100	0.9871	0.9000	1.0179	1.0414	1.0288
$T_{39\text{-}57}$	0.951	0.9900	1.0132	1.1000	0.9913	0.9189	0.9000
$T_{9\text{-}55}$	0.911	1.0200	0.9372	1.1000	1.0695	1.0019	0.9721
Q_{sh18}	0.02	0.0800	0.0463	0.3000	-	-	-
Q_{sh25}	0.097	0.1080	0.0590	0	-	-	-
Q_{sh53}	0.042	0.0780	0.0628	0.3000	0.2133	0.2606	0.2770
Q_{sh31}	-	-	-	-	0.1380	0.1634	0.1699
Q_{sh38}	-	-	-	-	0.1972	0.3000	0.3000
TVD (pu)	0.9430	1.1100	0.6982	0.9737	1.2184	0.6998	0.6759

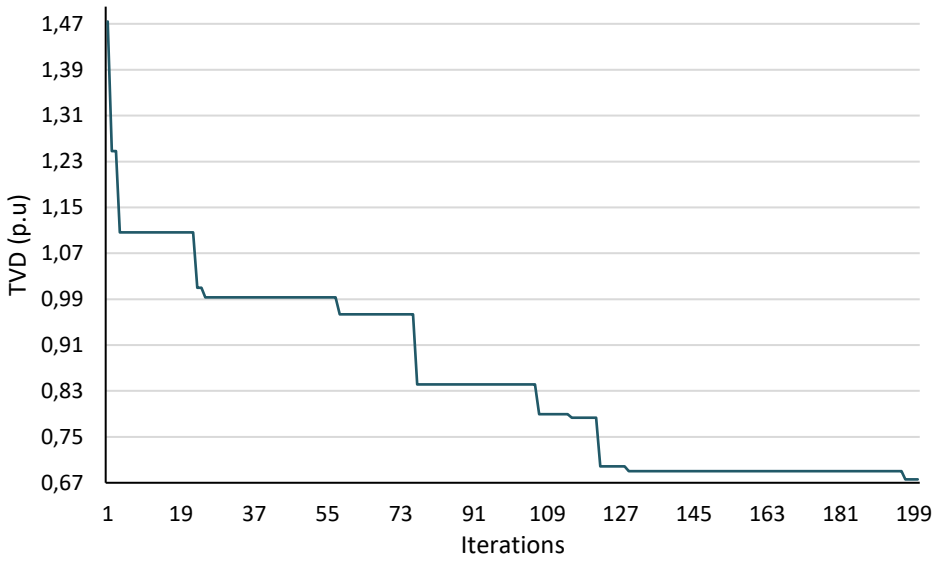

Figure 4.17. Convergence characteristic of the TVD minimization.

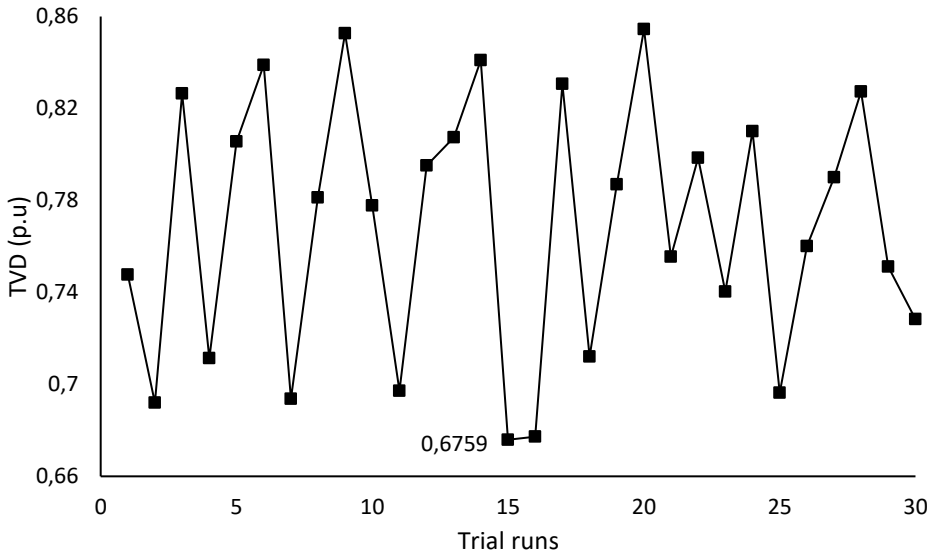

Figure 4.18. Performance of 30 independent runs of the IEEE 57-bus system ((case 2))

4.4.3. PSO-TS algorithm based ORPD considering discrete control variables

In this section, the ORPD is considered as a mixed integer nonlinear optimization problem that includes both continuous and discrete control variables. The bus voltages are considered as continuous variables on the other hand reactive powers of shunt compensators and the transformer taps are discrete variables with the step size of 0.01. The hybrid PSO-TS algorithm is implemented on IEEE 14-bus, IEEE 30-bus, IEEE 57-bus and Algerian 114-bus test systems. The objective function is the active power losses (P_{Loss}) for IEEE 14-bus, IEEE 30-bus and IEEE 57-bus, but for the Algerian 114-bus we have considered two objective

functions (active power losses and total voltage deviation). As in previous simulations, the inequality constraints are handled by penalty coefficients. The obtained results are compared with other evolutionary algorithms.

4.4.3.1. *IEEE 14-bus test system*

The PSO-TS method is applied to the ORPD problem taking into account continuous and discrete control variables for the active power loss minimization. Tables 4.16 summarizes the results of the optimal control variables obtained by PSO, TS, PSO-TS and the results obtained by several algorithms in literature. The results indicate that PSO-TS leads to active power losses of 12.1479 MW (initially these losses were 13.4919 MW) indicating a lower value than those of PSO and TS as well as the algorithms reported in the literature, namely PSO-TVAC [91], WOA [124], MGBTLBO [95], MTLA [130], DDE [130], MTLA-DDE [130] and SARGA [82]. In addition, the percentage reductions are presented in these tables. We can see that the proposed PSO-TS was able to reduce the active losses by 9.9615%. The proposed method was able to keep all the control variables within their bounds. Figures 4.19 shows the superiority of our algorithm over the others. The convergence curve of PSO-TS is given by Figure 4.20 indicating convergence after 190 iterations for the case of discrete variables. As illustrated by Figure 4.21, the performances of the PSO-TS are shown for 40 independent runs.

Table 4.16. Simulation results of TS, PSO and PSO-TS algorithms (case of discrete variables).

CV	Initial	MTLA **[130]**	DDE **[130]**	MTLA-DDE **[130]**	MGBTLBO **[95]**	PSO-TVAC **[91]**	WOA **[124]**	SARGA **[82]**	TS	PSO	PSO-TS
V_1	1.0600	1.0746	1.0743	1.0753	1.100	1.1013	1.1000	1.0000	1.0787	1.1000	1.1000
V_2	1.0450	1.0566	1.0561	1.0573	1.0791	1.0882	1.0859	1.0960	1.0464	1.0952	1.0932
V_3	1.0100	1.0272	1.0266	1.0284	1.0484	1.0585	1.0566	1.0360	1.0601	1.1000	1.0600
V_6	1.0700	1.0506	1.0469	1.0505	1.0553	1.0418	1.0858	1.0990	1.0158	1.1000	1.1000
V_8	1.0900	1.0111	1.0401	1.0353	1.0326	1.0440	1.1000	1.0780	1.0383	1.1000	1.1000
T_{4-7}	0.9780	1.0400	1.0400	1.0800	1.0100	1.0420	0.9585	0.9500	1.0300	0.9100	1.0500
T_{4-9}	0.9690	0.9300	0.9700	0.9100	1.0100	1.0176	1.0453	0.9500	1.0400	1.100	0.9000
T_{5-6}	0.9320	1.0400	1.0100	1.0100	1.0300	1.0747	1.0163	0.9600	1.0600	0.9900	0.9900
Q_{C9}	0.1800	0.3000	0.3000	0.3000	0.0300	0.171 0	0.1249	0.1800	0.1800	0.1800	0.1700
Q_{C14}	0.1800	0.0700	0.0700	0.0800	0.0700	0.0820	0.0801	0.0600	0.1700	0.0700	0.0800
*P*loss (MW)	13.491	12.910	12.928	12.897	12.310	12.279	12.255	13.216	13.042	12.257	12.147
Red (%)	-	4,308	4,175	4,403	8,760	8,989	9,167	2,044	3,334	9,147	9,961

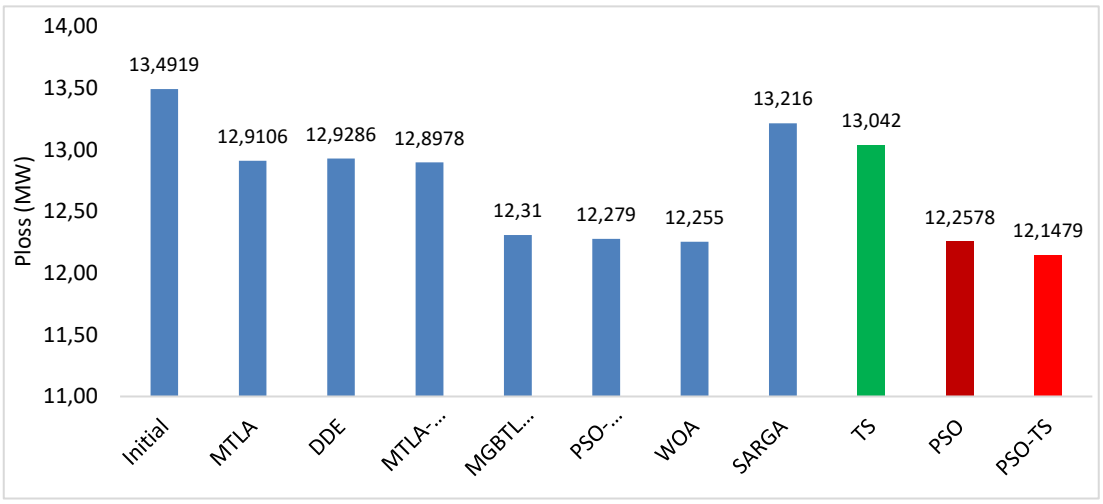

Figure 4.19. Comparative graph of the active power losses (Case of discrete variables)

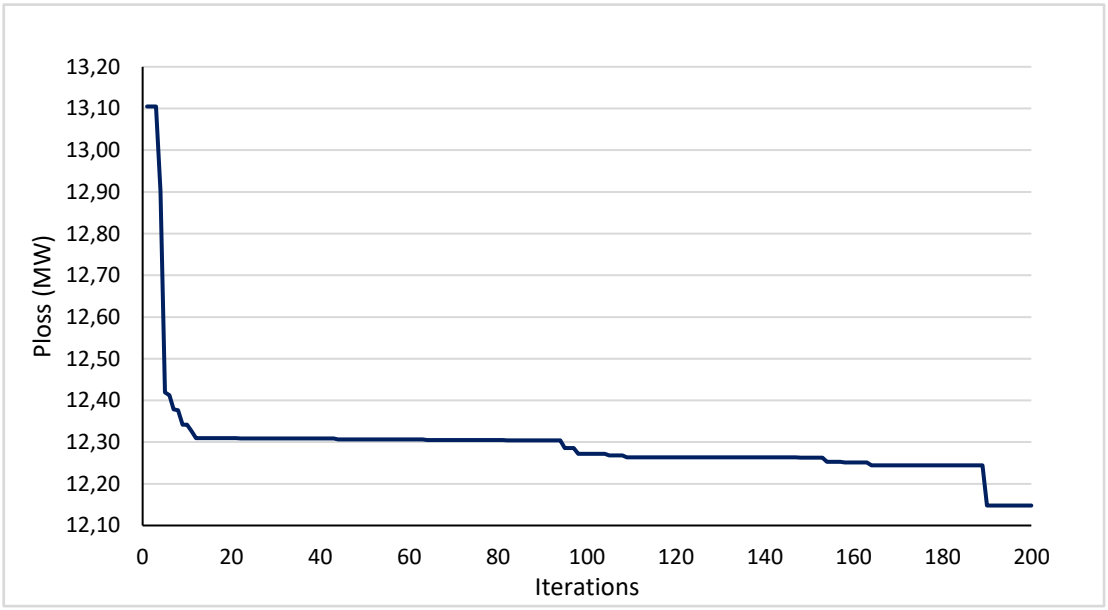

Figure 4.20. Convergence characteristic for power losses objective (case of discrete variables)

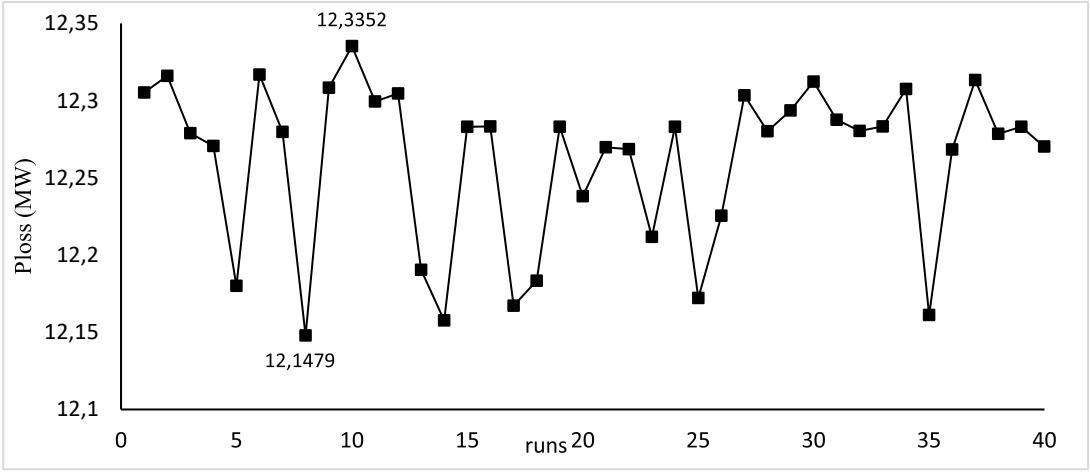

Figure 4.21. Performance for 40 independent runs

4.4.3.2. *IEEE 30-bus test system*

In order to verify the performance and feasibility of the proposed PSO-TS based reactive power optimization approach, the PSO-TS algorithm has also been tested on IEEE 30-bus power system [134]. It consists of 30 buses, out of which 6 are generator buses. Bus 1 is the slack bus, 2, 5, 8, 11 and 13 are taken as PV buses and the remaining 24 are PQ buses. The network has 41 branches, 4 transformers and 2 capacitor banks. The four branches 6–9, 9–10, 4–12, 27–28 are under load tap changing transformers within the interval [0.9, 1.1]. The two capacitor banks are set at buses 10 and 24 and take their values within the interval [0, 30] MVAr. The number of control variables is 12, which consist of six PV generator voltages within the range of [0.95, 1.1], four tap changing transformers and two shunt capacitor banks. The initial operating conditions of this system are given by [147]. In this part, the adopted objective function is the active power losses minimization. The best settings of the control variables obtained via the PSO-TS algorithm and the other algorithms are reported in Tables 4.17 and 4.18. Figure 4.24 shows the convergence curves of the considered algorithm. As noticeably, the PSO-TS technique converges to high quality solution in the last quarter of iterations. In addition, it can be seen that the PSO-TS algorithm outperforms the other methods namely: RGA [150], CMAES [150], MNSGA-II [150], MOPSO NSGA-II [150], [150], PSO [151], DE [388], ICA [89], IWO [89], MICA-IWO [89], SGA [3], MAPSO [3] (Figure 4.22). Figure 4.23 shows 40 independent runs of the proposed algorithm. The Best (4.5708), worst (4.6578), mean (4.6130) and the standard deviation (0.02121) of Ploss minimization results show that the solution is relatively stable.

Table 4.17. Simulation results of TS, PSO and PSO-TS algorithms (case of discrete variables).

Control Variables	TS	PSO	PSO-TS
V_1	1.0974	1.1000	1.1000
V_2	1.0968	1.1000	1.0949
V_5	1.0513	1.1000	1.0738
V_8	1.0868	1.1000	1.1000
V_{11}	1.0690	1.1000	1.1000
V_{13}	1.0739	1.1000	1.0999
T_{6-9}	0.9500	1.1000	0.9900
T_{6-10}	0.9800	1.1000	1.0600
T_{4-12}	1.0300	0.9000	0.9000
T_{27-28}	1.0800	0.9900	0.9600
Q_{Sh10}	0.0900	0.0700	0.0800
Q_{Sh24}	0.0600	0.0200	0.0100
P_{loss} *(MW)*	5.0607	4.6173	4.5708

Table 4.18. Best solutions comparison

Methods	Ploss (MW)	Loss reduction (%)
RGA [150]	4.9510	6.200
CMAES [150]	4.9450	6.314
MOPSO [150]	4.9510	6.200
NSGA-II [150]	4.9520	6.181
MNSGA-II [150]	4.9454	6.307
DE [151]	5.0110	5.064
ICA [89]	4.9444	6.325
IWO [89]	4.9995	5.282
MICA-IWO [89]	4.9178	6.829
SGA [3]	4.9800	5.651
MAPSO [3]	4.8747	7.646
TS	5.0607	4.122
PSO	4.6173	12.523
PSO-TS	**4.5708**	**13.403**

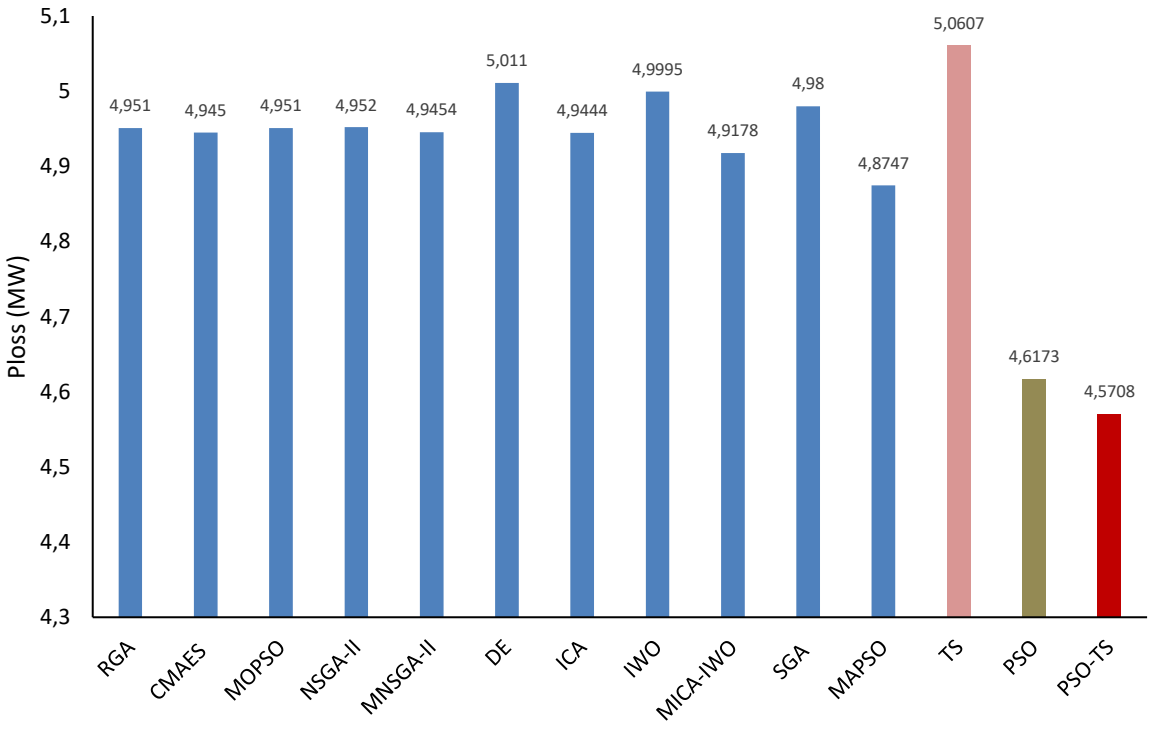

Figure 4.22. Comparative graph of the active power losses (Case of discrete variables)

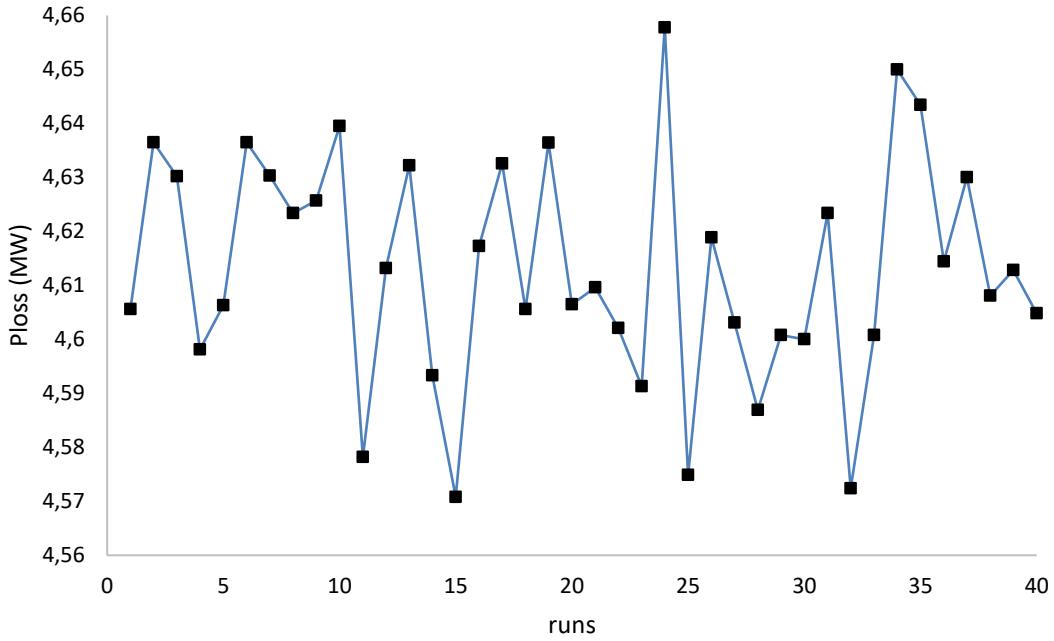

Figure 4.23. Performance of 40 independent runs

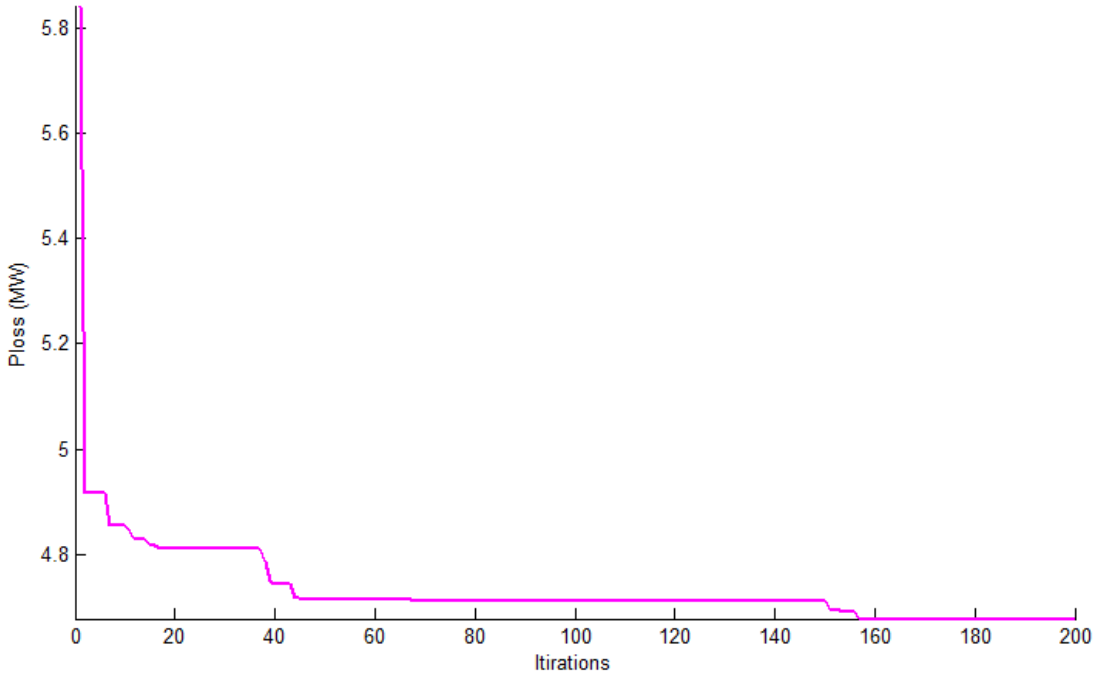

Figure 4.24. Convergence characteristic for the power losses

4.4.3.3. *IEEE 57-bus system*

In order to evaluate the effectiveness and performance of the PSO-TS method for large scale power system, the standard IEEE 57-bus test system already described in Chapter 3 is introduced as a test system for minimizing active power losses. Table 4.19 depicts the solution result for P_{Loss} minimization objective. In this table, PSO-TS based results are compared to

other optimization technique reported in the literature like NLP, CGA, AGA, PSO-w, PSO-cf, CLPSO, SPSO, L-DE, L-SACP-DE, L-SaDE, SOA [127], OGSA [79] and GSA [19]. From Table 4.19, it may be observed that PSO-TS reduced active power losses from 28.4623 MW (initial losses) to 21.3315 MW, i.e. a reduction of 25.053%, which is less than the amount obtained by TS and PSO as well as those of other algorithms. Figure. 4.25 shows the Convergence characteristic of real power loss based PSO-TS and indicates a convergence around 190 iterations while the Figure 4.26 gives the objective function minimum values for 30 independent runs and shows the relative stability of the proposed PSO-TS method as indicated by the statistical indicators below:

The best result= 21,3315 MW, the worst result=22.7303 MW, the mean=21.7629 MW and the standard deviation =0.4043.

Table 4.19. Simulation results of TS, PSO and PSO-TS algorithms (case of discrete variables).

Control variables	OGSA [79]	GSA [19]	NLP [127]	CGA [127]	AGA [127]	PSO-w [127]	PSO-cf [127]
V_1	1.0600	1.0600	1.0600	0.9686	1.0276	1.0600	1.0600
V_2	1.0594	1.0600	1.0600	1.0493	1.0117	1.0578	1.0586
V_3	1.0492	1.0600	1.0538	1.0567	1.0335	1.0438	1.0464
V_6	1.0433	1.0081	1.0600	0.9877	1.0010	1.0356	1.0415
V_8	1.0600	1.0550	1.0600	1.0223	1.0517	1.0546	1.0600
V_9	1.0450	1.0098	1.0600	0.9918	1.0518	1.0369	1.0423
V_{12}	1.0407	1.0186	1.0600	1.0044	1.0570	1.0334	1.0371
$T_{4\text{-}18}$	0.9000	1.1000	0.9100	0.9200	1.0300	0.9000	0.9800
$T_{4\text{-}18}$	0.9947	1.0826	1.0600	0.9200	1.0200	1.0200	0.9800
$T_{20\text{-}21}$	0.9000	0.9220	0.9300	0.9700	1.0600	1.0100	1.0100
$T_{24\text{-}26}$	0.9001	1.0167	1.0800	0.9000	0.9900	1.0100	1.0100
$T_{7\text{-}29}$	0.9111	0.9963	1.0000	0.9100	1.1000	0.9700	0.9800
$T_{34\text{-}32}$	0.9000	1.1000	1.0900	1.1000	0.9800	0.9700	0.9700
$T_{11\text{-}41}$	0.9000	1.0746	0.9200	0.9400	1.0100	0.9000	0.9000
$T_{15\text{-}45}$	0.9000	0.9543	0.9100	0.9500	1.0800	0.9700	0.9700
$T_{14\text{-}46}$	1.0464	0.9377	0.9800	1.0300	0.9400	0.9500	0.9600
$T_{10\text{-}51}$	0.9875	1.0168	0.9800	1.0900	0.9500	0.9600	0.9700
$T_{13\text{-}49}$	0.9638	1.0526	0.9800	0.9000	1.0500	0.9200	0.9300
$T_{11\text{-}43}$	0.9000	1.1000	0.9800	0.9000	0.9500	0.9600	0.9700
$T_{40\text{-}56}$	0.9000	0.9800	0.9800	1.0000	1.0100	1.0000	0.9900
$T_{39\text{-}57}$	1.0148	1.0247	1.0800	0.9600	0.9400	0.9600	0.9600
$T_{9\text{-}55}$	0.9830	1.0373	1.0300	1.0000	1.0000	0.9700	0.9800
Q_{sh18}	0.0682	0.0783	0.0835	0.0840	0.0168	0.0514	0.0998
Q_{sh25}	0.0590	0.0059	0.0086	0.0082	0.0154	0.0590	0.0590
Q_{sh53}	0.0630	0.0469	0.0110	0.0538	0.0389	0.0629	0.0629
Ploss (MW)	23.4300	23.4612	25,9023	25.2441	24.5648	24.2705	24.2802
Red (%)	17.6797	17.5701	8.9934	11.3060	13.6926	14.7267	14.6926

Table 4.19 (continued)

Control variables	CLPSO [127]	SPSO [127]	L-DE [127]	L-SACP-DE [127]	L-SaDE [127]	SOA [127]	TS	PSO	PSO-TS
V_1	1.0541	1.0596	1.0397	0.9884	1.0600	1.06	1.0877	1.1000	1.1000
V_2	1.0529	1.0580	1.0463	1.0543	1.0574	1.0580	1.0353	1.1000	1.1000
V_3	1.0337	1.0488	1.0511	1.0278	1.0438	1.0437	1.0988	1.1000	1.1000
V_6	1.0313	1.0362	1.0236	0.9672	1.0364	1.0352	1.0343	1.0941	1.1000
V_8	1.0496	1.0600	1.0538	1.0552	1.0537	1.0548	1.0730	1.1000	1.1000
V_9	1.0302	1.0433	0.94518	1.0245	1.0366	1.0369	0.9834	1.1000	1.0953
V_{12}	1.0342	1.0356	0.99078	1.0098	1.0323	1.0336	1.0378	1.1000	1.0810
$T_{4\text{-}18}$	0.9900	0.9500	1.0200	1.0500	0.9400	1.0000	1.0800	1.1000	1.0800
$T_{4\text{-}18}$	0.9800	0.9900	0.9100	1.0500	1.0000	0.9600	1.0600	0.9000	0.9000
$T_{20\text{-}21}$	0.9900	0.9900	0.9700	0.9500	1.0100	1.0100	1.0400	1.1000	1.1000
$T_{24\text{-}26}$	1.0100	1.0200	0.9100	0.9800	1.0100	1.0100	0.9200	1.0000	1.1000
$T_{7\text{-}29}$	0.9900	0.9700	0.9600	0.9700	0.9700	0.9700	1.0200	0.9000	0.9000
$T_{34\text{-}32}$	0.9300	0.9600	0.9900	1.0900	0.9700	0.9700	0.9700	1.1000	1.0100
$T_{11\text{-}41}$	0.9100	0.9200	0.9800	0.9200	0.9000	0.9000	0.9700	0.9000	1.1000
$T_{15\text{-}45}$	0.9700	0.9600	0.9600	0.9100	0.9700	0.9700	0.9800	0.9000	0.9000
$T_{14\text{-}46}$	0.9500	0.9500	1.0500	1.0800	0.9600	0.9500	1.0100	0.9000	0.9000
$T_{10\text{-}51}$	0.9800	0.9700	1.0700	0.9900	0.9600	0.9600	0.9800	0.9000	0.9000
$T_{13\text{-}49}$	0.9500	0.9200	0.9900	0.9100	0.9200	0.9200	1.0600	0.9000	0.9000
$T_{11\text{-}43}$	0.9500	1.0000	1.0600	0.9400	0.9600	0.9600	0.9800	0.9000	0.9000
$T_{40\text{-}56}$	1.0000	1.0000	0.9900	0.9900	1.0000	1.0000	0.9600	0.9900	1.1000
$T_{39\text{-}57}$	0.9600	0.9500	0.9700	0.9600	0.9600	0.9600	1.0000	0.9800	1.1000
$T_{9\text{-}55}$	0.9700	0.9800	1.0700	1.1000	0.9700	0.9700	1.1000	0.9000	0.9000
Q_{sh18}	0.0988	0.0393	0.0000	0.0000	0.0811	0.0998	-	-	-
Q_{sh25}	0.0542	0.0566	0.0000	0.0000	0.0580	0.0590	-	-	-
Q_{sh53}	0.0628	0.0355	0.0000	0.0000	0.0619	0.0628	0.0500	0.1000	0.1000
Q_{sh31}	-	-	-	-	-	-	0.1400	0.0600	0.0600
Q_{sh38}	-	-	-	-	-	-	0.1800	0.3000	0.3000
Ploss (MW)	24.51	24.43	27.81	27.91	24.26	24.26	25.6437	21.5229	21.3315
Red (%)	13.8852	14.1663	2.2908	1.9394	14.7635	14.7635	9.902	24.3802	25.0527

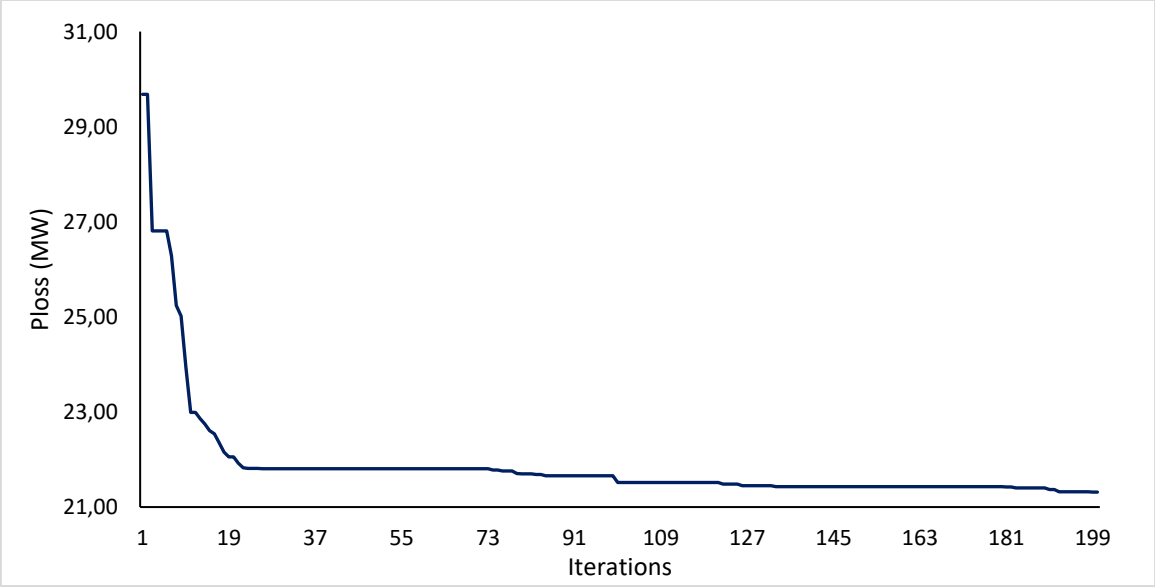

Figure 4.25. Convergence characteristic for the power losses

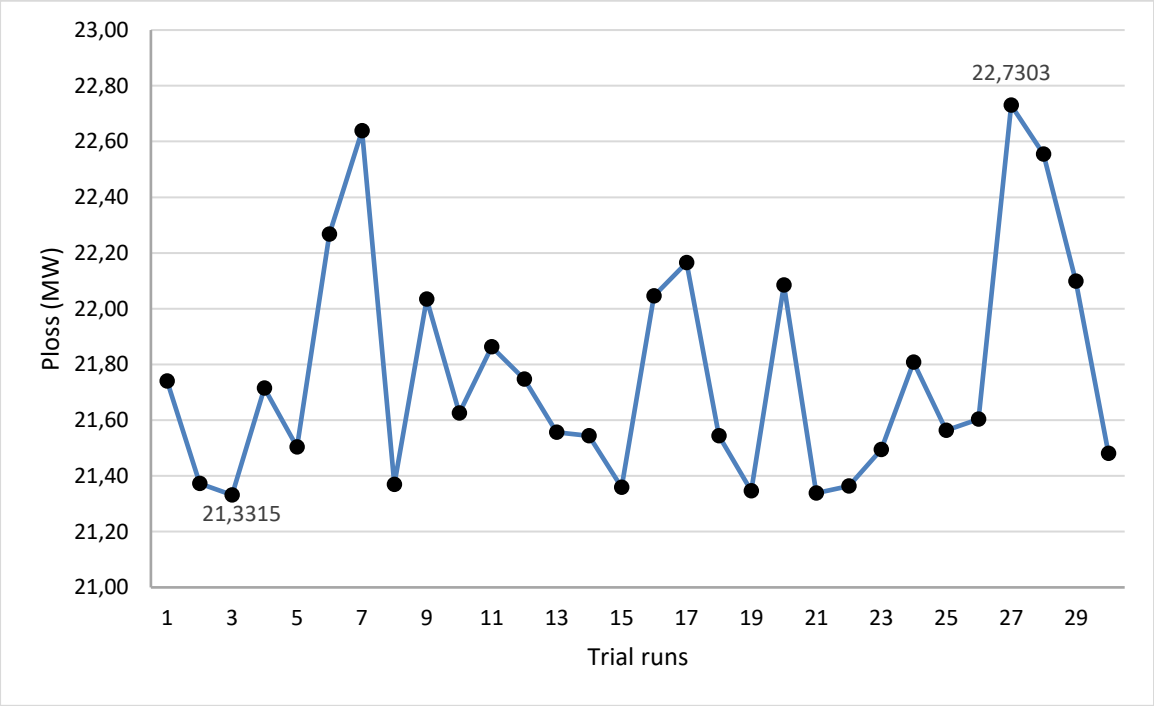

Figure 4.26. Performance of 30 independent runs

4.4.3.4. *Practical Algerian 114-bus power system*

In order to conduct deeper study of performance and efficiency of the proposed Hybrid PSO-TS algorithm, it is applied to the practical large-scale Algerian power test system with 114 bus (figure 4.27). The Algerian power system data are given in Appendix A. This system comprises 175 transmissions lines, 15 generators, and 16 tap changer transformers. In addition, shunt capacitors are also considered as control variables. The shunt capacitor locations are determined by the sensitive buses approach. The total system real and reactive power demands in initial state are 3727 MW and 2070 MVAr. Bus 4 is selected as the slack-bus. Using the sensitive bus approach, we have classified the busses of the Algerian network. The table 4.20 shows the classification of the busses from the most sensitive to the least sensitive. To identify the number of the shunt capacitors to install, we optimized the active power losses by inserting them gradually (one by one). After inserting the seventh reactive power source, there was no further improvement in the value of active power losses, so we have an optimum number of 6 shunt capacitors. Therefore, the system has a total of 37 variables to be optimized, including fifteen generators, sixteen transformers and six shunt capacitors. The minimum and maximum limits for the control variables are depicted in Table 4.21 [152].

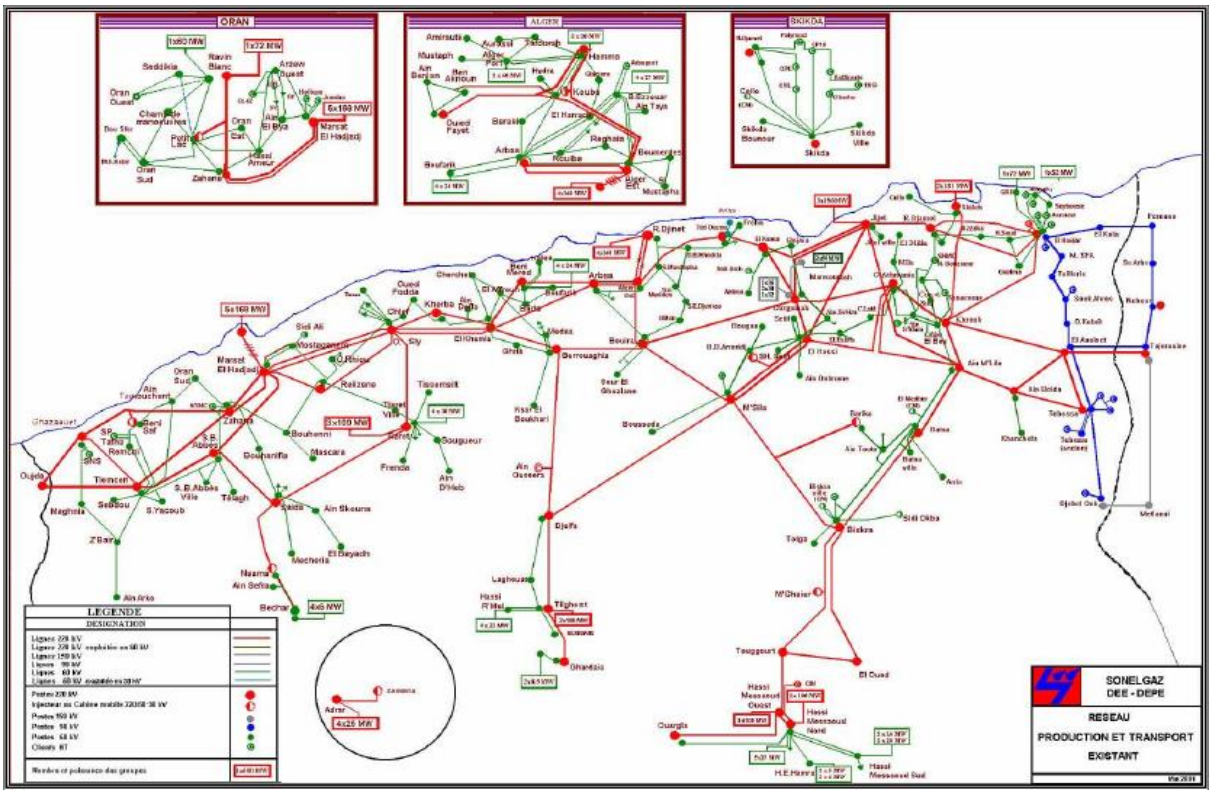

Figure 4.27. Single line diagram of Algerian 114-bus system [153]

Table 4.20. Classification of load buses.

bus	P_{Loss}	bus	P_{Loss}	bus	P_{Loss}	bus	P_{Loss}	bus	P_{Loss}	bus	P_{Loss}
66	76.0772	24	76.9634	69	77.1144	76	77.2217	113	77.2758	47	77.3824
56	76.3162	82	76.9733	29	77.1204	77	77.2248	50	77.2888	40	77.3846
91	76.3693	68	76.9755	87	77.1326	71	77.2250	110	77.2892	6	77.4251
73	76.3895	59	77.0097	70	77.1496	20	77.2366	49	77.3189	10	77.5197
63	76.5254	92	77.0289	39	77.1634	38	77.2495	45	77.3200	13	77.5599
89	76.6521	106	77.0623	33	77.1875	102	77.2593	43	77.3201	8	77.5781
54	76.8517	90	77.0851	23	77.1879	99	77.2620	112	77.3251	1	77.9258
85	76.8857	94	77.0878	97	77.1879	51	77.2672	3	77.3265	41	78.0063
61	76.9155	34	77.0968	25	77.2053	104	77.269	9	77.3438	26	78.0125
67	76.9203	32	77.1047	95	77.2072	79	77.2697	103	77.3498	12	78.2962
53	76.9272	65	77.1070	36	77.2078	78	77.2725	114	77.3530	21	78.3947
62	76.9324	107	77.1089	88	77.2080	37	77.2732	84	77.3605		
55	76.9410	57	77.1134	30	77.2166	108	77.2744	7	77.3681		

Table 4.21. Algerian 114-bus test system variable limits

Variables	Lower limits (p.u)	Upper limits (p.u)
Generator buses voltage	0.9	1.1
Load buses voltage	0.9	1.1
Transformers tap setting	0.9	1.1
shunt compensators (MVAr)	0	25

a. Simulation results for active power losses minimization

The PSO-TS method was applied to a real Algerian network of 114-bus, taking into account continuous and discrete variables and the two objective functions earlier defined. Table 4.22 shows the optimal control variables for the 114-bus Algerian network, obtained by TS, PSO and PSO-TS. According to these results, the lowest active power losses are obtained using the PSO-TS method. The proposed algorithm reduced the active power losses from 77.2746 MW (initial losses) to 59.9319 MW with a reduction rate of 22.443% in the case of continuous variables and from 77.2746 MW to 60.4422 MW, i.e. a reduction of 21.783% in the case of

Table 4.22. Simulation results of TS, PSO and PSO-TS for the Ploss (Algerian 114-bus system)

Control variables	Continuous variables			Discrete variables		
	TS	PSO	PSO-TS	TS	PSO	PSO-TS
V_4	0.9820	1.1000	1.1000	1.0632	1.0889	1.1000
V_5	1.0122	1.1000	1.1000	1.0243	1.1000	1.1000
V_{11}	0.9165	1.1000	1.1000	1.0946	1.0889	1.1000
V_{15}	0.9592	1.1000	1.0995	1.0656	1.0677	1.1000
V_{17}	1.0828	1.1000	1.1000	1.0426	1.1000	1.1000
V_{19}	0.9826	1.1000	1.1000	0.9857	1.0942	1.1000
V_{22}	1.0656	1.1000	1.1000	1.0286	1.1000	1.1000
V_{52}	0.9822	1.1000	1.1000	1.0734	1.1000	1.1000
V_{80}	0.9374	1.0942	1.1000	1.0267	1.1000	1.1000
V_{83}	1.0048	1.1000	1.1000	1.0263	1.1000	1.1000
V_{98}	1.0875	1.1000	1.1000	0.9984	1.0748	1.1000
V_{100}	1.0331	1.1000	1.1000	1.0032	1.1000	1.1000
V_{101}	1.0646	1.1000	1.1000	1.0473	1.1000	1.1000
V_{109}	1.0678	1.1000	1.1000	1.0557	1.1000	1.1000
V_{111}	1.0892	1.1000	1.1000	1.0372	1.1000	1.1000
$T_{80–88}$	1.0745	0.9000	0.9000	1.04	0.90	0.90
$T_{81–90}$	0.9528	1.0456	0.9000	1.00	0.90	0.98
$T_{86–93}$	1.0327	1.1000	0.9000	0.99	0.94	0.98
$T_{42–41}$	1.0360	0.9605	0.9449	0.95	0.96	0.90
$T_{58–57}$	1.0679	0.9000	0.9472	1.08	0.90	0.90
$T_{44–43}$	1.0357	0.9000	0.9517	0.94	0.90	0.90
$T_{60–59}$	1.0040	0.9734	0.9905	0.98	0.97	0.98
$T_{64–63}$	0.9575	0.9460	0.9535	0.96	0.90	0.97
$T_{72–71}$	0.9111	0.9000	0.9002	1.05	0.90	0.90
$T_{17–18}$	1.0130	1.0233	1.0403	1.01	1.04	1.03
$T_{21–20}$	0.9695	0.9996	1.0079	1.09	1.00	0.98
$T_{27–26}$	1.0413	1.1000	0.9000	1.09	1.10	0.90
$T_{28–26}$	0.9894	0.9563	1.1000	0.93	0.90	1.10
$T_{31–30}$	1.0012	0.9772	0.9822	1.03	0.98	0.97
$T_{48–47}$	1.0118	0.9843	0.9577	1.09	0.98	0.98
$T_{74–76}$	0.9527	1.1000	0.9187	1.09	1.10	1.10
Q_{C56}	0.1159	0.2500	0.2500	0.15	0.25	0.25
Q_{C63}	0.2068	0.0000	0.2005	0.17	0.25	0.25
Q_{C66}	0.0844	0.2500	0.2088	0.01	0.25	0.25
Q_{C73}	0.2467	0.2500	0.2500	0.15	0.25	0.25
Q_{C89}	0.1613	0.2500	0.2500	0.19	0.10	0.25
Q_{C91}	0.2084	0.2500	0.0440	0.20	0.25	0.25
P_{Loss} (MW)	76.1048	61.1138	59.9319	75.0614	61.4602	60.4422
Red (%)	1.514	20.913	22.443	2.864	20.465	21.783

discrete variables. Figure 4.28 shows the superiority of PSO-TS over the other two algorithms. The evolution of active power losses over the iterations is shown in Figure 4.29, where we observe convergence of PSO-TS for continuous variables at the 102nd iteration and convergence at the 164th iteration for discrete variables. The performance of the proposed method for 20 independent runs is shown in Figure 4.30 with the minimum and maximum active losses obtained. The mean of the results obtained (60.9770) and their standard deviation (0.6092) show that the solution is relatively stable.

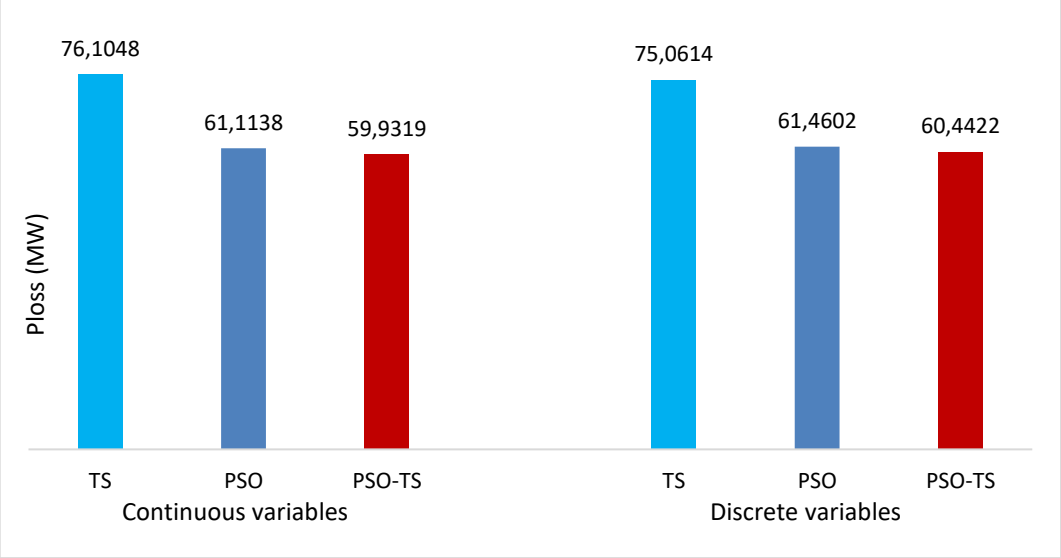

Figure 4.28. Comparative graph of active power losses (Algerian 114-bus system)

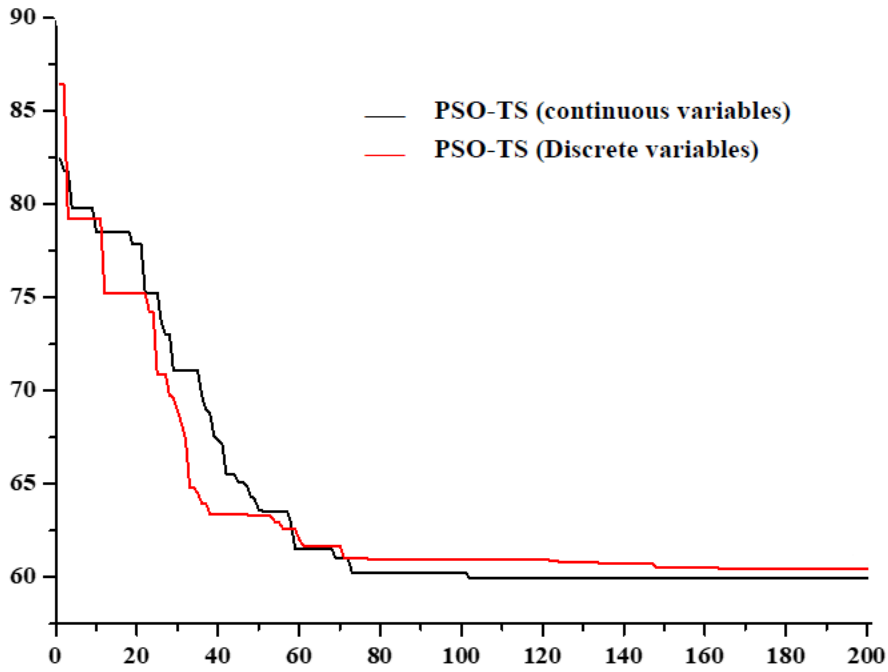

Figure 4.29. Convergence characteristic of Algerian 114-bus system for P_{Loss} minimization

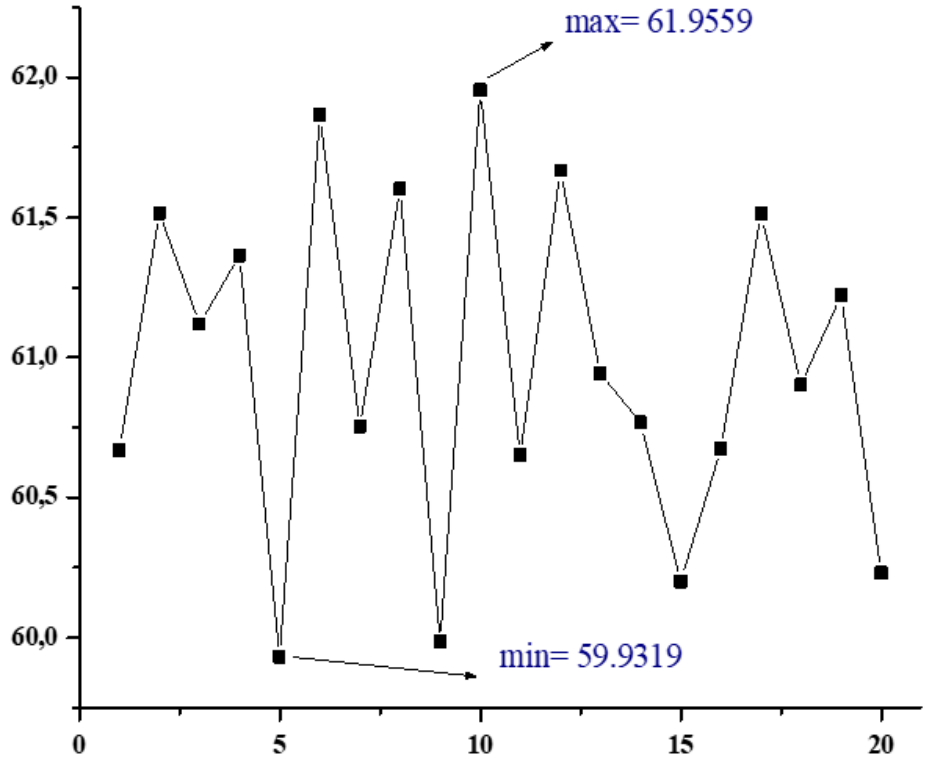

Figure 4.30. Performance of 24 particles for 20 runs (Ploss minimization)

b. Simulation results for total of voltage deviation minimization

In this case, the proposed algorithm is also applied to minimize the total voltage deviation. Table 4.23 shows the simulation results obtained by the three algorithms with discrete and continuous variables. The TVD value obtained by the PSO-TS algorithm is better than that obtained by the TS and PSO algorithms for both types of variables. Indeed, the PSO-TS reduced the total of voltage deviation from 3.7650 pu (initial TVD) to 1.6834 pu, i.e. a reduction of 55.288% in the case of continuous variables and from 3.7650 pu to 1.6753 pu in the case of discrete variables with a reduction rate of 55.503%. The proposed algorithm is therefore effective in giving solutions that are close to optimality (Figures 4.31). The convergence curves of this method are presented in Figure 4.32, we note that the PSO-TS converges for continuous variables at the 180th iteration and for the case of discrete variables, it converges at the 139th iteration. An overview of the voltage profile is given in Figures 4.34. We note that the voltages at each busbar respect the limits set and are close to the reference voltage (1 p.u). Figure 4.33 shows several tests carried out, with the minimum and maximum TVD obtained. The mean of the results obtained (1.80588) and their standard deviation (0.0990) show that the solution is relatively stable.

Table 4.23. Simulation results of TS, PSO and PSO-TS for the TVD (Algerian 114-bus system)

Control variables	Continuous variables			Discrete variables		
	TS	PSO	PSO-TS	TS	PSO	PSO-TS
V_4	1.0657	1.0033	1.0402	1.0498	1.0051	1.0046
V_5	1.0968	1.1000	0.9000	0.9023	1.0914	1.1000
V_{11}	1.0446	0.9149	0.9000	1.0050	0.9000	0.9000
V_{15}	1.0089	0.9169	0.9194	1.0540	0.9000	0.9000
V_{17}	0.9912	0.9927	0.9924	1.0469	1.0090	1.1000
V_{19}	1.0254	1.0139	0.9979	1.0466	1.0191	0.9996
V_{22}	1.0822	1.1000	1.1000	0.9019	0.9815	0.9010
V_{52}	0.9069	1.1000	1.1000	1.0711	1.1000	1.1000
V_{80}	1.0673	0.9691	0.9000	0.9480	1.1000	0.9000
V_{83}	0.9863	1.1000	1.1000	1.0064	1.1000	1.0534
V_{98}	1.0120	0.9000	1.1000	1.0662	0.9526	1.1000
V_{100}	1.0259	1.0442	1.0617	1.0737	1.0942	1.0985
V_{101}	1.0040	1.1000	0.9615	0.9903	1.0553	0.9466
V_{109}	1.0156	1.1000	1.0029	1.0052	1.0091	1.0375
V_{111}	1.0106	0.9810	1.0371	0.9477	0.9000	1.0134
T_{80-88}	0.9555	0.9308	0.9251	0.95	1.10	0.90
T_{81-90}	0.9212	0.9000	0.9000	1.01	0.90	0.99
T_{86-93}	0.9836	1.0004	0.9917	0.95	0.99	0.99
T_{42-41}	1.0079	0.9229	0.9686	1.08	0.90	0.92
T_{58-57}	0.9486	0.9275	0.9176	0.99	0.97	0.99
T_{44-43}	0.9213	0.9645	0.9000	0.97	0.90	0.90
T_{60-59}	1.0776	0.9005	0.9226	0.95	0.90	1.01
T_{64-63}	0.9292	0.9744	0.9225	0.96	0.97	1.00
T_{72-71}	0.9822	0.9000	0.9074	1.05	0.90	0.96
T_{17-18}	0.9945	1.0304	1.1000	1.06	1.10	1.02
T_{21-20}	0.9951	1.1000	1.1000	0.93	1.02	1.05
T_{27-26}	1.0818	0.9333	0.9016	0.96	1.10	0.92
T_{28-26}	1.0308	1.1000	0.9000	1.02	1.10	0.91
T_{31-30}	0.9881	0.9000	0.9681	1.06	0.98	1.00
T_{48-47}	1.0150	0.9593	0.9620	1.06	0.97	1.04
T_{74-76}	1.0575	0.9796	0.9000	0.91	0.97	0.96
Q_{C56}	0.1850	0.0000	0.0456	0.18	0.24	0.25
Q_{C63}	0.2493	0.2500	0.0000	0.11	0.25	0.25
Q_{C66}	0.1654	0.2500	0.2500	0.23	0.00	0.21
Q_{C73}	0.0472	0.2500	0.0728	0.19	0.25	0.23
Q_{C89}	0.1414	0.2500	0.0212	0.20	0.00	0.25
Q_{C91}	0.1558	0.2500	0.2248	0.09	0.15	0.20
TVD (pu)	3.1207	1.7059	1.6834	3.3029	1.7684	1.6753
Red (%)	17.113	54.691	55.288	12.274	53.031	55.503

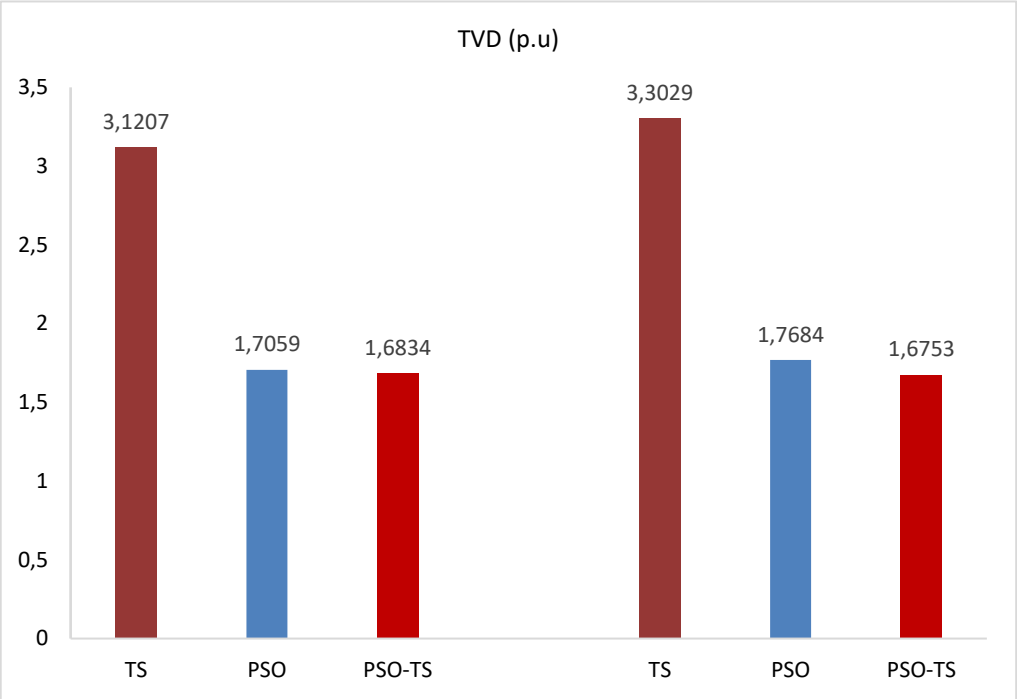

Figure 4.31. Comparative graph of TVD (Algerian 114-bus system)

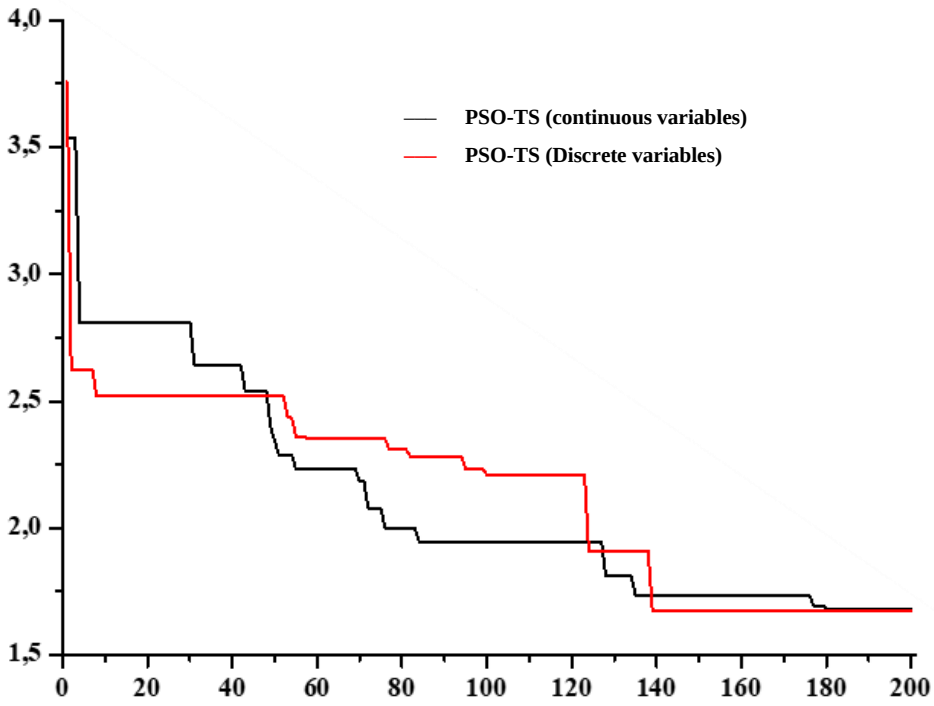

Figure 4.32. Convergence characteristic of Algerian 114-bus system for TVD minimization

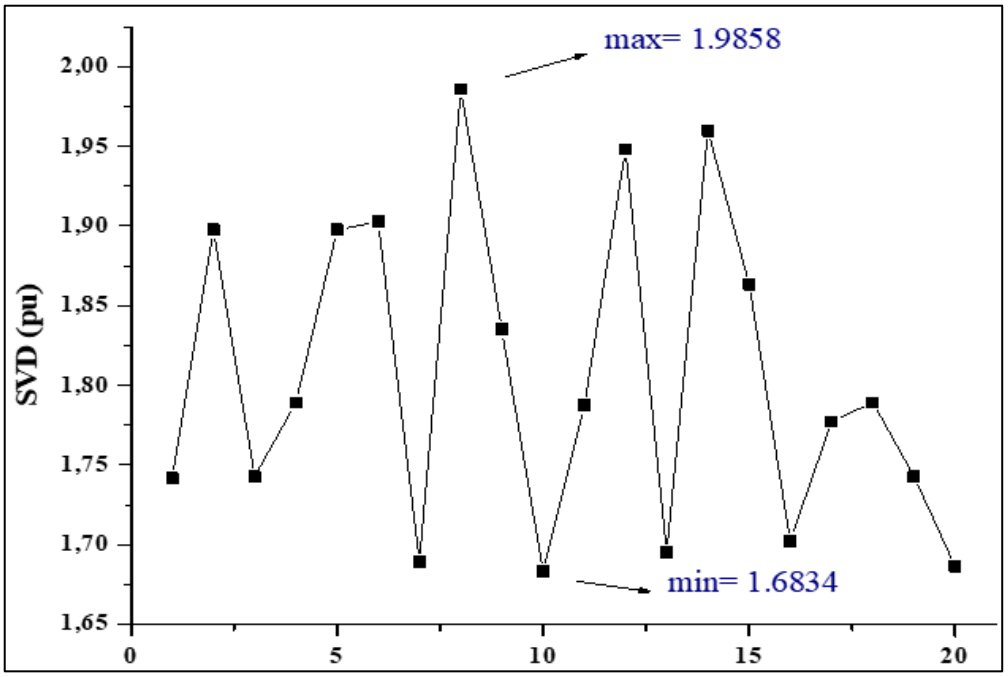

Figure 4.33. Performance of 24 particles for 20 trial runs (TVD minimization)

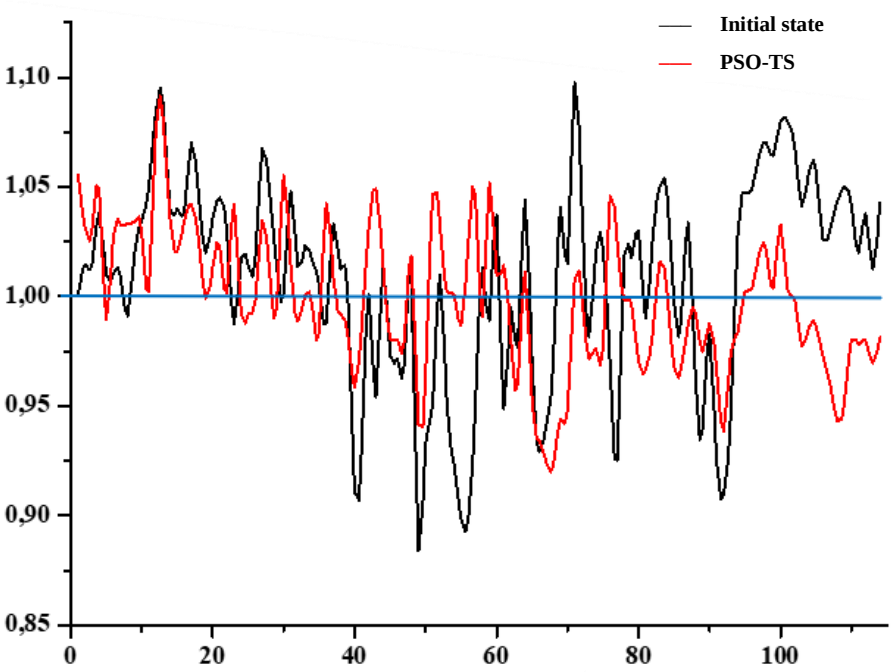

Figure 4.34. Voltage profile of the Algerian 114-bus system

4.5. Conclusion

The importance of hybridization algorithms lies in their ability to enhance performance, adapt to different problem characteristics, and provide effective solutions in a wide range of domains. They offer a flexible and powerful approach to optimization and problem-solving challenges.

These algorithms combine different optimization techniques or problem-solving methods to exploit their strengths and mitigate their weaknesses. In this chapter an efficient hybrid PSO with TS techniques called PSO-TS is implemented to solve the ORPD problem. The combination of these two metaheuristic methods can outperform the algorithms when used individually in solving power system optimization problems. First, the proposed PSO-TS algorithm based ORPD is implemented considering continuous control variables. In the second part, a new approach to identify the sensitive buses was presented. Afterwards, the proposed hybrid algorithm based sensitive approach is implemented to solve the ORPD problem with two distinct objective functions, namely, active power losses and voltage deviation. In the third part, the PSO-TS method based ORPD considering discrete control variables is presented. The proposed optimization approach was tested on IEEE 14-bus, IEEE 30-bus, IEEE 57-bus and the practical Algerian electric 114-bus power system. To demonstrate the effectiveness of the proposed PSO-TS algorithm, the obtained results were compared with TS, PSO and with several methods published in the literature.

Chapter 5

ORPD PROBLEM CONSIDERING FACTS DEVICES

5.1. Introduction

FACTS (Flexible Alternating Current Transmission Systems) are a set of innovative technologies and devices designed to improve the management, control and transmission of alternating current (AC) electricity on power grids. They have been developed to solve a number of major challenges facing power system operators around the world. These challenges include voltage regulation, reactive power management, improving system stability, increasing transmission capacity and improving the quality of electricity supplied to consumers. FACTS use advanced electronic technologies such as thyristors, power converters, filters and sensors to dynamically control and adjust AC parameters on the network. They offer network operators unprecedented flexibility to respond to variations in demand, network disturbances and power quality problems. With their ability to reduce power losses, improve energy efficiency and enhance grid stability, FACTS play a crucial role in improving the reliability of electricity supply and in the transition to more sustainable and resilient power systems.

Transmission lines are an important part of the network. They are made up of series and shunt impedances. The series impedance can affect the maximum power transited through the line and the shunt impedance is predominantly capacitive, and has an influence on the voltage along the transmission line. The series impedance of the line, the sending-end and receiving-end voltages and the phase shift between the voltages, determine the power transited. FACTS are used to change the series and shunt parameters as well as the phase shift voltages in order to control power flow.

Because the progress of power electronics, FACTS devices have taken more attention in transmission power systems. Based on the use of reliable high-speed power electronics, powerful analytical tools, advanced control and microcomputer technologies, FACTS represent a new concept for the operation of power transmission systems. They have the capability to change the network parameters with a rapid response and enhanced flexibility, such as, improving voltage profile and minimizing system losses [154]. Generally speaking, FACTS devices act by supplying or absorbing reactive power, increasing or reducing busbar voltage, controlling line impedance or modifying voltage phases. Furthermore, FACTS controllers, in

comparison with mechanical devices such as transformer tap changers or shunt capacitor switches that have enabled the AC power system to be controlled so far are not subject to mechanical wear and offer them an important advantage to FACTS devices in addition to high flexibility and speed [155].

In order to observe the effects of FACTS devices on electrical systems, it is necessary to model them. FACTS modelling is based on the elements used in power flow calculations. These are, in particular, the generators, the loads, the shunts, the lines and the transformers. FACTS devices are considered as ideal elements and their active losses are not taken into account.

Since the FACTS devices can significantly improve power systems performance by controlling power flows without generation rescheduling or topological changes, two FACTS devices named Static Var Compensator (SVC) and Thyristor Controlled Series Capacitor (TCSC) are used in this work. In this thesis, the settings of FACTS devices are considered as additional control parameters in the ORPD formulation and studied the impact on active power losses minimization. The above FACTS device power flow models are briefly described below [156].

5.2. FACTS devices.

5.2.1. Definition

Flexible Alternating Current Transmission Systems, commonly known as FACTS, are a set of advanced power system technologies and devices designed to enhance the controllability and flexibility of AC (alternating current) power systems. FACTS devices are static power-electronic devices installed in AC transmission networks to increase power transfer capability, stability, and controllability of the networks through series and/or shunt compensation. These devices are also employed for congestion management and power losses optimization. The static synchronous series compensator (SSSC) and thyristor-controlled series capacitor (TCSC) are some of the FACTS control devices which provide series compensation to reactance of the lines to which they are connected, while the static synchronous compensator (STATCOM) and static VAR compensator (SVC) (where VAR stands for volt–ampere reactive) are FACTS devices which provide shunt compensation to transmission lines [157]. FACTS technologies are used to optimize the operation and performance of power systems, improve voltage stability, increase power transfer capacity, and enhance the overall reliability of electricity transmission and distribution. FACTS devices are crucial components in modern power systems, helping

utilities manage complex grid operations more efficiently.

5.2.2. Technology Overview

The principle behind FACTS can be explained by formula (5.1) that states (neglecting active and reactive losses) that the power flow between two nodes (substation 1 and substation 2) along an AC transmission line (see Figure. 5.1) can be expressed as:

$$\boldsymbol{S_{1,2} = \frac{V_1 V_2 \sin(\delta_{1,2})}{X} - j\left(\frac{V_1 V_2 \cos(\delta_{1,2})}{X} - \frac{V_1^2}{X}\right)} \quad (5.1)$$

Being the real part of Eq. 5.1, the active power flow, therefore,

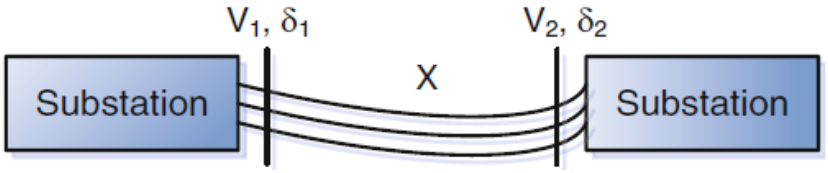

Figure 5.1. Simplified connection diagram between two substations

$$\boldsymbol{P_{1,2} = \frac{V_1 V_2 \sin(\delta_{1,2})}{X}} \quad (5.2)$$

where $P_{1,2}$ is the active power flow between the two nodes along the line, V_1 and V_2 represent the respective nodal voltage magnitudes at both ends of the line, X expresses the line reactance and $\delta_{1,2}$ represents the voltage angular difference between the two nodes. By improving the control of one or more of the above-mentioned parameters (voltage, line reactance or phase angle), it becomes possible to increase the flexibility of any line or any part of an electrical system, in particular increasing or decreasing the power flow on a given line or part of the system. This control enhancement leads to a corresponding improvement in operation of the power transmission system. In this case, FACTS devices enable the controllability and power transmission capability of electrical systems to be enhanced in term of both flexibility [155].

5.2.3. General classification of FACTS devices

FACTS devices can be classified into several categories based on their functionality, the control they provide and the way they are connected to the power system (shunt or series). Here are some common classifications of FACTS devices (figure 5.2) [158]:

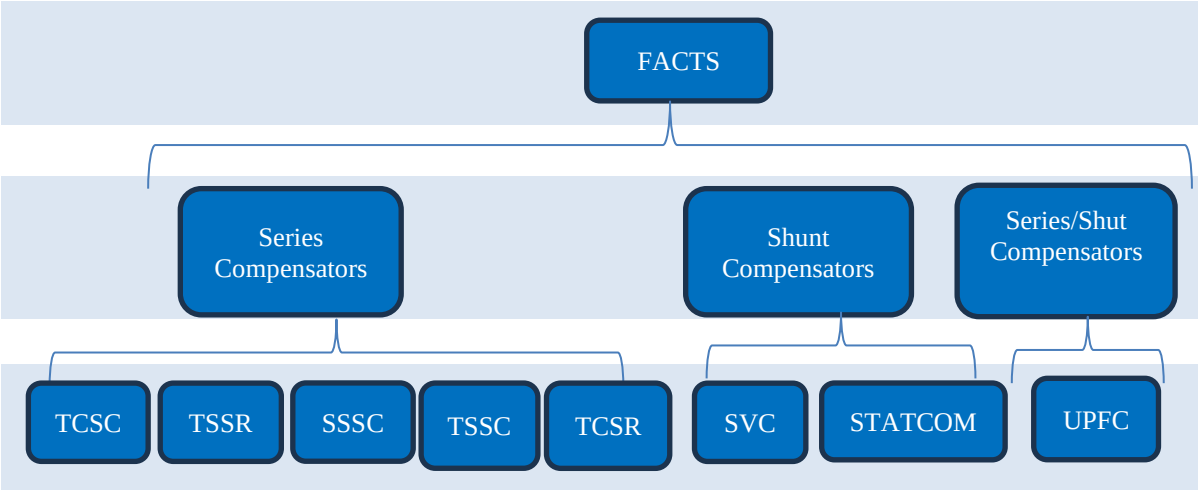

Figure 5.2. General classification of FACTS devices

5.2.3.1. *Shunt compensators*

Shunt compensators have long been used in electrical networks, their main objectives are to control voltages at the desired levels when there is a change in system conditions and to increase the transmissible power in the lines. Shunt controllers are connected in shunt with the line to inject current into the system at the point of connection. They can also be variable impedance, variable source or a combination of the two. If the injected line current is in quadrature with the line voltage, variable reactive power supply or consumption could be achieved. However, any other phase relationship could also involve real power handling. This category includes STATCOM (Static Synchronous Compensator) and SVC (Static Var Compensator). The most common Static VAR Compensators (SVC) are: TCR (Thyristor controlled reactor), TSR (Thyristor switched reactor) and TSC (Thyristor switched capacitor).

5.2.3.2. *Series compensators*

Series compensators are being connected in series with the line as they are meant for injecting voltage in series with the line. These devices could be variable impedances like capacitor, reactor or power electronics based variable source of main frequency, sub synchronous or harmonic frequency, or can be a combination of these, to meet the requirements. If the injected voltage is in phase quadrature with the line current, then only supply or consumption of variable reactive power is possible. These types of controllers include:

- SSSC: Static synchronous series compensator
- TCSC: Thyristor controlled series capacitor
- TCSR: Thyristor controlled series reactor

- TSSC: Thyristor switched series capacitor
- TSSR: Thyristor switched series reactor.

5.2.3.3. *Combined Series-Shunt compensators*

The FACTS devices described above can only act on one of the three parameters determining the power transmitted in a line (voltage, impedance and angle). By combining the two types of devices (shunt and series), it is possible to obtain hybrid devices capable of simultaneously controlling the different variables mentioned above. Hence, they are capable of injecting current into the line using the shunt part and injecting series voltage with the series part of the respective controller. If they are unified, there can be real power exchange between the shunt and series controllers via the common DC power link, as in the case of Unified Power Flow Controllers (UPFC).

5.2.4. FACTS devices modeling

Modeling FACTS devices is essential for understanding their operation, simulating their impact on power systems, and optimizing their control. The modeling process involves representing the behavior of FACTS devices mathematically or through simulation tools. The developed models are integrated into calculation programs so that they can simulate their effects throughout the system. FACTS device modeling is a critical aspect of power system analysis and control. Accurate models help power system engineers and operators assess the impact of FACTS devices, design control strategies, and ensure grid stability and efficiency. The complexity and level of detail in the models will depend on the specific analysis or simulation objectives.

Below are some key aspects of how FACTS devices are modelled:

- Mathematical Models: FACTS devices are typically modeled using mathematical equations that describe their electrical and control characteristics. The level of detail in the model can vary depending on the simulation objectives.
- Device-Specific Models: Different FACTS devices require specific models to capture their unique features. Here are common models for some FACTS devices:
  - SVC (Static VAR Compensator): SVC models include control characteristics and can be described as a set of voltage and current equations. A simple SVC model may include equations representing its susceptance (B) and voltage setpoints.
  - STATCOM (Static Synchronous Compensator): STATCOM models include the voltage-source inverter and its control algorithms. These models describe the

relationship between the inverter's control signals, the injected reactive power, and the grid voltage.

- TCSC (Thyristor-Controlled Series Capacitor): TCSC models incorporate the switching action of thyristors and describe how the capacitive reactance can be controlled. The model accounts for the voltage and current across the TCSC.
- SSSC (Static Synchronous Series Compensator): SSSC models typically include synchronous generator models and power electronics for voltage control. These models describe the device's control capabilities, including real and reactive power injection.
- UPFC (Unified Power Flow Controller): UPFC models combine the functionalities of various FACTS devices and include detailed power electronics and control algorithms. They encompass voltage source converters and are often more complex than single-device models.

The methods used to integrate FACTS into the load flow are mainly different. The three most common methods in the literature are: injection of equivalent power, creation of a fictitious node or modification of the admittance matrix. In general, FACTS devices can be inserted either at the nodes of the network, or in series with the lines. In practice, devices whether shunt or series are often inserted at existing stations. This thesis focuses only on series devices (TCSC) and shunt devices (SVC).

5.2.4.1. *Static VAR Compensator (SVC)*

a. Definition

SVC is one of the most important shunt controllers in FACTS technology used in electric power systems to regulate voltage and manage reactive power. SVCs are shunt-connected devices that can rapidly control the flow of reactive power into or out of the power system, helping to stabilize voltage levels and improve system performance. SVCs are typically connected in parallel with the transmission lines or at specific buses in the power system. They are primarily used for voltage regulation and can quickly adjust the reactive power output to maintain the desired voltage levels within the power system. When the system voltage is too low, the SVC injects reactive power to raise it, and when the voltage is too high, it absorbs reactive power to lower it. SVCs have a fast response time which makes them suitable for dealing with rapid voltage fluctuations caused by sudden load changes or system disturbances. SVCs help in preventing voltage instability and voltage collapse during contingencies. By maintaining voltage stability, SVCs can increase the power transfer capacity of transmission lines. SVCs are equipped with sophisticated control systems that monitor the voltage levels and adjust the

reactive power output accordingly. In some cases, SVCs are used in conjunction with other FACTS devices to optimize voltage and power flow control. Coordinated operation with other FACTS devices like series compensators can lead to more comprehensive grid control.

b. Modeling of Static VAR Compensator (SVC)

The Static VAR Controller (SVC) is one of the shunt FACTS devices widely installed in the world. As well shown in Figure. 5.3., the basic structure of SVC consists of connected anti-parallel thyristors to provide controllability. The SVC has the ability to control dynamically the voltage at critical buses by exchanging dynamically capacitive or inductive reactive power with the network [120].

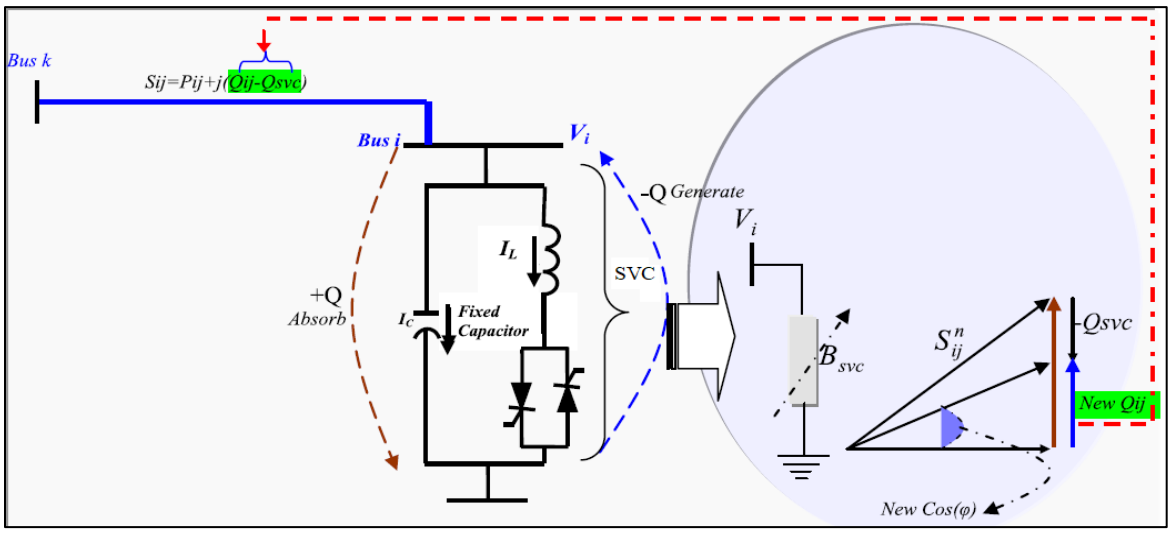

Figure 5.3. Basic circuit and operation principle of SVC

The static reactive power compensator is modeled by Y_{SVC} as shunt variable admittance as shown in Figure 5.4. Since the power loss of SVC is negligible, its admittance is assumed to be purely imaginary:

$$\boldsymbol{Y_{SVC} = jb_{SVC}} \qquad (5.3)$$

Were $\boldsymbol{b_{SVC}}$ is the susceptance of the SVC device

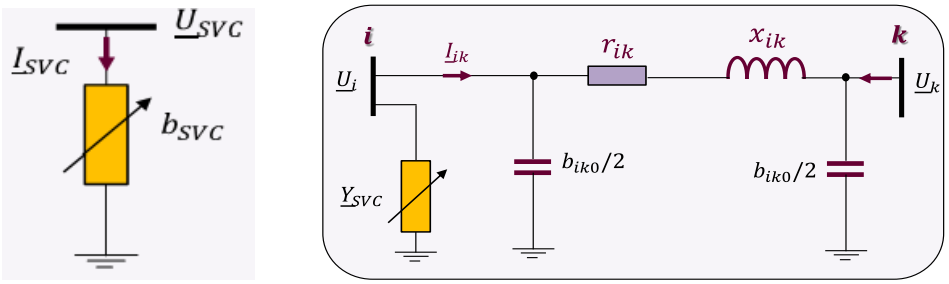

(a) (b)

Figure 5.4. Basic structure of SVC

SVC can be utilized for both inductive and capacitive compensation Figure 5.5. In power flow study, the SVC is modeled as a device for reactive power injection on the bus to which it is connected to as:

$$Q_{SVC} = U_i^2 b_{SVC} \quad (5.4)$$

where U_i is the amplitude of bus voltage where the compensator is installed.

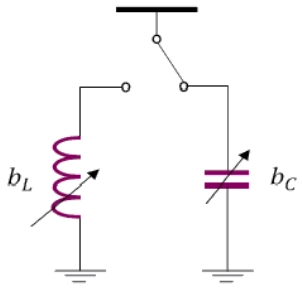

Figure 5.5. Equivalent circuit representation of SVC

5.2.4.2. *Thyristor-Controlled Series Capacitor (TCSC)*

a. Definition

A Thyristor-Controlled Series Capacitor (TCSC) is a type of FACTS device used in electrical power systems to control power flow and enhance system stability. TCSCs are series-connected devices that consist of a series capacitor in conjunction with thyristor-controlled reactors. These devices can adjust the impedance and phase angle of the transmission line, allowing power flow control and voltage stability improvement. TCSCs are primarily used to control power flow on transmission lines by dynamically changing the line impedance. They can be used in coordination with other FACTS devices like Static VAR Compensators (SVCs) and Unified Power Flow Controllers (UPFCs) to provide comprehensive power system control and optimization.

b. Modeling of the Thyristor series compensator

The TCSC is a series compensation component which consists of a series capacitor bank shunted by Thyristor controlled reactor as presented in Figure 5.6. It can vary the series impedance continuously to levels below and above the line's natural impedance. This is a powerful means of increasing and controlling power transfer. TCSCs can respond rapidly to control signals to increase or decrease the capacitance or inductance [155]. The static model of TCSC inserted particular line is shown in Figure 5.7. Since the devices are considered ideal, only the reactive part of the impedance is taken into account. The basic idea behind power flow

control with the TCSC is to decrease or increase the overall lines effective series transmission impedance, by adding a capacitive or inductive reactance to the line impedance. The TCSC is modelled as variable reactance. After installing TCSC, the new reactance of TCSC is presented by:

$$\boldsymbol{X_{TCSC} = (1 - k_{TCSC}).X_{ligne}} \quad (5.5)$$

Where X_{ligne} is the transmission line reactance and $\boldsymbol{k_{TCSC}}$ is the level of reactance compensation. The level of the applied compensation of the TCSC varies generally between 20% in inductive mode and 80% in capacitive mode [159].

$$\boldsymbol{-0.8 \leq k_{TCSC} \leq 0.2} \quad (5.6)$$

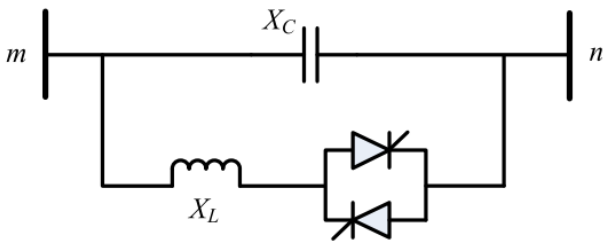

Figure 5.6. Basic circuit structure of TCSC

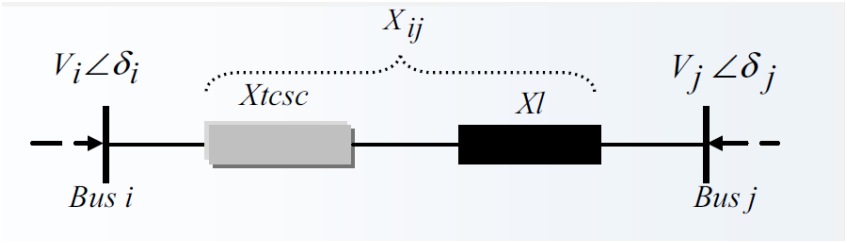

Figure 5.7. The basic model of TCSC device

5.3. Formulation of ORPD problem considering FACTS devices

Optimal Reactive Power Dispatch is a crucial aspect of power system operation aiming to optimize the allocation of reactive power resources to enhance voltage profile of the power system, reduce line losses, and improve system performance. When considering FACTS devices in ORPD formulation, it involves incorporating these devices into the optimization process to achieve better control over system parameters. Integrating FACTS devices into ORPD formulation enhances the system's efficiency and reliability. In this study, the objective of the optimal reactive power dispatch considering FACTS is same as that of conventional

ORPD that is to minimize the active power losses (P_{Loss}) which is described in Equation (2.2). Like in conventional ORPD, we take into account power balance constraints to ensure that the total power injected is equal to the total power consumed at each bus, maintain voltages within specified limits at all buses, constraints on the reactive power generated by each generator and the capacity constraints of the FACTS devices. SVC and TCSC are the two FACTS controllers considered along with conventional OPRD for further active power losses reduction of the power system. The settings of the FACTS devices are the additional control variable in ORPD in addition with generator voltages, tap ratio of tap changing transformers and amount of VAR injection by shunt capacitors.

The SVC device is modeled by Y_{SVC} as shunt variable admittance. When SVC is connected at the bus i (Figure 5.4 (b)), only the element $\underline{Y_{ii}}$ of the nodal admittance matrix is modified (Equations 5.7 and 5.8).

$$\boldsymbol{Y'_{ii} = Y_{ii} + y_{SVC}} \tag{5. 7}$$

$$\boldsymbol{Y' = \begin{pmatrix} y_{ik} + \frac{y_{ik0}}{2} + y_{SVC} & -y_{ik} \\ -y_{ik} & y_{ik} + \frac{y_{ik0}}{2} \end{pmatrix}} \tag{5. 8}$$

When a TCSC is inserted in a line connecting the bus i and the bus k (Figure 5.8), the new reactance of this line becomes:

$$\boldsymbol{x'_{ik} = x_{ik} + x_{TCSC}} \tag{5. 9}$$

The matrix admittance of the line is modified as follows:

$$\boldsymbol{Y' = \begin{pmatrix} y'_{ik} + \frac{y_{ik0}}{2} & -y'_{ik} \\ -y'_{ik} & y'_{ik} + \frac{y_{ik0}}{2} \end{pmatrix}} \tag{5. 10}$$

$$\boldsymbol{y'_{ik} = \frac{1}{r_{ik} + j(x_{ik} + x_{TCSC})}} \tag{5. 11}$$

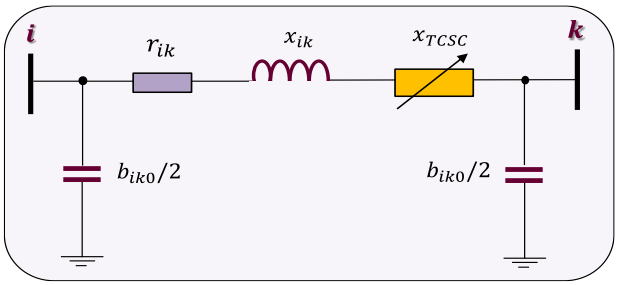

Figure 5.8. TCSC connected in a line

To incorporate SVC and TCSC devices with ORPD, the following constraints are added with conventional ORPD problem constraints.

5.3.1. SVC VAr limits

SVC reactance values are restricted within the limits as follows

$$\boldsymbol{Q_{SVCmin} \leq Q_{SVC} \leq Q_{SVCmax}} \quad (5.12)$$

Q_{SVC} is the VAR rating of SVC and Q_{SVCmin} and Q_{SVCmax} are the minimum and maximum VAr limits of SVC.

5.3.2. TCSC Reactance limits

TCSC reactance values are restricted within the limits as follows

$$\boldsymbol{-0.8X_{line} \leq X_{TCSC} \leq 0.2X_{line}} \quad (5.13)$$

X_{line} is the reactance of the line where TCSC is connected. X_{TCSC} is the reactance of the TCSC.

5.4. Simulation Results and Discussions

For investigating the effect of optimal setting of FACTS devices in minimizing the total active power losses and in order to demonstrate the applicability and the validity of the proposed PSO-TS algorithm for ORPD problem with FACTS devices, studies are conducted on the standard IEEE 30-bus and on practical Algerian power test system with 114 buses.

5.4.1. IEEE 30 bus test system

This network consists of 41 branches, 6 generator buses, and 24 load buses. Four branches are under tap setting transformer branches. In addition, buses 10 and 24 have been selected as shunt VAR compensation buses. Bus 1 is selected as the slack bus, and buses 2, 5, 8, 11, and 13 are the generator buses. The others are load buses. A total of 12 optimal control variables are utilized for this ORPD problem. The branch parameters and loads are taken from [160]. The voltage magnitudes limits of all buses are [0.9 p.u, 1.1 p.u.]. The tap settings limits of regulating transformers are [0.9 p.u., 1.1 p.u.]. The VAR injection of the shunt capacitors is within the interval of [0 MVAr, 30 MVAr]. This study has considered the setting of the FACTS devices as additional control parameters in the ORPD formulation and studied the impact on active power losses minimization. Static models of the two types of FACTS devices consisting of SVC and TCSC have been included in the ORPD formulation. The SVC device is considered as a generator (or an absorber) of reactive power which varies continuously between −0.3 p.u and 0.3 p.u. The number of FACTS and their limits are chosen at the beginning. The reactance of TCSC is considered as continuous variable which varies between 20% inductive and 80% capacitive of the line reactance. Table 5.1 shows the limits of the control variables of IEEE 30-

bus system considering FACTS devices [161]. In the present work, several cases in terms of use of FACTS devices are considered namely:

Case 1. P_{Loss} minimization considering one SVC device.

Case 2. P_{Loss} minimization considering two SVC devices.

Case 3. P_{Loss} minimization considering one TCSC device.

Case 4. P_{Loss} minimization considering two types of FACTS devices (one SVC and one TCSC).

For each case, we will study the impact of the FACTS when installed with and without shunt capacitors on the quality of the solution. The locations of shunt capacitors, SVC and TCSC devices are as bellow fixed:

The locations of the shunt capacitors are as given by reference [147] for this test network. The SVC location is identified using the bus sensitivity approach (developed in section 4.4.2) whereas the TCSC location is as indicated in reference [162].

Table 5.1. Limits of the control variable considering FACTS devices (IEEE 30-bus)

V_G^{max}	V_G^{min}	T_k^{max}	T_k^{min}	Q_c^{max}	Q_c^{min}	Q_{SVC}^{max}	Q_{SVC}^{min}	X_{TCSC}^{max}	X_{TCSC}^{min}
1.1	0.9	1.1	0.9	0.3	0.0	0.3	-0.3	$0.2X_{ij}$	$-0.8X_{ij}$

5.4.1.1. *Case 1: ORPD using one SVC device*

In this case, we aim to use the proposed PSO-TS algorithm to find the optimal SVC MVAR rating in addition to the other control variables, namely the generator voltages and the tap setting transformers, which minimize active power losses. The SVC location is determined based on the buses sensitivities developed in section 4.4.2. The most sensitive bus is, for the studied network, that numbered 21. The simulation results obtained by the proposed PSO-TS method for the three cases listed below are presented in Table 5.2.

Case 1a: P_{Loss} minimization with shunt capacitors (bus 10 and 24).

Case 1b: P_{Loss} minimization with only SVC device (bus 21).

Case 1c: P_{Loss} minimization with shunt capacitors and SVC device.

From this table, it can be seen that the proposed PSO-TS algorithm based ORPD optimization implemented with the combination of capacitor banks and one SVC device reduced the total active power losses from 5.2783 MW to 4.3327 MW, which represents a reduction of 17.915%. Whereas, these losses were reduced by 12.745% if the SVC device is used without the capacitor banks. While capacitor banks without FACTS devices reduce power losses by only 12,27% (Figure 5.9). Also, the evolution of power losses versus the iterations number, given by Figure 5.10, shows that after 57 iterations, the power losses value, i.e. 4.296 MW, remains stable

until reaching the 176th iteration where the power losses become equal to 4.332 MW.

Table 5.2. Simulation results considering SVC device (case 1)

Control variables	Initial state	PSO-TS (case 1a)	PSO-TS (case 1b)	PSO-TS (case 1c)
V_1	1.0600	1.0992	1.1000	1.1000
V_2	1.0450	1.0948	1.1000	1.0890
V_5	1.0100	1.0766	1.1000	1.1000
V_8	1.0100	1.0977	1.1000	1.1000
V_{11}	1.0820	1.0837	1.1000	1.1000
V_{13}	1.0710	1.0754	1.0215	1.1000
T_{6-9}	0.9780	0.9257	1.0361	0.9504
T_{6-10}	0.9690	1.0291	1.1000	0.9701
T_{4-12}	0.9320	0.9265	1.1000	1.1000
T_{27-28}	0.9680	0.9422	1.0346	0.9578
Q_{Sh10}	0.0000	0.2864	-	0.3000
Q_{Sh24}	0.0000	0.1363	-	0.0714
SVC (21)	-	-	0.3000	0.1317
Ploss (MW)	5.2783	4.6304	4.6056	4.3327

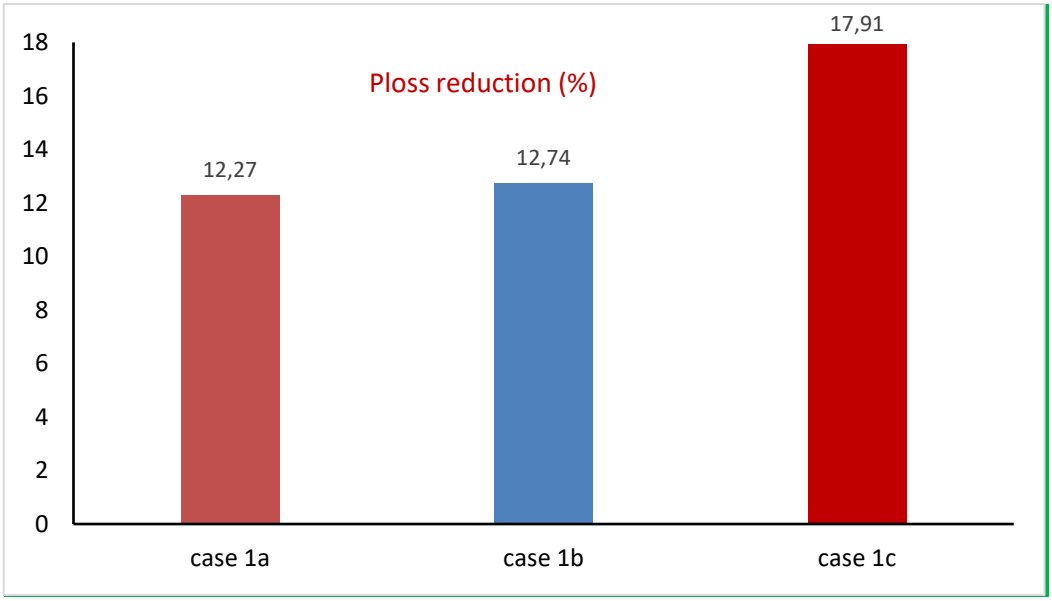

Figure 5.9. Reduction of active power losses (case 1)

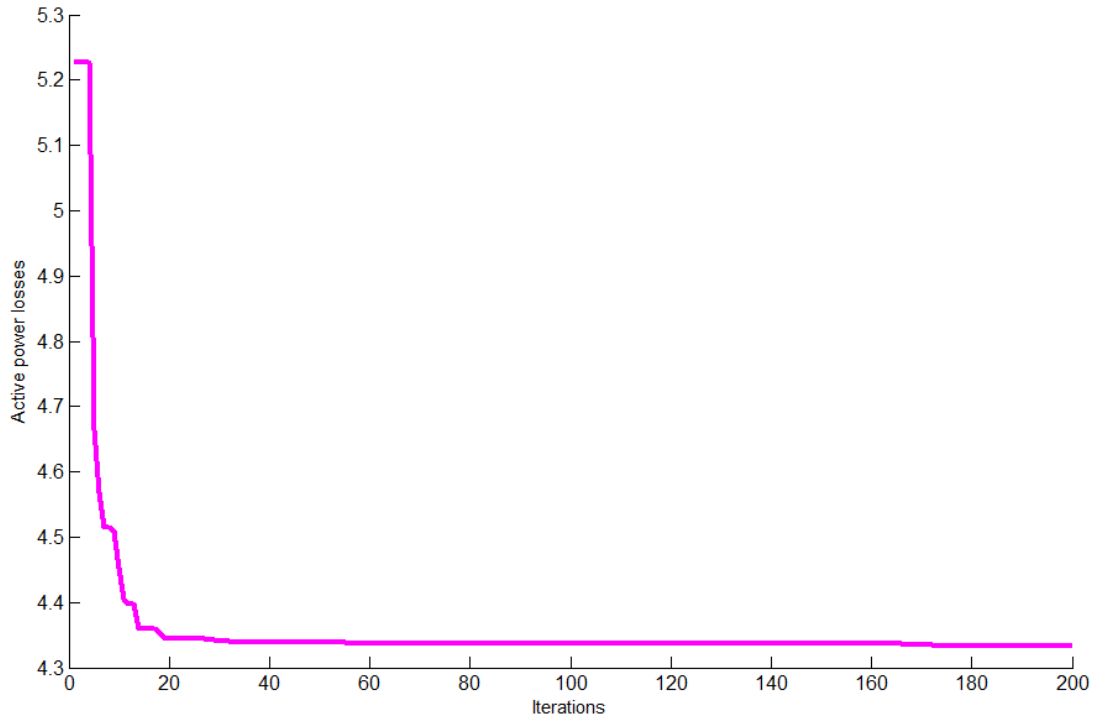

Figure 5.10. Convergence characteristic of IEEE 30-bus system for case 1c

5.4.1.2. *Case 2: ORPD using two SVC devices*

In this case, two SVC devices are inserted at buses 21 and 24. The optimal setting of control variables (voltage of generator buses, tap settings of the regulating transformers, VAR injections of the shunt capacitors, and VAr setting of SVC devices) and active power losses that are obtained by the proposed method for the three cases namely:

Case 2a: P_{Loss} minimization with only shunt capacitors.

Case 2b: P_{Loss} minimization with two SVC devices.

Case 2c: P_{Loss} minimization with shunt capacitors and SVC devices.

The Cases 2a, 2b and 2c are presented in Table 5.3. From this table and Figure 5.11, the results clearly show that the active power loss has improved from 5.2783 MW to 4.6510 MW in the case 2a, from 5.2783 MW to 4.5360 MW in the case 2b and from 5.2783 MW to 4.2645 MW in the case 2c. It may be noticed that the objective function value obtained in case 2c is better than those of the other cases. In fact, the installation of two SVCs in the presence of shunt capacitors reduced the power losses by 19.207% compared with the power losses reduction observed in the case where the shunt capacitors are installed alone (11.884%) and the case where the SVCs are installed alone (14.063%) (Figure 5.11). Figure 5.12 illustrates the convergence characteristic of power loss minimization in case 2c which indicates a much better solution for the proposed hybrid algorithm.

Table 5.3. Simulation results considering SVC devices (case 2)

Control variables	Initial state	PSO-TS (case 2a)	PSO-TS (case 2b)	PSO-TS (case 2c)
V_1	1.0600	1.1000	1.1000	1.1000
V_2	1.0450	1.1000	1.1000	1.1000
V_5	1.0100	1.1000	1.1000	1.0795
V_8	1.0100	1.1000	1.1000	1.1000
V_{11}	1.0820	1.0968	0.9500	1.1000
V_{13}	1.0710	1.1000	1.1000	1.1000
T_{6-9}	0.9780	0.9671	1.0359	0.9329
T_{6-10}	0.9690	1.1000	1.1000	1.0484
T_{4-12}	0.9320	0.9000	0.9000	0.9000
T_{27-28}	0.9680	0.9564	0.9919	0.9370
Q_{Sh10}	-	0.3000	-	0.2632
SVC (21)	-	-	0.3000	0.0648
SVC (24)	-	-	-0.3000	0.1202
Ploss (MW)	5.2783	4.6510	4.5360	4.2645

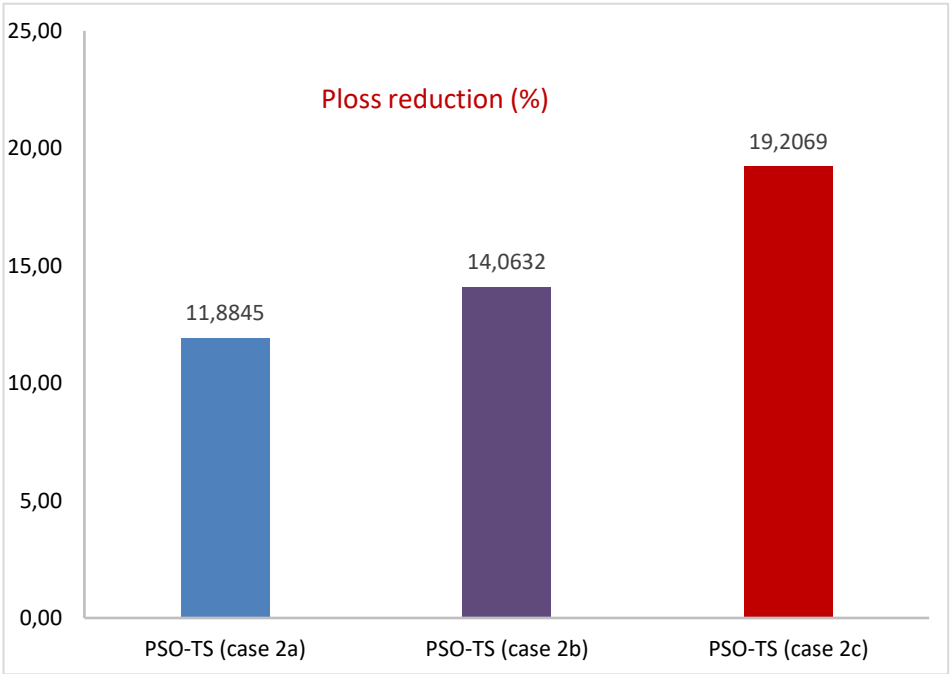

Figure 5.11. Reduction of active power losses (case 2)

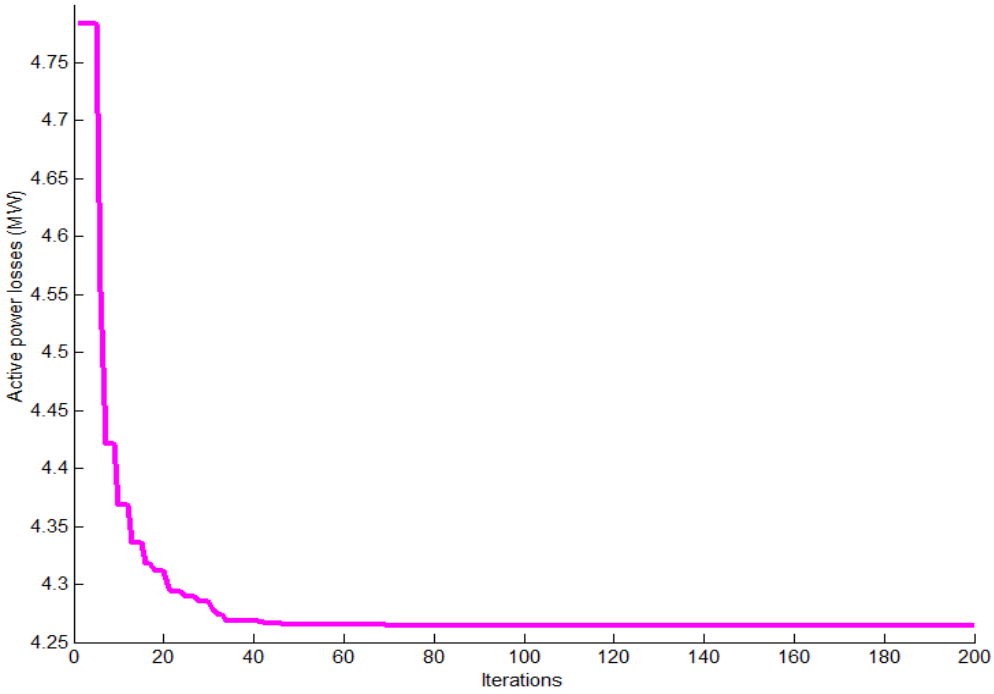

Figure 5.12. Convergence characteristic of IEEE 30-bus system for case 1c

5.4.1.3. *Case 3: ORPD using TCSC device*

In this case, we are going to install another type of FACTS which is the TCSC. The proposed algorithm tries to find, in addition to the usual control variables, the TCSC reactance setting which minimize the active power losses. The best results of P_{Loss} minimization achieved by PSO-TS are tabulated in Table 5.4 for the different cases cited bellow:

Case 3a: P_{Loss} minimization with only shunt capacitors.

Case 3b: P_{Loss} minimization with TCSC device (line (2-5))

Case 3c: P_{Loss} minimization with shunt capacitors and TCSC device.

It can be pointed from table 5.4 and figure 5.13, that PSO-TS in cases 3a, 3b and 3c is able to reduce power losses from 5.2783 MW to 4.6304 MW, 4.5631 MW and 4.3703 MW respectively, which represents a reduction of 12.275%, 13.550%, and 17.203%. Comparing these results, we can notice that the minimum active power losses is obtained in case 3c where TCSC is combined with shunt capacitors. In the case where shunt capacitors are installed alone, the result is not as good as with TCSC taken alone. However, when we took into account both shunt capacitors and the TCSC device, the result became better. Figure 5.14 shows the power loss reduction process for PSO-TS for the case 3c. From this figure it can be seen that the best result can be achieved after about 40 iterations, which reflects the good search capability of this proposed hybrid algorithm.

Table 5.4. Simulation results considering TCSC device (case 3)

Control variables	Initial state	PSO-TS (case 3a)	PSO-TS (case 3b)	PSO-TS (case 3c)
V_1	1.0600	1.0992	1.1000	1.1000
V_2	1.0450	1.0948	1.1000	1.1000
V_5	1.0100	1.0766	1.0796	1.1000
V_8	1.0100	1.0977	1.1000	1.1000
V_{11}	1.0820	1.0837	1.1000	1.1000
V_{13}	1.0710	1.0754	1.1000	1.1000
T_{6-9}	0.9780	0.9257	1.1000	0.9766
T_{6-10}	0.9690	1.0291	1.0357	0.9669
T_{4-12}	0.9320	0.9265	0.9856	1.1000
T_{27-28}	0.9680	0.9422	1.0138	0.9673
Q_{Sh10}	-	0.2864	-	0.3000
Q_{Sh24}	-	0.1363	-	0.0938
TCSC (2-5)	-	-	-0.2388	-0.1944
Ploss (MW)	5.2783	4.6304	4.5631	4.3703

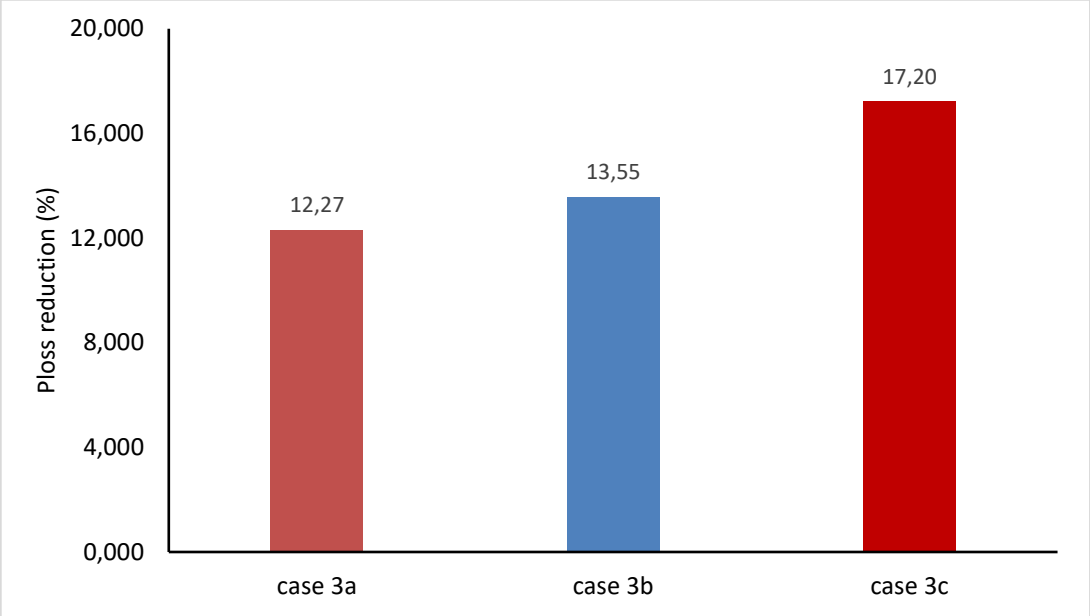

Figure 5.13. Reduction of active power losses (case 3)

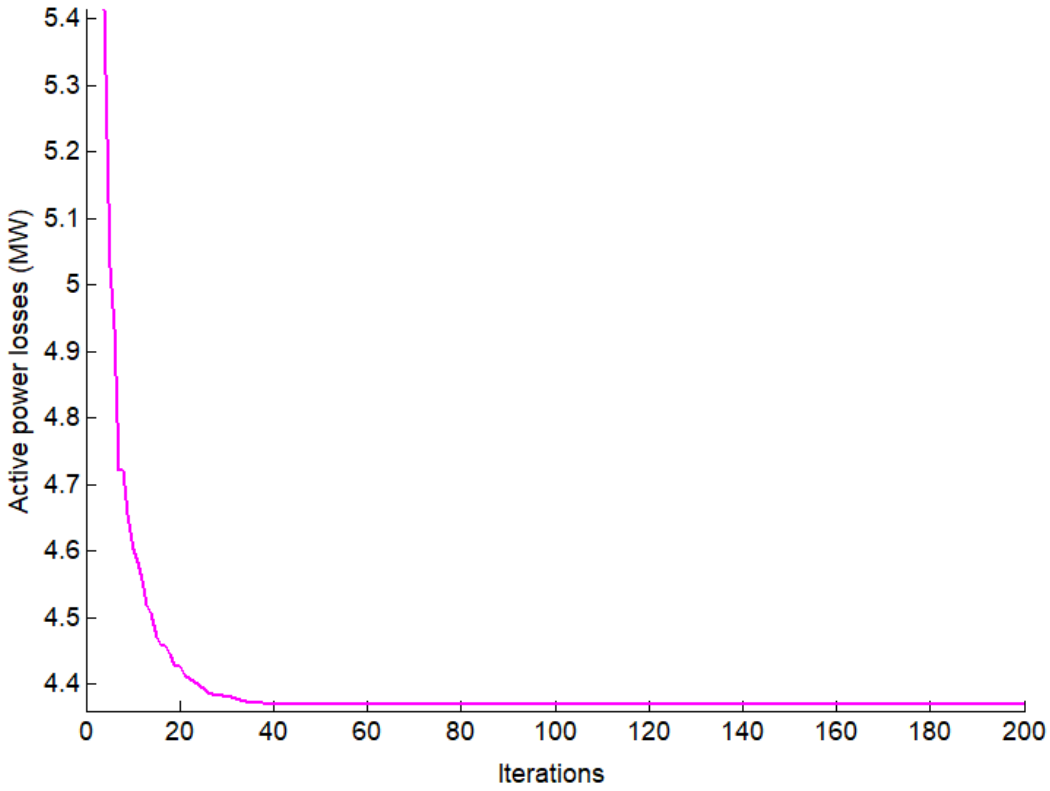

Figure 5.14. Convergence characteristic of IEEE 30-bus system (case 3c)

5.4.1.4. *Case 4: ORPD using two types of FACTS devices*

In this case, two type of FACTS devices were integrated, namely SVC and TCSC in order to optimize the active power losses. Table 5.5 shows the detailed results of the control variables including the optimal sizes of the SVC and TCSC as well as the active power losses obtained by the proposed algorithm for the different following cases:

Case 4a: P_{Loss} minimization with shunt capacitors.

Case 4b: P_{Loss} minimization with TCSC and SVC devices (one SVC and one TCSC)

Case 4c: P_{Loss} minimization with shunt capacitors and FACTS devices (SVC and TCSC).

The SVC has been connected at bus 21, the TCSC at line (2-5) and the shunt capacitor at bus 10. Table 5.4 shows that the power losses obtained by PSO-TS algorithm in case 4b is 4.435 MW and in case 4c is 4.2437 MW. Table 5.5 and Figure 5.15 present the results and a comparison of reduction in active power losses for different cases. According to this Table and Figure, ORPD considering FACTS devices and shunt capacitors significantly decrease the active power losses (case 4c). To conclude, we can say that the installation of single type FACTS device (one SVC) brings the active power loss to 4.6056 MW and the installation of two SVC devices brings the power loss to 4.5360 MW. Similarly, the use of a single TCSC lowers power losses to 4.5631 MW. For the cases mentioned above, i.e. either SVC or TCSC,

adding shunt capacitors to the facts devices, further enhances results. On the other hand, simultaneous installation of the two type FACTS devices (SVC and TCSC) reduce better the power loss in comparison to the results obtained by FACTS devices installed separately (Table 5.6).

Table 5.5. Simulation results considering SVC and TCSC devices (case 4)

Control variables	Initial state	PSO-TS (case 4a)	PSO-TS (case 4b)	PSO-TS (case 4c)
V_1	1.0600	1.0992	1.1000	1.1000
V_2	1.0450	1.0948	1.1000	1.1000
V_5	1.0100	1.0766	1.1000	1.0940
V_8	1.0100	1.0977	1.1000	1.1000
V_{11}	1.0820	1.0837	1.1000	1.0965
V_{13}	1.0710	1.0754	1.1000	1.1000
T_{6-9}	0.9780	0.9257	0.9848	0.9184
T_{6-10}	0.9690	1.0291	1.0932	0.9515
T_{4-12}	0.9320	0.9265	0.9000	1.0349
T_{27-28}	0.9680	0.9422	0.9706	0.9288
Q_{Sh10}	0.0000	0.2864	-	0.2997
Q_{Sh24}	-	0.1363	-	0.0628
SVC (21)	-	-	0.3000	0.1191
TCSC (2-5)	-		-0.1913	-0.2528
Ploss (MW)	5.2783	4.6304	4.4358	4.2437

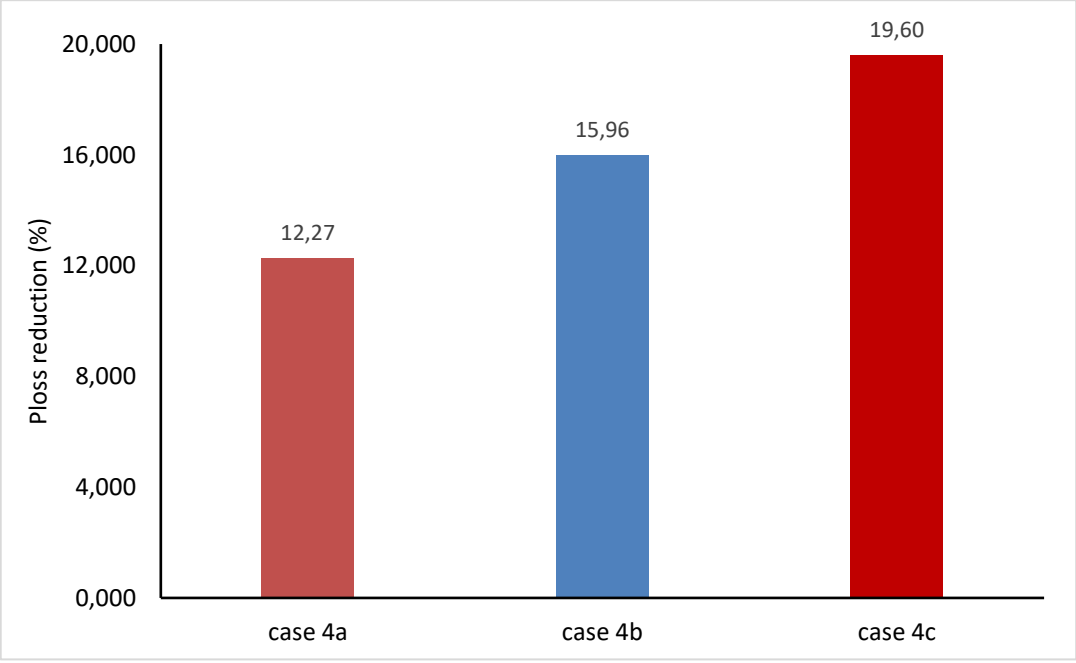

Figure 5.15. Reduction of active power losses (case 4)

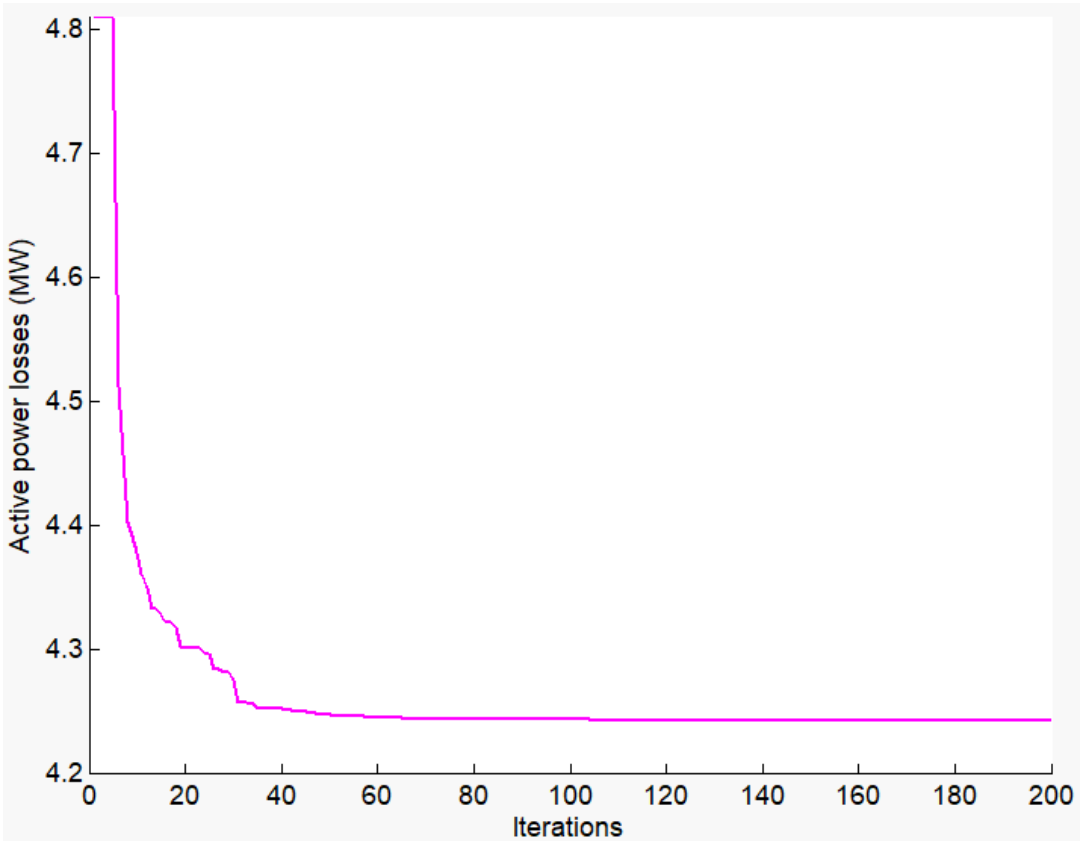

Figure 5.16. Convergence characteristic of IEEE 30-bus system for case 4c

Table 5.6. comparison of reduction in Ploss considering SVC and TCSC devices

	Ploss reduction (%)	
	Without shunt capacitors	With shunt capacitors
Installation of SVC device	12.74	17.91
Installation of TCSC device	13.55	17.20
Installation of SVC and TCSC devices	15.96	19.60

5.4.2. Practical Algerian electric power system

The effectiveness of the proposed PSO-TS algorithm in solving large scale nonlinear problems is validated by the ORPD problem carried out on a practical large scale Algerian electrical network having 114 buses, using FACTS devices. This problem has 38 decision variables namely, 15 generator voltages, 16 tap changer transformers and 7 reactive compensation devices which are installed at buses 50, 55, 66, 67, 77, 89 and 93 [152]. The total load demand is (37.27+ j 20.70) p.u at 100 MVA base. This study has considered the setting of the SVC devices as additional control parameters in the ORPD formulation and studied the impact on

active power losses minimization. The SVC device is modeled as shunt variable admittance (Y_{SVC}) as already explained in section 5.4.1. The upper and the lower operating limits of the control variables are given in Table 5.7. For this network, the impact of installing shunt capacitors and SVC devices on power losses is examined. Firstly, the power losses are calculated without shunt capacitors, which corresponds to case 1. Case 2 is devoted to minimizing power losses in the presence of shunt capacitors in the initial state [152]. Case 3 is the minimization of power losses in the presence of shunt capacitors, but this time installed on sensitive buses (already identified in section 4.4.3.4). Case 4 is the optimization of power losses in the presence of shunt capacitors and SVC devices (shunt capacitors are installed as in the initial state and the SVC devices are installed on the sensitive buses). The above cases are summarized as follows:

Case 1. P_{Loss} without shunt capacitors.

Case 2. P_{Loss} minimization considering shunt capacitors (Initial state).

Case 3. P_{Loss} minimization considering shunt capacitors (Sensitivite bus approach).

Case 4. P_{Loss} minimization considering shunt capacitors and SVC devices.

Table 5.8 summarizes the optimal control variables of Algerian 114-buses, obtained by PSO-TS for the four cases (case1, 2, 3 and 4). These results show that the most degraded active power losses are obtained in the first case since no reactive compensation have been used. After installation of the shunt capacitors at buses 50, 55, 66, 67, 77, 89 and 93 (initial state), the power losses are reduced from 77.2746 MW to 70.7003 MW, i.e. a reduction in power losses of 8.51%. The 3rd case is the case where the shunt capacitors are installed on the most sensitive buses (56, 63, 66, 73, 89 and 91). In this case the power losses are reduced to 59.9319 MW, i.e. a reduction of 22.442%. This reduction is better than that found in the 2nd case, which again shows that the sensitive bus approach is effective and gives better results. The 4th case shows the usefulness of installing FACTS devices in addition to shunt capacitors. It can be seen from Table 5.8 and Figure 5.17 that after integration the SVC devices in addition to the shunt capacitors, the losses were reduced to 55.0110, i.e. a reduction in losses of 28.8109% which is improved compared to case 2 (initial state). This electrical energy saving shows the considerable advantages offered by the FACTS devices in electrical networks. The objective function, i.e. active power losses, convergence characteristics for the three cases (2, 3 and 4) are shown in Figure 5.18. This figure

indicates a much better solution in other words, a better minimum and faster convergence, for the proposed hybrid algorithm considering SVC devices.

Table 5.7. Control variable limits

Variables	Lower limits (p.u)	Upper limits (p.u)
Generator buses voltage	0.9	1.1
Load buses voltage	0.9	1.1
Transformers tap setting	0.9	1.1
shunt compensators	0	0.25
SVC device	-0.25	0.25

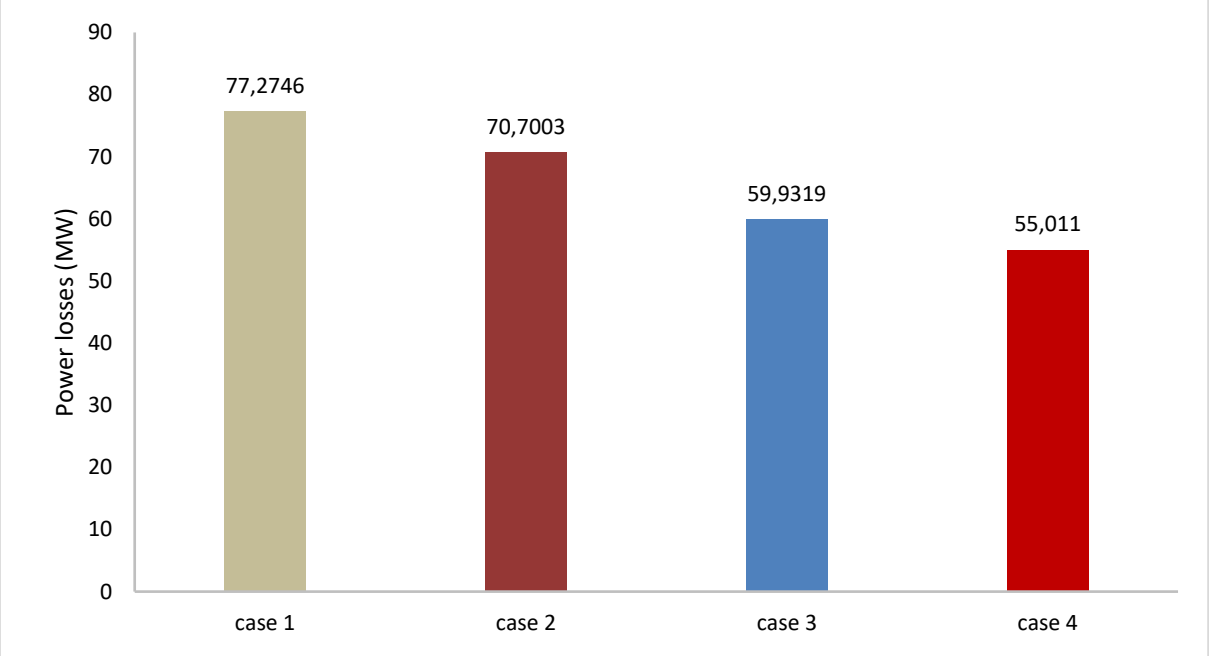

Figure 5.17. Reduction of active power losses (case 4)

Table 5.8. Simulation results of PSO-TS considering SVC devices (Algerian 114-bus system)

Control variables	Case 1	Case 2	Case 3	Case 4
V_4	1.0700	1.1000	1.1000	1.0498
V_5	1.0500	1.1000	1.1000	1.0753
V_{11}	1.0500	1.1000	1.1000	1.1000
V_{15}	1.0400	1.1000	1.0995	1.0199
V_{17}	1.0800	1.1000	1.1000	1.0382
V_{19}	1.0300	1.1000	1.1000	0.9000
V_{22}	1.0400	1.1000	1.1000	0.9000
V_{52}	1.0500	1.1000	1.1000	0.9000
V_{80}	1.0800	1.1000	1.1000	1.0936
V_{83}	1.0500	1.1000	1.1000	1.1000
V_{98}	1.0500	1.1000	1.1000	1.1000
V_{100}	1.0800	1.1000	1.1000	1.1000
V_{101}	1.0800	1.1000	1.1000	1.1000
V_{109}	1.0500	1.1000	1.1000	1.1000
V_{111}	1.0200	1.1000	1.1000	1.1000
$T_{80–88}$	1.0300	0.9000	0.9000	0.9000
$T_{81–90}$	1.0300	0.9000	0.9000	1.1000
$T_{86–93}$	1.0300	0.9000	0.9000	1.1000
$T_{42–41}$	1.0300	0.9821	0.9449	1.1000
$T_{58–57}$	1.0300	1.0083	0.9472	1.1000
$T_{44–43}$	1.0300	1.1000	0.9517	1.1000
$T_{60–59}$	1.0300	0.9966	0.9905	0.9900
$T_{64–63}$	1.0300	1.1000	0.9535	0.9000
$T_{72–71}$	1.0300	0.9000	0.9002	0.9000
$T_{17–18}$	1.0300	0.9000	1.0403	1.1000
$T_{21–20}$	1.0300	1.0166	1.0079	1.1000
$T_{27–26}$	1.0300	0.9000	0.9000	1.1000
$T_{28–26}$	1.0300	0.9000	1.1000	0.9308
$T_{31–30}$	1.0300	1.1000	0.9822	1.1000
$T_{48–47}$	1.0300	1.1000	0.9577	1.1000
$T_{74–76}$	1.0300	0.9000	0.9187	1.1000
Q_{C50}	-	0.2500	-	0.2496
Q_{C55}	-	0.2500	-	0.2500
Q_{C56}	-	-	0.2500	-
Q_{C63}	-	-	0.2005	-
Q_{C66} / Q_{C66}	-	0.2500	0.2088	-
Q_{C67}	-	0.2500	-	0.2323
Q_{C73}	-	-	0.2500	-
Q_{C77}	-	0.0371	-	0.2500
Q_{C89} / Q_{C89}	-	0	0.2500	-
Q_{C91}	-	-	0.0440	-
Q_{C93}	-	0	-	0.2500
SVC_{56}	-	-	-	0.2500
SVC_{63}	-	-	-	0.2500
SVC_{66}	-	-	-	-0.2500
SVC_{73}	-	-	-	0.1875
SVC_{89}	-	-	-	0.2500
SVC_{91}	-	-	-	0.1292
P_{Loss} (MW)	77.2746	70.7003	59.9319	55.0110
Reduction (%)	-	8.510	22.443	28.8109

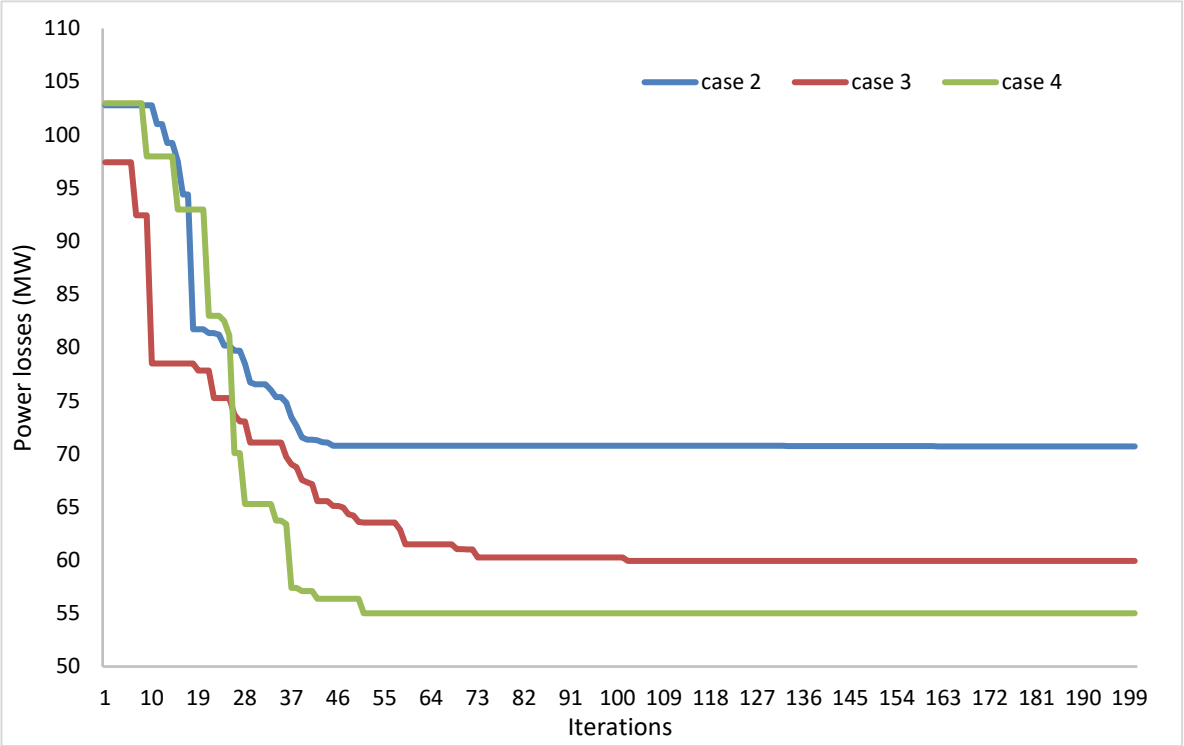

Figure 5.18. Convergence characteristic of Algerian electric power system (case 2, 3 and 4)

5.5. Conclusion

Flexible AC Transmission Systems (FACTS) can provide benefits in increasing system transmission capacity and power flow control flexibility and speed. The FACTS have the capability to control various electrical parameters in electrical transmission network. These devices include Thyristor Controlled Series Compensator (TCSC), Static Var Compensator (SVC), Unified Power Flow Controller (UPFC), Static Compensator (STATCOM), and others. The SVC and the TCSC are the most widely used FACTS devices in power networks. In this chapter, a brief introduction to the FACTS is presented. Afterwards the proposed PSO-TS method was applied to the ORPD problem considering SVC and TCSC devices. The setting of FACTS devices is taken as additional control variable along with generator voltages, tap ratio of transformer and shunt capacitors. The performance evaluation of the proposed algorithms on ORPD problem in presence of FACTS devices is carried out and the results obtained are discussed. The first time only one type of FACTS was considered. Then the two type of FACTS, SVC and TCSC were installed simultaneously. The results indicate that the ORPD considering FACTS devices significantly decrease the active power losses. The results show also that the simultaneous application of these two type FACTS devices with shunt capacitors reduces better the system active power losses in comparison to the results obtained by FACTS devices when each type is installed separately.

Chapter 6

MONITORING AND CONTROL OF FACTS DEVICES IN POWER NETWORK

6.1. Introduction

FACTS (Flexible Alternating Current Transmission Systems) remote monitoring in a power transmission network is crucial to ensure efficient and reliable transmission of electricity over long distances. FACTS devices are used to control and optimize power flow, reduce energy losses and improve power system stability. These devices can include equipment such as STATCOMs (Static Synchronous Compensators), SVCs (Static Var Compensators), TCSCs (Thyristor-Controlled Series Compensators) and other similar technologies. More specifically, SVCs (Static Var Compensators) are FACTS devices used to regulate the voltage and flow of reactive power in an electrical network. They can rapidly adjust the voltage on a transmission line by injecting or absorbing reactive power, keeping voltage levels within safe limits and improving the quality of the electricity transmitted. Remote monitoring of these FACTS devices is essential for several reasons:

- Network management and control: Monitoring the real-time performance of SVCs and other FACTS equipment enables effective network control and preventive action to be taken in the event of problems or unexpected variations.
- Proactive maintenance: Remote monitoring can detect signs of potential failure or performance problems before they cause outages, facilitating maintenance planning and reducing service interruptions.
- System optimization: By analyzing remotely collected data, operators can adjust and optimize the parameters of SVCs and other FACTS devices to improve energy efficiency and system stability.
- Remote monitoring systems often use sensors, communication devices and data analysis software to collect real-time information on the performance of SVCs and other FACTS equipment. This enables network operators to have an overview and precise control of the power system, which is essential for efficient and reliable transmission of electrical energy over long distances.

In this chapter, we propose a method for monitoring and controlling FACTS. We have simulated one type of FACTS which is the SVC. Each SVC device will be automatically connected or disconnected to the most sensitive bus already identified. The SVC device will be connected according to the size optimized by the metaheuristic method executed in MATLAB. This control will be done directly between MATLAB and the SVC device via a microcontroller. Communication between the SVC device and MATLAB will be via an interface created by GUI MATLAB which will be described in more detail later. This interface was chosen to avoid programming the microcontroller. We can monitor the status (connected or disconnected) of the SVC device using an application that runs on different operating systems (Windows, Android, IOS).

6.2. Monitoring and control of electrical transmission network

6.2.1. Monitoring of electrical power system

Electrical transmission monitoring is crucial for ensuring the efficient and reliable operation of power systems. It involves the continuous observation, analysis, and management of various parameters within the transmission network to prevent failures, optimize performance, and enhance overall grid resilience.

Remote monitoring is capable of analyzing and synthesizing the information received to automatically and continuously provide all the information needed to operate the network in real time. It brings together all the signals from the network, such as the triggering or possible switching on of equipment, the measurement of instantaneous or weighted consumption in the various parts of the electricity network, and any other information that provides information on the actual state of the network. The monitoring part continuously collects all the signals from the process and the control, reconstructs the real state of the controlled system, and makes all the necessary inferences to produce the data used to draw up operating histories. The objectives of the monitoring part of a supervisor are:

- Detect abnormal operation.
- Identify the causes and consequences of unexpected or uncontrolled operation.
- Modifying the models used during planned operation to return to this operation: changing the control, resetting, ... etc.
- In particular, the synoptic images are created according to the actual installation and the needs of the operator. They are also animated in real time. The operator can therefore view:
    - operating diagrams (electrical network, substation, etc.).
    - installation status (equipment positions, etc.).

- values of operating parameters (currents, voltages, power, etc.).

6.2.1.1. *Different aspects of monitoring in electrical transmission*

- Voltage and Current Monitoring: Continuous measurement of voltage and current levels at different points in the transmission system to ensure they are within safe operating limits.
- Line Loading and Congestion Management: Monitoring the load on transmission lines to prevent overloading, which can lead to equipment damage or system failures.
- Fault Detection and Diagnosis: Detecting faults (like short circuits or equipment failures) promptly and accurately is essential for minimizing downtime and ensuring grid reliability.
- Temperature and Thermal Monitoring: Monitoring equipment temperatures to prevent overheating, which can damage components and lead to failures.
- Remote Sensing and Control: Using remote sensing technologies and control systems to monitor and manage the transmission network from a centralized location.
- Data Analytics and Predictive Maintenance: Utilizing data analytics and machine learning algorithms to analyze collected data, predict potential failures, and schedule maintenance proactively to prevent unplanned outages.

6.2.2. Control of electrical power system

The control of an electrical transmission network involves managing the flow of electricity, maintaining system stability, and responding to various operational conditions to ensure a reliable and secure power supply. The Continuous monitoring, advanced control algorithms, and effective communication are essential for the successful control of an electrical transmission network. These measures collectively contribute to the reliability, stability, and efficiency of the power grid.

6.2.2.1. *Different aspects of controlling in electrical transmission network.*

- Load Balancing: Ensure a balance between electricity generation and consumption to maintain stable grid conditions.
- Frequency Control: Maintain a stable frequency within acceptable limits.
- Voltage Control: Regulate voltage levels within specified limits to ensure the safe and efficient operation of the network. Use devices like tap-changing transformers, shunt reactors, and FACTS devices for voltage control.
- Generator Control: Control the operation of power generators to meet the demand and maintain grid stability.

- HVDC (High Voltage Direct Current) Control: Manage the power flow and voltage levels on HVDC transmission links. Utilize control systems to regulate the converters and maintain the desired DC voltage levels.
- Contingency Management: Implement automatic remedial actions during contingencies or disturbances.
- Grid Synchronization: Coordinate the connection and disconnection of power plants or substations to the grid.
- Communication Systems: Establish reliable communication between control centers and field devices. Enable fast and accurate exchange of information for timely decision-making.
- Emergency Response: Develop and implement emergency response plans to address severe disturbances or unforeseen events.
- Demand Response: Implement strategies to manage and control electricity demand. Engage with demand-side resources to adjust consumption during peak periods or emergency situations.
- Predictive Maintenance: Use data analytics and predictive maintenance models to anticipate equipment failures.

6.3. Monitoring applications

Monitoring applications allow remote access and exchange of electrical information in order to assess the state of the electrical network (see example in figure 6.1).

Monitoring applications in the context of electrical transmission encompass various software, tools, and systems designed to observe, analyze, and manage different aspects of the power grid. These applications serve to ensure the smooth functioning, reliability, and efficiency of the transmission network. Here are some monitoring applications:

SCADA (Supervisory Control and Data Acquisition): SCADA systems collect real-time data from remote locations within the power grid. They monitor and control equipment, such as substations, transformers, and switches, allowing operators to visualize the system, detect issues, and make informed decisions.

EMS (Energy Management System): EMS applications optimize the generation, transmission, and distribution of electrical power. They provide tools for monitoring grid conditions, managing generation and load, and ensuring grid stability.

PMU (Phasor Measurement Unit) Applications: PMUs measure the electrical waves' phasors (amplitude and phase angle) across the grid in real-time. Applications utilizing PMU data help in monitoring grid stability, detecting disturbances, and enabling faster corrective actions.

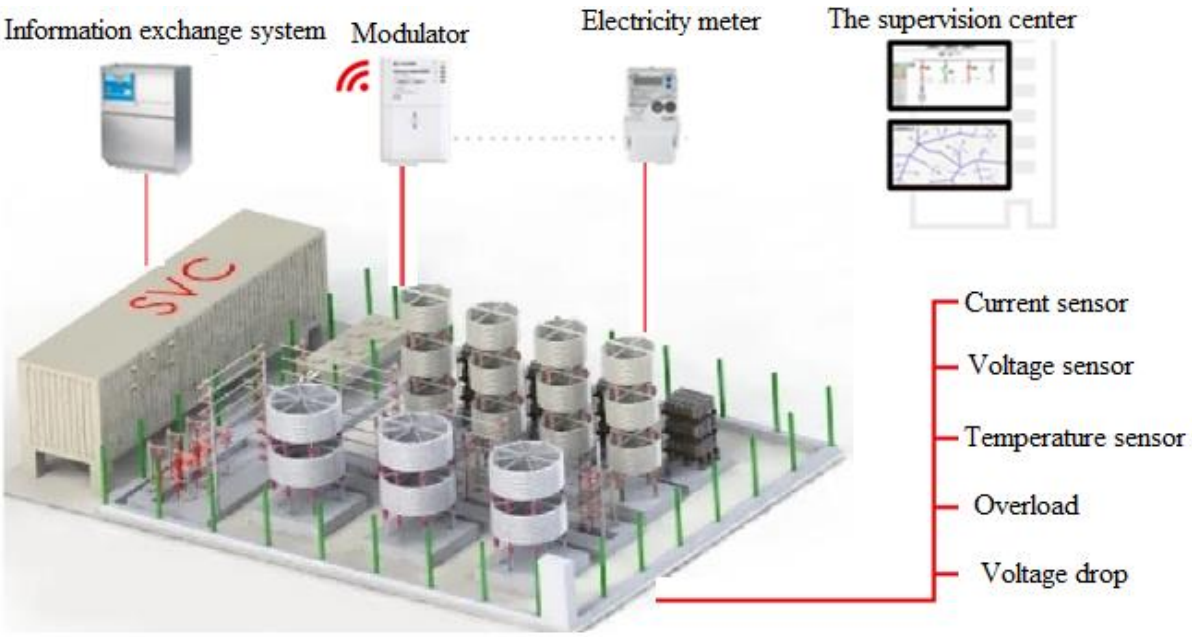

Figure 6.1. Example of Monitoring of SVC

6.4. Monitoring and control of SVC devices in electrical transmission system.

Monitoring and control of Static Voltage Compensators (SVCs) in a power transmission network is essential to ensure their efficient operation and to maintain voltage stability and power quality. SVCs are power electronics-based devices used to regulate voltage, control reactive power and improve network performance. The various steps followed to supervise and control the SVC devices in our case are described below:

1. Execution of the program in MATLAB for optimizing the size of SVCs

2. Once the sizes are optimized the MATLAB program calls the relevant functions (connected function or disconnected function) of each SVC generated by MATLAB GUI.

3. The GUI MATLAB functions called by the programs are sent to the microcontroller.

4. The microcontroller, via the relays, connects or disconnects the SVC devices according to the information sent by GUI MATLAB.

5. The microcontroller also sends information on the status of each SVC device (connected or disconnected) to an application (Windows or Mobile).

6. The application will also be used to see the different types of networks used as well as the different simulations found by the proposed methods namely GWO, ALO, AHA and MFO.

6.5. Monitoring and control of SVC devices block diagram

Our developed monitoring and control system comprises the following blocks (Figure 6.2):

1. MATLAB program to optimize the size of the SVC device.
2. Communication block to send the results found to the microcontroller via WIFI, GSM network or wired connection.
3. A Relay Module that receives the command from the microcontroller to connect or disconnect the SVC to the sensitive bus in the transmission network.
4. Power restoration and interruption equipment
5. Mobile phone: When the microcontroller instructs the relay module to connect or disconnect the SVC device in the transmission network, information will also be sent to a mobile application to monitor the status of the SVC in real time.

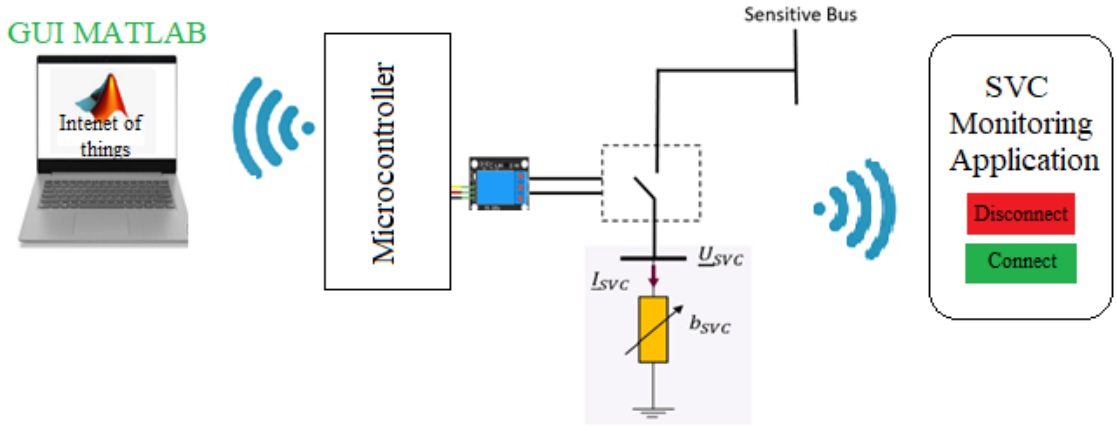

Figure 6.2. Block diagram of SVC device monitoring

6.6. The GUI MATLAB interface

6.6.1. Definition

A GUI (Graphical User Interface) is a type of user interface that allows users to interact with software or applications through graphical elements, as opposed to a command-line interface. GUI typically includes visual components like buttons, sliders, text boxes, and menus, making it easier for users to interact with and control the software.

6.6.2. GUI in MATLAB

When people refer to a GUI in MATLAB, they are usually talking about creating a graphical user interface for a MATLAB application. MATLAB provides a guide (Graphical User Interface Development Environment) for designing and creating GUIs. This environment allows users to design the layout and appearance of the GUI and link it to MATLAB code for functionality.

6.7. Control of SVC devices with GUI MATLAB

To control SVC devices with GUI MATLAB, we First need to install the MATLAB support package for the microcontroller. Once the package has been installed, all we need to do is to connect the relay module to the microcontroller and then connect it to the computer. Figure 6.3 illustrates how the GUI MATLAB interface can control the fact device directly via a microcontroller.

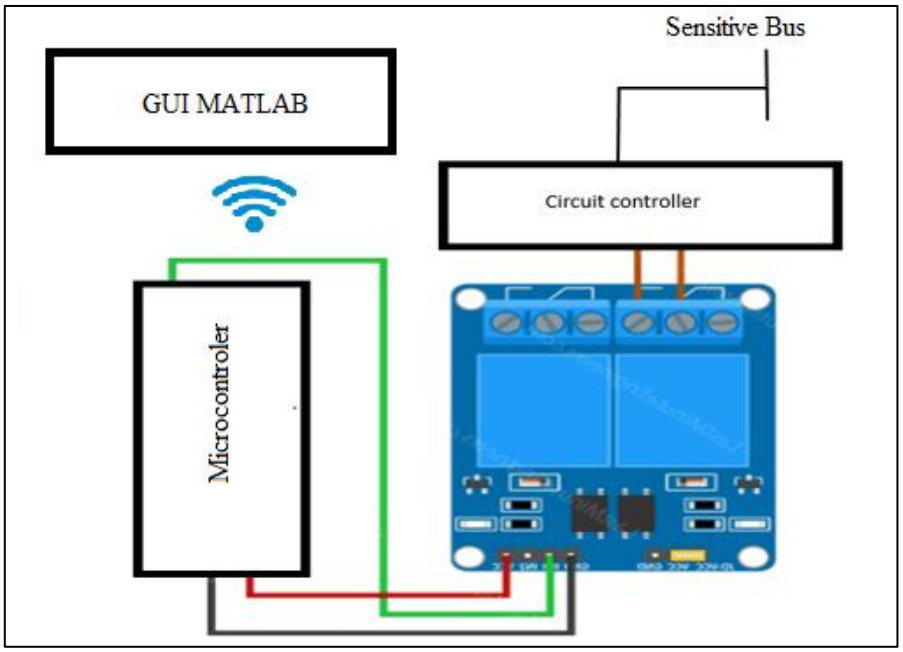

Figure 6.3. Control with MATLAB GUI interface

6.7.1. Creation of the GUI application

To create a new GUI application, select the file menu and then click on new GUI application (Figure 6.4)

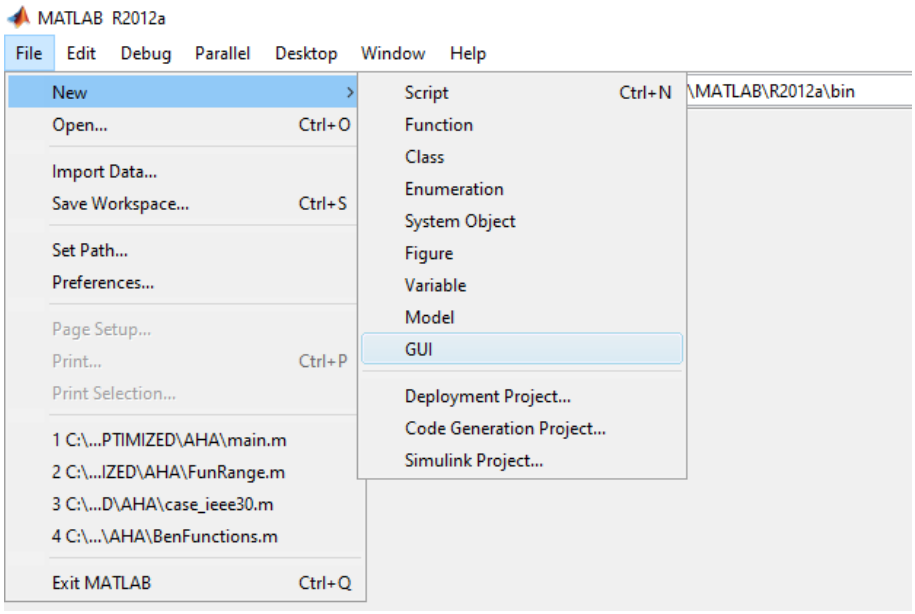

Figure 6.4. Menu to create a new GUI application

Once a new GUI application has been chosen (figure 6.5), we get a new window that lets us add buttons, images and text to create our remote control and monitoring interface.

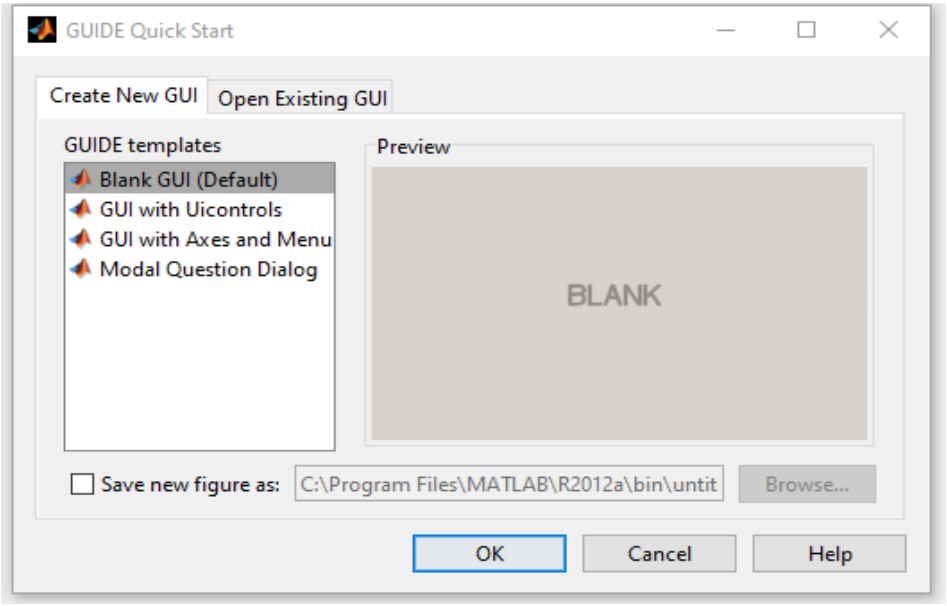

Figure 6.5. GUI application selection window

The GUI window appears (figure 6.6) and we're now going to create two buttons that will be used to connect or disconnect the SVC device. So, we're going to click on the push button and drag it to the size we want.

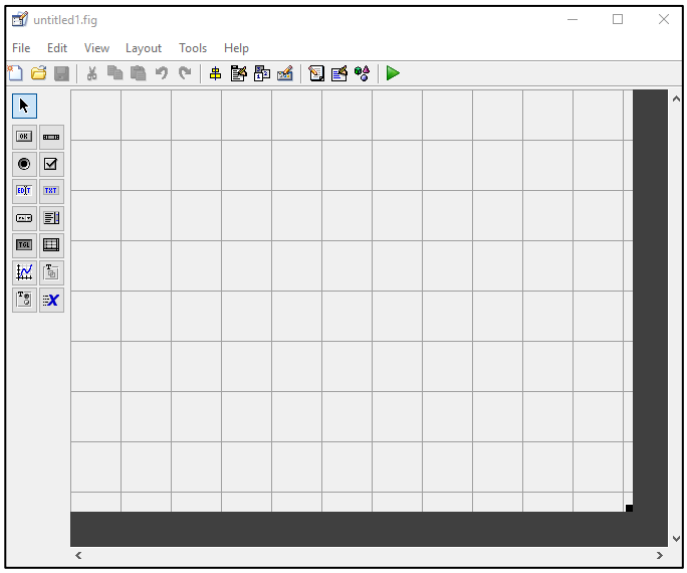

Figure 6.6. Window for creating the control and monitoring application

The window in figure 6.7 shows how to create the two buttons for connecting and disconnecting the SVC device from the electrical system

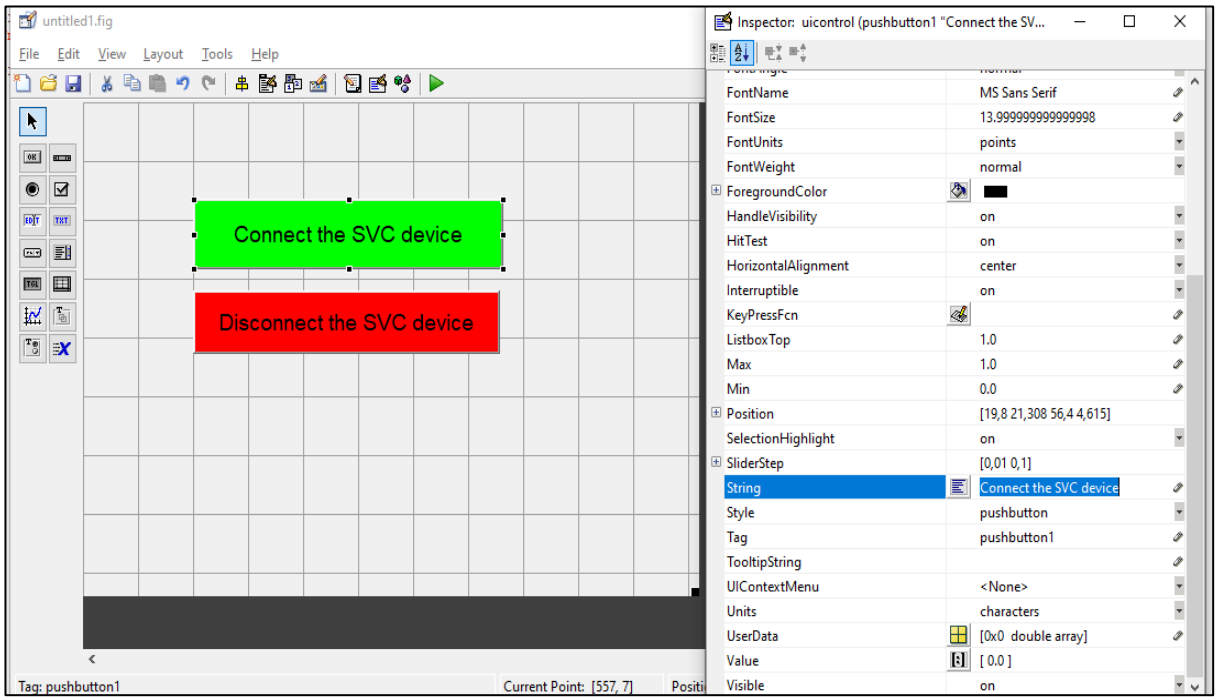

Figure 6.7. Window to create the SVC control button

Now, to add a label, we click on the "static text" label and click on the graphical interface, then resize the label and write the text we want to display. In our case, we'll start with the text "SVC device control".

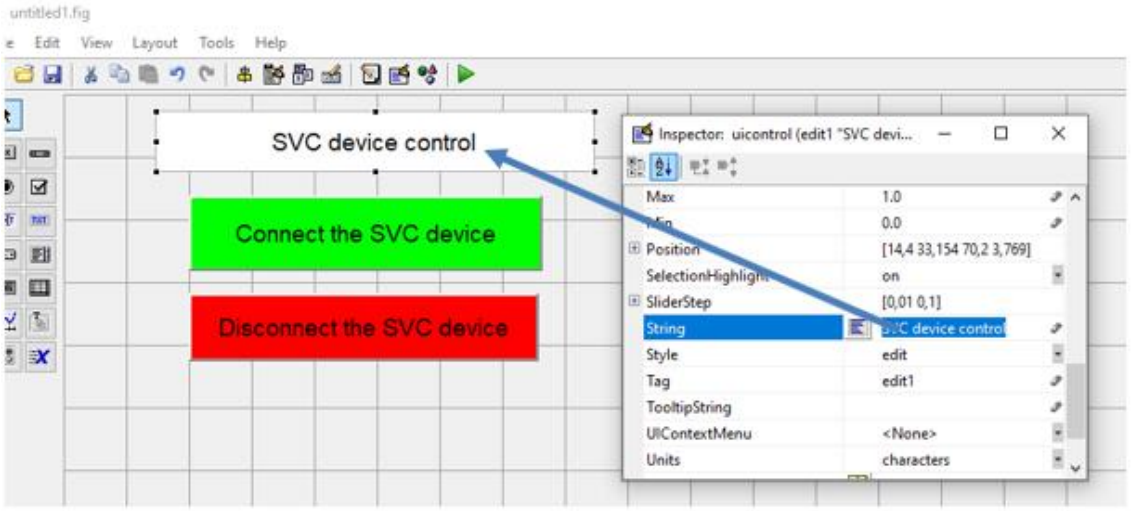

Figure 6.8. Window to add text title

6.7.2. Programming the two control buttons

Now we have to declare all the functions that we are going to use. Before that, we need to declare some variables.

The pseudo-code below gives the function where we declare the variables

```
function varargout = SVC_control_OutputFcn(hObject, eventdata, handles)
% varargout  cell array for returning output args (see VARARGOUT);
% hObject    handle to figure
% eventdata  reserved - to be defined in a future version of MATLAB
% handles    structure with handles and user data (see GUIDATA)
 % Get default command line output from handles structure
varargout{1} = handles.output;
```

A function called Communication, to establish communication between MATLAB and the microcontroller.

```
function Communication
global a;
a = microcontroller;
```

We will declare the function, when we press the button "SVC device connect" the relay module connects the SVC device to the power grid. for this, we need to write a function called “Connect_SVC”.

```
function Connect_SVC(hObject, eventdata, handles)
% hObject    handle to on (see GCBO)
% eventdata  reserved - to be defined in a future version of MATLAB
% handles    structure with handles and user data (see GUIDATA)
global a;
Pin(a,'D3',1);
```

When we click on the "Disconnect SVC device" button, the SVC disconnects from the electrical network.

```
function Disconnect_SVC(hObject, eventdata, handles)
% hObject    handle to off (see GCBO)
% eventdata  reserved - to be defined in a future version of MATLAB
% handles    structure with handles and user data (see GUIDATA)
global a;
lPin(a,'D3',0);
```

6.8. The main application of visualization and control

In order to be able to add and visualize the simulations carried out in this thesis and at the same time be able to control the SVC devices through the same menu, a main application has been designed to avoid having several separate applications.

6.8.1. Application login window

Creating a login window for an application is a common design element that provides a secure

way for users to access the application. Figure 6.9 represents the application connection window for our application.

Figure 6.9. Application login Window

6.8.2. The main menu

The main menu of the application (Figure 6.10) has the following icons:

- ✓ Add a new electrical network;
- ✓ Add line data;
- ✓ Add bus data;
- ✓ Add new algorithm
- ✓ Add simulation;
- ✓ View simulation;
- ✓ Monitoring of SVC devices;
- ✓ Administrator settings to add or modify access rights to the application.

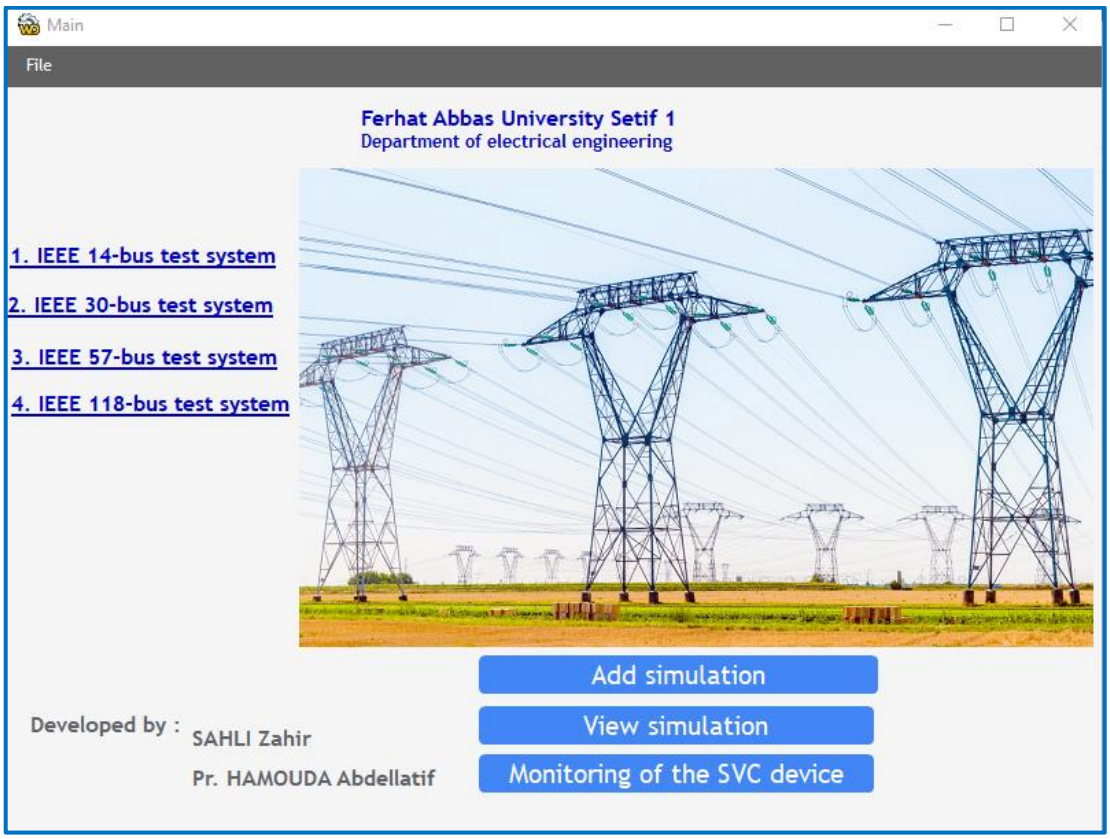

Figure 6.10. The main window

6.8.3. Simulation Results window

A simulation results window generally refers to a graphical interface or display that presents the results and analysis of a simulation. It is in this window that users can view and interpret the results of their simulated experiments. The specifics of a simulation results window may vary depending on the simulation tool or software used. The Simulation Results Window is a central component in simulation software, providing users with a visual and interactive platform to explore, analyze, and understand the outcomes of their simulated experiments. Figure 6.11 shows the Simulation results widow of our application.

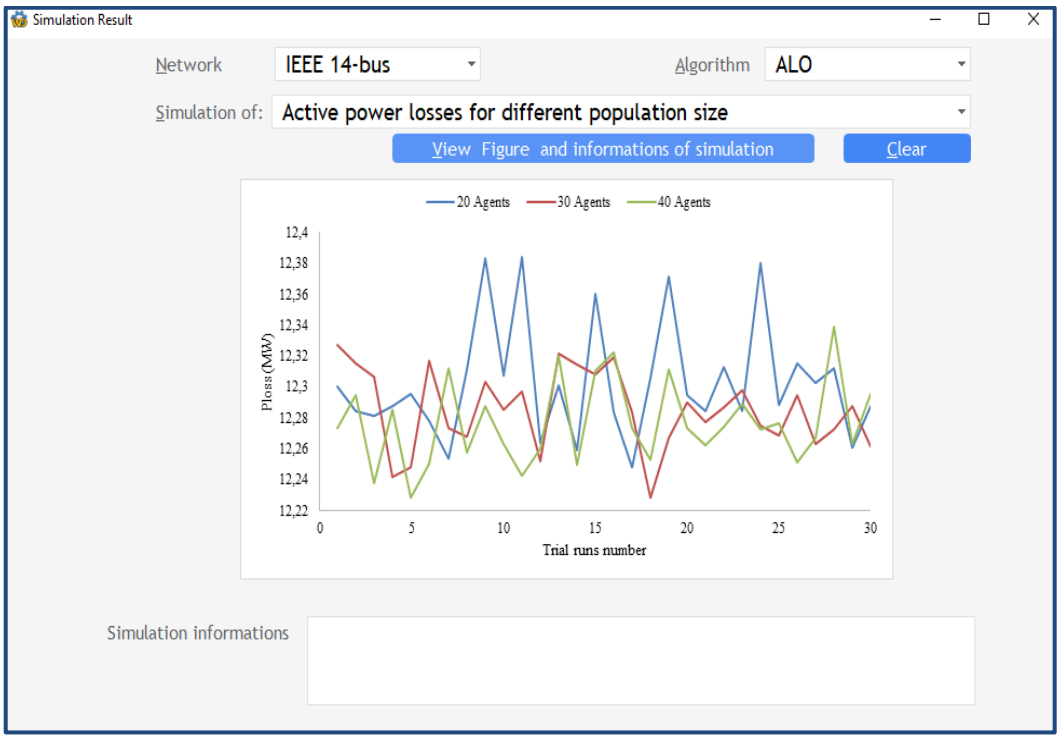

Figure 6.11. Simulation results widow

6.8.4. Interface for monitoring and controlling SVC devices

This figure shows the interface for monitoring and controlling SVC devices. We can connect or disconnect either all the SVCs or each SVC on its own.

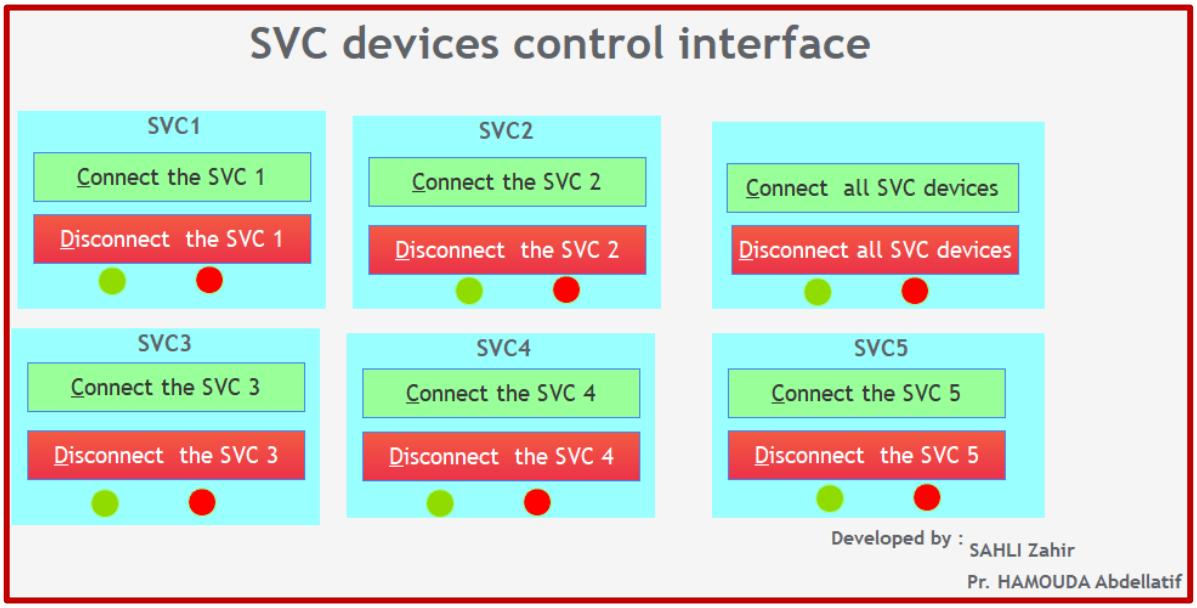

Figure 6.12. Interface for monitoring and controlling SVC devices

6.9. Practical implementation

we built a mock-up to test the control and command of the SVC devices via a human-machine interface running under Windows and Android. The SVC devices in our handling has been replaced by lamps. We controlled the relay modules, which can in turn connect or disconnect the lamps.

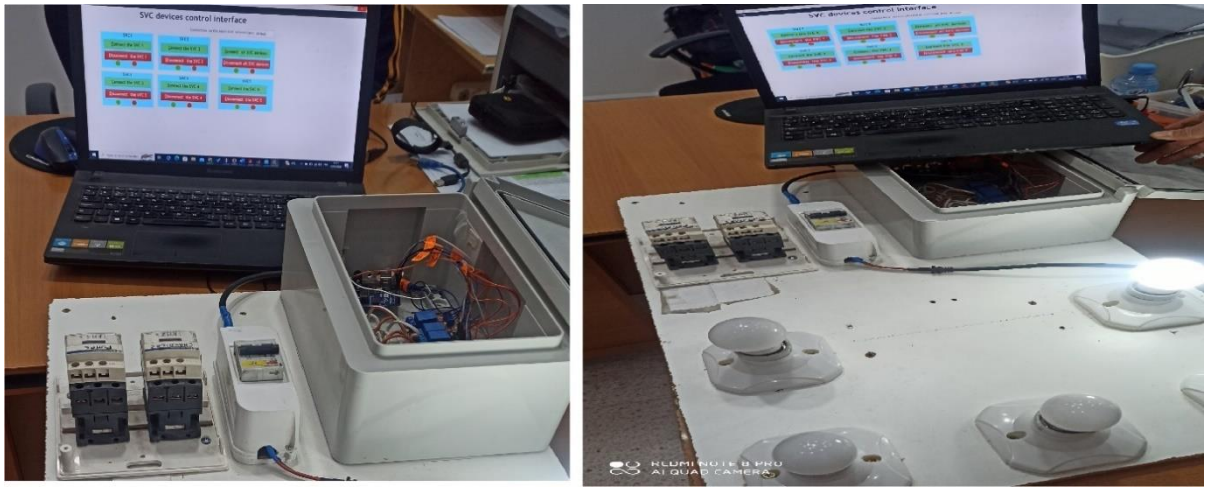

Figure 6.13. Practical implementation for controlling SVC devices

6.10. Conclusion

Monitoring and control are critical aspects of managing electrical transmission power networks. These activities involve real-time observation, analysis, and manipulation of various parameters within the power network. The Operators interact with the power system through Human-Machine Interface (HMI) which provide a user-friendly interface for monitoring and controlling the network. In this chapter, we have presented the various components used for the remote monitoring and control of SVC devices. An Android and Windows applications were developed to simulate monitoring of SVC devices connected to the electrical network. We have built a mock-up to test the control and command of the SVC devices via a human-machine interface running under Windows and Android. We controlled the relay modules, which can in turn connect or disconnect the SVC devices to or from the electrical network. An application has been designed to visualize all the curves obtained during the simulations carried out in this thesis.

Chapter 7

GENERAL CONCLUSION

7.1. General conclusion

Optimal Reactive Power Dispatch (ORPD) is one of the most classical and difficult problems among researchers' community of electrical power engineering. In addition to the size of the variables involved, its multi-objective aspect and the number of constraints constitute a real challenge for conventional optimization methods. These methods often using advanced mathematical analyses are not successful in realizing the global optimal results for ORPD problem. Therefore, in the last decade, there has been intense research activity proposing new algorithms that are inspired by the nature and called bio-inspired algorithms to solve optimization problems.

In the first part of this research work, four different bio-inspired methods are applied to evaluate ORPD problem. The first one is MFO, a metaheuristic optimization algorithm inspired by the behavior of moths which are a flying insect. The second one is ALO algorithm modeled on the hunting mechanism of Antlions (crawling insects). The third one is AHA algorithm which is based on the behavior of hummingbirds (a bird species). The last one is GWO algorithm inspired from the real life of an organized group of Grey Wolf (kind of animals) by analyzing their behavior and communication for hunting in nature. Usefulness and efficiency of the proposed techniques are evaluated on small, medium and large-scale power systems (IEEE 14-bus, IEEE-30 bus, IEEE-57 bus, IEEE-118 bus). Several tests were carried out throughout this work in order to conduct statistical studies and confirm the effectiveness of the proposed bio-inspired methods. The statistical analysis achieved in this study are: Box-and-whisker plot and One-way ANOVA. The software we have used to create box plots is R-software, which offers solid capabilities for creating, visualizing and analyzing data using box-plots.

In the second part of this study, a new efficient hybrid algorithm for ORPD has been proposed. It is based on the combination of the well-known metaheuristic algorithms, PSO (Particle Swarm Optimization) and TS (Tabu Search) algorithms to form a hybrid one called PSO-TS algorithm. The latter is a power tool that outperform the two algorithms alone for solving power system optimization problems. This hybridization has proved its effectiveness

in solving the optimal reactive power dispatch problem considering continues and discrete variables across four test networks, i.e. the IEEE 14-bus, the IEEE 30-bus, the IEEE 57-bus and the practical Algerian 114-bus network. Simulation results have shown that the obtained results by the PSO-TS were very satisfactory and better than the other algorithms. The ORPD problem based PSO-TS using Sensitive Bus approach is also presented. The bus locations of the shunt capacitors are identified according to this approach. To identify this type of buses and their location, we have studied three cases. The two first cases are based on the active power losses and the third one is based on the total voltage deviation. To show the effectiveness of the proposed method based sensitive approach, the IEEE 14-bus, IEEE 30-bus, IEEE 57-bus and the practical Algerian 114-bus electrical systems have been considered and the results compared with those given by PSO, TS and some other published approaches.

In the third part of this research work, we have studied the effects of FACTS devices since they can significantly improve system performance by controlling power flows in power system without generation rescheduling or topological changes. Two FACTS devices named Static Var Compensator (SVC) and Thyristor Controlled Series Capacitor (TCSC) were used in this work. This study has considered the setting FACTS devices as additional control parameters in the ORPD formulation and studied their impact on active power loss minimization. The proposed PSO-TS algorithm for ORPD problem including FACTS devices such as Static Var Compensator (SVC) and Thyristor Controlled Series Capacitor (TCSC) are conducted on IEEE 30-bus test system. To investigate the effect of optimal setting of FACTS devices in minimizing total active power losses, studies were conducted on the IEEE 30-bus test system using the proposed algorithm. Several cases in terms of use of FACTS devices are considered namely: P_{Loss} minimization considering one SVC device, P_{Loss} minimization considering two SVC devices, P_{Loss} minimization considering one TCSC device and P_{Loss} minimization considering two type FACTS devices (one SVC and one TCSC). For each case, the impact of the FACTS when installed with and without shunt capacitors on the quality of the solution is investigated.

To give a practical aspect to this work, we have tried to get closer to reality by controlling and monitoring the connection and disconnection of a type of FACTS called SVCs. To do this, we first designed a Windows application to display all the simulations carried out during the various test systems. A mock-up to test the control and command of the SVC devices via a human-machine interface running under Windows and Android has been developed. The relays are controlled to connect or disconnect the SVC devices from the electrical network. To control directly the SVCs via MATLAB, a MATLAB package called GUI MATLAB is

required. The GUI MATLAB functions called by the programs are sent to the microcontroller. The microcontroller, via the relays, connects or disconnects the SVC devices according to the information sent by GUI MATLAB. The microcontroller also sends information on the status of each SVC device (connected or disconnected) to an application (Windows or Mobile).

The optimization topics in modern power systems are vast and varied. In the future, we plan to cover more subjects related to power system optimization. Below are the development outlooks for the present work.

7.2. Future Works

- More objectives can be considered in solving ORPD problem such as maximizing power transfer and enhancing system stability.
- In addition to loss minimization and voltage deviation minimization, cost of reactive installation may be considered as another and conflicting objective.
- The proposed methods to solve the ORPD problem for minimizing the active power losses and voltage deviation could be extended to be applied for multi-objectives.
- The study of performance comparison on various proposed metaheuristic algorithms can be done for ORPD problem in deregulated environment.
- In addition to shunt capacitors and FACTS, we can study the ORPD problem in the presence of decentralized energy sources.

Appendix A. The Algerian Electric Power System 114 bus

Table A.1. Bus DATA.

Bus	Type	Pd (MW)	Qd (MVAr)	Bus	Type	Pd (MW)	Qd (MVAr)	Bus	Type	Pd (MW)	Qd (MVAr)
1	1	0	0	39	1	20	10	77	1	7	3
2	1	36	17	40	1	21	10	78	1	13	7
3	1	64	31	41	1	53	32	79	1	14	7
4	3	210	150	42	1	0	0	80	2	157	107
5	2	335	250	43	1	31	18	81	1	0	0
6	1	78	37	44	1	0	0	82	1	75	36
7	1	55	26	45	1	12	6	83	2	70	51
8	1	50	24	46	1	0	0	84	1	46	34
9	1	40	19	47	1	21	10	85	1	45	22
10	1	42	21	48	1	0	0	86	1	0	0
11	2	96	47	49	1	13	6	87	1	32	15
12	1	31	15	50	1	4	2	88	1	46	22
13	1	13	6	51	1	1	1	89	1	34	17
14	1	136	65	52	2	56	27	90	1	18	9
15	2	0	0	53	1	16	8	91	1	44	21
16	1	0	0	54	1	21	10	92	1	10	5
17	2	0	0	55	1	18	9	93	1	0	0
18	1	0	0	56	1	33	20	94	1	48	23
19	2	11	5	57	1	35	21	95	1	35	17
20	1	14	9	58	1	0	0	96	1	0	0
21	1	70	52	59	1	36	17	97	1	42	20
22	2	42	25	60	1	0	0	98	2	13	6
23	1	23	11	61	1	27	13	99	1	105	50
24	1	60	36	62	1	22	11	100	2	33	16
25	1	17	8	63	1	49	29	101	2	50	24
26	1	55	26	64	1	0	0	102	1	34	16
27	1	0	0	65	1	11	5	103	1	66	32
28	1	0	0	66	1	35	21	104	1	18	9
29	1	37	18	67	1	10	5	105	1	0	0
30	1	30	15	68	1	11	5	106	1	64	31
31	1	0	0	69	1	20	10	107	1	65	37
32	1	40	24	70	1	7	3	108	1	22	11
33	1	29	14	71	1	36	22	109	2	37	18
34	1	29	14	72	1	0	0	110	1	13	6
35	1	33	16	73	1	36	22	111	2	94	56
36	1	17	8	74	1	0	0	112	1	24	12
37	1	11	5	75	1	0	0	113	1	23	11
38	1	20	10	76	1	12	6	114	1	24	12

1: P-Q bus 2: P-V bus 3: V-θ bus.

Table A.2. Generator DATA.

Bus	Pg (MW)	Qg (MVAr)	Qmax (MVAr)	Qmin (MVAr)	Vg (pu)	Pmax (MW)	Pmin (MW)
4	750	0	400	-20	1.07	1200	0
5	450	0	200	-20	1.05	650	0
11	100	0	100	-50	1.05	150	0
15	100	0	100	0	1.04	150	0
17	450	0	400	0	1.08	600	0
19	115	0	60	0	1.03	150	0
52	115	0	50	0	1.04	150	0
22	115	0	50	0	1.05	150	0
80	115	0	60	0	1.08	150	0
83	100	0	200	-50	1.05	150	0
98	100	0	50	0	1.05	150	0
100	200	0	270	0	1.08	250	0
101	200	0	200	-50	1.08	250	0
109	100	0	100	-50	1.05	150	0
111	100	0	155	-50	1.02	150	0

Table A 3. Branch DATA.

Fbus	Tbus	R	X	B	Rate	Fbus	Tbus	R	X	B	Rate
2	1	0.0085	0.0403	0.0303	250	107	101	0.0334	0.1577	0.1189	250
6	1	0.0122	0.0578	0.0436	250	64	97	0.0178	0.0654	0.0470	200
2	6	0.0140	0.0498	0.0355	200	72	96	0.0152	0.0540	0.0386	200
4	42	0.0274	0.1295	0.0976	250	96	98	0.0203	0.0720	0.0515	200
4	42	0.0139	0.0122	0.1474	450	96	95	0.0015	0.0070	0.0053	200
4	3	0.0033	0.0158	0.0482	500	18	22	0.0290	0.1397	0.0017	80
5	3	0.0028	0.0189	0.0294	450	18	37	0.0256	0.1233	0.0015	80
5	4	0.0018	0.0126	0.0197	450	37	22	0.0171	0.0822	0.0010	80
4	7	0.0144	0.0678	0.0512	250	19	26	0.0058	0.0077	0.0017	60
15	16	0.0038	0.0135	0.0097	200	19	26	0.0058	0.0077	0.0017	60
16	3	0.0041	0.0144	0.0103	200	19	34	0.0019	0.0126	0.0001	80
16	14	0.0013	0.0045	0.0032	200	20	18	0.1348	0.2944	0.0013	50
8	42	0.0171	0.0629	0.0454	200	20	24	0.0376	0.1390	0.0006	40
8	4	0.0184	0.0870	0.0657	250	20	24	0.0368	0.1361	0.0006	40
10	7	0.0150	0.0709	0.0535	250	20	29	0.0319	0.1178	0.0005	40
10	11	0.0228	0.1076	0.0811	250	20	35	0.0428	0.1528	0.0006	40
7	6	0.0157	0.0740	0.0558	250	35	29	0.0458	0.1639	0.0007	40
11	42	0.0170	0.0806	0.0608	250	20	32	0.0708	0.2365	0.0010	60
6	3	0.0288	0.1012	0.0730	200	22	32	0.0342	0.1142	0.0005	60
9	2	0.0042	0.0284	0.0442	450	22	24	0.0239	0.0799	0.0003	60
9	3	0.0088	0.0600	0.0933	450	22	24	0.0239	0.0799	0.0003	60
13	12	0.0501	0.2365	0.1784	250	23	30	0.0239	0.0799	0.0003	60
10	13	0.0464	0.2190	0.1652	250	23	36	0.0136	0.0457	0.0002	60
17	21	0.0065	0.0244	0.0176	200	36	30	0.0273	0.0913	0.0004	60
17	21	0.0073	0.0278	0.0202	200	33	18	0.0205	0.0685	0.0003	60
17	72	0.0197	0.0732	0.0530	200	32	33	0.0239	0.0799	0.0003	60
17	27	0.0046	0.0237	0.1003	300	26	25	0.0139	0.0517	0.0002	30
17	31	0.0061	0.0311	0.0617	350	24	25	0.0164	0.0608	0.0003	60
31	28	0.0017	0.0088	0.0746	300	26	34	0.0049	0.0318	0.0002	60
17	64	0.0198	0.0727	0.0525	200	29	26	0.0119	0.0158	0.0034	60
21	44	0.0240	0.0861	0.0615	200	29	39	0.0126	0.0820	0.0004	80
60	31	0.0037	0.0253	0.0393	450	38	34	0.0047	0.0307	0.0002	80
21	60	0.0056	0.0263	0.0198	250	18	73	0.1557	0.3427	0.0015	50
60	44	0.0122	0.0578	0.0436	250	18	73	0.0854	0.3028	0.0012	60
58	44	0.0121	0.0569	0.0429	250	62	18	0.0508	0.1941	0.0008	60
72	101	0.0213	0.1007	0.0760	250	20	52	0.0873	0.2162	0.0011	50
72	58	0.0183	0.0863	0.0651	250	20	52	0.0875	0.2167	0.0011	50
58	75	0.0148	0.0701	0.0528	250	54	59	0.1188	0.3063	0.0015	50
75	107	0.0185	0.0876	0.0660	250	52	59	0.0360	0.1014	0.0005	50
75	74	0.0006	0.0026	0.0026	250	57	51	0.1227	0.4098	0.0018	60
44	42	0.0248	0.0903	0.0649	200	57	77	0.1366	0.4566	0.0020	60
44	42	0.0183	0.0864	0.0651	250	52	53	0.0937	0.1788	0.0007	35
42	48	0.0074	0.0506	0.0786	450	53	54	0.0937	0.1788	0.0007	35
48	44	0.0025	0.0158	0.0245	450	52	30	0.0722	0.1789	0.0009	50
71	70	0.1599	0.3148	0.0013	35	98	97	0.0121	0.0448	0.0325	200
40	41	0.0586	0.1623	0.0008	50	99	100	0.0231	0.1089	0.0821	250
40	50	0.1343	0.3645	0.0016	35	87	100	0.0102	0.0694	0.0105	450
71	69	0.1093	0.3653	0.0016	60	100	84	0.0065	0.0442	0.0687	450
70	68	0.1204	0.2180	0.0009	35	84	80	0.0074	0.0506	0.0786	450
43	46	0.1025	0.3425	0.0015	60	86	81	0.0055	0.0379	0.0589	450
51	43	0.2067	0.3556	0.0015	35	98	99	0.0163	0.0580	0.0414	200
54	55	0.1196	0.3996	0.0018	60	101	102	0.0116	0.0547	0.0413	250
55	43	0.1708	0.5708	0.0025	60	99	102	0.0116	0.0547	0.0413	250
73	62	0.0410	0.1370	0.0006	60	99	101	0.0111	0.0759	0.1179	450
73	67	0.3347	0.7007	0.0031	40	98	94	0.0357	0.1275	0.0918	200
68	67	0.1648	0.3569	0.0015	40	94	82	0.0056	0.0263	0.0198	250
29	26	0.0119	0.0158	0.0034	60	92	93	0.1624	0.4088	0.0099	60
73	66	0.1623	0.5752	0.0023	60	93	91	0.0304	0.1074	0.0021	60
63	66	0.0683	0.2283	0.0010	60	93	91	0.0379	0.1342	0.0027	60
63	65	0.0557	0.1861	0.0008	60	90	89	0.0776	0.2400	0.0052	60
63	65	0.0557	0.1861	0.0008	60	88	89	0.1354	0.4100	0.0089	60
56	54	0.1025	0.3425	0.0015	60	90	93	0.1852	0.3189	0.0068	60
57	56	0.1196	0.3996	0.0018	60	103	110	0.0185	0.0876	0.0660	250
57	56	0.1196	0.3996	0.0018	60	110	112	0.0185	0.0876	0.0660	250
47	50	0.1196	0.3996	0.0018	60	103	114	0.0419	0.1979	0.1493	250
47	46	0.0342	0.1142	0.0005	60	109	108	0.0148	0.0701	0.0528	250
67	66	0.1128	0.2794	0.0014	50	109	107	0.0388	0.1833	0.1382	250
49	41	0.1265	0.4225	0.0019	50	112	114	0.0190	0.0896	0.0675	250
19	78	0.0042	0.0055	0.0012	60	112	111	0.0297	0.1402	0.1057	250
19	79	0.0105	0.0139	0.0030	60	113	111	0.0167	0.0787	0.0608	250
59	61	0.0513	0.1816	0.0007	60	80	88	0.0123	0.3140	0.0000	400
45	46	0.0171	0.0605	0.0002	60	81	90	0.0062	0.1452	0.0000	240
85	87	0.0158	0.0745	0.0562	250	86	93	0.0012	0.0742	0.0000	240

Fbus	Tbus	R	X	B	Rate	Fbus	Tbus	R	X	B	Rate
85	86	0.0139	0.0657	0.0495	250	42	41	0.0012	0.0742	0.0000	240
85	81	0.0099	0.0467	0.0352	250	58	57	0.0012	0.0742	0.0000	240
87	106	0.0105	0.0495	0.0373	250	44	43	0.0029	0.1053	0.0000	120
87	82	0.0056	0.0266	0.0200	250	60	59	0.0014	0.0516	0.0000	360
87	99	0.0322	0.1249	0.0909	200	64	63	0.0019	0.0700	0.0000	180
103	105	0.0130	0.0613	0.0462	250	72	71	0.0012	0.0742	0.0000	240
105	101	0.0171	0.0806	0.0608	250	17	18	0.0014	0.0516	0.0000	360
105	104	0.0015	0.0070	0.0053	250	21	20	0.0016	0.0525	0.0000	240
103	106	0.0208	0.0983	0.0741	250	27	26	0.0024	0.1484	0.0000	120
81	82	0.0303	0.1075	0.0768	200	28	26	0.0024	0.1484	0.0000	120
80	82	0.0319	0.1129	0.0807	200	31	30	0.0007	0.0495	0.0000	360
80	84	0.0191	0.0676	0.0483	200	48	47	0.0012	0.0742	0.0000	240
84	83	0.0051	0.0180	0.0129	200	74	76	0.0089	0.3340	0.0000	40
82	83	0.0191	0.0676	0.0483	200						
100	98	0.0102	0.0598	0.0754	250						
100	97	0.0111	0.0759	0.1179	450						

Bibliography

1. Dai, W.; Liu, Z. Study on Modeling of Unified Power Flow Controller.
2. Saadat, H. *Power Systems Analysis*; McGraw-Hill: New York, 1999;
3. Zhao, B.; Guo, C.X.; Cao, Y.J. A Multiagent-Based Particle Swarm Optimization Approach for Optimal Reactive Power Dispatch. *IEEE Trans. Power Syst.* 2005, *20*, 1070–1078, doi:10.1109/TPWRS.2005.846064.
4. Deeb, N.; Shahidehpour, S.M. Linear Reactive Power Optimization in a Large Power Network Using the Decomposition Approach. *IEEE Trans. Power Syst.* 1990, *5*, 428–438, doi:10.1109/59.54549.
5. Lee, K.Y.; Park, Y.M.; Ortiz, J.L. A United Approach to Optimal Real and Reactive Power Dispatch. *IEEE Trans. Power Appar. Syst.* 1985, *104*, 1147–1153.
6. C. Mamandur, K.R.; Chenoweth, R.D. Optimal Control of Reactive Power Flow for Improvements in Voltage Profiles and for Real Power Loss Minimization. *IEEE Trans. Power Appar. Syst.* 1981, *PAS-100*, 3185–3194, doi:10.1109/TPAS.1981.316646.
7. Horton, J.S.; Grigsby, L.L. Voltage Optimization Using Combined Linear Programming & Gradient Techniques. *IEEE Trans. Power Appar. Syst.* 1984, *PAS-103*, 1637–1643, doi:10.1109/TPAS.1984.318645.
8. Sachdeva, S.S.; Billinton, R. Optimum Network Var Planning by Nonlinear Programming. *IEEE Trans. Power Appar. Syst.* 1973, *PAS-92*, 1217–1225, doi:10.1109/TPAS.1973.293803.
9. Mahadevan, K.; Kannan, P.S. Comprehensive Learning Particle Swarm Optimization for Reactive Power Dispatch. *Appl. Soft Comput.* 2010, *10*, 641–652, doi:10.1016/j.asoc.2009.08.038.
10. Quintana, V.H.; Santos-Nieto, M. Reactive-Power Dispatch by Successive Quadratic Programming. *IEEE Trans. Energy Convers.* 1989, *4*, 425–435, doi:10.1109/60.43245.
11. Granville, S. Optimal Reactive Dispatch through Interior Point Methods. *IEEE Trans. Power Syst.* 1994, *9*, 136–146, doi:10.1109/59.317548.
12. Abido, M.A. Optimal Power Flow Using Particle Swarm Optimization. *Int. J. Electr. Power Energy Syst.* 2002, *24*, 563–571, doi:10.1016/S0142-0615(01)00067-9.
13. Abdullah, W.N.W.; Saibon, H.; Zain, A.A.M.; Lo, K.L. Genetic Algorithm for Optimal Reactive Power Dispatch. In Proceedings of the Proceedings of EMPD '98. 1998 International Conference on Energy Management and Power Delivery (Cat. No.98EX137); IEEE: Singapore, 1998; Vol. 1, pp. 160–164.
14. Ela, A.A.A.E.; Abido, M.A.; Spea, S.R. Differential Evolution Algorithm for Optimal Reactive Power Dispatch. *Electr. Power Syst. Res.* 2011, *81*, 458–464, doi:10.1016/j.epsr.2010.10.005.
15. Wu, Q.H.; Ma, J.T. Power System Optimal Reactive Power Dispatch Using Evolutionary Programming. *IEEE Trans. Power Syst.* 1995, *10*, 1243–1249, doi:10.1109/59.466531.

16. Badar, A.Q.H.; Umre, B.S.; Junghare, A.S. Reactive Power Control Using Dynamic Particle Swarm Optimization for Real Power Loss Minimization. *Int. J. Electr. Power Energy Syst.* 2012, *41*, 133–136, doi:10.1016/j.ijepes.2012.03.030.
17. Yoshida, H.; Kawata, K.; Fukuyama, Y.; Takayama, S.; Nakanishi, Y. A Particle Swarm Optimization for Reactive Power and Voltage Control Considering Voltage Security Assessment.
18. Bhattacharya, A.; Chattopadhyay, P.K. Solution of Optimal Reactive Power Flow Using Biogeography-Based Optimization. 2010, *4*.
19. Duman, S.; Sönmez, Y.; Güvenç, U.; Yörükeren, N. Optimal Reactive Power Dispatch Using a Gravitational Search Algorithm. *IET Gener. Transm. Distrib.* 2012, *6*, 563, doi:10.1049/iet-gtd.2011.0681.
20. Niknam, T.; Narimani, M.R.; Azizipanah-Abarghooee, R.; Bahmani-Firouzi, B. Multiobjective Optimal Reactive Power Dispatch and Voltage Control: A New Opposition-Based Self-Adaptive Modified Gravitational Search Algorithm. *IEEE Syst. J.* 2013, *7*, 742–753, doi:10.1109/JSYST.2012.2227217.
21. Solution of Optimal Reactive Power Dispatch by Chaotic Krill Herd Algorithm - Mukherjee - 2015 - IET Generation, Transmission & Distribution - Wiley Online Library Available online: https://ietresearch.onlinelibrary.wiley.com/doi/10.1049/iet-gtd.2015.0077 (accessed on 31 December 2023).
22. Dutta, S.; Mukhopadhyay, P.; Roy, P.K.; Nandi, D. Unified Power Flow Controller Based Reactive Power Dispatch Using Oppositional Krill Herd Algorithm. *Int. J. Electr. Power Energy Syst.* 2016, *80*, 10–25, doi:10.1016/j.ijepes.2016.01.032.
23. Khazali, A.H.; Kalantar, M. Optimal Reactive Power Dispatch Based on Harmony Search Algorithm. *Int. J. Electr. Power Energy Syst.* 2011, *33*, 684–692, doi:10.1016/j.ijepes.2010.11.018.
24. Mandal, B.; Roy, P.K. Optimal Reactive Power Dispatch Using Quasi-Oppositional Teaching Learning Based Optimization. *Int. J. Electr. Power Energy Syst.* 2013, *53*, 123–134, doi:10.1016/j.ijepes.2013.04.011.
25. Abaci, K.; Yamaçli, V. Optimal Reactive-Power Dispatch Using Differential Search Algorithm. *Electr. Eng.* 2017, *99*, 213–225, doi:10.1007/s00202-016-0410-5.
26. Abou El-Ela, A.A.; Kinawy, A.M.; El-Sehiemy, R.A.; Mouwafi, M.T. Optimal Reactive Power Dispatch Using Ant Colony Optimization Algorithm. *Electr. Eng.* 2011, *93*, 103–116, doi:10.1007/s00202-011-0196-4.
27. Ayan, K.; Kılıç, U. Artificial Bee Colony Algorithm Solution for Optimal Reactive Power Flow. *Appl. Soft Comput.* 2012, *12*, 1477–1482, doi:10.1016/j.asoc.2012.01.006.
28. Rajan, A.; Malakar, T. Exchange Market Algorithm Based Optimum Reactive Power Dispatch. *Appl. Soft Comput.* 2016, *43*, 320–336, doi:10.1016/j.asoc.2016.02.041.
29. Roy, P.K.; Ghoshal, S.P.; Thakur, S.S. Optimal VAR Control for Improvements in Voltage Profiles and for Real Power Loss Minimization Using Biogeography Based Optimization. *Int. J. Electr. Power Energy Syst.* 2012, *43*, 830–838, doi:10.1016/j.ijepes.2012.05.032.
30. Estimating the Voltage Stability of a Power System | IEEE Journals & Magazine | IEEE Xplore Available online: https://ieeexplore.ieee.org/document/4308013 (accessed on 31 December 2023).
31. Devaraj, D.; Roselyn, J.P. Genetic Algorithm Based Reactive Power Dispatch for Voltage Stability Improvement. *Int. J. Electr. Power Energy Syst.* 2010, *32*, 1151–1156, doi:10.1016/j.ijepes.2010.06.014.
32. (4) FVSI Based Reactive Power Planning Using Evolutionary Programming Available online: https://www.researchgate.net/publication/241177323_FVSI_based_Reactive_Power_Planning_using_Evolutionary_Programming (accessed on 31 December 2023).

33. Sayah, S.; Hamouda, A. A Hybrid Differential Evolution Algorithm Based on Particle Swarm Optimization for Nonconvex Economic Dispatch Problems. *Appl. Soft Comput.* 2013, *13*, 1608–1619, doi:10.1016/j.asoc.2012.12.014.
34. Niknam, T.; Narimani, M.R.; Jabbari, M.; Malekpour, A.R. A Modified Shuffle Frog Leaping Algorithm for Multi-Objective Optimal Power Flow. *Energy* 2011, *36*, 6420–6432, doi:10.1016/j.energy.2011.09.027.
35. Özgür, Y. Penalty Function Methods for Constrained Optimization with Genetic Algorithms. *Math. Comput. Appl.* 2005, *10*, 45–56.
36. Bouchekara, H.R.E.H.; Abido, M.A.; Boucherma, M. Optimal Power Flow Using Teaching-Learning-Based Optimization Technique. *Electr. Power Syst. Res.* 2014, *114*, 49–59, doi:10.1016/j.epsr.2014.03.032.
37. Shaheen, A.M.; Spea, S.R.; Farrag, S.M.; Abido, M.A. A Review of Meta-Heuristic Algorithms for Reactive Power Planning Problem. *Ain Shams Eng. J.* 2018, *9*, 215–231, doi:10.1016/j.asej.2015.12.003.
38. Rapport Metaheuristiques Optimisation Combinatoire Available online: https://pdfcoffee.com/rapport-metaheuristiques-optimisation-combinatoire-pdf-free.html (accessed on 31 December 2023).
39. Nanda, S.J.; Panda, G. A Survey on Nature Inspired Metaheuristic Algorithms for Partitional Clustering. *Swarm Evol. Comput.* 2014, *16*, 1–18, doi:10.1016/j.swevo.2013.11.003.
40. Boussaïd, I.; Lepagnot, J.; Siarry, P. A Survey on Optimization Metaheuristics. *Inf. Sci.* 2013, *237*, 82–117, doi:10.1016/j.ins.2013.02.041.
41. Ettappan, M. Evolutionary Algorithms Based Optimal Reactive Power Dispatch for Real Power Loss Minimization and Voltage Stability Enhancement.
42. Civicioglu, P. Backtracking Search Optimization Algorithm for Numerical Optimization Problems. *Appl. Math. Comput.* 2013, *219*, 8121–8144, doi:10.1016/j.amc.2013.02.017.
43. Duman, S.; Güvenç, U.; Sönmez, Y.; Yörükeren, N. Optimal Power Flow Using Gravitational Search Algorithm. *Energy Convers. Manag.* 2012, *59*, 86–95, doi:10.1016/j.enconman.2012.02.024.
44. Kaveh, A.; Mahdavi, V.R. Colliding Bodies Optimization: A Novel Meta-Heuristic Method. *Comput. Struct.* 2014, *139*, 18–27, doi:10.1016/j.compstruc.2014.04.005.
45. Hatamlou, A. Black Hole: A New Heuristic Optimization Approach for Data Clustering. *Inf. Sci.* 2013, *222*, 175–184, doi:10.1016/j.ins.2012.08.023.
46. Mirjalili, S.; Mirjalili, S.M.; Lewis, A. Grey Wolf Optimizer. *Adv. Eng. Softw.* 2014, *69*, 46–61, doi:10.1016/j.advengsoft.2013.12.007.
47. Rajan, A.; Malakar, T. Optimal Reactive Power Dispatch Using Hybrid Nelder–Mead Simplex Based Firefly Algorithm. *Int. J. Electr. Power Energy Syst.* 2015, *66*, 9–24, doi:10.1016/j.ijepes.2014.10.041.
48. Yang, X.-S.; Deb, S. Cuckoo Search via Lévy Flights. In Proceedings of the 2009 World Congress on Nature & Biologically Inspired Computing (NaBIC); December 2009; pp. 210–214.
49. Mirjalili, S. Moth-Flame Optimization Algorithm: A Novel Nature-Inspired Heuristic Paradigm. *Knowl.-Based Syst.* 2015, *89*, 228–249, doi:10.1016/j.knosys.2015.07.006.
50. Mukherjee, A.; Mukherjee, V. Chaotic Krill Herd Algorithm for Optimal Reactive Power Dispatch Considering FACTS Devices. *Appl. Soft Comput.* 2016, *44*, 163–190, doi:10.1016/j.asoc.2016.03.008.
51. Eusuff, M.; Lansey, K.; Pasha, F. Shuffled Frog-Leaping Algorithm: A Memetic Meta-Heuristic for Discrete Optimization. *Eng. Optim.* 2006, *38*, 129–154, doi:10.1080/03052150500384759.
52. Farhat, I.A.; El-Hawary, M.E. Dynamic Adaptive Bacterial Foraging Algorithm for Optimum

Economic Dispatch with Valve-Point Effects and Wind Power. *IET Gener. Transm. Distrib.* 2010, *4*, 989, doi:10.1049/iet-gtd.2010.0109.

53. Husseinzadeh Kashan, A. League Championship Algorithm (LCA): An Algorithm for Global Optimization Inspired by Sport Championships. *Appl. Soft Comput.* 2014, *16*, 171–200, doi:10.1016/j.asoc.2013.12.005.
54. Sadollah, A.; Bahreininejad, A.; Eskandar, H.; Hamdi, M. Mine Blast Algorithm: A New Population Based Algorithm for Solving Constrained Engineering Optimization Problems. *Appl. Soft Comput.* 2013, *13*, 2592–2612, doi:10.1016/j.asoc.2012.11.026.
55. Mirjalili, S. SCA: A Sine Cosine Algorithm for Solving Optimization Problems. *Knowl.-Based Syst.* 2016, *96*, 120–133, doi:10.1016/j.knosys.2015.12.022.
56. Soroudi, A.; Ehsan, M. Imperialist Competition Algorithm for Distributed Generation Connections. *IET Gener. Transm. Distrib.* 2012, *6*, 21, doi:10.1049/iet-gtd.2011.0190.
57. Civicioglu, P. Transforming Geocentric Cartesian Coordinates to Geodetic Coordinates by Using Differential Search Algorithm. *Comput. Geosci.* 2012, *46*, 229–247, doi:10.1016/j.cageo.2011.12.011.
58. Kaipa, K.; Ghose, D. Glowworm Swarm Optimization for Simultaneous Capture of Multiple Local Optima of Multimodal Functions. *Swarm Intell.* 2008, *3*, 87–124, doi:10.1007/s11721-008-0021-5.
59. Tamura, K.; Yasuda, K. Primary Study of Spiral Dynamics Inspired Optimization. *IEEJ Trans. Electr. Electron. Eng.* 2011, *6*, doi:10.1002/tee.20628.
60. Venkata Rao, R. Jaya: A Simple and New Optimization Algorithm for Solving Constrained and Unconstrained Optimization Problems. *Int. J. Ind. Eng. Comput.* 2016, 19–34, doi:10.5267/j.ijiec.2015.8.004.
61. Mirjalili, S.; Lewis, A. The Whale Optimization Algorithm. *Adv. Eng. Softw.* 2016, *95*, 51–67, doi:10.1016/j.advengsoft.2016.01.008.
62. Lenin, K.; Ravindhranath Reddy, B.; Suryakalavathi, M. Hybrid Tabu Search-Simulated Annealing Method to Solve Optimal Reactive Power Problem. *Int. J. Electr. Power Energy Syst.* 2016, *82*, 87–91, doi:10.1016/j.ijepes.2016.03.007.
63. Eskandar, H.; Sadollah, A.; Bahreininejad, A.; Hamdi, M. Water Cycle Algorithm – A Novel Metaheuristic Optimization Method for Solving Constrained Engineering Optimization Problems. *Comput. Struct.* 2012, *110–111*, 151–166, doi:10.1016/j.compstruc.2012.07.010.
64. Zhao, W.; Wang, L.; Mirjalili, S. Artificial Hummingbird Algorithm: A New Bio-Inspired Optimizer with Its Engineering Applications. *Comput. Methods Appl. Mech. Eng.* 2022, *388*, 114194, doi:10.1016/j.cma.2021.114194.
65. Zhang, W.; Liu, Y. Multi-Objective Reactive Power and Voltage Control Based on Fuzzy Optimization Strategy and Fuzzy Adaptive Particle Swarm. *Int. J. Electr. Power Energy Syst.* 2008, *30*, 525–532, doi:10.1016/j.ijepes.2008.04.005.
66. Ben Aribia, H.; Derbel, N.; Hadj Abdallah, H. The Active–Reactive – Complete Dispatch of an Electrical Network. *Int. J. Electr. Power Energy Syst.* 2013, *44*, 236–248, doi:10.1016/j.ijepes.2012.07.003.
67. Li, Y.; Wang, Y.; Li, B. A Hybrid Artificial Bee Colony Assisted Differential Evolution Algorithm for Optimal Reactive Power Flow. *Int. J. Electr. Power Energy Syst.* 2013, *52*, 25–33, doi:10.1016/j.ijepes.2013.03.016.
68. Rezaei Adaryani, M.; Karami, A. Artificial Bee Colony Algorithm for Solving Multi-Objective Optimal Power Flow Problem. *Int. J. Electr. Power Energy Syst.* 2013, *53*, 219–230, doi:10.1016/j.ijepes.2013.04.021.
69. Kılıç, U.; Ayan, K.; Arifoğlu, U. Optimizing Reactive Power Flow of HVDC Systems Using Genetic Algorithm. *Int. J. Electr. Power Energy Syst.* 2014, *55*, 1–12, doi:10.1016/j.ijepes.2013.08.006.

70. Ghasemi, A.; Valipour, K.; Tohidi, A. Multi Objective Optimal Reactive Power Dispatch Using a New Multi Objective Strategy. *Int. J. Electr. Power Energy Syst.* 2014, *57*, 318–334, doi:10.1016/j.ijepes.2013.11.049.
71. Martinez-Rojas, M.; Sumper, A.; Gomis-Bellmunt, O.; Sudrià-Andreu, A. Reactive Power Dispatch in Wind Farms Using Particle Swarm Optimization Technique and Feasible Solutions Search. *Appl. Energy* 2011, *88*, 4678–4686, doi:10.1016/j.apenergy.2011.06.010.
72. Durairaj, S.; Kannan, P.S.; Devaraj, D. Application of Genetic Algorithm to Optimal Reactive Power Dispatch Including Voltage Stability Constraint. *J. Energy* 2005.
73. Suresh, R.; Kumar, C.; Sakthivel, S.; Jaisiva, S. Application of Gravitational Search Algorithm for Real Power Loss and Voltage Deviation Optimization. 2013, *2*.
74. Varadarajan, M.; Swarup, K.S. Differential Evolutionary Algorithm for Optimal Reactive Power Dispatch. *Int. J. Electr. Power Energy Syst.* 2008, *30*, 435–441, doi:10.1016/j.ijepes.2008.03.003.
75. Li, Y.; Cao, Y.; Liu, Z.; Liu, Y.; Jiang, Q. Dynamic Optimal Reactive Power Dispatch Based on Parallel Particle Swarm Optimization Algorithm. *Comput. Math. Appl.* 2009, *57*, 1835–1842, doi:10.1016/j.camwa.2008.10.049.
76. Kumari, M.S.; Maheswarapu, S. Enhanced Genetic Algorithm Based Computation Technique for Multi-Objective Optimal Power Flow Solution. *Int. J. Electr. Power Energy Syst.* 2010, *32*, 736–742, doi:10.1016/j.ijepes.2010.01.010.
77. Lenin, K.; Reddy, B.R.; Kalavathi, M.S. Harmony Search (HS) Algorithm for Solving Optimal Reactive Power Dispatch Problem. *Int. J. Electron. Electr. Eng.* 2013, 269–274, doi:10.12720/ijeee.1.4.269-274.
78. Devaraj, D. Improved Genetic Algorithm for Multi-Objective Reactive Power Dispatch Problem. *Eur. Trans. Electr. Power* 2007, *17*, 569–581, doi:10.1002/etep.146.
79. Shaw, B.; Mukherjee, V.; Ghoshal, S.P. Solution of Reactive Power Dispatch of Power Systems by an Opposition-Based Gravitational Search Algorithm. *Int. J. Electr. Power Energy Syst.* 2014, *55*, 29–40, doi:10.1016/j.ijepes.2013.08.010.
80. Abido, M.A. Optimal Power Flow Using Tabu Search Algorithm. *Electr. Power Compon. Syst.* 2002, *30*, 469–483, doi:10.1080/15325000252888425.
81. Abdelmoumene, M.; Mohamed, B.; Boubakeur, A. Optimal Reactive Power Dispatch Using Differential Evolution Algorithm with Voltage Profile Control. *Int. J. Intell. Syst. Appl.* 2013, *5*, 28–34, doi:10.5815/ijisa.2013.10.04.
82. Subbaraj, P.; Rajnarayanan, P.N. Optimal Reactive Power Dispatch Using Self-Adaptive Real Coded Genetic Algorithm. *Electr. Power Syst. Res.* 2009, *79*, 374–381, doi:10.1016/j.epsr.2008.07.008.
83. Abido, M.A. Multiobjective Optimal VAR Dispatch Using Strength Pareto Evolutionary Algorithm. In Proceedings of the 2006 IEEE International Conference on Evolutionary Computation; IEEE: Vancouver, BC, Canada, 2006; pp. 730–736.
84. Smita, P.; Vaidya, B.N. Optimal Power Flow by Particle Swarm Optimization for Reactive Loss Minimization. 2012, *1*.
85. Dai, C.; Chen, W.; Zhu, Y.; Zhang, X. Reactive Power Dispatch Considering Voltage Stability with Seeker Optimization Algorithm. *Electr. Power Syst. Res.* 2009, *79*, 1462–1471, doi:10.1016/j.epsr.2009.04.020.
86. Suresh, R. Real Power Loss Minimization Using Big Bang Big Crunch Algorithm. *Int. J. Comput. Appl. 65*.
87. Xu, Y.; Zhang, W.; Liu, W.; Ferrese, F. Multiagent-Based Reinforcement Learning for Optimal Reactive Power Dispatch. *IEEE Trans. Syst. Man Cybern. Part C Appl. Rev.* 2012, *42*, 1742–1751, doi:10.1109/TSMCC.2012.2218596.
88. Heidari, A.A.; Ali Abbaspour, R.; Rezaee Jordehi, A. Gaussian Bare-Bones Water Cycle

Algorithm for Optimal Reactive Power Dispatch in Electrical Power Systems. *Appl. Soft Comput.* 2017, *57*, 657–671, doi:10.1016/j.asoc.2017.04.048.

89. Ghasemi, M.; Ghavidel, S.; Ghanbarian, M.M.; Habibi, A. A New Hybrid Algorithm for Optimal Reactive Power Dispatch Problem with Discrete and Continuous Control Variables. *Appl. Soft Comput.* 2014, *22*, 126–140, doi:10.1016/j.asoc.2014.05.006.
90. Rayudu, K.; Yesuratnam, G.; Jayalaxmi, A. Ant Colony Optimization Algorithm Based Optimal Reactive Power Dispatch to Improve Voltage Stability. In Proceedings of the 2017 International Conference on Circuit ,Power and Computing Technologies (ICCPCT); IEEE: Kollam, India, April 2017; pp. 1–6.
91. Ben Oualid Medani, K.; Sayah, S. Optimal Reactive Power Dispatch Using Particle Swarm Optimization with Time Varying Acceleration Coefficients. In Proceedings of the 2016 8th International Conference on Modelling, Identification and Control (ICMIC); IEEE: Algiers, Algeria, November 2016; pp. 780–785.
92. Zhang, X.; Chen, W.; Dai, C.; Cai, W. Dynamic Multi-Group Self-Adaptive Differential Evolution Algorithm for Reactive Power Optimization. *Int. J. Electr. Power Energy Syst.* 2010, *32*, 351–357, doi:10.1016/j.ijepes.2009.11.009.
93. Xiong, H.; Cheng, H.; Li, H. Optimal Reactive Power Flow Incorporating Static Voltage Stability Based on Multi-Objective Adaptive Immune Algorithm. *Energy Convers. Manag.* 2008, *49*, 1175–1181, doi:10.1016/j.enconman.2007.09.005.
94. Tripathy, M.; Mishra, S. Bacteria Foraging-Based Solution to Optimize Both Real Power Loss and Voltage Stability Limit. *IEEE Trans. Power Syst.* 2007, *22*, 240–248, doi:10.1109/TPWRS.2006.887968.
95. Ghasemi, M.; Taghizadeh, M.; Ghavidel, S.; Aghaei, J.; Abbasian, A. Solving Optimal Reactive Power Dispatch Problem Using a Novel Teaching–Learning-Based Optimization Algorithm. *Eng. Appl. Artif. Intell.* 2015, *39*, 100–108, doi:10.1016/j.engappai.2014.12.001.
96. Chakraborty, N.; Raha, S.B.; Mandal, K.K. Parametric Variation Based Simulated Annealing for Reactive Power Dispatch. In Proceedings of the IET Chennai Fourth International Conference on Sustainable Energy and Intelligent Systems (SEISCON 2013); Institution of Engineering and Technology: Chennai, India, 2013; pp. 29–34.
97. Sulaiman, M.H.; Mustaffa, Z. Cuckoo Search Algorithm as an Optimizer for Optimal Reactive Power Dispatch Problems. In Proceedings of the 2017 3rd International Conference on Control, Automation and Robotics (ICCAR); April 2017; pp. 735–739.
98. Raha, S.B.; Mandal, K.K.; Chakraborty, N. Hybrid SMES Based Reactive Power Dispatch by Cuckoo Search Algorithm. In Proceedings of the 2016 IEEE 1st International Conference on Power Electronics, Intelligent Control and Energy Systems (ICPEICES); July 2016; pp. 1–7.
99. Basu, M. Multi-Objective Optimal Reactive Power Dispatch Using Multi-Objective Differential Evolution. *Int. J. Electr. Power Energy Syst.* 2016, *82*, 213–224, doi:10.1016/j.ijepes.2016.03.024.
100. Nasouri Gilvaei, M.; Jafari, H.; Jabbari Ghadi, M.; Li, L. A Novel Hybrid Optimization Approach for Reactive Power Dispatch Problem Considering Voltage Stability Index. *Eng. Appl. Artif. Intell.* 2020, *96*, 103963, doi:10.1016/j.engappai.2020.103963.
101. Titare, L.S.; Singh, P.; Arya, L.D.; Choube, S.C. Optimal Reactive Power Rescheduling Based on EPSDE Algorithm to Enhance Static Voltage Stability. *Int. J. Electr. Power Energy Syst.* 2014, *63*, 588–599, doi:10.1016/j.ijepes.2014.05.078.
102. Kumar, S.K.N.; Renuga, D.P. Reactive Power Planning Using Differential Evolution: Comparison with Real GA and Evolutionary Programming. 2009, *2*.
103. Vishnu, M.; T. K., S.K. An Improved Solution for Reactive Power Dispatch Problem Using Diversity-Enhanced Particle Swarm Optimization. *Energies* 2020, *13*, 2862, doi:10.3390/en13112862.

104. Aljohani, T.M.; Ebrahim, A.F.; Mohammed, O. Single and Multiobjective Optimal Reactive Power Dispatch Based on Hybrid Artificial Physics–Particle Swarm Optimization. *Energies* 2019, *12*, 2333, doi:10.3390/en12122333.
105. Sahli, Z.; Hamouda, A.; Bekrar, A.; Trentesaux, D. Reactive Power Dispatch Optimization with Voltage Profile Improvement Using an Efficient Hybrid Algorithm. *Energies* 2018, *11*, 2134, doi:10.3390/en11082134.
106. Pal, B.B.; Biswas, P.; Mukhopadhyay, A. GA Based FGP Approach for Optimal Reactive Power Dispatch. *Procedia Technol.* 2013, *10*, 464–473, doi:10.1016/j.protcy.2013.12.384.
107. Al-Ammar, E.A.; Farzana, K.; Waqar, A.; Aamir, M.; Saifullah; Ul Haq, A.; Zahid, M.; Batool, M. ABC Algorithm Based Optimal Sizing and Placement of DGs in Distribution Networks Considering Multiple Objectives. *Ain Shams Eng. J.* 2021, *12*, 697–708, doi:10.1016/j.asej.2020.05.002.
108. Abaza, A.; Fawzy, A.; El-Sehiemy, R.A.; Alghamdi, A.S.; Kamel, S. Sensitive Reactive Power Dispatch Solution Accomplished with Renewable Energy Allocation Using an Enhanced Coyote Optimization Algorithm. *Ain Shams Eng. J.* 2021, *12*, 1723–1739, doi:10.1016/j.asej.2020.08.021.
109. Shaheen, M.A.M.; Hasanien, H.M.; Alkuhayli, A. A Novel Hybrid GWO-PSO Optimization Technique for Optimal Reactive Power Dispatch Problem Solution. *Ain Shams Eng. J.* 2021, *12*, 621–630, doi:10.1016/j.asej.2020.07.011.
110. Naderi, E.; Narimani, H.; Fathi, M.; Narimani, M.R. A Novel Fuzzy Adaptive Configuration of Particle Swarm Optimization to Solve Large-Scale Optimal Reactive Power Dispatch. *Appl. Soft Comput.* 2017, *53*, 441–456, doi:10.1016/j.asoc.2017.01.012.
111. Mehdinejad, M.; Mohammadi-Ivatloo, B.; Dadashzadeh-Bonab, R.; Zare, K. Solution of Optimal Reactive Power Dispatch of Power Systems Using Hybrid Particle Swarm Optimization and Imperialist Competitive Algorithms. *Int. J. Electr. Power Energy Syst.* 2016, *83*, 104–116, doi:10.1016/j.ijepes.2016.03.039.
112. Lenin, K.; Reddy, B.R.; Kalavathi, M.S. Hybrid Genetic Algorithm and Particle Swarm Optimization (HGAPSO) Algorithm for Solving Optimal Reactive Power Dispatch Problem. *Int. J. Electron. Electr. Eng.* 2013, 262–268, doi:10.12720/ijeee.1.4.262-268.
113. Yapıcı, H.; Çetinkaya, N. An Improved Particle Swarm Optimization Algorithm Using Eagle Strategy for Power Loss Minimization. *Math. Probl. Eng.* 2017, *2017*, 1–11, doi:10.1155/2017/1063045.
114. Subbaraj, P.; Rajnarayanan, P.N. Hybrid Particle Swarm Optimization Based Optimal Reactive Power Dispatch. *Int. J. Comput. Appl.* 2010, *1*, 79–85, doi:10.5120/121-236.
115. Binitha: A Survey of Bio Inspired Optimization Algorithms - Google Scholar Available online: https://scholar.google.com/scholar_lookup?title=A%20survey%20of%20bio%20inspired%20optimization%20algorithms&author=S.%20Binitha&publication_year=2012&pages=137-151 (accessed on 1 January 2024).
116. An Efficient Moth Flame Optimization (MFO) Algorithm for Solving Numerical Expressions Available online: https://transpireonline.blog/2019/07/30/an-efficient-moth-flame-optimization-mfo-algorithm-for-solving-numerical-expressions/ (accessed on 24 February 2024).
117. Taher, M.A.; Kamel, S.; Jurado, F.; Ebeed, M. An Improved Moth-Flame Optimization Algorithm for Solving Optimal Power Flow Problem. *Int. Trans. Electr. Energy Syst.* 2019, *29*, e2743, doi:10.1002/etep.2743.
118. Shi, J.-Y.; Zhang, D.-Y.; Xue, F.; Li, Y.-J.; Qiao, W.; Yang, W.-J.; Xu, Y.-M.; Yang, T. Moth-Flame Optimization-Based Maximum Power Point Tracking for Photovoltaic Systems Under Partial Shading Conditions. *J. Power Electron.* 2019, *19*, 1248–1258, doi:10.6113/JPE.2019.19.5.1248.

119. Mirjalili, S. The Ant Lion Optimizer. *Adv. Eng. Softw.* 2015, *83*, 80–98, doi:10.1016/j.advengsoft.2015.01.010.
120. Mahdad, B.; Srairi, K. Blackout Risk Prevention in a Smart Grid Based Flexible Optimal Strategy Using Grey Wolf-Pattern Search Algorithms. *Energy Convers. Manag.* 2015, *98*, 411–429, doi:10.1016/j.enconman.2015.04.005.
121. Naserbegi, A.; Aghaie, M.; Mahmoudi, S.M. PWR Core Pattern Optimization Using Grey Wolf Algorithm Based on Artificial Neural Network. *Prog. Nucl. Energy* 2020, *129*, 103505, doi:10.1016/j.pnucene.2020.103505.
122. Buchholz, M. Artificial Hummingbird Algorithm for Solving Optimization Problems in C++. *Medium* 2023.
123. Chen, K.; Chen, L.; Hu, G. PSO-Incorporated Hybrid Artificial Hummingbird Algorithm with Elite Opposition-Based Learning and Cauchy Mutation: A Case Study of Shape Optimization for CSGC–Ball Curves. *Biomimetics* 2023, *8*, 377, doi:10.3390/biomimetics8040377.
124. Medani, K.B.O.; Sayah, S.; Bekrar, A. Whale Optimization Algorithm Based Optimal Reactive Power Dispatch: A Case Study of the Algerian Power System. *Electr. Power Syst. Res.* 2018, *163*, 696–705, doi:10.1016/j.epsr.2017.09.001.
125. Mugemanyi, S.; Qu, Z.; Rugema, F.X.; Dong, Y.; Bananeza, C.; Wang, L. Optimal Reactive Power Dispatch Using Chaotic Bat Algorithm. *IEEE Access* 2020, *8*, 65830–65867, doi:10.1109/ACCESS.2020.2982988.
126. Pg_tca57bus Available online: https://labs.ece.uw.edu/pstca/pf57/pg_tca57bus.htm (accessed on 14 November 2023).
127. Chaohua Dai; Weirong Chen; Yunfang Zhu; Xuexia Zhang Seeker Optimization Algorithm for Optimal Reactive Power Dispatch. *IEEE Trans. Power Syst.* 2009, *24*, 1218–1231, doi:10.1109/TPWRS.2009.2021226.
128. Pg_tca118bus Available online: https://labs.ece.uw.edu/pstca/pf118/pg_tca118bus.htm (accessed on 18 November 2023).
129. Duong, T.L.; Duong, M.Q.; Phan, V.-D.; Nguyen, T.T. Optimal Reactive Power Flow for Large-Scale Power Systems Using an Effective Metaheuristic Algorithm. *J. Electr. Comput. Eng.* 2020, *2020*, 1–11, doi:10.1155/2020/6382507.
130. Ghasemi, M.; Ghanbarian, M.M.; Ghavidel, S.; Rahmani, S.; Mahboubi Moghaddam, E. Modified Teaching Learning Algorithm and Double Differential Evolution Algorithm for Optimal Reactive Power Dispatch Problem: A Comparative Study. *Inf. Sci.* 2014, *278*, 231–249, doi:10.1016/j.ins.2014.03.050.
131. Barrette, M. Méthode de comparaison statistique des performances d'algorithmes évolutionnaires. masters, École de technologie supérieure: Montréal, 2008.
132. Blum, C.; Roli, A. Hybrid Metaheuristics: An Introduction. In *Hybrid Metaheuristics: An Emerging Approach to Optimization*; Blum, C., Aguilera, M.J.B., Roli, A., Sampels, M., Eds.; Studies in Computational Intelligence; Springer: Berlin, Heidelberg, 2008; pp. 1–30 ISBN 978-3-540-78295-7.
133. Thangaraj, R.; Pant, M.; Abraham, A.; Bouvry, P. Particle Swarm Optimization: Hybridization Perspectives and Experimental Illustrations. *Appl. Math. Comput.* 2011, *217*, 5208–5226, doi:10.1016/j.amc.2010.12.053.
134. Vlachogiannis, J.G.; Lee, K.Y. A Comparative Study on Particle Swarm Optimization for Optimal Steady-State Performance of Power Systems. *IEEE Trans. Power Syst.* 2006, *21*, 1718–1728, doi:10.1109/TPWRS.2006.883687.
135. Chuanwen, J.; Bompard, E. A Hybrid Method of Chaotic Particle Swarm Optimization and Linear Interior for Reactive Power Optimisation. *Math. Comput. Simul.* 2005, *68*, 57–65, doi:10.1016/j.matcom.2004.10.003.
136. Hybrid Fuzzy Particle Swarm Optimization Approach for Reactive Power Optimization - UQ

eSpace Available online: https://espace.library.uq.edu.au/view/UQ:216731 (accessed on 16 December 2023).
137. Li, Y.; Jing, P.; Hu, D.; Zhang, B.; Mao, C.; Ruan, X.; Miao, X.; Chang, D. Optimal Reactive Power Dispatch Using Particle Swarms Optimization Algorithm Based Pareto Optimal Set. In *Advances in Neural Networks – ISNN 2009*; Yu, W., He, H., Zhang, N., Eds.; Lecture Notes in Computer Science; Springer Berlin Heidelberg: Berlin, Heidelberg, 2009; Vol. 5553, pp. 152–161 ISBN 978-3-642-01512-0.
138. Yiqin, Z. Optimal Reactive Power Planning Based on Improved Tabu Search Algorithm. In Proceedings of the 2010 International Conference on Electrical and Control Engineering; IEEE: Wuhan, China, June 2010; pp. 3945–3948.
139. Shen, Q.; Shi, W.-M.; Kong, W. Hybrid Particle Swarm Optimization and Tabu Search Approach for Selecting Genes for Tumor Classification Using Gene Expression Data. *Comput. Biol. Chem.* 2008, *32*, 53–60, doi:10.1016/j.compbiolchem.2007.10.001.
140. Kennedy, J.; Eberhart, R. Particle Swarm Optimization. In Proceedings of the Proceedings of ICNN'95 - International Conference on Neural Networks; November 1995; Vol. 4, pp. 1942–1948 vol.4.
141. Eberhart, R.; Kennedy, J. A New Optimizer Using Particle Swarm Theory. In Proceedings of the MHS'95. Proceedings of the Sixth International Symposium on Micro Machine and Human Science; October 1995; pp. 39–43.
142. Thangaraj, R.; Pant, M.; Abraham, A.; Bouvry, P. Particle Swarm Optimization: Hybridization Perspectives and Experimental Illustrations. *Appl. Math. Comput.* 2011, *217*, 5208–5226, doi:10.1016/j.amc.2010.12.053.
143. Hu, X.; Eberhart, R. Solving Constrained Nonlinear Optimization Problems with Particle Swarm Optimization. *Citeseer* 2002, *2002*, 203–206.
144. Yeniay, Ö. Penalty Function Methods for Constrained Optimization with Genetic Algorithms. *Math. Comput. Appl.* 2005, *10*, 45–56, doi:10.3390/mca10010045.
145. Pothiya, S.; Ngamroo, I.; Kongprawechnon, W. Application of Multiple Tabu Search Algorithm to Solve Dynamic Economic Dispatch Considering Generator Constraints. *Energy Convers. Manag.* 2008, *49*, 506–516, doi:10.1016/j.enconman.2007.08.012.
146. Chelouah, R.; Siarry, P. Enhanced Continuous Tabu Search: An Algorithm for Optimizing Multiminima Functions. In *Meta-Heuristics: Advances and Trends in Local Search Paradigms for Optimization*; Voß, S., Martello, S., Osman, I.H., Roucairol, C., Eds.; Springer US: Boston, MA, 1999; pp. 49–61 ISBN 978-1-4615-5775-3.
147. Pg_tca30bus Available online: http://labs.ece.uw.edu/pstca/pf30/pg_tca30bus.htm (accessed on 16 December 2023).
148. Mouassa, S.; Jurado, F.; Bouktir, T.; Raja, M.A.Z. Novel Design of Artificial Ecosystem Optimizer for Large-Scale Optimal Reactive Power Dispatch Problem with Application to Algerian Electricity Grid. *Neural Comput. Appl.* 2021, *33*, 7467–7490, doi:10.1007/s00521-020-05496-0.
149. Energies | Free Full-Text | Single and Multiobjective Optimal Reactive Power Dispatch Based on Hybrid Artificial Physics–Particle Swarm Optimization Available online: https://www.mdpi.com/1996-1073/12/12/2333 (accessed on 17 December 2023).
150. Jeyadevi, S.; Baskar, S.; Babulal, C.K.; Willjuice Iruthayarajan, M. Solving Multiobjective Optimal Reactive Power Dispatch Using Modified NSGA-II. *Int. J. Electr. Power Energy Syst.* 2011, *33*, 219–228, doi:10.1016/j.ijepes.2010.08.017.
151. Varadarajan, M.; Swarup, K.S. Differential Evolution Approach for Optimal Reactive Power Dispatch. *Appl. Soft Comput.* 2008, *8*, 1549–1561, doi:10.1016/j.asoc.2007.12.002.
152. Amrane, Y.; Boudour, M.; Ladjici, A.A.; Elmaouhab, A. Optimal VAR Control for Real Power Loss Minimization Using Differential Evolution Algorithm. *Int. J. Electr. Power Energy Syst.*

2015, *66*, 262–271, doi:10.1016/j.ijepes.2014.10.018.
153. Sayah, S. Modified Differential Evolution Approach for Practical Optimal Reactive Power Dispatch of Hybrid AC–DC Power Systems. *Appl. Soft Comput.* 2018, *73*, 591–606, doi:10.1016/j.asoc.2018.08.038.
154. Preedavichit, P. Optimal Reactive Power Dispatch Considering FACT§ Devices.
155. Ferreira, H.L.; L'Abbate, A.; Fulli, G.; Häger, U. Flexible Alternating Current Transmission Systems (FACTS) Devices. In *Advanced Technologies for Future Transmission Grids*; Migliavacca, G., Ed.; Power Systems; Springer London: London, 2013; pp. 119–156 ISBN 978-1-4471-4548-6.
156. Chakrabarti, A.; Halder, S. *Power System Analysis: Operation And Control 3Rd Ed.*; Prentice Hall India Pvt., Limited, 2010; ISBN 978-81-203-4015-2.
157. Singh, A.K.; Pal, B.C. Introduction. In *Dynamic Estimation and Control of Power Systems*; Elsevier, 2019; pp. 1–8 ISBN 978-0-12-814005-5.
158. Muhammad, Y.; Khan, R.; Raja, M.A.Z.; Ullah, F.; Chaudhary, N.I.; He, Y. Solution of Optimal Reactive Power Dispatch with FACTS Devices: A Survey. *Energy Rep.* 2020, *6*, 2211–2229, doi:10.1016/j.egyr.2020.07.030.
159. Nabil, M.; Mahdad, B.; Srairi, K.; Hamed, M. Multi Objective For Optimal Reactive Power Flow Using Modified PSO Considering TCSC. *Int. J. Energy Eng.* 2012, *2*.
160. Basu, M. Optimal Power Flow with FACTS Devices Using Differential Evolution. *Int. J. Electr. Power Energy Syst.* 2008, *30*, 150–156, doi:10.1016/j.ijepes.2007.06.011.
161. Karthikaikannan, D.; Ravi, G. Optimal Reactive Power Dispatch Considering Multi-Type FACTS Devices Using Harmony Search Algorithms. *Automatika* 2018, *59*, 311–322, doi:10.1080/00051144.2018.1541641.
162. Mahdad, B. Improvement Optimal Power Flow Solution Considering SVC and TCSC Controllers Using New Partitioned Ant Lion Algorithm. *Electr. Eng.* 2020, *102*, 2655–2672, doi:10.1007/s00202-020-01033-3.

ملخص:

الطاقة التفاعلية هي أحد مكونات الطاقة الكهربائية التي تتأرجح بين المصدر والحمل دون القيام بأي عمل مفيد. على الرغم من أنه لا يساهم بشكل مباشر في استهلاك الطاقة، إلا أن توزيعه المناسب يساعد على تقليل خسائر النقل وتحسين ملف الجهد وتعزيز الموثوقية العامة لشبكة الطاقة. يهدف إرسال الطاقة التفاعلية الأمثل (OPRD) إلى إدارة موارد الطاقة التفاعلية للنظام بشكل صحيح. غالبًا ما تواجه الطرق التقليدية لحل مشكلة ORPD صعوبات مرتبطة بالطبيعة المعقدة وغير الخطية والمقيدة للغاية للشبكات الكهربائية. في هذا السياق، ظهرت خوارزميات ما بعد الماهرة كأدوات فعالة لإيجاد حلول شبه مثالية لمشاكل التحسين المعقدة. في هذه الأطروحة، أولاً، تم تطوير وتنفيذ العديد من تقنيات التحسين الوصفية المستوحاة من البيولوجيا لمعالجة مشكلة ORPD. بعد ذلك، اقترحنا طريقة ميتايورستية هجينة جديدة تتكون من الطريقة السكانية (طريقة سرب الجسيمات) وطريقة بحث محلية (بحث التبو) تسمى تقنية PSO-TS. يتم استخدام نهج PSO-TS المقترح للعثور على معلمات متغيرات التحكم (أي جهد المولد وصنابير المحولات وأحجام مكثفات التحويل) التي تقلل من فقد الطاقة النشطة وتحسن ملف تعريف الجهد للشبكة الكهربائية. يتم تحديد مواقع مكثفات التحويل باستخدام طريقة قضيب التوصيل الحساس. في هذا العمل، قمنا أيضًا بحل مشكلة ORPD من خلال مراعاة أجهزة FACTS. تمتد عمليات المحاكاة لتشمل بعض نماذج أنظمة الطاقة واسعة النطاق مثل قضبان التوصيل IEEE 57 وخطوط التوصيل IEEE 118 والشبكة الجزائرية العملية 114 قضبان التوصيل. وأخيرًا، تم بناء نموذج لاختبار المراقبة والتحكم في أجهزة SVC عبر واجهة الإنسان والآلة التي تعمل بنظامي التشغيل Windows وAndroid. كما تم تصميم تطبيق لتصور جميع عمليات المحاكاة التي أجريت في هذه الرسالة

كلمات مفتاحية: التوزيع الأمثل للقدرة التفاعلية ; ميتاهيروستيك ; خوارزميات مستوحاة من الحيوية ; التقليل من فقدان الطاقة ; تقليل انحراف الجهد; أجهزة FACTS

Abstract:

Reactive power is the component of electrical power that oscillates between the source and load without performing any useful work. While it does not contribute directly to energy consumption, Its Proper dispatch helps of minimizing transmission losses, improving voltage profile and enhance the overall reliability of the electrical grid. The optimal reactive power dispatch (OPRD) Seeks to properly manage the reactive power resources of the system. Traditional methods for solving the ORPD problem often face challenges in handling the complex, non-linear, and highly constrained nature of power systems. In this context, metaheuristic algorithms have emerged as effective tools for finding near-optimal solutions to complex optimization problems. In this thesis, firstly, various bio-inspired meta-heuristic optimization techniques have been developed and implemented to deal with the ORPD problem. Then, we have proposed a new hybrid metaheuristic method composed of a population method (Particle Swarm Optimization) and a local search method (Tabu Search) named PSO-TS technique. The proposed PSO-TS approach is used to find the settings of the control variables (i.e. generation bus voltages, transformer taps, and shunt capacitor sizes) which minimize transmission active power losses and improve voltage profile of the electrical network. The bus locations of the shunt capacitors are identified according to sensitive buses approach. In this work, we have also solved the of ORPD problem considering FACTS devices. Simulations is extended to some large-scale power system models like IEEE 57-bus, IEEE 118-bus and a practical Algerian 114-bus power test system. Finally, a mock-up has been built to test the control and command of the SVC devices via a human-machine interface running under windows and android. An application has been designed to visualize all the simulations carried out in this thesis.

Keywords: optimal reactive power dispatch (ORPD); metaheuristic techniques; bio-inspired algorithms; power loss minimization; voltage deviation minimization; FACTS devices.

Résumé:

La puissance réactive est la composante de la puissance électrique qui oscille entre la source et la charge sans effectuer de travail utile. Bien qu'elle ne contribue pas directement à la consommation d'énergie, sa répartition appropriée permet de minimiser les pertes de transmission, d'améliorer le profil de tension et de renforcer la fiabilité globale du réseau électrique. La répartition optimale de la puissance réactive (OPRD) vise à gérer correctement les ressources de puissance réactive du système. Les méthodes traditionnelles de résolution du problème de l'ORPD se heurtent souvent à des difficultés liées à la nature complexe, non linéaire et très contraignante des réseaux électriques. Dans ce contexte, les algorithmes métaheuristiques sont apparus comme des outils efficaces pour trouver des solutions quasi-optimales à des problèmes d'optimisation complexes. Dans cette thèse, tout d'abord, diverses techniques d'optimisation méta-heuristiques bio-inspirées ont été développées et mises en œuvre pour traiter le problème de l'ORPD. Ensuite, nous avons proposé une nouvelle méthode métaheuristique hybride composée d'une méthode de population (la méthode des essaims de particules) et d'une méthode de recherche locale (la recherche tabou) appelée la technique du PSO-TS. L'approche PSO-TS proposée est utilisée pour trouver les paramètres des variables de contrôle (c'est-à-dire les tensions des générateurs, les prises des transformateurs et les tailles des condensateurs shunt) qui minimisent les pertes de puissance active et améliorent le profil de tension du réseau électrique. Les emplacements des condensateurs shunt sont identifiés selon l'approche des jeux de barres sensibles. Dans ce travail, nous avons également résolu le problème de l'ORPD en tenant en compte les dispositifs FACTS. Les simulations sont étendues à certains modèles de systèmes électriques à grande échelle tels que IEEE 57 jeux de barres, IEEE 118 jeux de barres et le réseau algérien pratique à 114 jeux de barres. Enfin, une maquette a été construite pour tester le contrôle et la commande des dispositifs SVC via une interface homme-machine fonctionnant sous Windows et Android. Une application a été conçue aussi pour visualiser toutes les simulations réalisées dans cette thèse.

Mots clés : répartition optimale de la puissance réactive (ORPD); techniques métaheuristiques; algorithmes bio-inspirés; minimisation des pertes de puissance; minimisation des déviations des tensions; dispositifs FACTS.